UNIVERSITEIT VAN PRETORIA
UNIVERSITY OF PRETORIA
YUNIBESITHI YA PRETORIA

Correlation between invasive abdominopelvic and lower limb procedures and the detailed anatomical description of the lumbar plexus in a South African population

by

Zithulele Nkosinathi Tshabalala

Dissertation submitted in full fulfilment of the requirements for the degree

Doctor of Philosophy in Anatomy

In the Faculty of Health Science

University of Pretoria

Supervisor: Prof. A-N van Schoor

2019

DECLARATION OF ORIGINALITY
UNIVERSITY OF PRETORIA

The Department of Anatomy places great emphasis upon integrity and ethical conduct in the preparation of all written work submitted for academic evaluation.

While academic staff teach you about referencing techniques and how to avoid plagiarism, you too have a responsibility in this regard. If you are at any stage uncertain as to what is required, you should speak to your lecturer before any written work is submitted.

You are guilty of plagiarism if you copy something from another author's work (e.g. a book, an article or a website) without acknowledging the source and pass it off as your own. In effect you are stealing something that belongs to someone else. This is not only the case when you copy work word-for-word (verbatim), but also when you submit someone else's work in a slightly altered form (paraphrase) or use a line of argument without acknowledging it. You are not allowed to use work previously produced by another student. You are also not allowed to let anybody copy your work with the intention of passing if off as his/her work.

Students who commit plagiarism will not be given any credit for plagiarised work. The matter may also be referred to the Disciplinary Committee (Students) for a ruling. Plagiarism is regarded as a serious contravention of the University's rules and can lead to expulsion from the University.

The declaration which follows must accompany all written work submitted while you are a student of the Department of Anatomy. No written work will be accepted unless the declaration has been completed and attached.

Full names of student: Zithulele Nkosinathi Tshabalala
Student number: 27356010
Topic of work: Correlation between invasive abdominopelvic and lower limb procedures and the detailed anatomical description of the lumbar plexus in a South African population

Declaration

1. I understand what plagiarism is and am aware of the University's policy in this regard.
2. I declare that this thesis is my own original work. Where other people's work has been used (either from a printed source, Internet or any other source), this has been properly acknowledged and referenced in accordance with departmental requirements.
3. I have not used work previously produced by another student or any other person to hand in as my own.
4. I have not allowed, and will not allow, anyone to copy my work with the intention of passing it off as his or her own work.

Zithulele Nkosinathi Tshabalala

Acknowledgements

In the name of the Father, of the Son and of the Holy Spirit.

To my wife, Ncuthukazi, thank you for your constant patience, love and understanding throughout this entire journey. I am still in awe at how amazing you are, can be and remain even in the most difficult of situations. I know it was not easy to have a zombie as a husband and I truly appreciate how you were my assistant, advisor, cheerleader, shoulder to cry on and my second brain when my mind was not be able to perform the most mundane of tasks. The snack runs when I have long sessions in the dissection hall and during writing up, none of the things you done went unnoticed. Ndiyabulela, enkosi, ke a leboha Mamorero Tshabalala, Khaleesi, The first of her name. Ndikuthanda gqithi Mamzangwa.

To my mother, Moitheri, I will forever be indebted to you. Your words of encouragement when I was in dark places shed a lot of light and pushed me forward. Your teachings throughout these years remain engraved in my heart and mind, they keep me grounded and sane. Thank you Nkhono MaTshabalala, Mshengu omukhulu. Ke o rata ka pelo, mmele le moya.

To my sisters, Minky and Thulisa and my niece, Luyanda, your calls and texts always reminded me why I needed to finish this thesis. Missing big and small moments was unintentional and will be rectified, I am sorry. Believe that I missed you as much as you constantly told me how much I missed you. Thank you for your understanding I love you. To my niece who is due soon, Siphosethu, you didn't make it on time to get a thank you, hade.

To my late grandmother, Mojabeng, you left us at a critical moment in the completion process of this thesis, but I got healing in knowing that you were at rest. I would have loved to have you see me walk on that stage one last time. I submitted this thesis in your honour in the week of your passing, determined that this journey should be laid to rest as well. We will always miss you, Anjeng. Thank you for getting me this far, you did your part. Robala ka khotso Motaung, o ratile, o ratuwe.

To the rest of my family, there are way too many of you to name, but you were just as important in this journey. Thank you for your support throughout the years and always being willing to step up when situations call for you to carry more weight. Ke leboha ho menahane.

To my supervisor, Prof. Albert-Neels van Schoor, thank you for always being by my side, especially during those times when I was struggling to find my feet. This would not have been possible had you not taken me under your wing and lifted me when I faltered. Thank you to Robyn and Neil for sharing your attention with me when you had to read through all of this. Thank you abundantly.

To Nkhensani Mogale, we started this madness on different ends of the spectrum, but yet we were able to carry each other through. Were one fell, the other would carry them, Thank you for the talks so I can regain my sanity knowing that I am not going through the struggles alone.

During the process of the write up, there are two people that helped in making the weight of my work lighter. So, a big Thank you to Niel van Tonder and Shavana Govender. The last 6 months of the write up were easy on the work front because of the both of you. Another word of appreciation to Jade Naicker for her illustration and Barbara Viljoen for the language editing. Thank you very much to all of you.

Thank you to all the staff of the Department of Anatomy for all the help with getting samples and ensuring that they are all ready and easy to locate. Ke lebohile Ntate Solly, Moses, Eric le Peter. Mam Johanna, ngibongela amazwi akho. Thank you Professor Marius Bosman and Professor Prashilla Soma for your support in the difficult admin process during this journey.

To the professional services staff, Natasha Jeftha (Research) and Natasha Muller (Human Resources), thank you for your assistance during the admin process of getting funding and sabbatical.

I owe one of my biggest thank you to the body donors and their families, for without your sacrifice this study would not have been possible. I cannot articulate how enormous your contribution to the success of this study was. A million times THANK YOU!

Lastly, I would like to National Research Foundation – Black Academic Advancement Program (NRF – BAAP) for their assistance in the funding of a replacement lecturer so I could go on sabbatical.

Amen

Tshabalala! Mshengu!

Ludvonga lukaMavuso waNgwane! Sdwabas'ilitfuli!
Esingabacwaba seza nomlandakazi!

Nine bakwa Wawawa!

Ena wela uLubombo ngokuhlehlethela!

Nine lolway'eMbo nabuyela!

Nine bengongoni yase mavaneni!

Abaduma bakhathala bezindlu

nezindlwana!

Bethi uMhlongamvula udilikile kanti kuzamazama lgcuku!

Nina abathenga amanga ngesitole esikone! Bethi kungcono amanga kunokuthakada!

Nina ebavala ngamakhanda amadoda eSimakade! Abanye bevala ngamahlahla!

Nina bakwa Mafu angalingani phansi naphezulu!

Aphezulu abhuhhalahhala afuze kithi

eSwatini lapho kubodle iNgonyama!

Bese basho bantu besizwe, bethi

Tshabalala! Mshengu!

Table of contents

List of figures

List of tables

List of abbreviations

Abbreviation	Meaning
ASIS	Anterior superior iliac spine
BMI	Body mass index
CI	Confidence interval
cm	Centimeters
CT	Computed tomography
FA	Femoral artery
FN	Femoral nerve
FV	Femoral vein
GFN	Genitofemoral nerve
IHN	Iliohypogastric nerve
IIN	Ilioinguinal nerve
L1	Lumbar verterbra 1
L1/L2	Intervertebral disc between lumbar vertebrae 1 and 2
L2	Lumbar verterbra 2
L2/L3	Intervertebral disc between lumbar vertebrae 2 and 3
L3	Lumbar verterbra 3
L3/L4	Intervertebral disc between lumbar vertebrae 3 and 4
L4	Lumbar verterbra 4
L4/L5	Intervertebral disc between lumbar vertebrae 4 and 5
L5	Lumbar verterbra 5
L5/S1	Intervertebral disc between lumbar vertebra 5 and sacral vertebra 1
LFCN	Lateral femoral cutaneous nerve
LPT	Trunk of the lumbar plexus
mm	Millimeters
MRI	Magnetic resonance imaging
n	Sample size
ON	Obturator nerve
PSIS	Posterior superior iliac spine
SD	Standard deviation
T12	Thoracic vertebra 12

Abstract

The lumbar plexus is a bundle of nerves which originate from the ventral rami of the L1-L4 spinal nerves. The terminal branches of the lumbar plexus are the iliohypogastric-, ilioinguinal-, genitofemoral-, lateral femoral cutaneous-, obturator- and femoral nerves. These nerves give motor and sensory innervation to the lower abdomen, lower limb and parts of the perineum as they exit the pelvis to enter the thigh. A number of clinical and surgical procedures are performed along the courses of these nerves. The aim of this study was to accurately describe the anatomy of all the branches of the lumbar plexus and correlate the results with currently used procedural guidelines.

One hundred and five (105) formalin-fixed cadavers (59 males and 46 females; 70.8 ± 15.3 years) were dissected bilaterally at the Department of Anatomy, University of Pretoria. Dissections were done along the course of each of the terminal branches from their origins paravertebrally until their termination in the thigh. Relation to bony and connective tissue landmarks were noted and measured.

Variations were observed in the anatomy of most of the terminal branches along their course. In some instances, the anatomy was observed to be as described in the literature. Measurements from bony landmarks to the nerves indicated some differences with what had been reported in the literature.

The results of the study lay a foundation for further clinical research in the areas where the terminal branches course and may be used in current and future teaching practices in anatomy.

Keywords: anterior superior iliac spine, lower limb nerve block, lower limb surgery, psoas compartment block, peripheral nerve blocks, lower limb anaesthesia, lower limb analgesia, pain management

Chapter 1 – Introduction and problem statement

A number of surgical and clinical procedures are performed on the lumbar plexus and its branches. The determination of the location of these nerves is essential in order to successfully complete these procedures. As these procedures are performed in close proximity to the nerves, extensive knowledge of their anatomy will ensure that the use of instrumentation is completed safely so not to damage them. Nerve damage after nerve blocks has been reported in the literature. This complication as a result of needles being advanced too far and has been reported as a common complication of these procedures (Horlocker et al., 2015; Xu and Hadzic, 2015; Bomberg et al., 2018). Post-operative pain has been reported as a complication of damage to the nerves by instruments used during surgery or mesh placed to reinforce the walls of the inguinal canal (Huri et al., 2015; Lange et al., 2015; Katzen, 2019)

Lower limb nerve blocks are performed on peripheral nerves in order to provide anaesthesia of joints and skin during surgical procedures. These nerve blocks are also utilized as a solution for the management of chronic pain and post-operative pain (Lewis et al., 2015; Guay et al., 2017; Yang et al., 2017). The nerve blocks provide analgesia to the regions of the lower limb and perineum which the nerves supply. The peripheral lower limb nerve blocks are performed on the lumbar plexus and its branches along their origin and course through different regions of the body, where they are in danger of damage during these blocks. Studies have reported the rate of complication as a result of these ultrasound-guided procedures between 0.27% and 19% worldwide. The common complications of peripheral nerve blocks are reported to be vascular puncture, nerve puncture and partial/incomplete blocks (Horlocker et al., 2015; Lewis et al., 2015; Williams et al., 2017). Complications may be attributed to the partial disregard of the anatomy of the peripheral lower limb nerves and their variations. It is essential that the anatomy of these nerves is understood and considered during peripheral nerve block of the lower limb to ensure that they are not damaged and the blocks are successful.

Surgical procedures in the lower limb where the nerve blocks are needed are executed along the course of the branches of the lumbar plexus. Invasive surgery such as iliac crest harvesting, inguinal hernia repair, transobturator tape and tension-free vaginal tape-obturator procedures have reported incidences of damage and entrapment of

these branches (Aydogmus et al., 2014; Bozkurt et al., 2015; Armaghani et al., 2016; Vasu and Sagar, 2018; Duckett et al., 2019; Suda et al., 2019). Damage to these branches will not only cause sensory loss to the lower limb and aspects of the perineum, but will also lead to paralysis and weakness of the lower limb muscles and muscle groups (Sugimoto et al., 2010; Lee et al., 2016; Park et al., 2016; Thomas et al., 2016). Visualization of the nerves peri-operatively will decrease the incidence of complications, as clinicians can avoid these nerves with the instruments used for the procedures. Accurately identifying the lumbar plexus and its branches using surface anatomy and imaging modalities will increase the success rate of these procedures. Therefore, it is essential that the anatomy and variations of the lumbar plexus and its branches be reviewed regularly to contribute to the worldwide knowledgebase.

Chapter 2 – Lumbar plexus

2.1. Introduction and problem statement

A number of surgical and clinical procedures are performed in the vicinity of and/or on the lumbar plexus and the branches thereof. These procedures are performed in order to provide treatment, anaesthesia or analgesia to patients pre-, peri- and/or post-operatively. This places the lumbar plexus and/or its branches in danger of injury. Damage to these nerves will have adverse effects on the motor and sensory function in certain areas of the thigh, groin and perineum. Instances of damage have also been reported in about 6-33% of surgical procedures performed in the area (Arnold et al., 2012; Pumberger et al., 2012; Grunert et al., 2017).

An extensive review of the available literature indicates that, apart from general anatomical descriptions and brief references in clinical articles, few actual studies have been done to describe the exact position, course, branching patterns or possible anatomical variations of the lumbar plexus and its branches in detail.

2.2. Literature review

2.2.1. Lumbar plexus

The lumbar plexus arises from the ventral rami of the lumbar spinal nerves 1 to 4 (L1– L4). This plexus gives origin to six terminal branches that course to, and innervate the area of the perineum as well as the anterior, medial and lateral surfaces of the thigh. These branches are the iliohypogastric nerve (IHN), ilioinguinal nerve (IIN), genitofemoral nerve (GFN), lateral femoral cutaneous nerve (LFCN), femoral nerve (FN) and the obturator nerve (ON), arising from different combinations of the spinal nerves within or posterior to the substance of the psoas major muscle, anterior to its attachment on the transverse processes of the lumbar vertebrae. In relation to the psoas major muscle, the nerves are described to exit lateral, medial and anterior to it, as they course to their target areas of innervation (Sim and Webb, 2004; Tubbs et al., 2005; Uzmansel et al., 2006; Anloague and Huijbregts, 2009; Ellis, 2010).

The first lumbar spinal nerve (L1) courses through the psoas major muscle, to then exit from its lateral border, subsequently splitting into the IHN and IIN. The combination of the first and second lumbar spinal nerves (L1 – L2) then gives rise to the GFN, which pierces the psoas major muscle and exits anteriorly between the muscles fibres.

The second and third lumbar spinal nerves (L2 – L3) give rise to LFCN, coursing to exit from the lateral border of the psoas major muscle. Lastly, the FN and ON arise from the second, third and fourth lumbar spinal nerves (L2 – L4), with the FN exiting lateral and the ON medial to the psoas major muscle (Tubbs et al., 2005; Anloague and Huijbregts, 2009; Ellis, 2010; Tagliafico et al., 2015).

2.2.2. Iliohypogastric nerve (IHN)

The IHN arises from the ventral rami of the L1 spinal nerve, to then traverse the anterior surface of the quadratus lumborum muscle, posterior to the kidneys. Along its course, it pierces the transversus abdominis muscle, running anteriorly between the transversus abdominis and internal oblique muscles. At the iliac crest, it terminates as the lateral cutaneous and the anterior cutaneous branches. The lateral cutaneous branch will pierce the internal oblique muscle before penetrating the external oblique muscle to supply the skin over the posterolateral surface of the gluteal region. The anterior cutaneous branch will course in the opposite direction, running anteriorly. It pierces the internal oblique muscle medial to the anterior superior iliac spine (ASIS), runs obliquely inferomedially and pierces the external oblique aponeurosis to supply skin over the pubic region. The IHN also has motor innervation to the transversus abdominis and internal oblique muscles (Amin et al., 2016; Kale et al., 2019). Variations have been reported where the subcostal nerve (SN), which usually arises from the twelfth thoracic spinal nerve (T12), also originates from the lumbar plexus. In that, the IHN would also have a contribution from T12 and L1 (Tubbs et al., 2005; Kotian et al., 2015; Tagliafico et al., 2015). A study by Amin et al. (2016) reported a contribution from both T12 and L2 to the IHN nerve.

2.2.3. Ilioinguinal nerve (IIN)

The IIN arises from the same ventral rami of L1 as the IHN. The IIN runs obliquely over the quadratus lumborum muscle, descending on the iliacus muscle and the iliac crest towards the inguinal canal. As it approaches the iliac crest, it pierces the transversus abdominis and internal oblique muscles; to enter the inguinal canal, in relation to the spermatic cord in males and the round ligament of the uterus in females. The IIN emerges from the superficial inguinal ring to then give sensory innervation to the upper medial thigh and the perineum, anterior part of the scrotum in males and the mons pubis and the anterior part of the labia majora in females. As in the case of

the IHN, the IIN gives motor innervation to the abdominal muscle as it travels through them (Al-dabbagh, 2002; Anloague and Huijbregts, 2009; Barazanchi et al., 2016).

2.2.4. Genitofemoral nerve (GFN)

The GFN arises from the ventral rami of the L1 and L2 spinal nerves. It exits the psoas major muscle anteriorly, to then descend along its anterior surface. In its descent, it passes posterior to the ureter. Before it reaches the inguinal canal, the nerve splits into its terminal branches, the genital and femoral branches (Anloague and Huijbregts, 2009; Celebi et al., 2013).

In males, the genital branch descends on the psoas major muscle to pass through the deep inguinal ring, entering the inguinal canal to form part of the content of the spermatic cord. It gives motor supply to the cremasteric muscle in males. It does not give any innervation within the inguinal canal in females. In the thigh, the genital branch provides sensory innervation to the skin of the anterior surface of the scrotum and upper thigh in males and accompanies the round ligament of the uterus to innervate the mons pubis and the labia majora in females (Anloague and Huijbregts, 2009; Celebi et al., 2013; Gossman and Bhimji, 2017). The innervation to the external genitalia is in combination with that of the IIN (Rab and Dellon, 2001; Tagliafico et al., 2015; Kumar and Zaidi, 2017)

The femoral branch descends lateral to the external iliac artery and then posterior to the inguinal ligament, to enter the femoral sheath. In the upper region of the anterior thigh, it then pierces the sheath and fascia lata anteriorly, to give sensory innervation to the skin of the upper area of the anterior thigh (Anloague and Huijbregts, 2009; Celebi et al., 2013).

A study by Anloague and Huijbregts (2009) reported a 47.1% variation in the bifurcation of the GFN into its terminal branches. They also found variations in the bifurcation, where the terminal branches originated within the substance of the psoas major muscle. Al-dabbagh (2002) found variations in the GFN in two out of 64 cases, where the IIN also originated from it.

2.2.5. Lateral femoral cutaneous nerve (LFCN)

The LFCN arises from the ventral rami L2 and L3 spinal nerves. After emerging from the lateral border of the psoas major muscle, it descends obliquely on the iliacus muscle, towards the ASIS. According to most anatomical texts, the LFCN passes deep to the inguinal ligament as it descends, to then enter the thigh. Thereafter, it gives sensory innervation to skin over the lateral and anterior surfaces of the thigh up to the level of the knee (Shannon et al., 1994; Anloague and Huijbregts, 2009).

A study by Anloague and Huijbregts (2009) found that there was variation with regard to the root values of the LFCN. The root values were reported to be from L1 and L2, whereas in the literature it is described as originating from the ventral rami of the L2 and L3 spinal nerves. The LFCN terminates as its femoral and genital branches as it passes deep to the inguinal ligament. Variation of the bifurcation of the LFCN into its terminal branches have been reported in the literature (Anloague and Huijbregts, 2009).

2.2.6. Obturator nerve (ON)

The ON arises from anterior divisions of the ventral rami of the L2, L3 and L4 spinal nerves. The ON is the only nerve of the lumbar plexus to emerge from the medial border of the psoas major muscle. It then descends towards the pelvis, running on the pelvic brim before entering the lesser pelvis at the level of the sacroiliac joint. The nerve enters through the obturator canal at the obturator foramen. After entering the obturator canal, the nerve terminates into anterior and posterior divisions, to give motor supply to the medial compartment of the thigh. The anterior and posterior divisions are separated by the obturator externus muscle as the ON extends into the medial compartment of the thigh. The branches of the anterior division of the ON give additional sensory innervation to the skin over the medial thigh up to the level of the knee (Anagnostopoulou et al., 2009; Anloague and Huijbregts, 2009; Arora et al., 2014).

2.2.7. Femoral nerve (FN)

The FN arises from the posterior divisions of the ventral rami of the L2, L3 and L4 spinal nerves. As it emerges from the lateral border of the psoas major muscle, it descends anterior to the iliacus muscle towards the inguinal ligament. It then passes

posterior to the inguinal ligament before entering the anterior compartment of the thigh lateral to the femoral sheath. Upon entering the thigh, it divides into various motor and sensory branches. The sensory branches innervate the skin over the anterior surface of the thigh and the medial surface of the leg. The motor branches innervate the iliacus, rectus femoris, sartorius, pectineus and the vastus medialis, -intermedius and -lateralis muscles (Anloague and Huijbregts, 2009; Moore and Stringer, 2011).

2.2.8. Psoas compartment block

The psoas compartment block was first described by Winnie et al. (1974). This block was later modified by Capdevila et al. (2002) who introduced a nerve stimulator for the procedure. The psoas compartment block is usually performed for analgesia for post-operative patient care after total hip arthroplasty surgery. The procedure has been reported to be a good alternative to epidural analgesia and easy to perform (Sharrock and Savarese, 2000; Becker et al., 2007; Singh et al., 2018; Yoo et al., 2019). In this technique, the patient is placed in a lateral position, where the side to be operated on faces superiorly; known as the Sim's position. A horizontal line is marked, posteriorly, between the iliac crests. A vertical line, parallel to the vertebral column, is drawn perpendicular to the line between the posterior parts of the iliac crests, ensuring that it passes through the posterior superior iliac spine. The spinous process of the L4 vertebra is marked and the line between it and the line through the PSIS was divided into thirds along the line between the posterior parts of the iliac crests (Figure 1) (Buckenmaier III et al., 2002; Capdevila et al., 2002; Di Benedetto et al., 2005; Jogdand and Sule, 2018). The junction between the medial two-thirds and the lateral third, along the perpendicular line, serves as the insertion point of the needle (Capdevila et al., 2002; Mannion, 2007). Furthermore, Jogdand and Sule (2018) reported a 45 - 50mm insertion site lateral to the midline of the body. A study by Awad and Duggan (2005) reported an insertion site of 40mm lateral to the midline of the vertebral column.

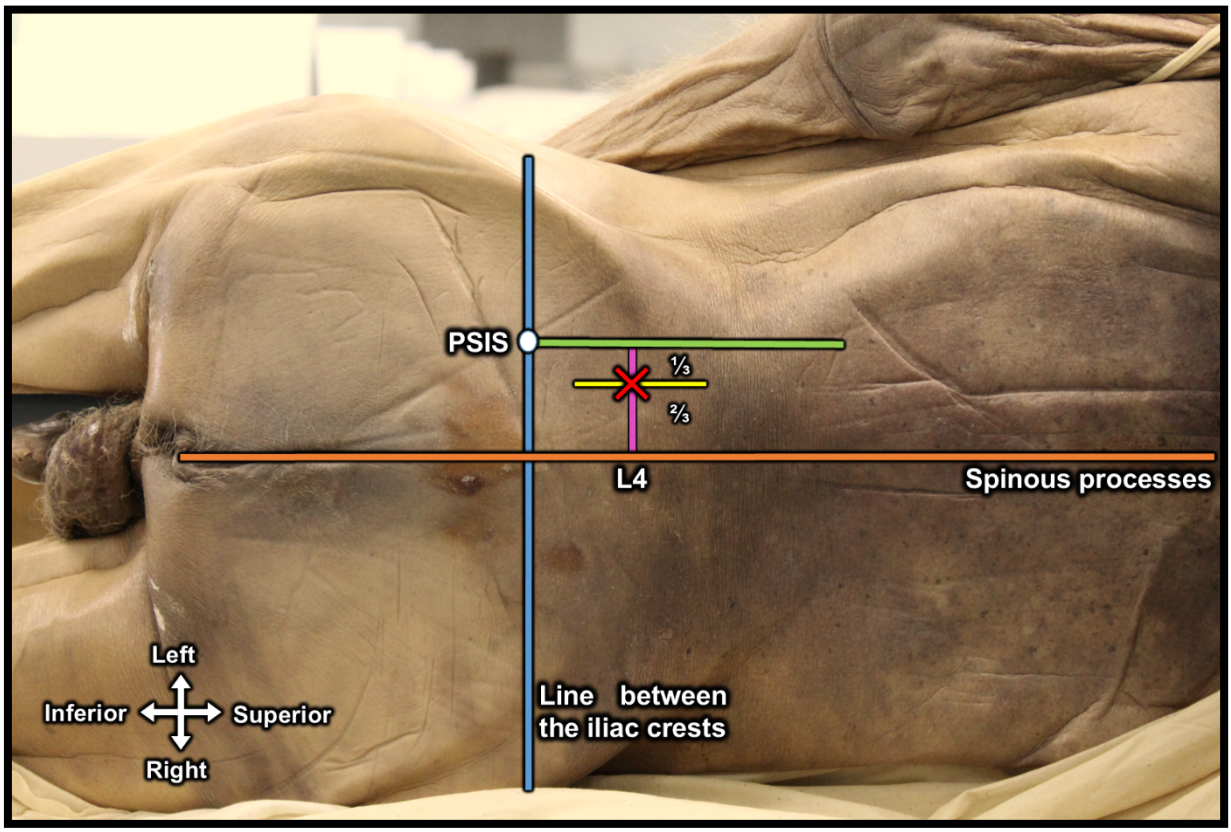

Figure 1: Posterior view of a cadaver placed in the Sim's position to simulate the psoas compartment block with annotated landmarks used to determine the needle insertion site (X).

Although there are reported successes for the procedure, the nerve block has been associated with complications such as nerve injury, intra-abdominal injury and pain caused by paravertebral muscle spasm, amongst others (Al-Nasser and Palacios, 2004; Jankovic, 2008; Kim et al., 2019). This is as a result of the needle coursing beyond the boundaries of the psoas major muscle.

Accurate knowledge of the anatomy and possible variations of the lumbar plexus, with its relation to the psoas compartment, will assist in improving the success rate of psoas compartment nerve blocks, to then decrease complication rates.

2.3. Aim

The aim of this chapter was to clearly and accurately describe the anatomy of the lumbar plexus – prior to the origin of the terminal branches – with specific application in the successful performance of a psoas compartment block.

2.4. Research objectives

1. Qualitatively describe the anatomy of the lumbar plexus by observing its origin from the lumbar nerve roots and their location in relation to the psoas major and quadratus lumborum muscles.
2. Quantitatively describe the location of the lumbar plexus by measuring distances between relevant anatomical landmarks as exhibited by computed tomography (CT) scans.
3. Correlate the results of this study to guidelines laid down for the performance of the psoas compartment block, in order to make suggestions and validations of current practices.

2.5. Materials and methods

Bilateral dissection of the posterior abdominal wall, pelvic cavity and upper thigh were performed on a sample of 105 formalin-fixed cadavers (59 males and 46 females; 70.8 ± 15.3 years [mean ± standard deviation]) from the Department of Anatomy, School of Medicine, Faculty of Health Sciences, University of Pretoria from 2017 to 2018. Factors such as height, weight or race were noted but were not a reason for exclusion from this study, although any cadavers with obvious pathology or previous surgery in the above-mentioned regions were omitted from the study.

Individual data for the lumbar plexus and each of its branches were collected in three phases. The first phase comprised of the qualitative description of the anatomy of the lumbar plexus with regard to its root values, variations and its location in relation to the psoas major and quadratus lumborum muscles. The second phase was a quantitative investigation of the lumbar plexus, using CT scans to determine the approximate location of the plexus using the skin, transverse process and the midline of the body as landmarks. The third phase was a meta-analysis of the psoas compartment block, for correlation of its guidelines to the results of this study, to assist in improving and/or further validating the procedure.

2.5.1. Root values and location within psoas major

To describe the anatomy of the lumbar plexus, bilateral dissections of the psoas major muscle were performed to expose the nerve roots. The nerves were exposed by removing the peritoneal and fascial layers that cover the anterior surface of them (Figure 2). Thereafter, the muscle fibres of the psoas major and minor (when present) muscles were carefully removed in layers, so not to disturb the underlying nerves, until all the roots of the plexus had been clearly exposed.

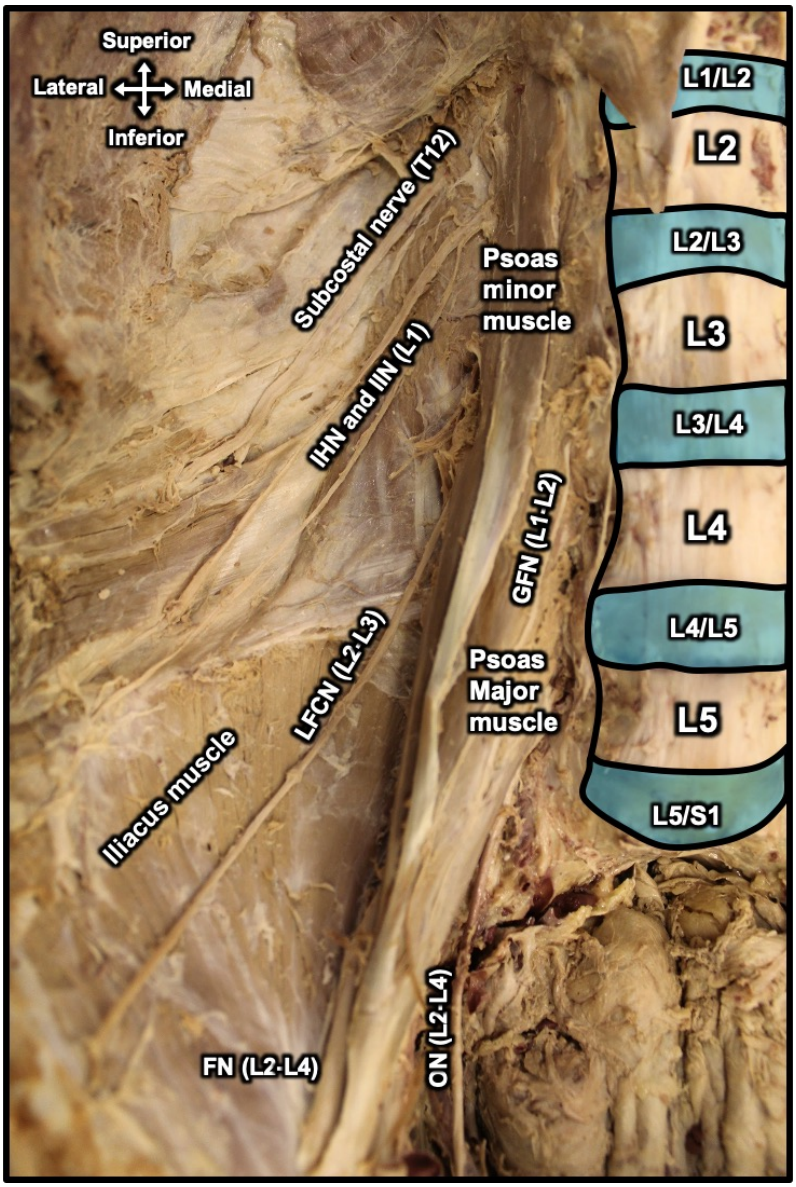

Figure 2: Anterior view of the branches of the lumbar plexus coursing on the posterior abdominal wall on the right side.

The investigation commenced with recording the position of the lumbar plexus in relation to the psoas major muscle. It was noted whether the plexus lay within the substance of the psoas major muscle or between the psoas major and quadratus lumborum muscles, posterior to the psoas major muscle. The data was captured in a 2013 Microsoft Office Excel spreadsheet.

2.5.2. Lumbar plexus depth using scans

In this phase, 69 axial computed tomography (CT) scans (23 male and 43 females; 52.7 ± 13.5 years) were used to determine nerve depth from the skin to the psoas compartment at the L4/L5 intervertebral disc level. This intervertebral level was chosen to avoid piercing the kidneys, where it is commonly situated and its inferior pole passes the vertebral level, should the needle be inserted beyond the lumbar plexus, into the abdominal cavity (Di Benedetto et al., 2005; Yoo et al., 2019). Each scan was viewed and measured using the Agfa Healthcare Impax EE CD Viewer R20. Bilateral measurements were taken in a straight line from the skin of the back to the transverse process of L4 (A). This was followed by a measurement from the skin of the back to the trunk of the lumbar plexus (B). The trunk of the lumbar plexus in this study is defined as the bundle of ventral rami of the spinal nerves before they divide into the various nerves. Two additional measurements taken from the midline of the body to the lateral border of the psoas major muscle (C) and to the trunk of the lumbar plexus (D). The midline of the body was determined by drawing a straight line through the spinous processes and body of the adjacent vertebrae (Figure 3).

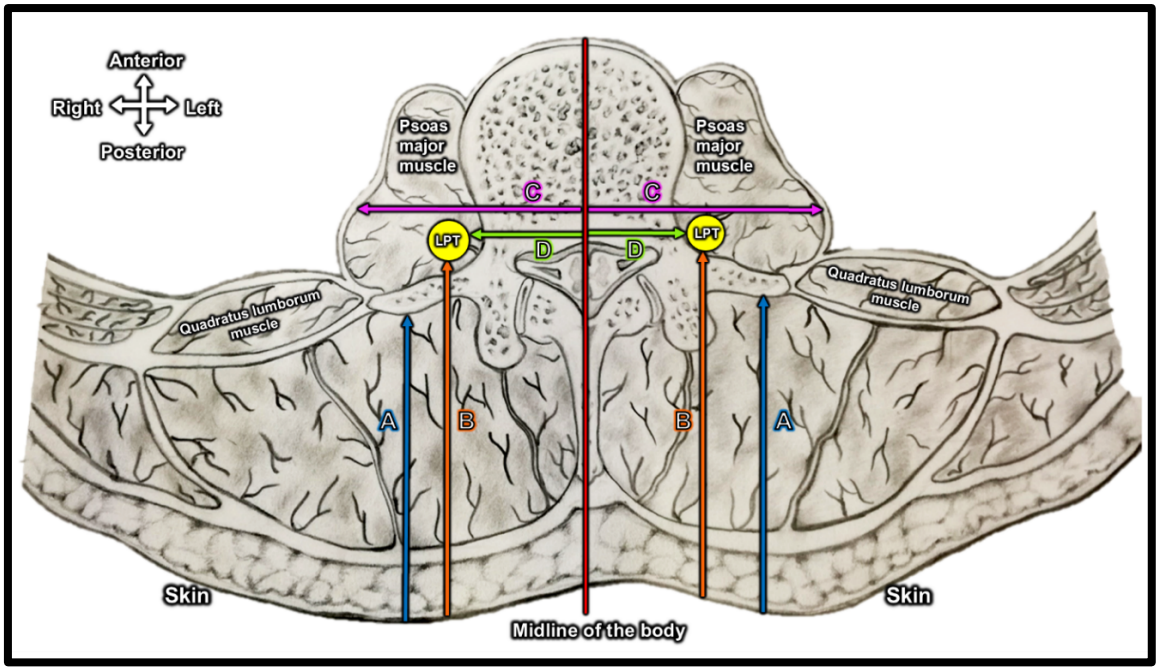

Figure 3: Illustration of a cross section through the posterior abdominal wall at the level of L4 as a representation of the measurements taken on the CT scans.

A – Skin of the back to the transverse process of L4

B – Skin of the back to the trunk of the lumbar plexus

C – Midline of the body to the lateral border of the psoas major muscle

D – midline of the body to the trunk of the lumbar plexus

LPT – Trunk of the lumbar plexus

All scans were retrospectively obtained from the databases of the Department of Radiology, Steve Biko Academic Hospital. The scans were taken using a Siemens Medical Somatom Sensation Cardiac 64 (64 slice) CT with a 5 mm slice thickness, with the patient placed in the supine position, at end tidal inspiration and with the arms abducted. Any scans of patients with an abnormal degree of kyphosis and/or scoliosis, as diagnosed by the consulting radiologist, those with a distorting space-occupying lesion (mass or fluid collection) and those with obvious visceromegaly (enlarged organ/s) were excluded from the study.

2.5.3. Clinical applications

The results of the first two phases were correlated with procedural guidelines for the posterior approach of the psoas compartment nerve block, in order to assist in altering or verifying the current technique. This was achieved by an extensive literature study

using the PubMed, Science Direct, Ovid and Google Scholar journal databases, as well as current anatomy-, surgical- and anaesthetic textbooks/guidelines.

2.5.4. Statistical analysis

All statistical tests were performed using IBM® SPSS® Statistics version 25. For the qualitative aspects of the study, a contingency table was drawn up to determine the frequency of the results of the nerve roots origins and locations. A Chi-squared test was then performed to determine whether sex had an influence on the observed root values and observations. For the measurements on computed tomography scans, a Shapiro-Wilk test was performed to determine the normality of the data. If the data was observed to be normally distributed, a Chi-squared test was performed to determine if sex had an influence on the measurements. A p-value above 0.05 would indicate no statistically significant difference observed. Thereafter, a paired t-test was performed to test whether there was a statistically significant difference ($p < 0.05$) between the left and right side measurements. After obtaining a p-value from the paired t-test, descriptive statistics (mean, standard deviation [SD] and a 95% confidence interval [CI]) were used on the obtained sample.

A Pearson's correlation test was performed to determine whether age had an influence on the measured parameters. A correlation was considered to be negative when the r-value is observed between 0 and -1 and positive when observed between 0 and 1. The strength of a correlation was determined according to a range between these values. A weak correlation was were an r-value was found between 0 and +/-0.30, a moderate correlation between +/-0.30 and +/-0.70 and a strong correlation between +/-0.70 and +/-1.

2.6. Results

2.6.1. Root values and location of the lumbar plexus in relation to the psoas major muscle

The root values of the lumbar plexus (L1-L4) were consistent in all samples and the left and right samples were pooled into an overall sample of 210 sides. However, variations were observed with regard to the root values of the branches of the lumbar plexus, these will be discussed in the respective chapters. The roots of the nerves were observed laying in order, from anterior to posterior, as the GFN, IIN and IHN,

LFCN, ON and then the FN. The roots were considered to be within the substance of the muscle if they had fibres of the psoas major muscle posterior to them (Figure 4). The LFCN, ON and FN complied with this criterion.

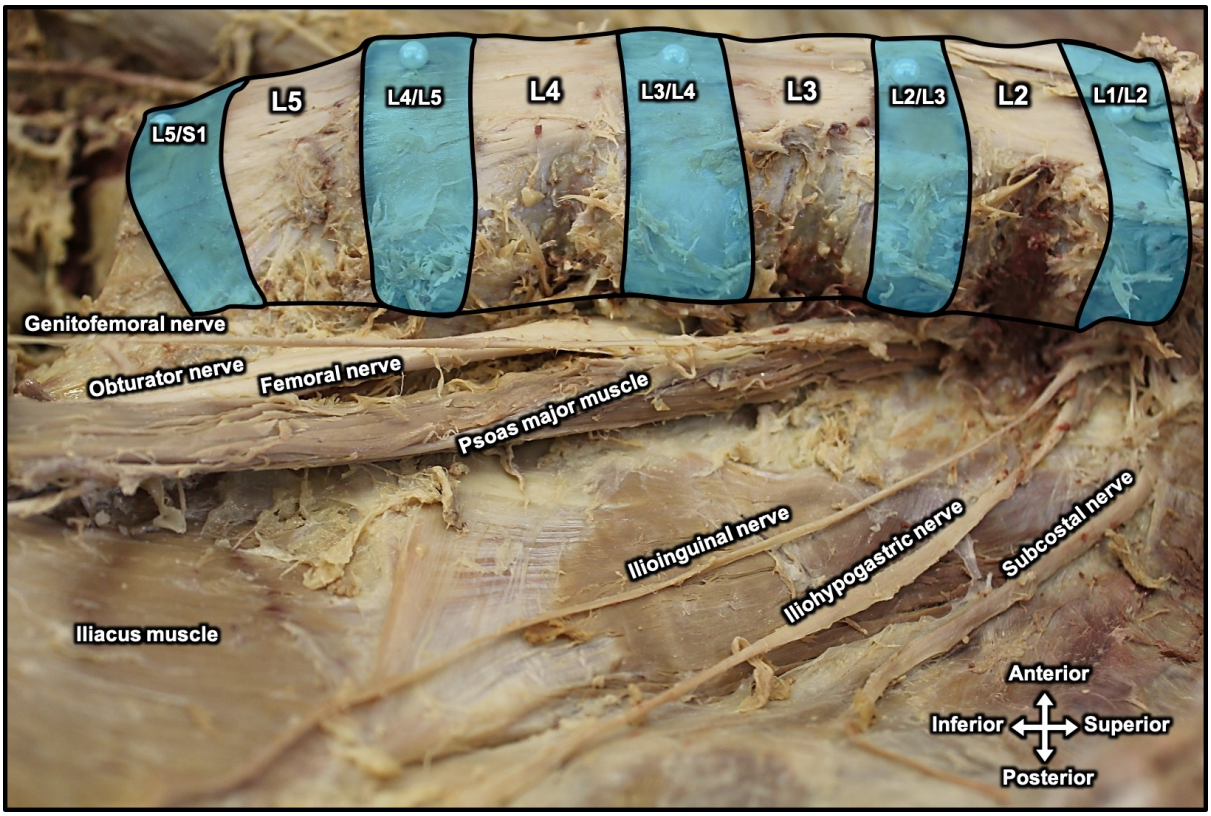

Figure 4: Lateral view of the lumbar plexus in relation to the psoas major muscle and the posterior abdominal wall on the left side.

Contingency tables were drawn up for the left and right sides to determine whether sex had an influence on the location of the roots of the lumbar plexus in relation to the psoas major muscle. On the left side (n = 105), the roots were observed within the psoas major muscle in 89 cases (84.8%), of which 48 (54%) were seen in the males and 41 (46%) in the females. The roots were found posterior to the psoas major muscle in 16 cases (15.2%); this was seen in 11 (68.75%) males and only 5 females (31.25%). These results are presented in figure 5. A Chi-squared test yielded a p-value of 0.27, which indicated that sex did not have a statistically significant influence on the location of the roots in relation to the psoas major muscle.

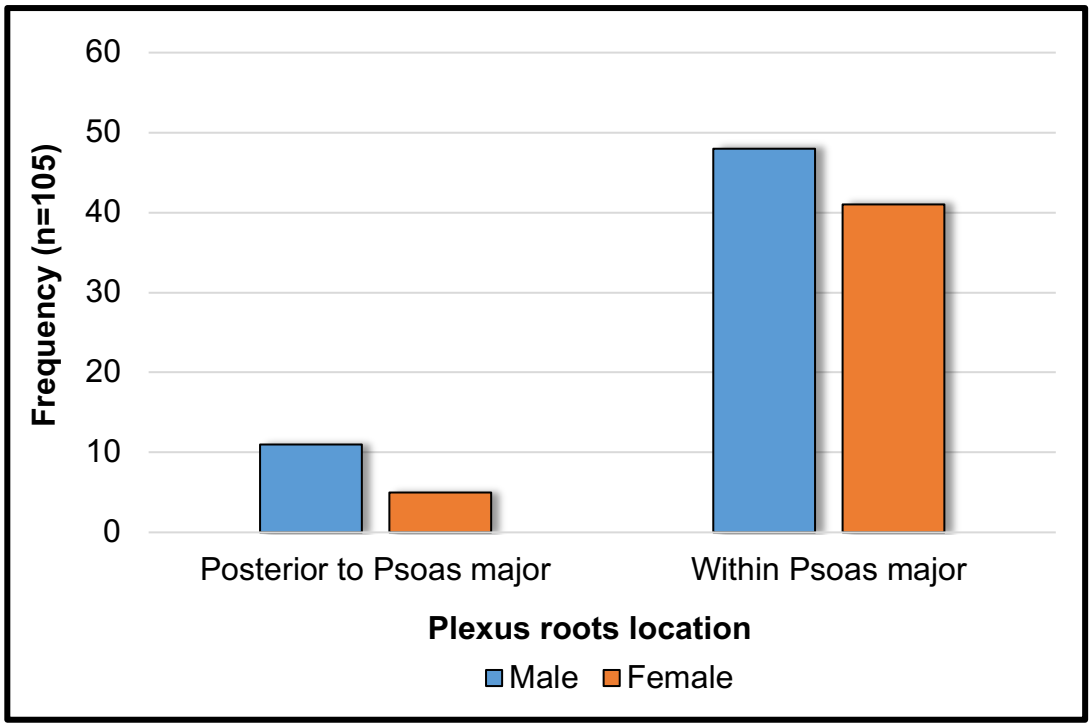

Figure 5: Bar graph indicating the frequency of the roots of the lumbar plexus at different locations in relation to the psoas major muscle on the left side of the abdomen.

On the right side (n = 105), the roots were observed within the psoas major muscle in 87 cases (82.9%), where 46 cases (52.87%) were male and 41 cases (47.13%) were female. The roots were posterior in 18 cases (17.1%) where 13 cases (72.22%) were male and 5 cases (27.78%) were female (Figure 6). A similar contingency table as for the left side revealed that sex did not have a statistically significant influence on the location of the roots in relation to the psoas major muscle on the right side. A Chi-squared test resulted in a p-value of 0.13.

Figure 6: Bar graph indicating the frequency of the location of the roots of the lumbar plexus on the right side in males and females.

These results allowed the locations of the different sides to be merged into one sample of 210. The overall sample was subdivided into 176 cases (83.8%) within the psoas major muscle and 34 cases (16.2%) posterior to it (Figure 7).

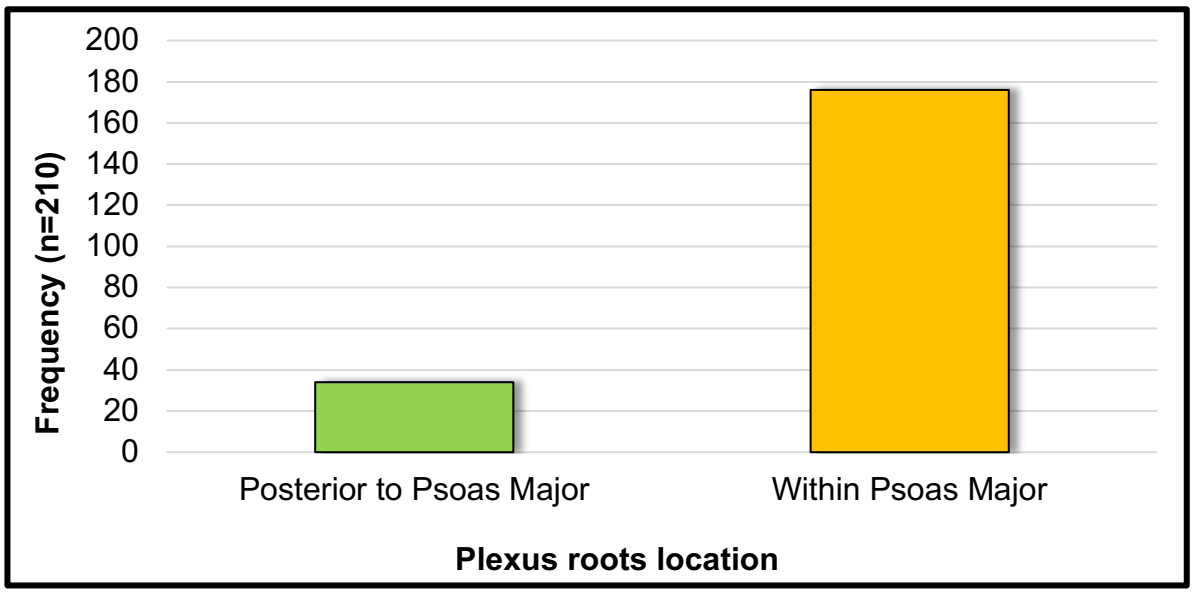

Figure 7: Bar graph indicating the frequency of the roots of the lumbar plexus at different locations in relation to the psoas major muscle.

2.6.2. Lumbar plexus depth using CT scans

This phase was performed on 69 CT scans to determine the depth at which the trunk of the lumbar plexus can be found. The trunk is seen as a white bundle of nerves that descend together in relation to the psoas major muscle. To determine the nerve depth, measurements were made from various anatomical landmarks. A Shapiro-Wilk test revealed a p-value above 0.05 for all the data sets, confirming that all data was normally distributed. Thereafter, contingency tables were drawn to test whether sex had an influence on any of the measurements taken. The Chi-squared test revealed p-values above 0.05 for all bilateral measurements, indicating that sex did not have an influence on any of the measurements. A paired t-test was performed to determine whether there was a significant difference between the measurements on the left and right sides of each person. For the measurement from the skin to the transverse process, the mean distance on the left (n=69) was 71.4 ± 18.7mm (mean ± SD) and 70.8 ± 19.0mm on the right (n = 69). A paired t-test revealed no statistically significant difference between the left and right sides (p = 0.20). This allowed the two side to be combined into one sample (N = 138). The mean distance for the new sample was 71.1mm, with a standard deviation of 18.9mm (CI - 66.8; 75.9).

To determine the depth of the lumbar plexus, measurements were taken from the skin to the lumbar plexus trunk bilaterally. The mean distance was 81.6 ± 19.3mm on the left side and 81.4 ± 18.8mm on the right side. A paired t-test was performed to compare the means of both sides. There was no statistically significant difference observed (p = 0.72) between the sides and the measurements were therefore pooled (N =138). The pooled mean distance was 81.5mm, with a standard deviation of 19.0mm (CI – 77.0; 86.3).

Similar bilateral measurements were taken from the midline of the body to the lumbar plexus, with a mean distance of 26.7 ± 3.7mm on the left side (CI - 25.8mm; 27.6mm) and 25.4 ± 3.5mm (CI - 24.6; 26.3) on the right side. A paired t-test revealed a statistically significant difference between the sides was present (p < 0.001). This was followed by determining the distance from the midline of the body to the lateral border of the psoas major muscle. The mean distance on the left side was 56.1 ± 6.9mm (CI – 54.4; 57.7) and 54.9 ± 7.5mm (CI – 53.1; 56.6) on the right side. A paired t-test was performed to compare the sides. A p-value of 0.04 was obtained, which indicated

that there was a statistically significant difference between the left and right sides. There were no observed correlations between the age of the subject and the measurements on the CT scans (Table 1).

Table 1: Representation of the results of a Pearson's correlation test between age and measurements taken on CT scans

Measurement	Side	r	p
Skin to transverse process	**Left**	-0.201	0.097
	Right	-0.211	0.082
Skin to lumbar plexus trunk	**Left**	-0.203	0.095
	Right	-0.196	0.107
Midline of the body to lateral border of psoas major muscle	**Left**	-0.050	0.682
	Right	0.011	0.931
Midline of the body to lumbar plexus trunk	**Left**	0.050	0.682
	Right	0.209	0.086

Inter- and intra-observer reliability test results may be found in Annexure A.

2.6.3. Clinical applications

An extensive literature study revealed that relevant clinical and surgical procedures were identified which could be used in conjunction with the results. The keywords in the database searches mentioned previously were: *lumbar plexus, lumbar plexus anatomy, lumbar plexus variation, lumbar plexus damage, lumbar plexus procedures, lumbar plexus surgery, lumbar plexus block approach* and *psoas compartment block*. As possible procedures were identified after results of the previous keywords, the following additional keywords were used to find the most relevant procedures: +*lumbar plexus block posterior approach* and *analgesia lumbar plexus*. The application of the results on the posterior approach of the psoas compartment nerve block procedure is detailed in the discussion.

2.7. Discussion

Knowledge of the anatomy, course and variation of the lumbar plexus and its branches is important for the successful performance of surgical and clinical procedures

performed on and/or around it. Despite there not being any deviation from the normal spinal nerve contributions of the lumbar plexus, the results in this chapter revealed variations in the origin and branching patterns of the terminal branches. The clear understanding of these aspects of the lumbar plexus and its branches will assist clinicians and surgeons in pre-, peri- and post-operative planning of these procedures, resulting in the decrease of the incidence of complications.

2.7.1. Root values and location

Exposing the root values of the lumbar plexus revealed that the plexus is found mostly within the substance of the psoas major muscle, with instances of some lying between the psoas major and quadratus lumborum muscles. Several studies have reported similar observation (Dietemann et al., 1987; Farny et al., 1994; Tubbs et al., 2005; Lu et al., 2011) (Table 2). On the contrary, a study by Anloague and Huijbregts (2009) reported that the plexus was observed predominantly posterior to the psoas major muscle. This is important to note when planning a procedure either on the plexus or in its vicinity, as the psoas major muscle might be a clear obstacle when attempting to access the lumbar plexus. Clear knowledge on the frequency of the location of the plexus in relation to the psoas major muscle will assist in targeting the nerves for nerve blocks and repairs.

Table 2: Comparison of results of the root values of the lumbar plexus

Study	Country	n	Plexus location
Farny et al. (1994)	France	4	Mostly within psoas major
Tubbs et al. (2005)	USA	22	Mostly within psoas major
Anloague and Huijbregts (2009)	USA	34	Mostly posterior to psoas major
Lu et al. (2011)	China	30	Mostly within psoas major
Current study	South Africa	210	Mostly within psoas major

The investigation of the root values of the lumbar plexus revealed that there were no variations with regard to the described contributions from L1-L4. It was also observed that sex does not have a statistically significant influence on the root values. This result

entails that procedural steps for the psoas compartment block may be used on both males and females with equal expected success.

The result found in this study is similar to results reported by other studies, where the root values were L1-L4 (Dietemann et al., 1987; Farny et al., 1994; Capdevila et al., 2005; Anloague and Huijbregts, 2009; Bendersky et al., 2015; Nontasaen et al., 2016; Abd-Elsayed, 2019). There are studies that have reported the addition of the ventral rami of the 12th thoracic (T12) and/or fifth lumbar (L5) spinal nerves to the root values of the lumbar plexus (Table 3). Several studies have described the addition of the T12 spinal root to the lumbar plexus. In these study, it is reported that the T12 spinal root contributes to the IHN and IIN, making their root values T12-L1 (Urbanowicz and Zaluska, 1969; Dalens et al., 1988; Tubbs et al., 2005). In a study by Lu et al. (2011), it was reported that the plexus had an additional L5 spinal nerve contribution. It is important to note that it was not mentioned as to which terminal branch of the lumbar plexus the L5 spinal nerve contributed towards. In addition, the term lumbar plexus might be considered as any ramus from the lumbar area.

Table 3: Comparison of results of the root values of the lumbar plexus

Study	Country	n	Nerve roots
Farny et al. (1994)	France	4	All normal root values (L1-L4)
Anloague and Huijbregts (2009)	USA	34	All normal root values (L1-L4)
Lu et al. (2011)	China	30	L5 contribution in entire sample
Nontasaen et al. (2016)	Thailand	131	8 contributions from T12
Current study (2019)	South Africa	210	All normal root values (L1-L4)

2.7.2. Lumbar plexus depth

It is of the utmost importance that surgeons and clinicians have accurate knowledge of the approximate location of nerves which they would like to avoid or to reach. Anaesthetists need to have clear knowledge of any variations of the nerve of interest to successfully accomplish anaesthesia for surgical procedures and/or analgesia to manage any discomfort experienced by patients post-operatively.

Investigation of the CT scans revealed a wide variation in the distance from the skin to the transverse process and lumbar plexus. This variation presented mean distances from the skin to the transverse process, and the skin to the lumbar plexus as 71.06mm and 81.49mm, respectively, with large standard deviations of 18.89mm and 18.98mm, respectively. These high standard deviations indicate the necessity to understand the location of the lumbar plexus on the posterior abdominal wall. A study by Farny et al. (1994), using CT scans, reported a subcutaneous fat thickness of 26.5 ± 16.7mm, further indicating a large standard deviation. A similar study by Yoo et al. (2019), using MRI, described the transverse process of L4 at a depth of 55 ± 10mm and the lumbar plexus depth at 67 ± 10mm. Not many studies have been conducted to determine the distance of the lumbar plexus from the skin. Table 4 compares results reported in the study by Farny et al. (1994) and Yoo et al. (2019) with those of the current study.

Table 4: Comparison of results of the root values of the lumbar plexus

Study	Country	n	Skin to transverse process	Skin to lumbar plexus
Farny et al. (1994)	France	44	70.2 ± 21.2mm	90.1 ± 24.3mm
Yoo et al. (2019)	Korea		55 ± 1mm	67 ± 1mm
Current study (2019)	South Africa	138	71.1 ± 18.9mm	81.5 ± 19.0mm

2.7.3. Clinical implications

The distance from the midline of the body to the lateral border of the psoas major muscle varies between the left and the right sides. The lateral border is further from the midline on the left side (56.1 ± 6.9mm) than it is on the right side (54.9 ± 7.5mm). This distance from the midline of the body to the lateral border of the psoas major muscle is smaller than that of a study by Farny et al. (1994), who reported a distance of 64.1 ± 16.1mm. The mean and standard deviation in the study by Farny et al. (1994) is larger than that of the current study. Regardless of the variation between the studies, the results of both studies validate the decision to insert a needle between 40 – 50mm from the midline of the body as stated by Chudinov et al. (1999) and Awad and Duggan (2005). This distance will allow the psoas major to be pierced by the needle, keeping in mind the variation in lumbar plexus depth.

The lumbar plexus was observed to be on average 26.7 ± 3.8mm on the left side and 25.6 ± 3.9mm on the right side from the midline of the body. Although these values fall within the limits of the distance of the needle insertion site from the midline of the body, the gap may lead to an unsuccessful block because the anaesthetic solution would have to travel further to get to the lumbar plexus and fail to spread evenly. This spread is key in the success of the block and the closer the needle insertion site and trajectory of the needle is to the target nerves, the higher the chance of a successful block.

The difference in the distance on the left and right sides of the plexus may be attributed to the width of the psoas major muscle. As the plexus will be more medially located within a narrow psoas major muscle, as opposed to a wide psoas major muscle. This can be observed in the results with the psoas major being narrower on the right side and the lumbar plexus similarly being more medial on the same side as well.

Inserting a needle at the suggested insertion site, angled medially, would allow clinicians to reach a closer distance to the lumbar plexus. Di Benedetto et al. (2005) reported an angle of 30º - 45º.

2.8. Conclusion

This study aimed to provide new information and expand present knowledge on the anatomy of the lumbar plexus and its relations to important bony- and soft tissue landmarks. No variations with regard to the root values of the lumbar plexus were observed, but there were differences with regard to the location of the plexus in relation to the psoas major- and quadratus lumborum muscles. The lumbar plexus was predominantly observed within the substance of the psoas major muscle, only being found posterior to it in 16% of cases. This is important for clinicians to note when administering anaesthetic solution with the aim of blocking the lumbar plexus, as the trajectory and depth of the needle must come close to the plexus without damaging it, especially where ultrasound machinery is unavailable. Anaesthesiologists will have to take the penetration of the anaesthetic solution between the fibres of psoas major into account when planning their block. This might also affect the concentration and volume of the solution that can safely be injected into the psoas compartment.

Clinicians must ensure that the solution is released in the correct area to block the branches of the lumbar plexus in a psoas compartment block. The needle must be inserted into the substance of the psoas major muscle, noting the mean distance from the midline of the body of 56.1mm on the left side and 54.9mm on the right side. As a result of variation in the thickness of subcutaneous tissue, the needle must be inserted approximately 81.5mm deep in order to reach the lumbar plexus, with a 95% confidence interval of 77.0mm and 86.3mm. The large standard deviation of 18.98mm must also be noted, keeping in mind that the thickness of the subcutaneous fat of a patient must be investigated prior to needle insertion. This will ensure that the correct equipment is used and the correct depth is reached to successfully block the lumbar plexus.

It must be noted that there was a significant difference in the distance of the lumbar plexus trunk from the midline of the body on the left- and right sides. This must be taken into consideration when planning a block on either side, taking into account the distance from the midline of the body to the needle insertion site, versus the distance from the midline of the body to the trunk of the lumbar plexus. The distance from the midline of the body to the needle insertion site was shorter on the right side than on the left side. Therefore, a needle insertion site that is further from the midline of the body may lead to an unsuccessful nerve block, as the anaesthetic solution may not have spread to the trunk as a result of the inability to travel the distance.

None of the results indicated a significant difference in the influence of sex on the observations and measurements of this study. Therefore, these results should be considered in nerve blocks in both males and females.

The main limitation of the cadaver study was the inability to make measurements from the skin to the lumbar plexus in order to compare them with the CT study, as a result of the embalming process. The limitations of the CT study was the lack of information of the height and weight of the patients. The correlation of the results to the body mass index (BMI) of the patients was thus not possible, especially with regard to subcutaneous fat.

As this was a retrospective study, the limitations of the CT scans include exact position of the patient for the scan, resulting in scans being excluded, as well as other demographic information. It is suggested that a prospective CT study with a larger sample size be done on the lumbar plexus, with a larger sample size. The study should focus on the influence of BMI, subcutaneous fat thickness and visible scoliosis on the depth and location of the lumbar plexus.

2.9. References

ABD-ELSAYED, A. 2019. Lumbar Plexus. *Pain.* Springer.

AL-DABBAGH, A. 2002. Anatomical variations of the inguinal nerves and risks of injury in 110 hernia repairs. *Surgical and radiologic anatomy,* 24**,** 102-107.

AL-NASSER, B. & PALACIOS, J. L. 2004. Femoral nerve injury complicating continuous psoas compartment block. *Regional anesthesia and pain medicine,* 29**,** 361-363.

AMIN, N., KRASHIN, D. & TRESCOT, A. M. 2016. Ilioinguinal and Iliohypogastric Nerve Entrapment: Abdominal. *Peripheral Nerve Entrapments.* Springer.

ANAGNOSTOPOULOU, S., KOSTOPANAGIOTOU, G., PARASKEUOPOULOS, T., CHANTZI, C., LOLIS, E. & SARANTEAS, T. 2009. Anatomic variations of the obturator nerve in the inguinal region: implications in conventional and ultrasound regional anesthesia techniques. *Regional anesthesia and pain medicine,* 34**,** 33-39.

ANLOAGUE, P. A. & HUIJBREGTS, P. 2009. Anatomical variations of the lumbar plexus: a descriptive anatomy study with proposed clinical implications. *Journal of Manual & Manipulative Therapy,* 17**,** 107E-114E.

ARNOLD, P. M., ANDERSON, K. K. & MCGUIRE JR, R. A. 2012. The lateral transpsoas approach to the lumbar and thoracic spine: a review. *Surgical neurology international,* 3**,** S198.

ARORA, D., KAUSHAL, S. & SINGH, G. 2014. VARIATIONS OF LUMBAR PLEXUS IN 30 ADULT HUMAN CADAVERS-A UNILATERAL PREFIXED PLEXUS. *IJPAES,* 4**,** 225-8.

AWAD, I. T. & DUGGAN, E. M. 2005. Posterior lumbar plexus block: anatomy, approaches, and techniques. *Reg Anesth Pain Med,* 30**,** 143-149.

BARAZANCHI, A. W. H., FAGAN, P. V. B., SMITH, B. B. & HILL, A. G. 2016. Routine neurectomy of inguinal nerves during open onlay mesh hernia repair: a meta-analysis of randomized trials. *Annals of surgery,* 264**,** 64-72.

BECKER, P., BOSCH, J. & SMITH, F. 2007. Analgesia after total hip replacement: epidural versus psoas compartment block. *Southern African Journal of Anaesthesia and Analgesia,* 13**,** 21-25.

BENDERSKY, M., SOLÁ, C., MUNTADAS, J., GRUENBERG, M., CALLIGARIS, S., MERELES, M., VALACCO, M., BASSANI, J. & NICOLÁS, M. 2015. Monitoring

lumbar plexus integrity in extreme lateral transpsoas approaches to the lumbar spine: a new protocol with anatomical bases. *European Spine Journal,* 24**,** 1051-1057.

BUCKENMAIER III, C. C., XENOS, J. S. & NILSEN, S. M. 2002. Lumbar plexus block with perineural catheter and sciatic nerve block for total hip arthroplasty. *The Journal of arthroplasty,* 17**,** 499-502.

CAPDEVILA, X., COIMBRA, C. & CHOQUET, O. 2005. Approaches to the lumbar plexus: success, risks, and outcome. *Regional anesthesia and pain medicine,* 30**,** 150.

CAPDEVILA, X., MACAIRE, P., DADURE, C., CHOQUET, O., BIBOULET, P., RYCKWAERT, Y. & D'ATHIS, F. 2002. Continuous psoas compartment block for post-operative analgesia after total hip arthroplasty: new landmarks, technical guidelines, and clinical evaluation. *Anesthesia & Analgesia,* 94**,** 1606-1613.

CELEBI, S., AKSOY, D., CEVIK, B., YILDIZ, A., KURT, S. & DOKUCU, A. I. 2013. An electrophysiologic evaluation of whether open and laparoscopic techniques used in pediatric inguinal hernia repairs affect the genitofemoral nerve. *Journal of pediatric surgery,* 48**,** 2160-2163.

CHUDINOV, A., BERKENSTADT, H., SALAI, M., CAHANA, A. & PEREL, A. 1999. Continuous psoas compartment block for anesthesia and peri-operative analgesia in patients with hip fractures. *Regional anesthesia and pain medicine,* 24**,** 563-568.

DALENS, B., TANGUY, A. & VANNEUVILLE, G. 1988. Lumbar plexus block in children: a comparison of two procedures in 50 patients. *Anesthesia and analgesia,* 67**,** 750-758.

DI BENEDETTO, P., PINTO, G., ARCIONI, R., DE BLASI, R., SORRENTINO, L., ROSSIFRAGOLA, I., BACIARELLO, M. & CAPOTONDI, C. 2005. Anatomy and imaging of lumbar plexus. *Minerva anestesiologica,* 71**,** 549.

DIETEMANN, J., SICK, H., WOLFRAM-GABEL, R., DA SILVA, R. C., KORITKE, J.-G. & WACKENHEIM, A. 1987. Anatomy and computed tomography of the normal lumbosacral plexus. *Neuroradiology,* 29**,** 58-68.

ELLIS, H. 2010. The lumbar and sacral plexuses. *Anaesthesia & Intensive Care Medicine,* 11**,** 93-94.

FARNY, J., DROLET, P. & GIRARD, M. 1994. Anatomy of the posterior approach to the lumbar plexus block. *Canadian journal of anaesthesia,* 41**,** 480-485.

GOSSMAN, W. & BHIMJI, S. 2017. Anatomy, Abdomen, Nerves, Genitofemoral.

GRUNERT, P., DRAZIN, D., IWANAGA, J., SCHMIDT, C., ALONSO, F., MOISI, M., CHAPMAN, J. R., OSKOUIAN, R. J. & TUBBS, R. S. 2017. Injury to the lumbar plexus and its branches after lateral fusion procedures: a cadaver study. *World neurosurgery,* 105**,** 519-525.

JANKOVIC, D. 2008. *Regional Nerve Blocks and Infiltration Therapy: Textbook and Color Atlas*, John Wiley & Sons.

JOGDAND, P. & SULE, P. M. 2018. Comparative study of psoas compartment block and sciatic nerve block with that of spinal block anesthesia for lower extremity surgeries. *Indian Journal of Clinical Anaesthesia,* 5**,** 141-146.

KALE, A., AYTULUK, H. G., CAM, I., BASOL, G. & SUNNETCI, B. 2019. Selective Spinal Nerve Block in Ilioinguinal, Iliohypogastric and Genitofemoral Neuralgia. *Turk Neurosurg,* 29**,** 530-537.

KIM, B.-G., YANG, C., SOH, S. & LEE, K. 2019. Inadvertent epidural anesthesia associated with catheterization following continuous psoas compartment block in a patient with scoliosis: A Case report. *Medicine,* 98.

KOTIAN, S. R., SOUZA, A. S. D., RAY, B. & SUMALATHA, S. 2015. Anatomical variations of the lumbar plexus in fetus. *Gaziantep Medical Journal,* 21**,** 17-20.

KUMAR, A. & ZAIDI, M. 2017. Ilioinguinal, Iliohypogastric, and Genitofemoral Nerve Pain Syndromes. *Musculoskeletal Sports and Spine Disorders.* Springer.

LU, S., CHANG, S., ZHANG, Y.-Z., DING, Z.-H., XU, X. M. & XU, Y.-Q. 2011. Clinical anatomy and 3D virtual reconstruction of the lumbar plexus with respect to lumbar surgery. *BMC musculoskeletal disorders,* 12**,** 76.

MANNION, S. 2007. Psoas compartment block. *Continuing Education in Anaesthesia, Critical Care & Pain,* 7**,** 162-166.

MOORE, A. E. & STRINGER, M. D. 2011. Iatrogenic femoral nerve injury: a systematic review. *Surgical and radiologic anatomy,* 33**,** 649-658.

NONTASAEN, P., DAS, S., NISUNG, C., SINTHUBUA, A. & MAHAKKANUKRAUH, P. 2016. A cadaveric study of the anatomical variations of the lumbar plexus with clinical implications. *Journal of the Anatomical Society of India,* 65**,** 24-28.

PUMBERGER, M., HUGHES, A. P., HUANG, R. R., SAMA, A. A., CAMMISA, F. P. & GIRARDI, F. P. 2012. Neurologic deficit following lateral lumbar interbody fusion. *European spine journal,* 21**,** 1192-1199.

RAB, M. & DELLON, A. 2001. Anatomic variability of the ilioinguinal and genitofemoral nerve: implications for the treatment of groin pain. *Plastic and reconstructive surgery,* 108**,** 1618-1623.

SHANNON, J., LANG, S., YIP, R. & GERARD, M. 1994. Lateral femoral cutaneous nerve block revisited. A nerve stimulator technique. *Regional anesthesia,* 20**,** 100-104.

SHARROCK, N. E. & SAVARESE, J. 2000. Anesthesia for orthopedic surgery. *Anesthesia. 5th ed. Philadelphia: Churchill Livingstone***,** 2118-2139.

SIM, I. & WEBB, T. 2004. Anatomy and anaesthesia of the lumbar somatic plexus. *Anaesthesia and intensive care,* 32**,** 178.

SINGH, R., BAJAJ, J. K. & SINGH, D. 2018. Comparison of psoas compartment block and epidural block for post-operative analgesia in hip surgeries. *Astrocyte,* 4**,** 221.

TAGLIAFICO, A., BIGNOTTI, B., CADONI, A., PEREZ, M. M. & MARTINOLI, C. 2015. Anatomical study of the iliohypogastric, ilioinguinal, and genitofemoral nerves using high-resolution ultrasound. *Muscle & nerve,* 51**,** 42-48.

TUBBS, R. S., SALTER, E. G., WELLONS III, J. C., BLOUNT, J. P. & OAKES, W. J. 2005. Anatomical landmarks for the lumbar plexus on the posterior abdominal wall. *Journal of Neurosurgery: Spine,* 2**,** 335-338.

URBANOWICZ, Z. & ZALUSKA, S. 1969. Formation of the lumbar plexus in man and macaca. *Folia Morphol (Warsz),* 28**,** 256-271.

UZMANSEL, D., AKTEKIN, M. & KARA, A. 2006. Multiple variations of the nerves arising from the lumbar plexus. *Neuroanatomy,* 5**,** 37-9.

WINNIE, A., RAMAMURTHY, S., DURRANI, Z. & RADONJIC, R. 1974. Plexus blocks for lower extremity surgery. *Anesthesiol Rev,* 1**,** 11-16.

YOO, S., CHOI, S.-N., PARK, S.-K., KIM, W. H., LIM, Y.-J. & KIM, J.-T. 2019. Safety margin for needle placement during lumbar plexus block: An anatomical study using magnetic resonance imaging. *Canadian Journal of Anesthesia/Journal canadien d'anesthésie,* 66**,** 302-308.

Chapter 3 – Iliohypogastric- (IHN) and Ilioinguinal nerves (IIN)

3.1. Introduction and problem statement

Inguinal hernias are a common occurrence in both infants and adults. It has been reported that the incidence rate of inguinal hernia repair in the United States is 800 000 annually (Samakar et al., 2019). A study by McDonnell and Wakefield (2018) estimated that approximately 20 million inguinal hernia repairs are performed worldwide annually. Direct hernias in adults are commonly observed in males, as a result of weakening of the anterior abdominal wall (Gatabi et al., 2018; McDonnell and Wakefield, 2018). A study by de Goede et al. (2015) reported that the incidence of inguinal hernias is highest in middle-aged and elderly males.

Several surgical procedures to repair these hernias have been introduced over the years, with varying success rates. A review of the literature indicated that surgeons are beginning to move towards the use of the Lichtenstein tension-free method (Lichtenstein et al., 1989; Amid, 2004b). The main focus, in decreasing the rate of complication incidence, is an absolute understanding of the anatomy of the structures in, and in relation to the inguinal canal, for placement of a mesh, specifically with regard to the IHN and IIN, as studies have reported the occurrence of nerve entrapment by the inserted mesh (Zwaans et al., 2017; Neogi et al., 2018). The entrapment of these nerves may be due to lack of knowledge of the anatomy and variations of the nerves in the inguinal area.

3.2. Literature review

3.2.1. Iliohypogastric and ilioinguinal nerves

The IHN and IIN are terminal branches of the ventral ramus of the L1 spinal nerve. Both of these nerves provide motor and sensory innervation to the abdominal muscles and the skin over the groin. Both these nerves traverse the anterior surface of the quadratus lumborum muscle obliquely and laterally, coursing towards the transversus abdominis muscle. Once they reach the muscle, they pierce it to course anteriorly between it and the internal oblique muscle (Barazanchi et al., 2016; Kale et al., 2019).

The IHN bifurcates into a lateral cutaneous- and anterior cutaneous branch. The lateral cutaneous branch perforates and further courses through the internal and external oblique muscles to supply the posterolateral surface of the skin over the gluteal region.

In addition, this nerve gives motor innervation to the internal oblique and transversus abdominis muscles. The anterior cutaneous branch similarly pierces the internal oblique muscle, to run between it and the external oblique muscle. In this plane, it runs to the level of the ASIS, where it pierces the external oblique muscle to give sensory innervation to the skin over the pubic-, groin- and inferior abdominal regions. In its course, it supplies the internal oblique and transversus abdominis muscles (Anloague and Huijbregts, 2009; Barazanchi et al., 2016; Kale et al., 2019).

At the level of the ASIS, the IIN will pierce the internal oblique muscle to enter the inguinal canal, accompanied by the spermatic cord in males and the round ligament of the uterus in females. It will exit the canal through the superficial inguinal ring and gives sensory innervation to the medial thigh, base of the penis and superior surface of the scrotum in males and the mons pubis and labia majora in females. This sensory innervation is shared with that of the GFN. The IIN will, additionally, give motor innervation to the internal oblique- and transversus abdominis muscles (Anloague and Huijbregts, 2009; Barazanchi et al., 2016; Kale et al., 2019). Some studies report a variation where both the IIN and GFN receive contributions from the twelfth spinal nerve (T12) (Klaassen et al., 2011; Tagliafico et al., 2015; Kale et al., 2019).

The IHN could be injured during inguinal hernia repairs (Rab and Dellon, 2001; Fateh et al., 2018). A study by Al-dabbagh (2002) found that there is variation with regard to the course of the IHN. The author reports that this variation could pose a risk during routine hernia repairs. In a similar study by Anloague and Huijbregts (2009), a complete absence of the nerve was observed in 20.6% of their sample.

The study by Al-dabbagh (2002) also reported that the IIN is similarly variable in its course as the IHN, reporting the IIN as being more susceptible to injury during open inguinal hernia repair. Contrarily, the study by Anloague and Huijbregts (2009) indicated that there was no variation in the course of the IIN. The difference in opinion could alter the technique used by different surgeons, possibly leading to nerve damage, should the anatomy of these nerves not be considered. The use of a mesh during inguinal hernia repair could in turn cause entrapment of both the IHN and IIN, causing patients prolonged – and unnecessary – post-operative pain (Rab and Dellon, 2001; Fateh et al., 2018)

For inguinal hernia repairs, the Bassini technique had been widely used, but with high incidence of complications and hernia recurrence (Zsolt and Csiky, 2001). This procedure involved the suturing of tissue at different fascial planes. A now commonly used technique by Lichtenstein et al. (1989) uses a mesh (Lichtenstein et al., 1989; Gatabi et al., 2018).

The Lichtenstein tension-free technique has now become the commonly used method for open inguinal hernia repair as a result of its low complication rate (Schumpelick and Klinge, 2003; Neogi et al., 2018; Tan and Blatnik, 2018; Vasu and Sagar, 2018). The procedure was first described by Lichtenstein et al. (1989) as an alternative to the techniques at that time that had high recurrence rate after repair. Since then, the method has been modified several times to what is best described in an article by Amid (2004b). That study states the guidelines for the Lichtenstein tension-free hernioplasty procedure, in males, as a 50mm skin incision from the pubic tubercle superolaterally towards the ASIS. This is followed by opening the inguinal canal by cutting through the external oblique muscle from the floor of the inguinal canal and freeing it from the spermatic cord. The external oblique muscle is then reflected superiorly for approximately 30-40mm from the inguinal ligament, which forms the floor of the canal, also freeing it from the internal oblique muscle. This will allow visualization of the IHN as it traverses the internal oblique muscle and the IIN as it courses on the spermatic cord. The importance of the visualization of these nerves was also reported by Ferzli et al. (2008), who reported that the IHN is most at risk of compression by placement of a mesh in the inguinal region.

3.3. Aim

The aim of this chapter was to clearly and accurately describe the anatomy of the IHN and IIN for application in the successful performance of the Lichtenstein tension-free inguinal hernia repair.

3.4. Research objectives

1. Qualitatively describe the anatomy of the IHN and IIN by observing their nerve root contributions, as well as bifurcation patterns from the ventral ramus of the L1 spinal nerve, either in the anterior abdominal wall, or closer to the vertebral column.
2. Quantitatively describe the location of the IHN and IIN in relation to the ASIS within the anterior abdominal wall.
3. Correlate the results of this study to guidelines for the performance of the Lichtenstein tension-free inguinal hernia repair, in order to make suggestions and validations of the current technique, based on the anatomical findings reported in this chapter.

3.5. Materials and methods

Bilateral dissections to expose the nerve roots of the IHN and IIN were performed according to the guidelines outlined in the materials and methods of chapter two, on the lumbar plexus.

3.5.1. Nerve roots and bifurcation pattern

After the nerve roots had been exposed from the lumbar plexus dissection, the nerves that form from plexus were investigated. The IHN and IIN were identified and their nerve root contributions recorded, together with any variations that were observed. Furthermore, the relation of the IHN and IIN to the psoas major muscle and where each exits the muscle was noted

The IHN and IIN were followed as they ran anterior to the posterior abdominal wall, before piercing the transversus abdominis muscle. What was also noted was whether the IHN and IIN bifurcated from the ventral ramus of the L1 spinal nerve at the vertebral column, or whether the bifurcation occurred after piercing the transversus abdominis muscle (Figure 8).

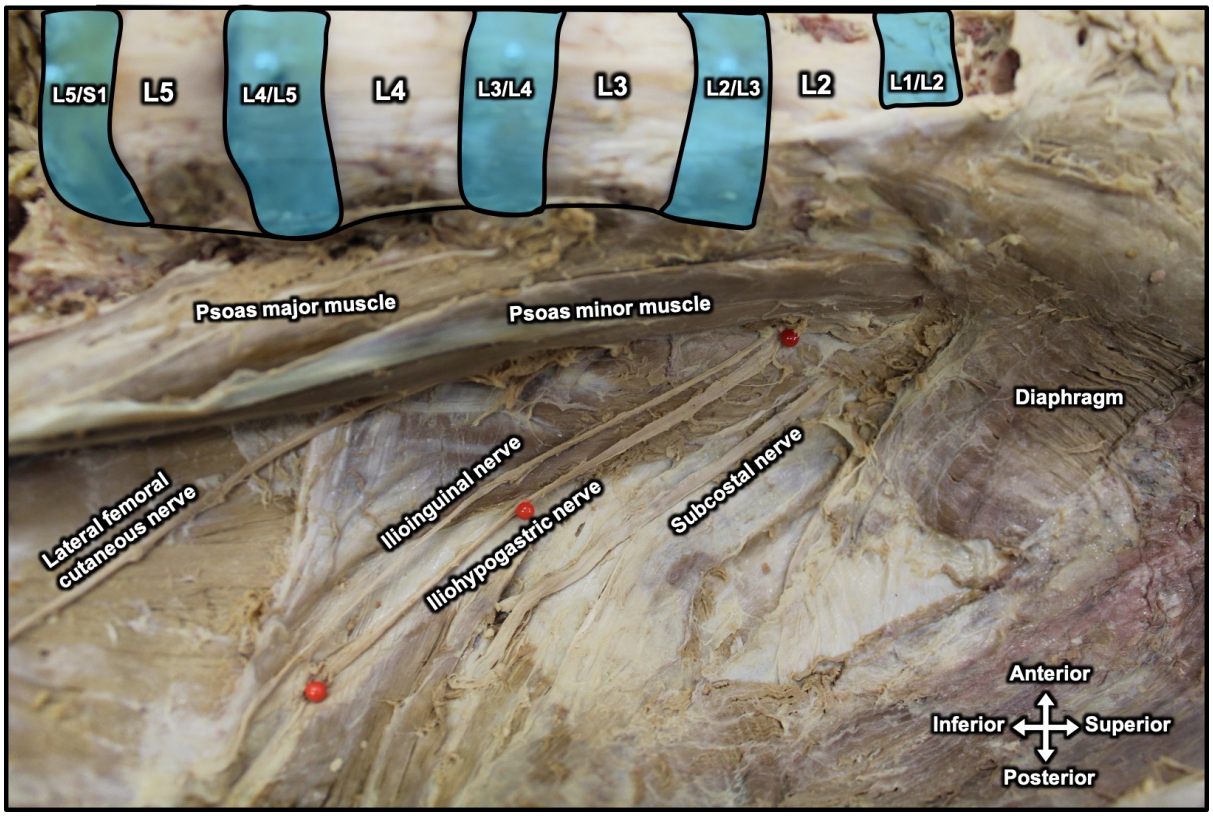

Figure 8: Anterior view of the posterior abdominal wall, indicating how the IHN and IIN originate from the anterior ramus of the L1 spinal nerve deep to the psoas major muscle on the left side

To expose the IHN and IIN along the anterior abdominal wall, at the level of the ASIS, the external oblique muscle was reflected laterally. To achieve this, three incisions were made in the external oblique muscle. A vertical incision was made along the linea semilunaris, a connective tissue junction at the lateral border of the rectus abdominis muscle, from the level of the umbilicus until the superficial inguinal ring. Thereafter, a horizontal incision is made at the level of the umbilicus, from the vertical incision laterally towards the midaxillary line. To allow the external oblique muscle to be reflected laterally from the anterior abdominal wall to be, an oblique incision was made from the superior border of the superficial inguinal ring to the ASIS, taking care not to damage nor disturb any underlying structures.

This opened up the inguinal canal with the IIN within it, as well as the IHN, as it courses over the internal oblique muscle towards the groin. Where there were visible contents in the inguinal canal, these were carefully removed so not to disturb the position of the IIN. The IHN and IIN were identified and pinned where each pierced the internal

oblique muscle. The ASIS was also pinned at the centre of its most anterior point (Figure 9). The course of the nerves was observed and followed to their termination.

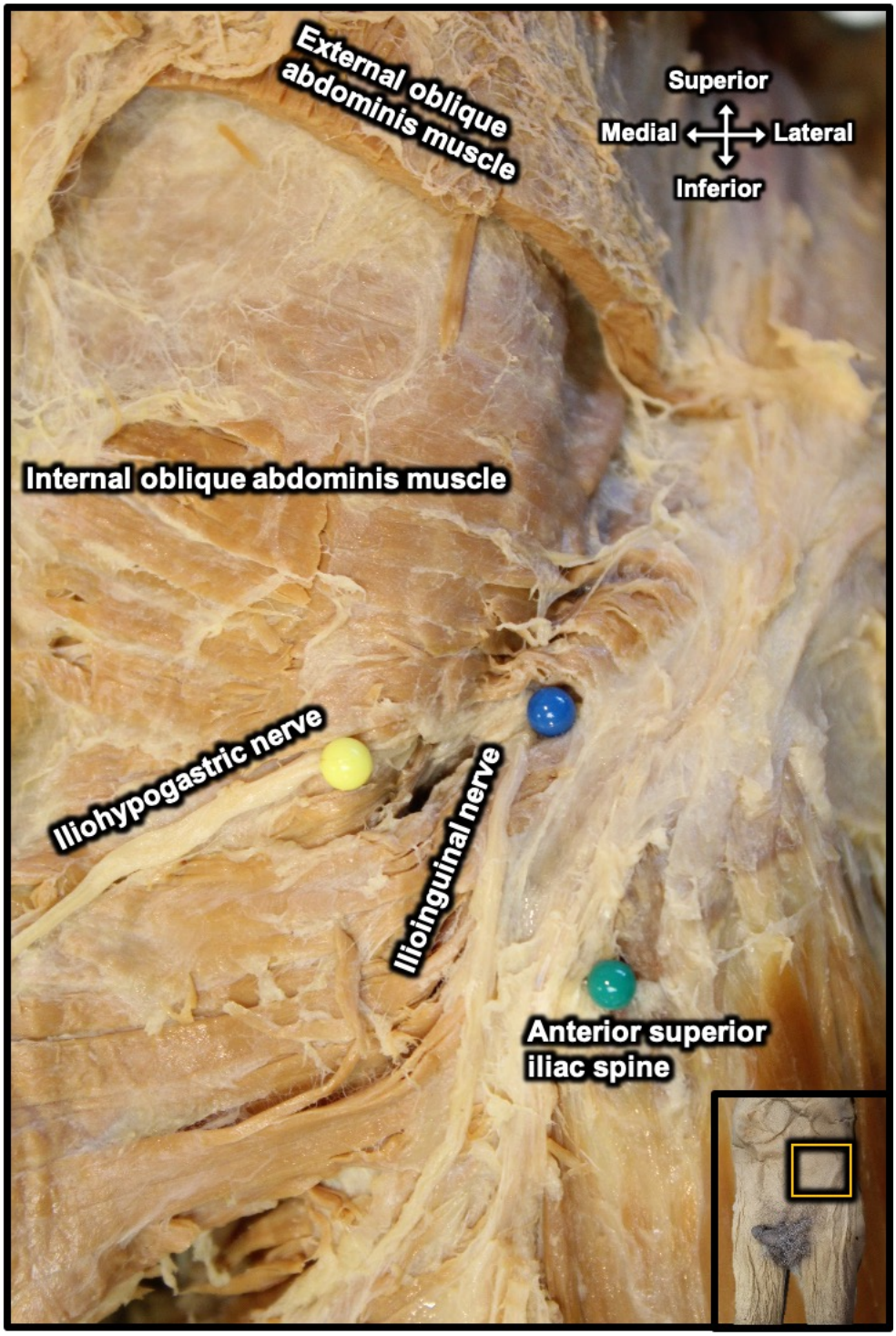

Figure 9: Anterior view of the left lower anterior abdominal wall with the external oblique muscle reflected laterally, indicating the ASIS, IHN and IIN in relation to each other.

3.5.2. Location of the IHN and IIN in relation to ASIS

To determine the location of the IHN and IIN in the anterior abdominal wall, measurements were taken, in a straight line, from the ASIS to where each nerve pierced the internal oblique muscle to run between it and the external oblique muscle. All measurements were taken using a mechanical dial sliding calliper (accuracy = 0.01mm). The measurements were recorded and captured in a 2013 Microsoft Office Excel spreadsheet.

3.5.3. Clinical applications

The results of the investigation of the root values of the IHN and the IIN, their course and their relations to the ASIS were correlated with clinical and surgical technique guidelines for the performance of Lichtenstein inguinal hernia repair, in order to assist in refining or verifying the current techniques. This was achieved through an extensive literature study using the PubMed, Science Direct, Ovid and Google Scholar journal databases, as well as current anatomy-, surgical- and anaesthetic textbooks and guidelines.

3.5.4. Statistical analysis

All statistical tests were performed using the IBM® SPSS® Statistics version 25 program. For the results on the nerve roots and their bifurcation patterns of the IHN and IIN, contingency tables were drawn up to determine the frequency of the observations. Furthermore, a Chi-squared test was executed on the left- and right sides to determine whether sex had an influence on the observations.

On the parts of the study involving measurements, a Shapiro-Wilk test for normality was performed to test for normality of the distribution of the data. Where the data was observed to not have normal distribution, a Related Samples Wilcoxon Sign Rank test was performed to compare the left- and right sides. A Chi-squared test was performed to determine whether sex had an influence on the observed results. Thereafter, descriptive statistics were executed to describe the mean, SD and 95% CI of the samples. Furthermore, a correlation test was executed to determine whether a linear relationship exists between the distances of the IHN and IIN to the ASIS with age, height, weight and BMI.

3.6. Results

3.6.1. Nerve roots and bifurcation pattern

Standard anatomical texts describe the roots of the IHN and IIN to originate from the ventral ramus of the L1 spinal nerve. This pattern was observed on both the left and on the right sides for the entire sample (n = 105) without any noted variation. As a result, no further tests were performed for the nerve roots. Regarding bifurcation of the ventral ramus of the L1 spinal nerve, a difference was observed on both sides. Firstly, a contingency table was constructed to describe the branching pattern of the spinal nerve. On the left side, the L1 spinal nerve bifurcated after piercing the transversus abdominis muscle in 79 cases (75.2%; 41 male and 38 female) and proximal to where they enter the transversus abdominis muscle in 26 cases (24.8%; 18 male and 8 female). On the right side, it bifurcated within the transversus abdominis muscle in 90 cases (85.7%; 49 male and 41 female) and in 15 cases (14.3%; 10 male and 5 female) at the vertebral column (Figure 3). A Chi-square test determined that there is no apparent influence of sex on the bifurcation pattern on both the left- ($p = 0.12$) and the right sides ($p = 0.38$). This allowed the overall sample to be combined into an overall sample size of 210. In the new sample, the bifurcation at the muscle was in 169 cases (80.6%) and 41 cases were at the vertebral column (9.4%). Where the L1 spinal nerve bifurcated proximal to where they enter the transversus abdominis muscle, the IHN was superior to the IIN (Figure 10).

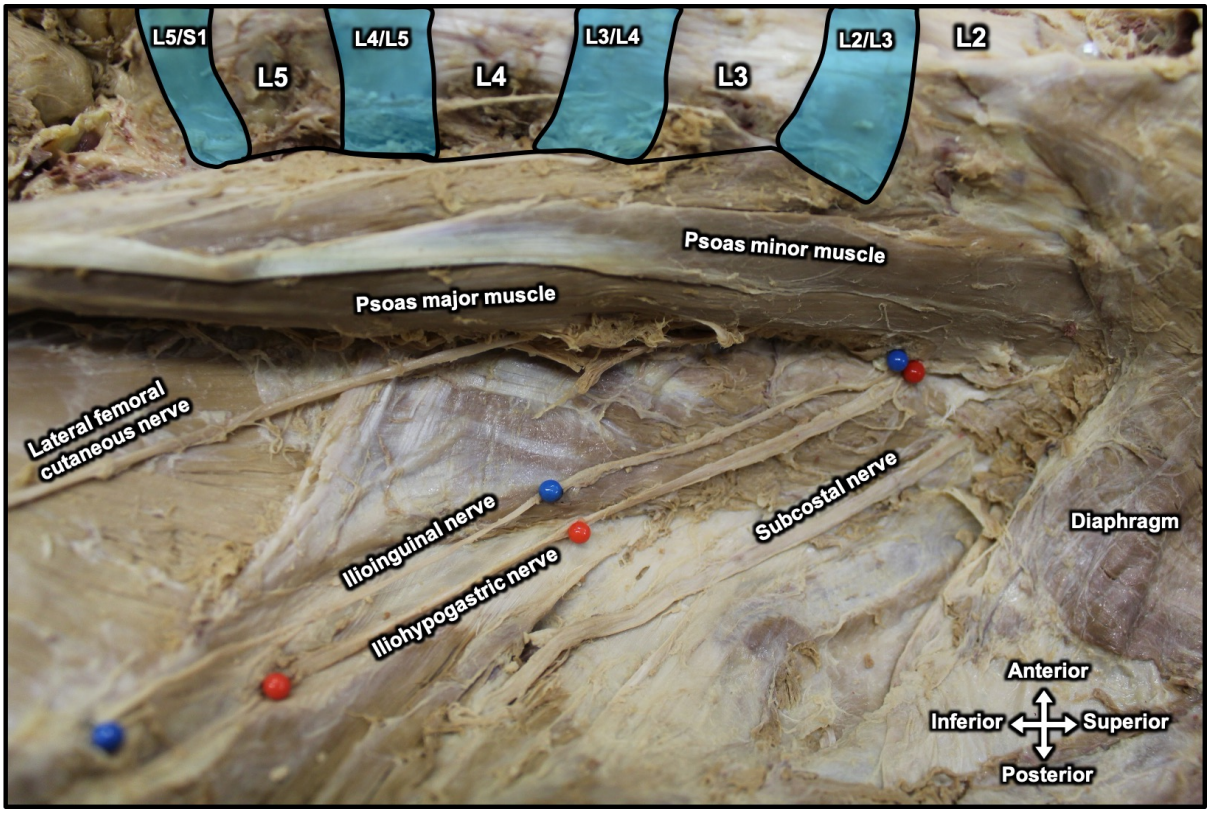

Figure 10: Lateral view of the posterior abdominal wall (left side), indicating the position and course of the IHN (red) , IIN (blue) and the other branches of the lumbar plexus on the posterior abdominal wall as they pass lateral to the psoas major muscle

3.6.2. Location of the IHN and IIN in relation to ASIS

As a result of the exclusion criteria, where there was evidence of pathology, previous dissection or disturbance to the area, only 36 cadavers were included in this sample. The measurement from the ASIS to the IHN (n = 33) was 25.2 ± 11.6mm (CI – 21.1; 29.4) on the left side and 23.6 ± 10.6mm (CI – 19.4; 27.8) on the right side (n = 36). A Chi-squared test resulted in p-values of 0.42 on the left- and 0.36 on the right sides, indicating no apparent influence of sex on the data. A Shapiro-Wilk test indicated that the data was not normally distributed on the two sides ($p < 0.05$). A Related Samples Wilcoxon Sign Rank test showed no statistically significant difference between the left- and right sides, with a p-value of 0.22.

Similar results were observed for the distance from the ASIS to the IIN. On the left side, the distance was 18.8 ± 8.4mm (CI – 16.0; 21.6) and the right side, 18.3 ± 9.77mm (CI – 14.8; 21.8). No statistically significant influence of sex on the data

was observed after a Chi-squared test on the left side (p = 0.48) and the right side (p = 0.37) was performed. The Shapiro-Wilk test revealed that the data was not normally distributed on the left- and right sides. As a result of the abovementioned result, a Wilcoxon Sign Rank test was performed, showing no statistically significant difference between the left- and right sides (p = 0.88). There was no statistically significant correlation observed between age, height, weight and BMI and measurements from the ASIS to the IHN and IIN (r < 0.30) (Table 5).

Table 5: Results of a Pearson's correlation test between measurements from the ASIS to the IHN and IIN and age, height, weight and BMI

		Age		**Height**		**Weight**		**BMI**	
Measurement	**Side**	**r**	**p**	**r**	**p**	**r**	**p**	**r**	**p**
ASIS to IHN	**Left**	-0.20	0.10	0.09	0.61	-0.07	0.71	-0.10	0.59
	Right	-0.21	0.08	-0.16	0.42	0.001	0.99	0.09	0.67
ASIS to IIN	**Left**	-0.20	0.10	-0.13	0.45	0.03	0.86	0.07	0.70
	Right	-0.20	0.11	-0.01	0.97	0.03	0.86	0.03	0.86

Inter- and intra-observer reliability test results may be found in Annexure A.

3.6.3. Clinical applications

An examination of the literature revealed a large amount of relevant clinical and surgical procedures that were selected to be compared to the results of this study. The keywords in the database searches mentioned previously were: *iliohypogastric nerve, ilioinguinal nerve, iliohypogastric and ilioinguinal nerve anatomy, iliohypogastric and ilioinguinal nerve injury*. To focus the search results, the following additional keywords were included: *inguinal hernia repair complications, iliohypogastric and ilioinguinal nerve analgesia, Pfannenstiel incision, iliohypogastric nerve, hernioplasty ilioinguinal iliohypogastric*. Several relevant surgical procedures were found during the search, but not all of them were reviewed for the study. The selected procedure was the Lichtenstein tension-free inguinal hernia repair. The applications of the results of these procedures are detailed in the discussion.

3.7. Discussion

3.7.1. Nerve roots and bifurcation pattern

This study aimed to accurately describe the anatomy of the IHN and IIN from its origin in the lumbar area to its innervation in the groin. The root value of the IHN and IIN was consistent throughout the entire study. Both nerves originated from the ventral ramus of the L1 spinal nerve. There have been studies that report the contribution of the T12 spinal nerve to the formation of IHN and IIN, but no incidences of this pattern could be found in the sample. These studies are compared in Table 6.

Table 6: Comparison of the root values of the IHN and IIN reported by different studies

Study	Country	n	IHN root values	IIN root values
Amid (2004a)	USA	-*	T12-L1	T12-L1
Tagliafico et al. (2015)	Italy	-*	T12-L1	L1
Amin et al. (2016)	USA	-*	T12-L2	T12-L2
Kale et al. (2019)	Turkey	-*	T12-L1	T12-L1
Current study (2019)	South Africa	210	L1	L1

*Study reported the root value, but not based on determining them

Of the studies that report the contribution of the T12 and L2 spinal roots, the most extensive was one by Klaassen et al. (2011) on 200 cadaver sides. In this study, they reported that the origin of IHN was from the ventral ramus of the L1 spinal nerve only. The variations arose with the IIN, where it originated from only the L1 spinal root in 65% of the cases, from T12-L1 in 14%, from L1-L2 in 11% and from L2-L3 in 10% of the cases. These variations were not observed in this current study. Nontasaen et al. (2016) also found the IHN and IIN originating from L1 in 96.5% and 90.1%, respectively, in a 131 lumbar plexus sample.

3.7.2. Location of the IHN and IIN in relation to ASIS

The location of the IHN and IIN in the anterior abdominal wall is important to consider when performing inguinal hernia repairs, especially regarding the IIN, as it lies within the inguinal canal (Rab and Dellon, 2001; Amid, 2004b; Ferzli et al., 2008; Kale et al., 2019). On the left side, the IHN was on average 25.24 ± 11.61mm from the ASIS and

on the right side, 23.60 ± 10.60mm from the ASIS. The IIN was 18.79 ± 8.38mm away from the ASIS on the left side and 18.26 ± 9.77mm on the right side. In a study of 11 fresh cadavers by Rahn et al. (2010), they found the IHN 25mm medial and 20mm inferior to the ASIS. The range for both measurements was 0 to 46mm. They also found that the IIN was 25mm medial and 24mm inferior to the ASIS, with ranges of 11 to 51mm and 0 to 53mm respectively. In a study by Whiteside et al. (2003), the IHN was found 21 ± 18mm medial and 9mm ± 28mm inferior to the ASIS. The IIN was on average 31 ± 15mm medial and 37 ± 15mm inferior to ASIS. These results differ from the results obtained in the current study. In this study, the IIN was observed closer to the ASIS than the IHN. In addition, the results of this study place both the IHN and IIN closer to the ASIS than in what is documented in literature, whereby Rahn et al. (2010) observed the nerves equidistant from the ASIS medially and the Whiteside et al. (2003) observed the IHN closer to the ASIS than the IIN. Being cognisant of the differences in the observed distances from the ASIS to the IHN and IIN is vital in the planning and performance of surgical and clinical procedures safely and successfully.

3.7.3. Clinical applications

The results of this study found that the IIN is closer to the ASIS than the IHN. This implies that the IIN is most likely in danger during procedures done on or around the ASIS and the structures that attach to it, such as the inguinal ligament. The results correspond to the described procedural guideline for the Lichtenstein tension-free repair, where the external oblique muscle is reflected superiorly for approximately 30 – 40mm. This will allow for clear visualization of the IHN and IIN, limiting the possibility of entrapment of the nerve when inserting the mesh, as both distances lie within the limits of the proposed muscle reflection distances.

It must be noted that even though the Wilcoxon test did not report a statistically significant difference in the distances on the opposite sides, the variability on the respective sides necessitates that each side be approached with caution. The finding that the data is not equally distributed on all sides for both the IHN and IIN indicates the presence of variation in the location of the nerves. This should be considered when undertaking inguinal hernia repairs. Knowledge of this variability will prevent the occurrence of nerve entrapment, which will require further surgical intervention. There was no apparent correlation of between the distance from the ASIS to the IHN and IIN

for age, height, weight and BMI, therefore it is suggested that the procedural approaches be universal for every patient, with detailed planning to safely complete the procedures with the variations of the nerves in mind.

3.8. Conclusion

The anatomy of the IHN and IIN was in line with what has been described in anatomical textbooks and literature. Further comparative studies could be performed in order to further investigate the presence of the T12 contribution that has been suggested by other studies. The L1 spinal nerve predominantly bifurcated into the IHN and IIN within the transversus abdominis muscle before coursing towards the ASIS. The distances of the IHN and IIN lie within the recommended 30-40mm muscle flap described for the Lichtenstein tension-free repair for visualization of the nerves. This reiterates the safety of the procedure and is recommended for inguinal hernia repairs. It is important to note the variability in the distances observed in the study on left- and right sides. It cannot be denied that the variability may be due to the limitation of a small sample size, as a result of exclusion criteria. It is recommended that the IHN and IIN be further investigated on a larger cadaver sample with an equal distribution of males and females, including an extension of the study by mapping the nerves using magnetic resonance imaging (MRI) and CT scans.

3.9. References

AL-DABBAGH, A. 2002. Anatomical variations of the inguinal nerves and risks of injury in 110 hernia repairs. *Surgical and radiologic anatomy,* 24**,** 102-107.

AMID, P. 2004a. Causes, prevention, and surgical treatment of postherniorrhaphy neuropathic inguinodynia: triple neurectomy with proximal end implantation. *Hernia,* 8**,** 343-349.

AMID, P. K. 2004b. Lichtenstein tension-free hernioplasty: its inception, evolution, and principles. *Hernia,* 8**,** 1-7.

AMIN, N., KRASHIN, D. & TRESCOT, A. M. 2016. Ilioinguinal and Iliohypogastric Nerve Entrapment: Abdominal. *Peripheral Nerve Entrapments.* Springer.

ANLOAGUE, P. A. & HUIJBREGTS, P. 2009. Anatomical variations of the lumbar plexus: a descriptive anatomy study with proposed clinical implications. *Journal of Manual & Manipulative Therapy,* 17**,** 107E-114E.

BARAZANCHI, A. W. H., FAGAN, P. V. B., SMITH, B. B. & HILL, A. G. 2016. Routine neurectomy of inguinal nerves during open onlay mesh hernia repair: a meta-analysis of randomized trials. *Annals of surgery,* 264**,** 64-72.

DE GOEDE, B., TIMMERMANS, L., VAN KEMPEN, B. J., VAN ROOIJ, F. J., KAZEMIER, G., LANGE, J. F., HOFMAN, A. & JEEKEL, J. 2015. Risk factors for inguinal hernia in middle-aged and elderly men: results from the Rotterdam Study. *Surgery,* 157**,** 540-546.

FATEH, O., WASI, M. S. I. & RAFIQ, S. U. 2018. Variability in Ilioinguinal nerve anatomy during open hernia repair and its association with post-operative pain. *Pak J Surg,* 34**,** 46-51.

FERZLI, G. S., EDWARDS, E., AL-KHOURY, G. & HARDIN, R. 2008. Postherniorrhaphy groin pain and how to avoid it. *Surgical Clinics of North America,* 88**,** 203-216.

GATABI, M. H., DARZI, A. A. & MOUDI, E. 2018. COMPARISON OF OUTCOMES BETWEEN THE LICHTENSTEIN AND BASSINI METHODS IN INGUINAL HERNIA-A RANDOMISED CONTROLLED TRIAL. *JOURNAL OF EVOLUTION OF MEDICAL AND DENTAL SCIENCES-JEMDS,* 7**,** 5305-5309.

KALE, A., AYTULUK, H. G., CAM, I., BASOL, G. & SUNNETCI, B. 2019. Selective Spinal Nerve Block in Ilioinguinal, Iliohypogastric and Genitofemoral Neuralgia. *Turk Neurosurg,* 29**,** 530-537.

KLAASSEN, Z., MARSHALL, E., TUBBS, R. S., LOUIS JR, R. G., WARTMANN, C. T. & LOUKAS, M. 2011. Anatomy of the ilioinguinal and iliohypogastric nerves with observations of their spinal nerve contributions. *Clinical Anatomy,* 24**,** 454-461.

LICHTENSTEIN, I. L., SHULMAN, A. G., AMID, P. K. & MONTLLOR, M. M. 1989. The tension-free hernioplasty. *The American Journal of Surgery,* 157**,** 188-193.

MCDONNELL, D. & WAKEFIELD, C. 2018. Adult groin hernias: acute and elective. *Surgery (Oxford),* 36**,** 238-244.

NEOGI, P., SINGH, S. K., MANWATKAR, S., SINGH, S. K., SAXENA, A. & KOLA, A. 2018. A prospective study comparing preservation of ilioinguinal nerve with neurectomy in open mesh repair of inguinal hernia. *International Surgery Journal,* 6**,** 114-118.

NONTASAEN, P., DAS, S., NISUNG, C., SINTHUBUA, A. & MAHAKKANUKRAUH, P. 2016. A cadaveric study of the anatomical variations of the lumbar plexus with clinical implications. *Journal of the Anatomical Society of India,* 65**,** 24-28.

RAB, M. & DELLON, A. 2001. Anatomic variability of the ilioinguinal and genitofemoral nerve: implications for the treatment of groin pain. *Plastic and reconstructive surgery,* 108**,** 1618-1623.

RAHN, D. D., PHELAN, J. N., ROSHANRAVAN, S. M., WHITE, A. B. & CORTON, M. M. 2010. Anterior abdominal wall nerve and vessel anatomy: clinical implications for gynecologic surgery. *American journal of obstetrics and gynecology,* 202**,** 234. e1-234. e5.

SAMAKAR, K., SANDHU, K. K. & KATKHOUDA, N. 2019. Inguinal Hernia Repair: Open. *Shackelford's Surgery of the Alimentary Tract, 2 Volume Set.* Elsevier.

SCHUMPELICK, V. & KLINGE, U. 2003. Prosthetic implants for hernia repair. *British journal of surgery,* 90**,** 1457-1458.

TAGLIAFICO, A., BIGNOTTI, B., CADONI, A., PEREZ, M. M. & MARTINOLI, C. 2015. Anatomical study of the iliohypogastric, ilioinguinal, and genitofemoral nerves using high-resolution ultrasound. *Muscle & nerve,* 51**,** 42-48.

TAN, W. H. & BLATNIK, J. A. 2018. Open Inguinal Hernia Repair. *Surgical Principles in Inguinal Hernia Repair.* Springer.

VASU, S. & SAGAR, K. 2018. A clinical study of post operative complications of Lichtenstein's hernioplasty for inguinal hernia. *International Surgery Journal,* 6**,** 13-16.

WHITESIDE, J. L., BARBER, M. D., WALTERS, M. D. & FALCONE, T. 2003. Anatomy of ilioinguinal and iliohypogastric nerves in relation to trocar placement and low transverse incisions. *American journal of obstetrics and gynecology,* 189**,** 1574-1578.

ZSOLT, B. & CSIKY, M. 2001. Recurrence rate in Bassini operation after five years. *Magyar sebeszet,* 54**,** 307-308.

ZWAANS, W. A., PERQUIN, C. W., LOOS, M. J., ROUMEN, R. M. & SCHELTINGA, M. R. 2017. Mesh removal and selective neurectomy for persistent groin pain following Lichtenstein repair. *World journal of surgery,* 41**,** 701-712.

Chapter 4 – Genitofemoral nerve (GFN)

4.1. Introduction and problem statement

Genitofemoral neuralgia is a condition where pain and paraesthesia are experienced in the groin and upper medial thigh (Cesmebasi et al., 2015; Verstraelen et al., 2015; Iwanaga et al., 2019; Sehgal, 2019). The condition was described by Magee (1942), whereby it was termed genitofemoral causalgia. Several years later, it was redefined by Lyon (1945) to what is now described as genitofemoral neuralgia. The prevalence of genitofemoral neuralgia in the USA has been reported at 7% in females (Verstraelen et al., 2015). No reference could be found in the literature stating the incidence rate in males. The lack of incidence reports may be as a result of patients failing to consult doctors when the symptoms occur and may possibly be misdiagnosed, as the GFN has a similar distribution with the IHN and IIN (Bugada and Peng, 2015; Kumar and Zaidi, 2017; Kale et al., 2019).

Several studies attributed the neuralgia to direct damage during surgery or impingement during implantation of a mesh in the inguinal region during hernia repair (Fritz et al., 2017; Cesmebasi et al., 2015). A study by Aasvang and Kehlet (2005) reported an incidence rate of 20% after inguinal hernia repair. In another study of inguinal hernia repairs, an incidence rate of 12-20% was reported (Shanthanna, 2014). Clear and accurate knowledge of the anatomy of the genitofemoral nerve and its branches in relation to bony landmarks can be used in pre-operative planning of surgical and clinical procedures performed in the groin region. In this study, observations, measurements and accurate descriptions of the anatomy of the GFN and its branches in relation to bony landmarks were done for use in clinical applications, especially during the performance of inguinal hernia repair.

4.2. Literature review

4.2.1. Genitofemoral nerve

The GFN is a predominantly sensory nerve, but also supplies motor fibres to the cremaster muscle in the spermatic cord in males. Its origin is from the ventral rami of the L1 and L2 spinal nerves. The nerve exits the psoas major muscle from its anterior surface, then descends along its midline towards the pelvis. Before reaching the inguinal ligament, the nerve terminates into its genital and femoral branches (Figure 11) (Anloague and Huijbregts, 2009; Celebi et al., 2013; Fritz et al., 2017).

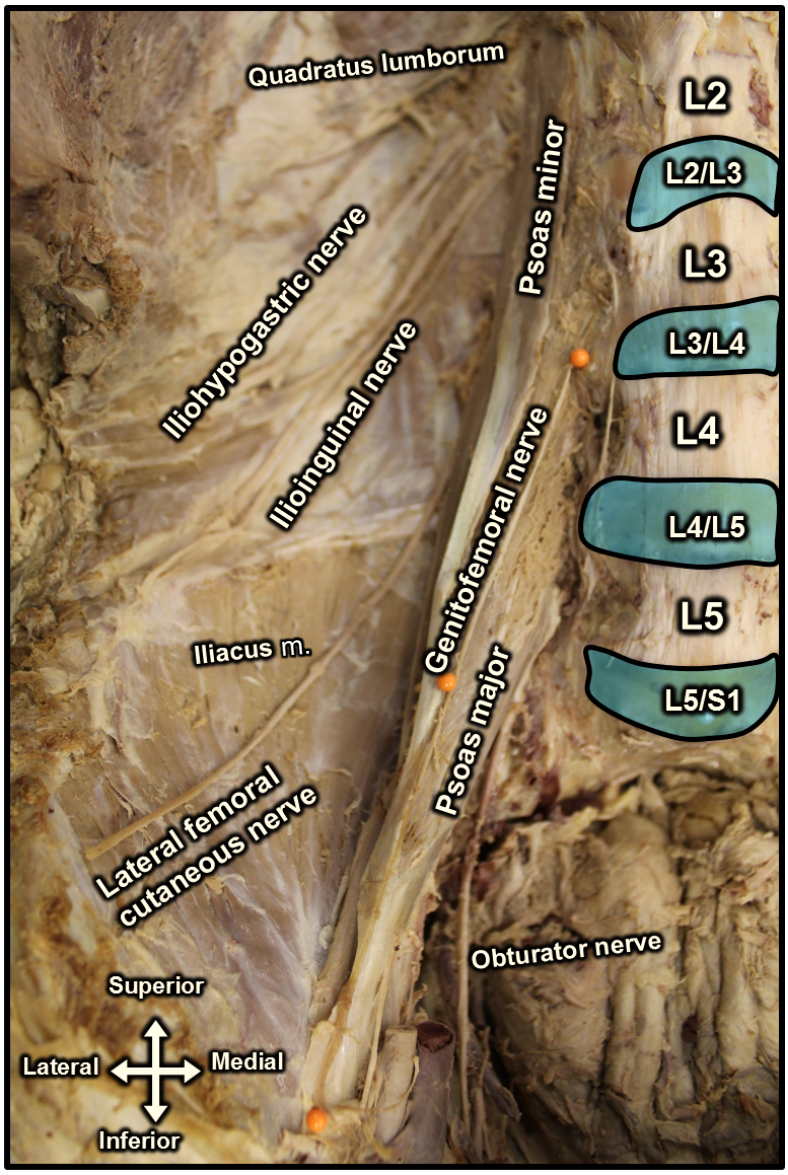

Figure 11: Anterior view of the lumbar plexus as it courses on the posterior abdominal wall. The GFN in indicated by orange pins as it descends on the psoas major muscle on the right side.

The genital branch descends on the anterior surface of the psoas major muscle towards the false pelvis, where it runs on the iliacus muscle towards the deep inguinal ring. After entering the deep inguinal ring, the nerve enters the inguinal canal and runs within the spermatic cord, innervating the cremaster muscle in males. The genital branch has no motor innervation in females. Thereafter, it exits the canal through the superficial inguinal ring. In males, it will give sensory innervation to the skin of the anterior surface of the scrotum and upper medial surface of the thigh. In females, it

will accompany the round ligament of the uterus to innervate the mons pubis and the superior surface of the labia majora in females (Anloague and Huijbregts, 2009; Celebi et al., 2013; Cesmebasi et al., 2015; Fritz et al., 2017). The innervation to the external genitalia overlaps with that of the IIN (Rab and Dellon, 2001; Tagliafico et al., 2015; Kumar and Zaidi, 2017).

Unlike the genital branch, the femoral branch does not enter the inguinal canal, but runs deep to the inguinal ligament. Thereafter, it enters the femoral sheath, running lateral to the femoral artery. In the upper region of the thigh, it pierces the femoral sheath and fascia lata anteriorly, to innervate the skin of the upper area of the anterior and medial thigh (Anloague and Huijbregts, 2009; Celebi et al., 2013; Tagliafico et al., 2015; Fritz et al., 2017).

A study by Anloague and Huijbregts (2009) (n = 34) reported that the there was a 47.1% (n = 16) variation in the bifurcation of the GFN into its terminal branches midway along its descent on the anterior surface of the psoas major muscle. The authors also found a variation in the bifurcation, where the terminal branches appeared within the substance of the psoas major muscle in 26.5% (n = 9) of the sample. Al-dabbagh (2002) found a variation in the origin of the GFN in two of 64 cases, where the IIN branched off from the GFN.

Injury to the GFN has been reported during laparoscopic varicocelectomy procedures. The incidence of injury has been reported in literature at a prevalence of between 2% and 9% (Jarow et al., 1993; Poulsen et al., 1994; Chrouser et al., 2004). A study by Muensterer (2008) reported a prevalence of 15% during the procedure in adolescents. Injury to the genital branch of the GFN has been observed during inguinal hernia repair surgery. This may be attributed to the existence of variations with regard to the bifurcation and course of the nerve, especially the genital branch (Sampath et al., 1995; Schulster et al., 2017), or a simple lack of anatomical knowledge of the course of the branches of the GFN.

4.2.2. GFN nerve block

The GFN block is commonly performed to provide pain relieve for patients with symptoms of genitofemoral neuralgia. To block the genital branch of the GFN, the patient is placed in a supine position. Before needle insertion, the pubic tubercle is identified by palpation. Once positively identified, a needle insertion site is marked 20mm lateral and 20mm superior to the pubic tubercle. The needle is then inserted and advanced obliquely and medially towards the pubic tubercle, ensuring not to pierce the spermatic cord. Once the needle reaches the pubic tubercle, it is slightly withdrawn and the anaesthetic solution is administered (Harmon, 2011; Waldman, 2011; Waldman, 2016).

For the blockade of the femoral branch of the GFN, the patient remains in a supine position. The inguinal ligament is identified and divided into thirds between the ASIS and pubic tubercle. The block is performed in the middle third of the inguinal ligament by inserting the needle into the groin. It is important to ensure that the needle is kept subcutaneous, so as not to puncture the femoral vessels or inadvertently block the femoral nerve which lies in close proximity to the femoral branch of the GFN (Harmon, 2011; Waldman, 2011; Waldman, 2016).

To ensure that these procedures are performed accurately and yield positive results, it is important that the anatomy of the GFN and its branches is understood, especially in relation to the pubic tubercle, which is a commonly used landmark.

4.3. Aim

The aim of this study was to investigate the anatomy of the genitofemoral nerve and its branches and to correlate these findings to the Lichtenstein inguinal hernia repair and GFN block.

4.4. Research objectives

The objectives to achieve the aim are as follows:

1. Expand the knowledge on the anatomy of the GFN and its branches through qualitative observation of its origin, course, branching patterns and possible variations.
2. Give a quantitative description of the GFN and its branches in relation to the pubic tubercle.
3. Correlate the anatomy of the GFN and its branches, as well as any observed variations, to the current literature and guidelines for the Lichtenstein tension-free inguinal hernia repair and GFN block.

4.5. Materials and methods

4.5.1. Vertebral level of exit, course and root values

Prior to any dissection of the posterior abdominal wall and the psoas major muscle, bilateral observations of 105 formalin-fixed cadavers (59 males and 46 females, 70 ± 15 years) of the vertebral level at which the GFN emerges from the psoas major muscle, were made. It was determined whether the GFN, on the anterior surface of the psoas major muscle, emerged in line with a vertebral body or an intervertebral disc and the level thereof. Thereafter, it was observed whether the GFN emerged as a single nerve, or whether it bifurcated into its terminal branches within the substance of the psoas major muscle. To determine its approximate location, the distance from the midline of the vertebral body/intervertebral disc was measured. The midline was determined by measuring the width of the vertebral body/intervertebral disc, followed by placement of a pin at the centre of the structure, on a horizontal line connecting to the GFN. In the cases where the GFN bifurcated at the psoas major muscle, measurements were made to the nearest terminal branch (Figure 12).

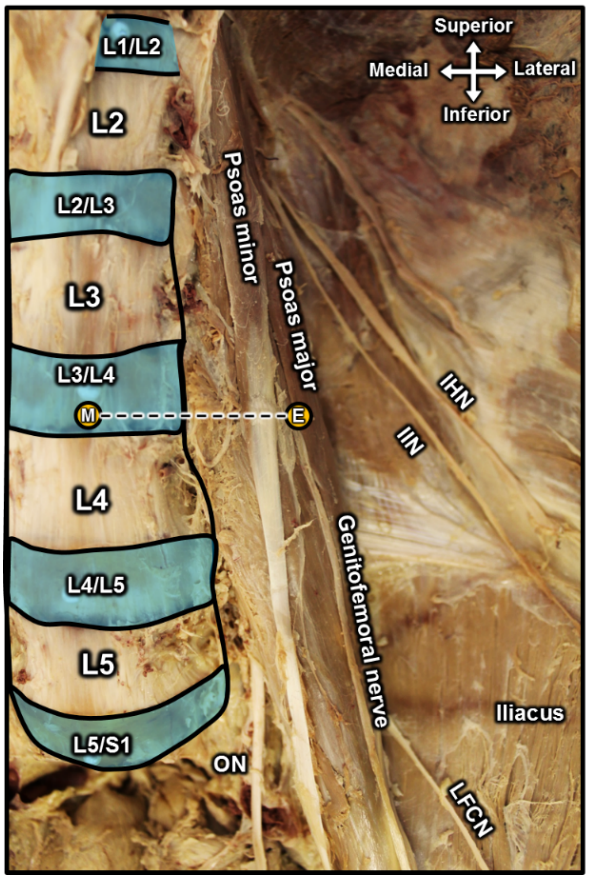

Figure 12: Anterior view of the measurement taken from the midline of the vertebral body to the GFN on the left side.

M = Midline of the vertebral body; E = Exit of the GFN on the psoas major muscle; IHN = Iliohypogastric nerve; IIN = Ilioinguinal nerve; LFCN – Lateral femoral cutaneous nerve; ON = Obturator nerve

Once the observations and measurements were completed, bilateral dissections of 105 formalin-fixed cadavers (59 males and 46 females, 70 ± 15 years), detailed in the chapter 2 on the lumbar plexus, were executed to expose the nerve roots. The GFN nerve roots were carefully separated from the nerves with which it shares root values, ensuring that only the nerve fibres of the GFN were identified (Figure 13).

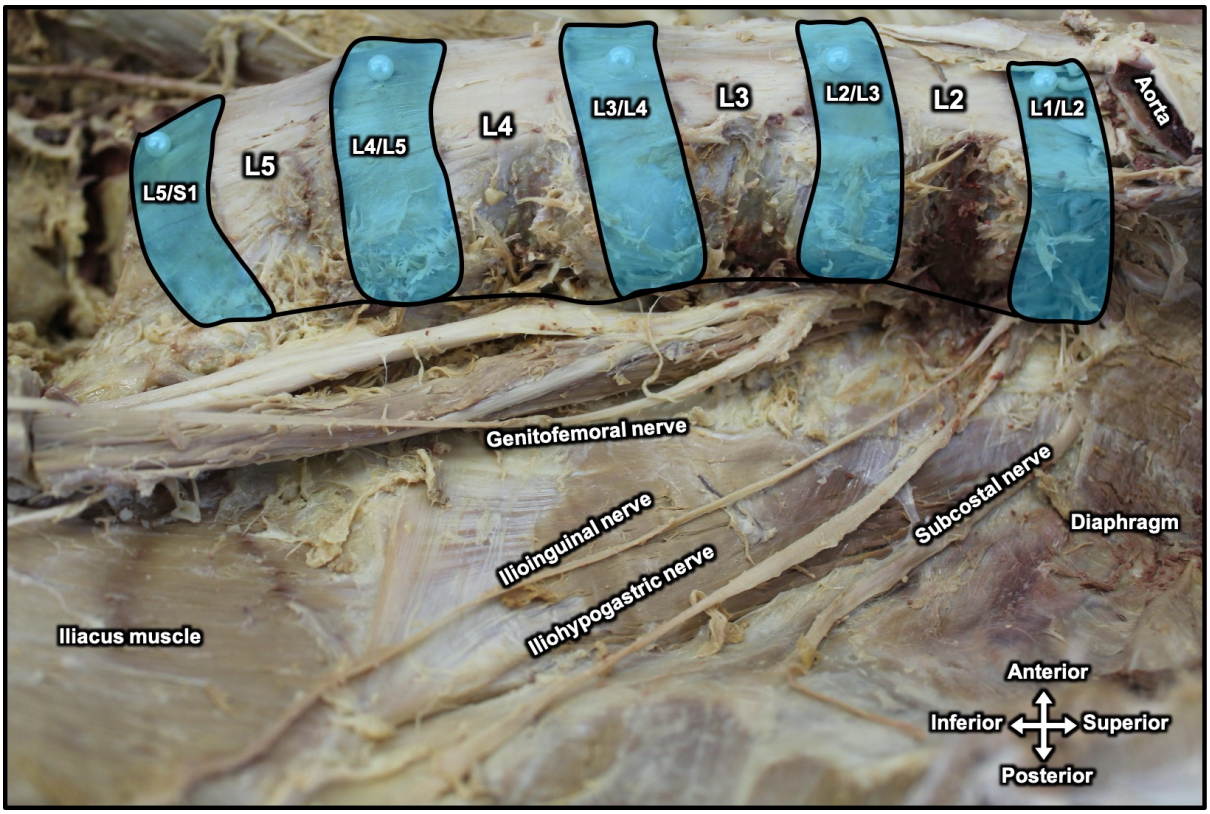

Figure 13: Lateral view indicating the GFN roots contributions without a contribution from the anterior ramus of the L2 spinal nerve.

4.5.2. Genitofemoral nerve in the inguinal region

The location of the femoral and genital branches of the GFN were investigated in relation to the pubic tubercle in the inguinal region. To determine the locations of the individual branches, measurements were taken from the attachment of the inguinal ligament on the pubic tubercle to the femoral and genital branches of the GFN. To identify the femoral branch, the subcutaneous fat was cleaned in the inguinal region, on the anterior thigh. After the nerve was exposed, just inferior to the inguinal ligament, the shortest distance from the pubic tubercle to the femoral branch was taken. The genital branch was similarly measured from the pubic tubercle to where it exits the inguinal canal at the superficial ring (Figure 14). Samples were excluded if there was visible evidence of pathology, previous dissection or disturbance to the area of interest.

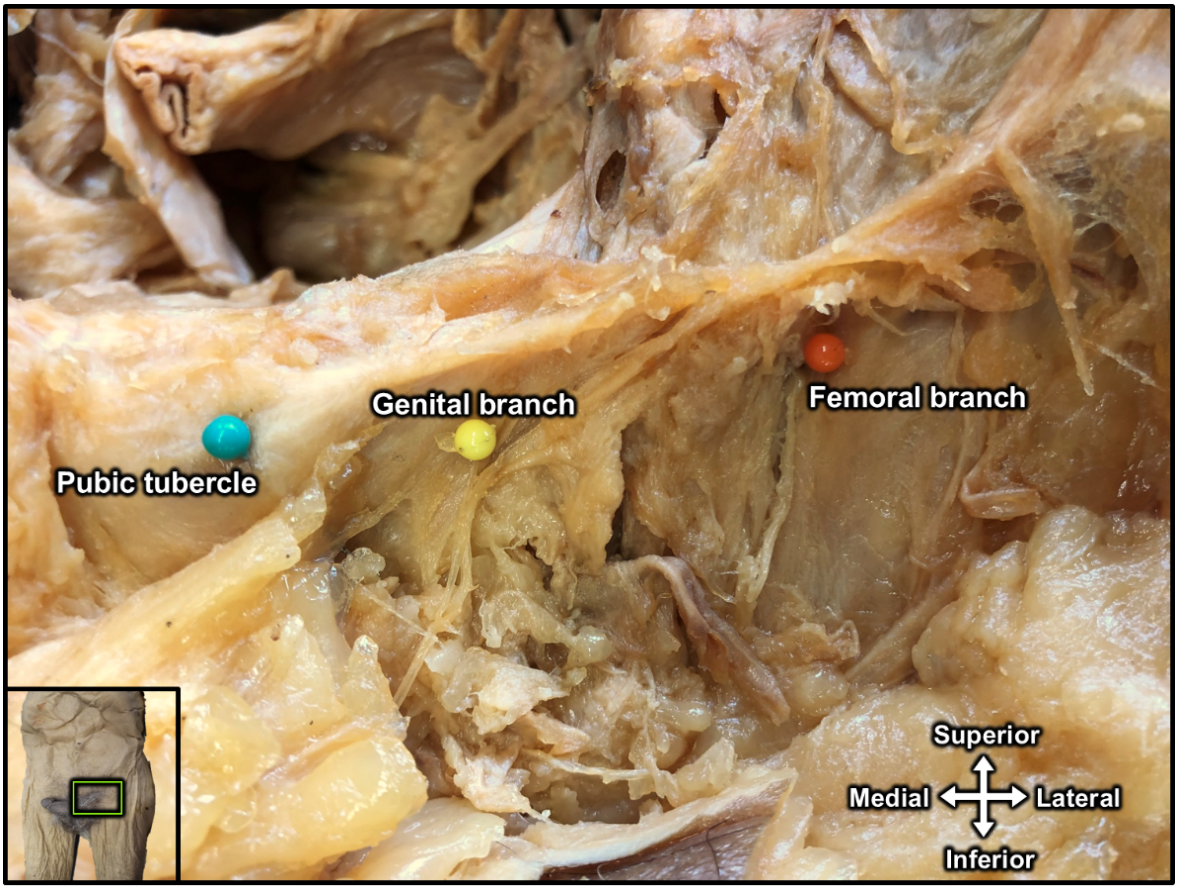

Figure 14: Anterior view of the inguinal region indicating the points where the distances from the pubic tubercle to the genital branch and femoral branch of the GFN on the left side were taken.

4.5.3. Clinical applications

After the cadaver results were obtained, they were correlated with the guidelines for genitofemoral nerve blocks and Lichtenstein tension-free inguinal hernia repair. An extensive literature search was performed using the PubMed, Science Direct, Ovid and Google Scholar journal databases, together with current anatomy-, surgical- and anaesthetic textbooks/guidelines.

4.5.4. Statistical analysis

All observation and measurement data were recorded in a 2013 Microsoft Office Excel spreadsheet. Statistical tests were performed as outlined in the preceding chapter three on the IHN and IIN.

4.6. Results

4.6.1. Vertebral level of exit, course and root values

Investigations into the vertebral level at which the GFN exits through the psoas major muscle resulted in observations where, on the left side, it was at the level of L3 in 7 cases (6.67%) in males and 6 cases (5.72%) in females. In addition, in males, it was found at L3/L4 intervertebral disc in 41 cases (39.05%), at L4 in 9 cases (8.57%) and L4/L5 intervertebral disc in 2 cases (1.90%). In females, it was found at L3/4 intervertebral disc in 34 cases (32.38%), L4 in 4 cases (3.81%) and at L4/L5 intervertebral disc in 2 cases (1.90%). On the right side, in males, it was observed at L3 in 5 cases, L3/L4 intervertebral disc in 45 cases, L4 in 6 cases and L4/L5 intervertebral disc in 3 cases. In females, it exited at L3 in 2 cases, L3/L4 intervertebral disc in 40 cases and L4 and L4/L5 intervertebral disc in 2 cases each. A Chi-squared test revealed no statistically significant influence of sex on the results on both the left side ($p = 0.90$) and the right side ($p = 0.70$). The pooled results for the levels at which the GFN exited through the psoas major muscle on the left side were at L3 in 13 cases (12.38%), at L3/L4 intervertebral disc in 75 cases (71.43%), 13 cases for L4 (12.43%) and at L4/L5 intervertebral disc in 4 cases (3.81%). Pooled results on the right side were recorded at L3 in 7 cases (6.67%), at L3/L4 intervertebral disc in 85 cases (80.95%), at L4 in 8 cases (7.62%) and at L4/L5 intervertebral disc in 5 cases (4.76%) (Figure 15). A Chi-squared test to determine whether a statistically significant difference existed between the two sides yielded a value of $p < 0.01$ indicating a positive result.

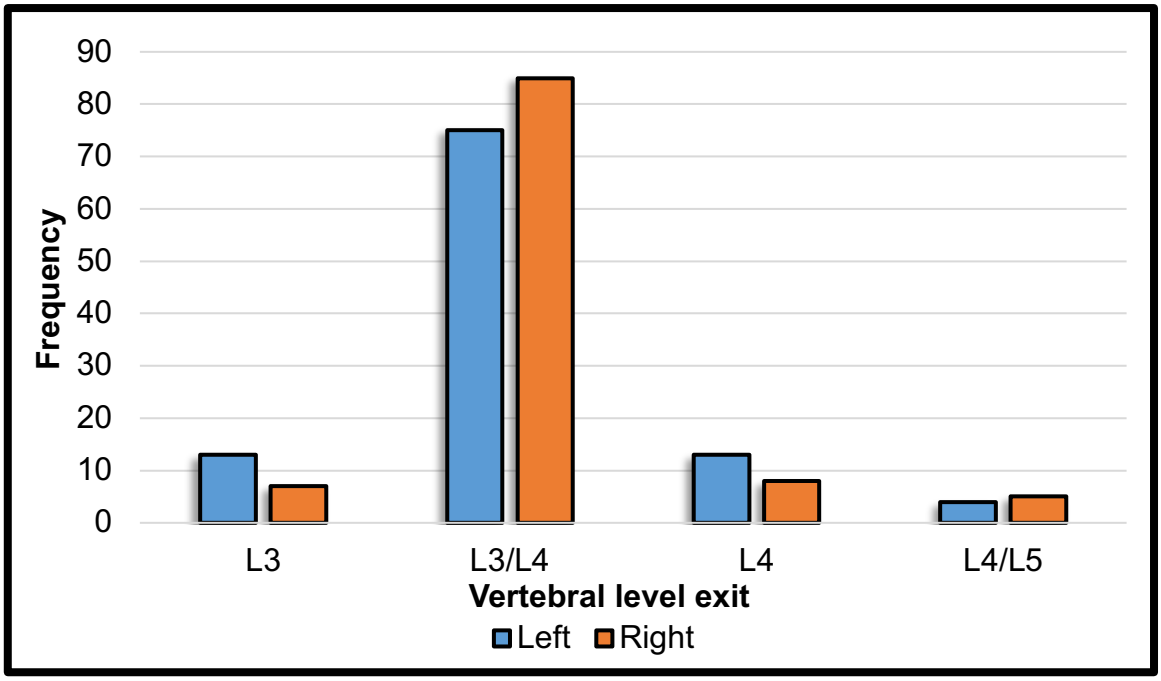

Figure 15: Histogram comparing the exit levels of the GFN from the anterior surface of the psoas major muscle on the left and right sides

The distance of the level at which the GFN exits from the psoas major muscle from the midline of the body was on average 25.20 ± 3.31mm on the left side and 26.35 ± 4.81mm on the right side. A Shapiro-Wilk test for the measurement from the midline of the vertebral body to the point where the GFN exits the psoas major muscle yielded p-values of 0.54 and 0.60 for the left side and right side, respectively. A Chi-squared test generated a p-value of 0.42 on the left side and 0.43 on the right side, indicating no significant influence of sex on the results. Thereafter, a paired t-test was performed to compare the sides. No significant difference was found between the sides ($p = 0.30$). Therefore, the results were pooled and resulted in a mean distance of 25.80 ± 4.18mm (CI – 14.86; 26.75). A Pearson's correlation test showed that there were weak negative- ($r > -0.30$) and weak positive correlations ($r < 0.30$) between the distance from the midline of the body to the exit of the GFN from the psoas major muscle and age, height, weight and BMI on both the left- and right sides (Table 7).

Table 7: Yielded results of a Pearson's correlation test between measurements from the midline of the body to the GFN exit through psoas major muscle and age, height, weight and BMI on the left- and right sides

		Age		Height		Weight		BMI	
Measurement	**Side**	**r**	**p**	**r**	**p**	**r**	**p**	**r**	**p**
Midline of the body to the GFN exit through psoas major muscle	**Left**	0.23	0.18	0.06	0.72	0.06	0.70	0.04	0.81
	Right	-0.12	0.46	0.07	0.67	0.02	0.89	0.10	0.53

After removing the psoas major muscle and exposing the nerve roots, it was found that in the male sample on the left side, the GFN originated from the L1 – L2 spinal nerves in 54 cases (91.53%), from L1 in 3 cases (5.08%) and from L2 in 2 cases (3.39%). In females, a L1-L2 origin was observed in 44 cases (95.66%), L1 in 2 cases (4.34%) and there were no observations of a L2 origin. On the right side, the observations of origin in males was from L1-L2 in 52 cases (88.14%), from L1 in 4 cases (6.78%) and from L2 in 3 cases (5.08%). For the female sample, a L1-L2 origin was observed in 43 cases (93.48%), L1 in 3 cases (6.52%) and no observations were made for L2. A Chi-squared test showed no significant influence of sex on the left side ($p = 0.65$) and the right side ($p = 0.49$). This allowed pooling of the observed left side origins of L1-L2 to 98 cases (93.33%), L1 to 5 cases (4.76%) and L2 to 2 cases (1.90%). On the right side, L1-L2 became 95 cases (90.48%), L1 was 7 cases (6.67%) and 3 cases (2.86%) for L2 (Figure 16). Another Chi-squared test was performed which revealed a statistically significant difference between the left- and right sides ($p < 0.01$).

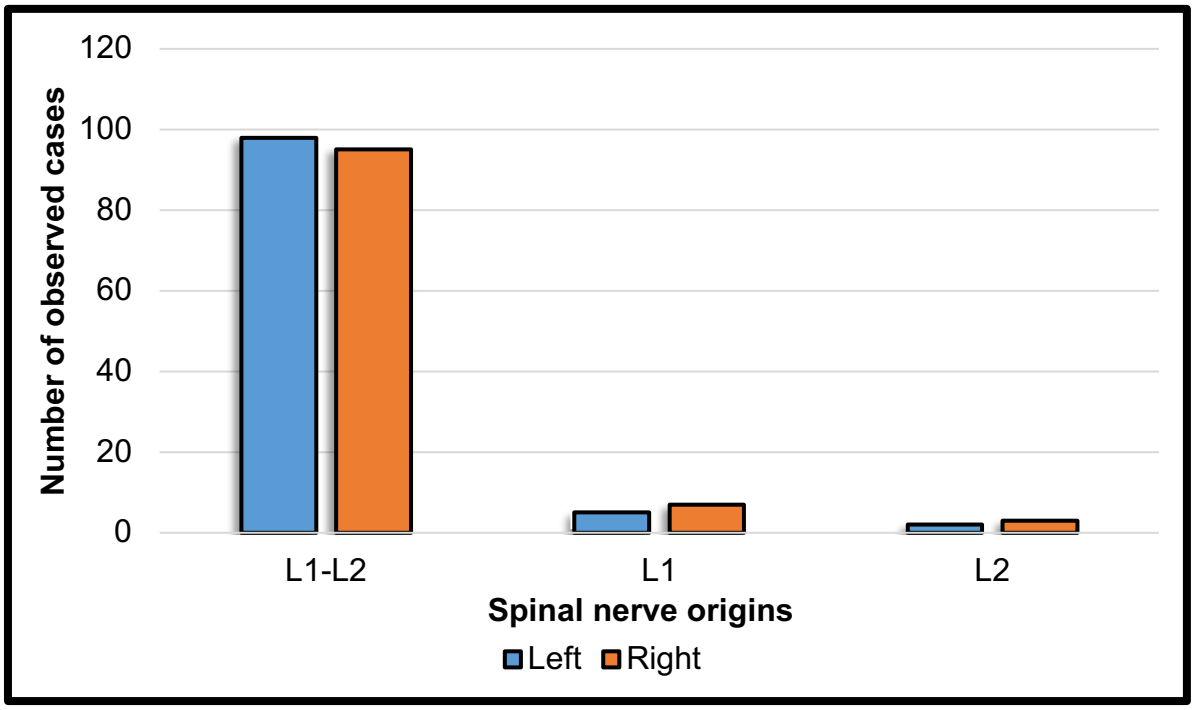

Figure 16: Histogram indicating the observed origins of the GFN from the spinal nerves L1-L2, L1 and L2 on the left- and right sides

4.6.2. Genitofemoral nerve in the inguinal region

When comparing males and females, the measurements from the pubic tubercle to the femoral branch of the GFN, a Shapiro-Wilk test revealed a p-value of 0.43 on the left side and 0.70 on the right side. For those of the genital branch, the p-values were 0.11 and 0.18 on the left and right sides, respectively. A Chi-squared test yielded p-values of 0.43 (left side) and 0.37 (right side) for measurements from the pubic tubercle to the femoral branch and 0.43 (left side) and 0.41 (right side) to the genital branch. These values did not suggest an influence of sex on the results. The average distance from the pubic tubercle to the femoral branch on the left side was 65.6 ± 8.5mm and 65.7 ± 7.6mm on the right side. The mean distance to the genital branch on the left side was 22.0 ± 8.8mm and 22.7 ± 6.9mm on the right side. A paired t-test showed no statistically significant difference between the two sides for the femoral branch ($p = 0.33$), nor for the genital branch ($p = 0.40$) of the GFN. The results were pooled and yielded a mean distance of 65.6 ± 8.1mm (CI – 63.8; 67.5) for the femoral branch and 22.3 ± 8.0mm (CI – 20.4; 24.2) for the genital branch.

A Pearson's correlation test yielded no statistically significant correlation between the distances from the pubic tubercle to the femoral- and genital branches of the GFN and age, height, weight. For BMI, a moderate positive correlation (r = 0.32) was observed for the distance from the pubic tubercle to the genital branch on the right side. On the left side, a weak positive correlation was observed (r = 0.13) (Table 8).

Table 8: Results of a Pearson's correlation test between measurements from the pubic tubercle to the femoral- and genital branches and age, height, weight and BMI

		Age		**Height**		**Weight**		**BMI**	
Measurement	**Side**	**r**	**p**	**r**	**p**	**r**	**p**	**r**	**p**
Pubic tubercle to the femoral branch	**Left**	-0.13	0.43	0.03	0.83	0.21	0.18	-0.04	0.79
	Right	0.10	0.60	0.13	0.48	<0.01	0.98	0.16	0.39
Pubic tubercle to the genital branch	**Left**	-0.14	0.41	0.14	0.38	0.13	0.42	0.13	0.42
	Right	-0.10	0.59	0.24	0.20	-0.08	0.69	0.32	0.08

Inter- and intra-observer reliability test results may be found in Annexure A.

4.6.3. Clinical applications

An extensive literature search revealed clinical and surgical procedures which were identified to be relevant to use in conjunction with the results. The keywords in the database searches mentioned previously were: *lumbar plexus, lumbar plexus anatomy, lumbar plexus variation, lumbar plexus damage, lumbar plexus procedures, lumbar plexus surgery, lumbar plexus block approach* and *psoas compartment block*. As possible procedures were identified by using the previous keywords, the following additional keywords were used to find the most relevant procedures: *total hip arthroplasty, lumbar plexus block posterior approach* and *analgesia lumbar plexus*. The application of the results on the posterior approach of the psoas compartment nerve block procedure is detailed in the discussion.

4.7. Discussion

4.7.1. Vertebral level of exit, course and root values

Deep to the psoas major muscle, the roots of the GFN were observed to have varying origins. The predominant origin was from the ventral rami of the L1-L2 spinal nerves, accounting for 98 cases on the left side and 95 cases on the right side. This was followed by L1 only, with 5 left side and 7 right side cases and the least frequent was L2 only with 2 left and 3 right cases. Other studies have investigated the roots of the GFN and found similar results as the current study (Gindha et al., 2015; Paul and Shastri, 2019). These studies reported variations that were not found in the current study. Gindha et al. (2015) reported contributions of T12-L1, L1-L3 and L2-L3 to the formation of the GFN. In addition, they reported instances where the GFN was absent. The study by Paul and Shastri (2019) also reported L2-L3 and L3 origin of the GFN. A comparison of these results is indicated in Table 9.

Table 9: Comparison of the root values of the GFN in different studies

Study	Country	n	T12-L1	L1	L1-L2	L1-L3	L2	L2-L3	L3
Gindha et al. (2015)*	India	60	2	1	41	3	4	2	-
Paul and Shastri (2019)	India	61	-	2	15	-	28	15	1
Current study	RSA	210	-	12	193	-	5	-	-

*Results of the sides were combined by the current study for comparison purposes. The nerve was absent in 7 cases.

The GFN was observed exiting anterior to the psoas major muscle predominantly at the vertebral level of the L3/4 intervertebral disc on both sides of the body. This is followed by the level of the L4 vertebral body, then the L3 vertebral body, with the L4/L5 intervertebral disc being the least common level at which the GFN exited the muscle. These observations are similar to those by Fritz et al. (2017), who reported the presence of the nerve initially at the level of the L3/L4 intervertebral disc and further at the level of the L4/L5 intervertebral disc. The nerve was not reported at L3, as was in the current study. Similarly, Cesmebasi et al. (2015) reported the exit at the level of the L3/L4 intervertebral disc.

A number of studies qualitatively described the location of the GFN on the psoas major muscle. Fritz et al. (2017) described the location of the nerve as anteromedial on the psoas major muscle. Gupton and Varacallo (2019) described the GFN originating from the "midsection" of the psoas major, to emerge from its anterior surface. Quantitatively describing the location will provide a standard on how to approximate the location of the nerve. Feigl et al. (2014) measured the distance between the emergence of the GFN and the trunk of the lumbar sympathetic trunk. Although quantitative, the methods cannot be standardized, as soft tissue is involved, which may differ in its position between individuals. The midline of the vertebral body was used in this study to standardize the position from which the distance to the GFN can be measured. The GFN was observed 25.8 ± 4.2mm from the midline of the body. Using this description, together with that of the level at which it exits, will allow for clear identification of the GFN in relation to the psoas major muscle as it descends towards the inguinal region.

4.7.2. Genitofemoral nerve in the inguinal region

The aim of this study was to quantify the location of the femoral and genital branches of the GFN in relation to the pubic tubercle. It was observed that the genital branch (22.3 ± 8.0mm) is closer to the pubic tubercle than the femoral branch (65.6 ± 8.1mm), as it travels through the inguinal canal to exit through the superficial inguinal ring, while the femoral branch remains along the mid-inguinal plane. A study by Rosenberger et al. (2000) reported the femoral branch to be 93 ± 15mm from the pubic tubercle. In the study, measurements for the genital branch were not made from the pubic tubercle, but from the ASIS (56mm). The current study suggests that the pubic tubercle is an alternative landmark, as it is closer to the branches of the GFN and is clinically relevant as it is used as a landmark during procedures. This is supported by the literature (Harmon, 2011; Waldman, 2011; Bugada and Peng, 2015; Waldman, 2016). This is especially true when considering the incision made for the Lichtenstein tension-free inguinal hernia repair, which starts at the pubic tubercle and continues laterally (Lichtenstein et al., 1989; Amid, 2004).

4.7.3. Clinical implications

As highlighted in the previous chapter on the IHN and IIN, the Lichtenstein tension-free inguinal hernia repair is performed in the inguinal area. This procedure is

performed by making a 5cm incision from the pubic tubercle laterally towards the ASIS (Lichtenstein et al., 1989; Amid, 2004). The results of the current study place the genital branch of the GFN within the closest proximity to the incision at 22.3 ± 8.0mm from the pubic tubercle as it exits the superficial inguinal ring, placing the nerve in danger of damage during this procedure. The femoral branch of the GFN is beyond the limit of the incision at a distance of 65.6 ± 8.1mm from the pubic tubercle. Therefore, the femoral branch is less likely to be damaged during the Lichtenstein tension-free inguinal hernia repair, but may be damaged as the standard deviation falls within the area where the incision is made. The short distance of the genital branch of the GFN from the pubic tubercle places it within the path of the incision and makes it more likely to be damaged, which may cause loss of sensation, pain and/or paraesthesia to the groin area.

The importance of the visualization of the genital branch has been reported in some studies (Amid, 2004; Cesmebasi et al., 2015). These studies report that the genital branch, together with the IIN, need to be visualized in order to safely complete the Lichtenstein tension-free inguinal hernia repair. Visualization of these nerves will minimise the probability of damaging them. In GFN blocks, the procedure is performed “blind” by using anatomical landmarks as a guide to locate the nerve branches. The pubic tubercle has been reported as the ideal bony landmark to use in the blocks (Harmon, 2011; Waldman, 2011; Bugada and Peng, 2015; Waldman, 2016). The guidelines for the block of the genital branch of the GFN place the needle insertion site at a safe distance from the nerve. The results of the current study agree with the location of the needle insertion site. The guidelines for the block state that the site is 20mm superolateral to the pubic tubercle (Harmon, 2011; Waldman, 2011; Waldman, 2016) placing the site, located obliquely superolateral from the pubic tubercle, close to the 22.3 ± 8.0mm distance observed in the current study. This ensures that the needle will be in close proximity to the nerve, but will not be in contact with it. Furthermore, the guidelines suggest that the site be placed 20mm superior to this point. This will allow for safe insertion of the needle, advancing it medially towards the pubic tubercle, without intercepting the genital branch of the GFN.

In the blockade of the femoral branch of the GFN, the inguinal ligament is divided into thirds in order to locate the nerve. Thereafter, the needle is inserted at the junction

between the medial two-thirds and the lateral third of the inguinal ligament and advanced towards the nerve medially (Waldman, 2011; Waldman, 2016). For a more accurate positioning of the needle insertion site, the results of the current study suggest that a numeric distance be used from the pubic tubercle to the femoral branch. With that, the nerve can be located by using the pubic tubercle as a consistent bony landmark. Using a consistent landmark such as the pubic tubercle will increase the accuracy of locating the femoral branch of the GFN and thereby decrease the incidence of incomplete blocks as a result of not enough spread of the anaesthetic solution on the nerve. In addition to the risk of incomplete blocks, using a bony landmark and a standard distance to the nerve will decrease the risk of damaging the nerve when inserting the needle.

4.8. Conclusion

The Lichtenstein tension-free inguinal hernia repair is a common procedure that is performed worldwide. The results of the current study agree with the guidelines used for the performance of the procedure. Despite the genital branch of the GFN being in danger during the incision over the superficial ring of the inguinal canal, as well as during regional suturing. Knowing the importance of visualizing the genital branch together with the IHN and IIN, as stated in the guidelines, is supported by the results of the current study. The 50mm incision proposed, places the IIN and genital branch of the GFN in danger, so visualization of these nerves, as recommended by the guidelines, is supported by the results of this study in order to decrease the probability of damaging them.

For the blockade of the femoral and genital branches of the GFN, it is recommended that the pubic tubercle be used as a landmark to assist in the approximation of the location of the GFN. This landmark will be used in conjunction with other vascular landmarks.

The main limitation of the study was the small sample size as a result of exclusion of samples. It is recommended that the sample size be increased and that ultrasound scans be included in the study to correlate the cadaveric anatomy with that of live patients.

4.9. References

AASVANG, E. & KEHLET, H. 2005. Surgical management of chronic pain after inguinal hernia repair. *British Journal of Surgery: Incorporating European Journal of Surgery and Swiss Surgery,* 92**,** 795-801.

AL-DABBAGH, A. 2002. Anatomical variations of the inguinal nerves and risks of injury in 110 hernia repairs. *Surgical and radiologic anatomy,* 24**,** 102-107.

AMID, P. K. 2004. Lichtenstein tension-free hernioplasty: its inception, evolution, and principles. *Hernia,* 8**,** 1-7.

ANLOAGUE, P. A. & HUIJBREGTS, P. 2009. Anatomical variations of the lumbar plexus: a descriptive anatomy study with proposed clinical implications. *Journal of Manual & Manipulative Therapy,* 17**,** 107E-114E.

BUGADA, D. & PENG, P. W. 2015. Ilioinguinal, Iliohypogastric, and Genitofemoral Nerve Blocks. *Regional Nerve Blocks in Anesthesia and Pain Therapy.* Springer.

CELEBI, S., AKSOY, D., CEVIK, B., YILDIZ, A., KURT, S. & DOKUCU, A. I. 2013. An electrophysiologic evaluation of whether open and laparoscopic techniques used in pediatric inguinal hernia repairs affect the genitofemoral nerve. *Journal of pediatric surgery,* 48**,** 2160-2163.

CESMEBASI, A., YADAV, A., GIELECKI, J., TUBBS, R. S. & LOUKAS, M. 2015. Genitofemoral neuralgia: a review. *Clinical Anatomy,* 28**,** 128-135.

CHROUSER, K., VANDERSTEEN, D., CROCKER, J. & REINBERG, Y. 2004. Nerve injury after laparoscopic varicocelectomy. *The Journal of urology,* 172**,** 691-693.

FEIGL, G., DREU, M., ULZ, H., BRESCHAN, C., MAIER, C. & LIKAR, R. 2014. Susceptibility of the genitofemoral and lateral femoral cutaneous nerves to complications from lumbar sympathetic blocks: is there a morphological reason? *British journal of anaesthesia,* 112**,** 1098-1104.

FRITZ, J., DELLON, A. L., WILLIAMS, E. H., ROSSON, G. D., BELZBERG, A. J. & ECKHAUSER, F. E. 2017. Diagnostic Accuracy of Selective 3-T MR Neurography–guided Retroperitoneal Genitofemoral Nerve Blocks for the Diagnosis of Genitofemoral Neuralgia. *Radiology,* 285**,** 176-185.

GINDHA, G., ARORA, D., KAUSHAL, S. & CHHABRA, U. 2015. Variations in origin of the genitofemoral nerve from the lumbar plexuses in North Indian Population (A cadaveric study). *MOJ Anat Physiol,* 1**,** 00015.

GUPTON, M. & VARACALLO, M. 2019. Anatomy, Abdomen and Pelvis, Genitofemoral Nerve.

HARMON, D. B., JACK; LOUGHNANE, FRANK; FINUNCANE, BRENDAN; SHORTEN, GEORGE 2011. Peripheral nerve blocks & peri-operative pain relief. 2nd ed. ed. [St. Louis]: Saunders/Elsevier.

IWANAGA, J., SIMONDS, E., SCHUMACHER, M., KIKUTA, S., WATANABE, K. & TUBBS, R. S. 2019. Revisiting the genital and femoral branches of the genitofemoral nerve: Suggestion for a more accurate terminology. *Clinical Anatomy,* 32**,** 458-463.

JAROW, J. P., ASSIMOS, D. G. & PITTAWAY, D. E. 1993. Effectiveness of laparoscopic varicocelectomy. *Urology,* 42**,** 544-547.

KALE, A., AYTULUK, H. G., CAM, I., BASOL, G. & SUNNETCI, B. 2019. Selective Spinal Nerve Block in Ilioinguinal, Iliohypogastric and Genitofemoral Neuralgia. *Turk Neurosurg,* 29**,** 530-537.

KUMAR, A. & ZAIDI, M. 2017. Ilioinguinal, Iliohypogastric, and Genitofemoral Nerve Pain Syndromes. *Musculoskeletal Sports and Spine Disorders.* Springer.

LICHTENSTEIN, I. L., SHULMAN, A. G., AMID, P. K. & MONTLLOR, M. M. 1989. The tension-free hernioplasty. *The American Journal of Surgery,* 157**,** 188-193.

LYON, E. K. 1945. Genitofemoral causalgia. *Canadian Medical Association Journal,* 53**,** 213.

MAGEE, R. 1942. Genitofemoral causalgia:(a new syndrome). *Canadian Medical Association Journal,* 46**,** 326.

MUENSTERER, O. J. 2008. Genitofemoral nerve injury after laparoscopic varicocelectomy in adolescents. *The Journal of urology,* 180**,** 2155-2158.

PAUL, L. & SHASTRI, D. 2019. Anatomical Variations in Formation and Branching Pattern of the Border Nerves of Lumbar Region. *National Journal of Clinical Anatomy,* 8**,** 057-061.

POULSEN, E. U., WILLUMSEN, H., COLSTRUP, H. & JENSEN, K. 1994. Varicocele of the testis. A comparison between laparoscopic and conventional surgery. *Ugeskrift for laeger,* 156**,** 5683-5685.

RAB, M. & DELLON, A. 2001. Anatomic variability of the ilioinguinal and genitofemoral nerve: implications for the treatment of groin pain. *Plastic and reconstructive surgery,* 108**,** 1618-1623.

ROSENBERGER, R., LOEWENECK, H. & MEYER, G. 2000. The cutaneous nerves encountered during laparoscopic repair of inguinal hernia. *Surgical endoscopy,* 14**,** 731-735.

SAMPATH, P., YEO, C. J. & CAMPBELL, J. N. 1995. Nerve injury associated with laparoscopic inguinal herniorrhaphy. *Surgery,* 118**,** 829-833.

SCHULSTER, M. L., COHN, M. R., NAJARI, B. B. & GOLDSTEIN, M. 2017. Microsurgically assisted inguinal hernia repair and simultaneous male fertility procedures: Rationale, technique and outcomes. *The Journal of Urology*.

SEHGAL, N. 2019. Genitofemoral Nerve. *Pain.* Springer.

SHANTHANNA, H. 2014. Successful treatment of genitofemoral neuralgia using ultrasound guided injection: a case report and short review of literature. *Case reports in anesthesiology,* 2014.

TAGLIAFICO, A., BIGNOTTI, B., CADONI, A., PEREZ, M. M. & MARTINOLI, C. 2015. Anatomical study of the iliohypogastric, ilioinguinal, and genitofemoral nerves using high-resolution ultrasound. *Muscle & nerve,* 51**,** 42-48.

VERSTRAELEN, H., DE ZUTTER, E. & DE MUYNCK, M. 2015. Genitofemoral neuralgia: adding to the burden of chronic vulvar pain. *Journal of pain research,* 8**,** 845.

WALDMAN, S. D. 2011. Pain management. Second Edition ed. Philadelphia, PA: Elsevier/Saunders.

WALDMAN, S. D. 2016. *Atlas of Pain Management Injection Techniques E-Book*, Elsevier Health Sciences.

Chapter 5 – Lateral femoral cutaneous nerve (LFCN)

5.1. Introduction and problem statement

Meralgia paraesthetica is a condition that causes sensations of burning, paraesthesia, pain and numbness in the anterior thigh. This sensation is due to damage to the LFCN as a result of trauma to the inguinal region, compression of the nerve along its course to the thigh, or due to iatrogenic injury during surgery (Harney and Patijn, 2007; Ataizi et al., 2019). Incidence of damage to the LFCN has been reported in the literature at a rate of 7-10% (Ataizi et al., 2019; Aras et al., 2019)

In order to accurately diagnose a patient or perform procedures in the region of the LFCN, it is essential that the anatomy of the LFCN and its relation to bony landmarks be understood and easily located pre- and peri-operatively. The anatomy is equally important to understand when using imaging modalities during invasive procedures.

5.2. Literature review

5.2.1. Lateral femoral cutaneous nerve

The LFCN arises from the ventral rami of the L2 and L3 spinal nerves. After emerging from the lateral border of the psoas major muscle, it descends obliquely over the iliacus muscle towards the ASIS. Along its descent it runs posterior to the inguinal ligament before entering the thigh. Thereafter, it gives sensory innervation to skin over the lateral and anterior surfaces of the thigh up to the level of the knee (Shannon et al., 1994; Anloague and Huijbregts, 2009).

A study by Anloague and Huijbregts (2009) found that there was variation with regard to the root values of the LFCN. The root values were reported to be from L1 and L2 in four of 64 cases, while the LFCN described in literature to originate from the L2 and L3 spinal nerve rami. An additional variation was observed in the early bifurcation of the nerve at the level of the inguinal ligament (Anloague and Huijbregts, 2009).

Accurate knowledge of the anatomy of the LFCN will assist in the successful performance of the LFCN block for analgesia after total hip arthroplasty (Vandebroek et al., 2014; Ozaki et al., 2017). A study by Shannon et al. (1994) reported a nerve block failure of approximately 60% as a result of LFCN variation. A prevalence of 42% failure was reported by Thybo et al. (2016). The danger that the LFCN is placed under

during iliac crest bone harvest has been reported in the literature as well. This is mainly because of its close relation to the ASIS. Compression of the LFCN between the inguinal ligament and bony elements has also been reported. Both the latter two conditions will present as paraesthesia of the anterolateral thigh, a condition known as meralgia paraesthetica (Massey, 1980; Kurz et al., 1989; Banwart et al., 1995).

5.2.2. Iliac crest bone graft

An iliac crest bone graft is commonly performed for arthroplasty across the body. The incidence rate of complications during the procedure, including nerve damage causing meralgia paraesthetica, has been reported at 2 – 40% (Armaghani et al., 2016; Fontaine et al., 2016; Sheha et al., 2018). For the procedure, the patient is placed in a lateral decubitus position, where the side that is to be operated on faces superiorly (Malatray et al., 2018). To determine the incision initiation site, the ASIS and the iliac crest are palpated and marked by drawing their outlines on the skin of the patient. The incision is then made 20 – 30mm posterolateral to the ASIS. The length of the incision, further posterior to the incision initiation site, is determined by the size of the bone graft that will be removed (Armaghani et al., 2016; Suda et al., 2019). During this procedure, the LFCN may be damaged, should it lie on the iliac crest or should the bone that is grafted be from the ASIS, as the LFCN lies close to it.

5.2.3. LFCN block

The LFCN block is performed in the inguinal region for anaesthesia and analgesia during and after procedures done in the inguinal region while the patient is in a supine position. The procedures can be performed using a landmark or an ultrasound-guided technique. In the landmark technique, the ASIS is first palpated. The needle insertion site is located 20mm medial to the ASIS, just inferior to the inguinal ligament. In the ultrasound-guided technique, the linear probe is placed near the ASIS, at a perpendicular angle to the skin. Once the LFCN is identified, the needle is inserted and advanced towards the nerve, ensuring not to pierce it, thereby injuring it. Thereafter, the anaesthetic solution is injected and gravity will assist to spread it to the nerve (Jankovic, 2008; Nersesjan et al., 2018; Aras et al., 2019).

In these procedures, the ASIS is an important landmark in the location of the LFCN. Knowledge of the anatomy of the LFCN in relation to the ASIS will assist in the location of the nerve for safe performance of an iliac crest bone graft and a LFCN block.

5.3. Aim

The aim of this study was to accurately describe the anatomy of the LFCN from its paravertebral origin to the point where it enters the thigh in relation to the ASIS for the iliac crest bone graft and LFCN block.

5.4. Research objectives

1. Describe the root value origins of the LFCN and its variations by observing the roots as they exit the vertebral column laterally.
2. Describe the location of the LFCN in the inguinal region using the distance from the ASIS to the LFCN where it crosses the inguinal ligament.
3. Use the results of the study to determine the anatomical basis of the safe performance of the iliac crest bone graft and LFCN block.

5.5. Materials and methods

5.5.1. Root values of the LFCN

In order to observe the roots of the LFCN, bilateral dissection of the psoas major muscle of 105 formalin-fixed cadavers (59 males and 46 females, 70 ± 15 years) were performed, as outlined under the “Materials and methods” in chapter two on the lumbar plexus. To observe the root contributions of the LFCN, the fibres of the LFCN were carefully separated from those of the ON. The level at which each root contribution originated was followed back to the intervertebral foramen it exited from. After the roots were identified, the LFCN was followed as it descended inferolaterally towards the thigh (Figure 1).

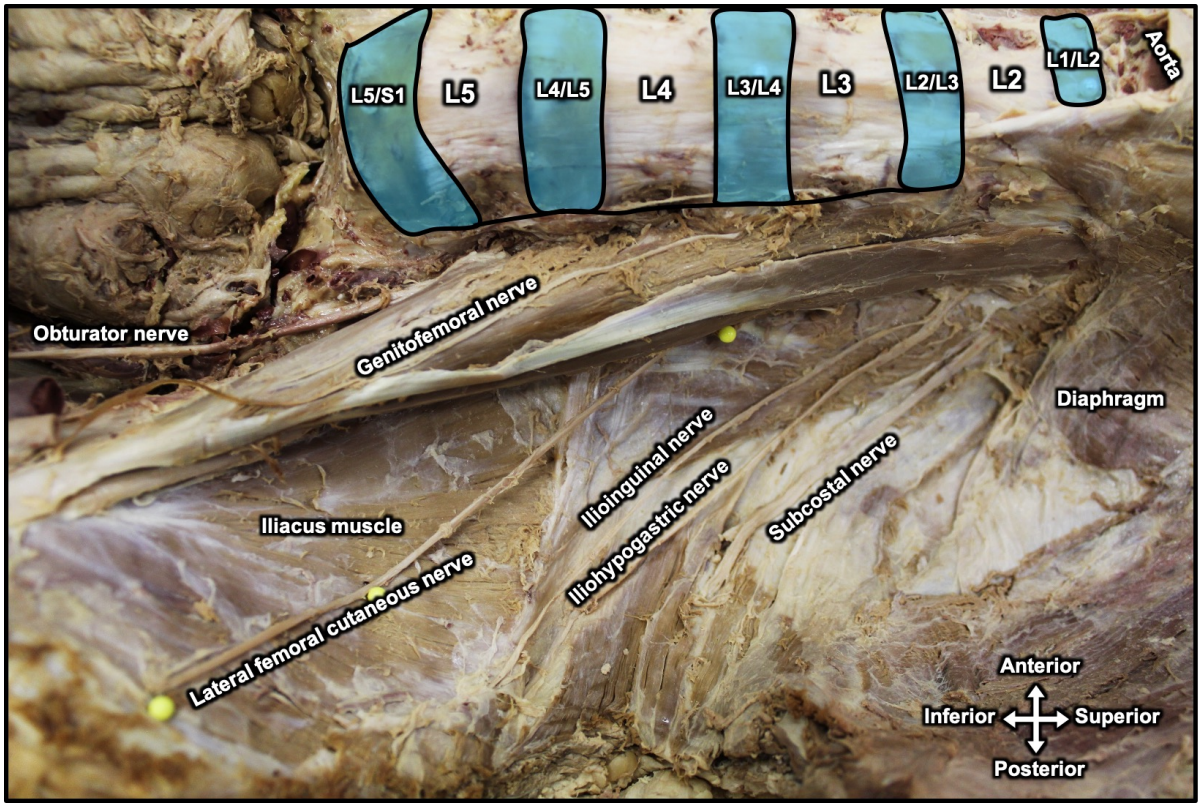

Figure 17: Anterolateral view of the posterior abdominal wall indicating the course of the LFCN lateral to the psoas major muscle and its course on the iliacus muscle towards the thigh

5.5.2. Relation of the LFCN to the ASIS

To determine the location of the LFCN within the inguinal region, the oblique distance from the most anterior point of the ASIS, to the lateral border of the LFCN, where it passes deep to the inguinal ligament to enter the thigh, was measured. This distance was measured with the use of a mechanical dial sliding calliper (accuracy = 0.01mm). The calliper was recalibrated after each measurement.

5.5.3. Clinical applications

To correlate the results of this study with the current procedural guidelines for the iliac crest bone graft and the LFCN block, a study of the literature was conducted using the PubMed, Science Direct, Ovid and Google Scholar journal databases, as well as current anatomy, surgical and anaesthetic textbooks/guidelines.

5.5.4. Statistical analysis

The statistical tests, Chi-squared, Shapiro-Wilks, paired t-test and Pearson's correlation, were performed as outlined in chapter 3 on the IHN and IIN.

5.6. Results

5.6.1. Root values and relation to inguinal ligament

The roots of the LFCN were observed as they exit their intervertebral foramina paravertebrally. On the left side (n = 105), the LFCN in males stemmed from the L2 and L3 ventral rami in 51 cases (48.57%), from L2 alone in 7 cases (6.67%) and from L3 alone in 1 case (0.95%). In females, the LFCN on the left side was observed as originating from L2 and L3 in 37 cases (35.24%), from L2 alone in 9 cases (8.57%), while there were no instances of any origin from L3 alone (Figure 18). On the right side (n = 105) the LFCN in males originated from L2 and L3 in 53 cases (50.48%), from L2 alone in 6 cases (5.71%), whie there were no observed origins from L3. In females, the LFCN was seen coming off from L2 and L3 in 39 cases (37.14%), from L2 alone in 7 cases (6.67%) and no cases of an only L3 origin were observed (Figure 19).

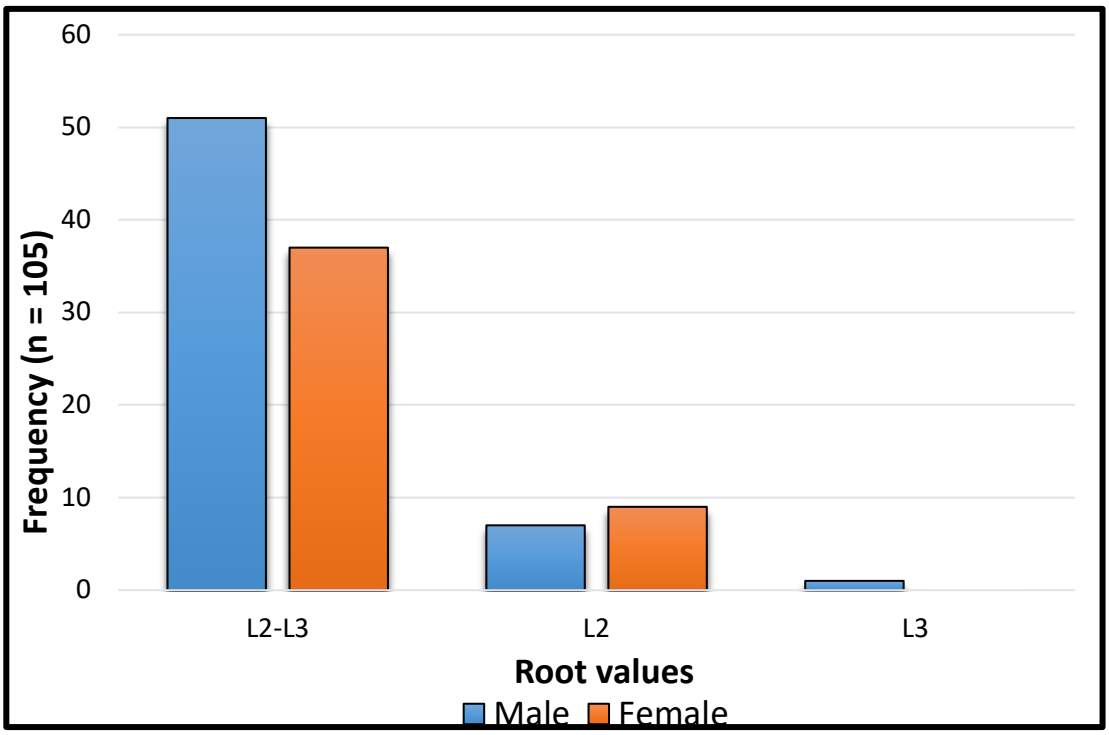

Figure 18: Histogram showing the frequency of the origins of the LFCN on the left side from L2-L3, L2 and L3 in males and females

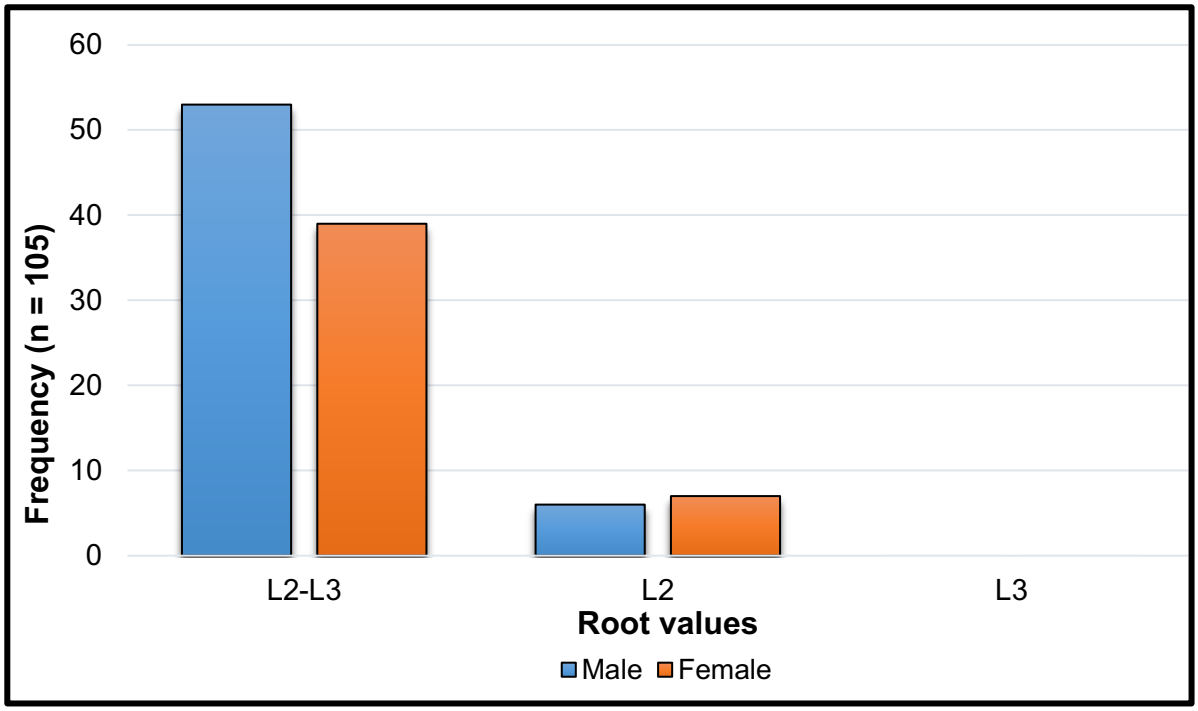

Figure 19: A histogram presenting the frequency of the origins of the LFCN from L2-L3, L2 and L3 on the right side in males and females

Contingency tables were drawn up to investigate whether sex had an influence on the root values of the LFCN. The Chi-squared test revealed no statistically significant influence of sex on the left ($p = 0.39$) and right ($p = 0.436$) sides. This permitted the sample to be pooled, by sides, into 88 cases (83.81%) of L2-3 origin, 16 cases (15.24%) of L2 origin and an L3 origin in 1 case (0.95%) on the left side. On the right side the LFCN originate from L2-L3 in 92 cases (87.62%), L2 in 13 cases (12.38%) and no observed cases of origin from only L3 (Figure 20). Another Chi-squared test of the sides presented a statistically significant difference between the left and right sides ($p < 0.01$).

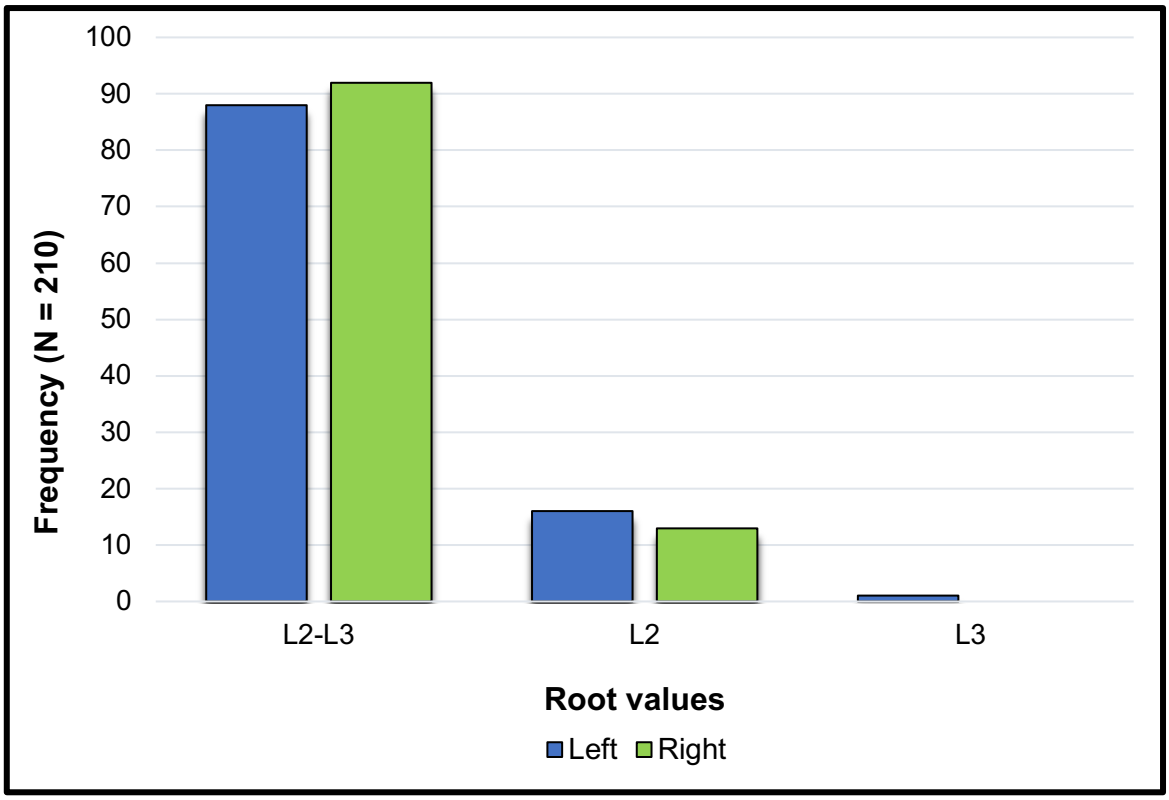

Figure 20: A histogram displaying the pooled results of the root value origins of the LFCN on the left and right sides

The LFCN, after exiting lateral to the psoas major muscle, descended anterolaterally towards the inguinal ligament and ASIS. In all samples (N = 210), the nerve was observed running deep to the inguinal ligament to enter the thigh.

5.6.2. Relation of the LFCN to the ASIS

The mean distances from the ASIS to the LFCN were 9.4 ± 2.9mm on the left side and 8.8 ± 2.3mm on the right side. A Shapiro-Wilk test indicated that the measurements from the ASIS to the LFCN were normally distributed on both the left and the right sides ($p > 0.05$). Thereafter, a paired t-test revealed no statistically significant difference between the sides ($p = 0.85$). The pooled results yielded a mean distance of 9.1 ± 2.7mm (CI – 8.7; 9.5).

Inter- and intra-observer reliability test results may be found in Annexure A.

5.6.3. Clinical applications

To obtain relevant literature, a study was conducted using the following keywords in the databases: *lateral femoral cutaneous nerve block, lateral femoral cutaneous nerve injury, lateral femoral cutaneous nerve iliac procedures.* The study yielded the iliac crest bone graft and the LFCN block as the most relevant procedures for correlation with the results of the current study.

5.7. Discussion

5.7.1. Root values and relation to the inguinal ligament

A review of the literature has shown that the LFCN had some variability in the root values from which it originates. In this study, it predominantly originated from the commonly described roots L2-L3 on both the left (83.81%) and the right (87.62%) sides. This was followed by an L2 origin in 15.24% of cases on the left side and 12.38% on the right side. The least common origin was from L3, where there was only a 0.95% prevalence on the left side and none on the right side. A study of the literature indicated that little research had been done on the nerve roots of the LFCN. A study by Anloague and Huijbregts (2009) revealed results which correlate with those of this study. In 34 lumbar left and right sides, they observed L2-L3 root origin in 19 cases, L1-L2 in 4 cases and L2 origin in one case. A recent study by Haładaj et al. (2018), reported 47 cases of L2-L3 origin (n = 80), 12 cases of L1-L20origin and 9 cases of L2 origin. An origin that was not observed in the current study was an origin from the femoral nerve, which was observed in 6 cases in the study by Haładaj et al. (2018). A comparison of these results is presented in Table 10.

Table 10: Comparison of the results of different studies into the root value origins of the LFCN

Study	Country	n	L1-L2		L2-L3		L2		L3		Femoral	
Anloague and Huijbregts (2009)	USA	34	4		29		1		-		-	
Haładaj et al. (2018)	Poland	74	12		47		9		-		6	
Current study	South Africa	210	**L**	**R**	**L**	**R**	**L**	**R**	**L**	**R**	**L**	**R**
			-	-	88	92	16	13	1	-	-	-

L = Left and R = Right

The LFCN first descended over the quadratus lumborum muscle, then over the iliacus muscle, before it passed deep to the inguinal ligament in all the samples. A meta-analysis of 18 studies by Tomaszewski et al. (2016) reported the location of the LFCN medial to the ASIS/sartorius muscle in 86.8% of cases, superficial to the inguinal ligament in 0.9% and other locations accounting for the remaining 12.3%. The studies that were analysed in the meta-analysis agree with the results of this study, namely that the LFCN courses mostly medial to the ASIS and deep to the inguinal ligament (Aszmann et al., 1997; De Ridder et al., 1999; Murata et al., 2000; Damarey et al., 2009; Üzel et al., 2011).

5.7.2. Relation of the LFCN to the ASIS

The use of bony landmarks to locate nerves is reliable because of the consistency that it affords. The ASIS is an important landmark that has been used in studies on the LFCN as it enters the thigh (Rudin et al., 2016; Tomaszewski et al., 2016; Nielsen et al., 2018). A study by Reinpold et al. (2015) reported a distance from the ASIS to the LFCN of 6mm lateral (n = 3), 20 ± 9mm medial (n = 55), 6 ± 4mm cranial and 5 ± 3mm caudal to the ASIS. A study by Grothaus et al. (2005) reported a distance of 36 ± 20 mm medial to the ASIS in 29 cadavers' sides. In another study of 39 LFCNs by Hanna (2017) the researcher observed the LFCN at an average distance of 65mm medial (n = 35) to ASIS and 60mm (n = 4) lateral to ASIS. A LFCN is defined as lateral to the ASIS if it is observed crossing over the anterior part of the iliac crest.

In a study by Murata et al. (2000), the position of the LFCN in relation to the ASIS was divided into four types according to their location and distance from the ASIS. Type A was lateral to the ASIS, traversing over the iliac crest, at a distance exceeding 20mm. Type B was similar to Type A in its location, but differed in that the nerve was at a distance of less that 20mm from the ASIS. The nerves classified as Type C entered the thigh at the ASIS, while Type D nerves were observed medial to ASIS and deep to the inguinal ligament. In the current study, all the nerves were observed as Type D, at an average distance of 9.1 ± 2.7mm. Lee et al. (2017) documented a similar observation, where all the LFCNs (n = 60) were located inferomedial to the ASIS, as it crossed the inguinal ligament, at an average distance of 8.8 ± 11.7mm. The absence

of the other types, as compared to the literature, suggests variability across study populations. This is essential to keep in mind when preparing to perform procedures on and in the area of the LFCN in the inguinal region.

5.7.3. Clinical implications

Safety is the main priority in the performance of any procedure. Accurate knowledge of the current anatomy of essential areas of access for clinical and surgical procedures is essential for the successful execution of these procedures. The location and course of the LFCN in relation to the ASIS should be considered prior to the start of any invasive procedure in order to avoid damaging the LFCN during iliac crest bone grafts involving the anterior region of the ilium. Meralgia paraesthetica, as a result of the iliac crest bone graft, has been reported in the literature, resulting in pain, a burning sensation and numbness in the anterior thigh (De Ridder et al., 1999; Murata et al., 2000; Ahlmann et al., 2002; Paul et al., 2015; Lee et al., 2017).

The results of the current study place the LFCN closer to the ASIS, medially, than in the literature (Murata et al., 2000; Rosenberger et al., 2000; Reinpold et al., 2015; Hanna, 2017). Although the LFCN was not observed traversing the iliac crest, the close proximity of 9.1 ± 2.7mm to the ASIS places it in danger during iliac crest bone grafts, should it be performed too far anteriorly. The bone graft is performed for transfer of excised bone to areas where there is an absence thereof. The results of the current study concur with the current outlined guideline of beginning the skin incision 20-30mm posterior to the ASIS in order to access the iliac crest (Armaghani et al., 2016; Shin and Tornetta III, 2016; Suda et al., 2019). The incision will allow for a safe distance from the LFCN and keep it from being damaged. Although the current study and that of Lee et al. (2017) did not report any cases of the LFCN lateral to the ASIS, it is important to note and consider reports of variations where the LFCN crossed over the iliac crest and could be in danger during the procedure. It is important to use the ASIS as a palpable landmark for locating the LFCN.

Having an understanding of the position and course of the LFCN is also essential in the performance of a LFCN block, where it is imperative that the needle be inserted as close to the LFCN as possible in order to successfully block the nerve. Although the LFCN block is predominantly performed with the aid of ultrasound, it is important

that the operator understands the anatomy of the LFCN in order to accurately track the course of the needle towards the nerve (Özçakar et al., 2015; Aras et al., 2019). Understanding the various locations of the LFCN in relation to the ASIS and approximate distance from the ASIS, will allow the ultrasound operator to accurately locate the nerve much quicker, decreasing the time necessary to perform the block. A study by Nersesjan et al. (2018) reported a 15% (n = 20) block failure rate using ultrasound guidance. The researchers suggested that failure was as a result of variation in the course of the LFCN, therefore the anaesthetic solution did not spread to the nerves. The suggestions of the study reiterate the importance of understanding the anatomy of the LFCN, even with the assistance of ultrasound.

5.8. Conclusion

Meralgia paraesthetica is a condition where the LFCN is injured or compressed, causing pain in the anterior thigh. The iliac bone graft is a procedure over the iliac crest where the nerve is in danger of iatrogenic injury. Surgeons should keep the proximity and reported variations of the relative positions of the LFCN to the ASIS in mind when performing the iliac bone graft to avoid damaging the nerve. When performing the LFCN block, it is important to consider the relation of the LFCN to the ASIS – in this study it was found approximately 1cm medial to the ASIS in all cases – for easier identification of the nerve when performing the procedure using a landmark or ultrasound-guided technique.

The study had a limitation in that the cadavers had already been dissected and the branches were not able to be followed into the thigh. This is because the course and area of distribution of the nerve were disturbed and would not be trustworthy. It is recommended that further studies be conducted on the LFCN in the thigh on cadavers and the results of the cadaver study should be supplemented by a ultrasound study. It is further suggested that the ultrasound component also includes measurements of the LFCN to the ASIS.

5.9. References

AHLMANN, E., PATZAKIS, M., ROIDIS, N., SHEPHERD, L. & HOLTOM, P. 2002. Comparison of anterior and posterior iliac crest bone grafts in terms of harvest-site morbidity and functional outcomes. *JBJS,* 84**,** 716-720.

ANLOAGUE, P. A. & HUIJBREGTS, P. 2009. Anatomical variations of the lumbar plexus: a descriptive anatomy study with proposed clinical implications. *Journal of Manual & Manipulative Therapy,* 17**,** 107E-114E.

ARAS, B., ADIGUZEL, E. & TOK, F. 2019. Blind Versus Ultrasound Guidance Injections: Lateral Femoral Cutaneous Nerve Blockage Revisited/Lateral Femoral Kutanoz Sinirinin Kor ve Ultrason Esliginde Yapilan Blokajinin Degerlendirilmesi. *Turkish Journal of Neurology,* 25**,** 54-58.

ARMAGHANI, S. J., EVEN, J. L., ZERN, E. K., BRALY, B. A., KANG, J. D. & DEVIN, C. J. 2016. The evaluation of donor site pain after harvest of tricortical anterior iliac crest bone graft for spinal surgery: a prospective study. *Spine,* 41**,** E191-E196.

ASZMANN, O. C., DELLON, E. S. & DELLON, A. L. 1997. Anatomical course of the lateral femoral cutaneous nerve and its susceptibility to compression and injury. *Plastic and reconstructive surgery,* 100**,** 600-604.

ATAIZI, Z. S., ERTILAV, K. & ERCAN, S. 2019. Surgical options for meralgia paresthetica: long-term outcomes in 13 cases. *British journal of neurosurgery,* 33**,** 188-191.

BANWART, J. C., ASHER, M. A. & HASSANEIN, R. S. 1995. Iliac crest bone graft harvest donor site morbidity: a statistical evaluation. *Spine,* 20**,** 1055-1060.

DAMAREY, B., DEMONDION, X., BOUTRY, N., KIM, H. J., WAVREILLE, G. & COTTEN, A. 2009. Sonographic assessment of the lateral femoral cutaneous nerve. *Journal of Clinical Ultrasound,* 37**,** 89-95.

DE RIDDER, V., DE LANGE, S. & POPTA, J. V. 1999. Anatomical variations of the lateral femoral cutaneous nerve and the consequences for surgery. *Journal of orthopaedic trauma,* 13**,** 207-211.

FONTAINE, V., VILLENEUVE, P., BELZILE, E. & LAFLAMME, M. 2016. Hernia through an Iliac Crest Bone Graft Harvest Site: Two Cases Treated Differently. *J Clin Case Rep,* 6**,** 2.

GROTHAUS, M. C., HOLT, M., MEKHAIL, A. O., EBRAHEIM, N. A. & YEASTING, R. A. 2005. Lateral femoral cutaneous nerve: an anatomic study. *Clinical Orthopaedics and Related Research (1976-2007),* 437**,** 164-168.

HAŁADAJ, R., WYSIADECKI, G., MACCHI, V., DE CARO, R., WOJDYN, M., POLGUJ, M. & TOPOL, M. 2018. Anatomic variations of the lateral femoral cutaneous nerve: remnants of atypical nerve growth pathways revisited by intraneural fascicular dissection and a proposed classification. *World neurosurgery,* 118**,** e687-e698.

HANNA, A. 2017. The lateral femoral cutaneous nerve canal. *Journal of neurosurgery,* 126**,** 972-978.

HARNEY, D. & PATIJN, J. 2007. Meralgia paresthetica: diagnosis and management strategies. *Pain Medicine,* 8**,** 669-677.

JANKOVIC, D. 2008. *Regional Nerve Blocks and Infiltration Therapy: Textbook and Color Atlas*, John Wiley & Sons.

KURZ, L. T., GARFIN, S. R. & BOOTH JR, R. E. 1989. Harvesting autogenous iliac bone grafts: a review of complications and techniques. *Spine,* 14**,** 1324-1331.

LEE, S. H., SHIN, K. J., GIL, Y. C., HA, T. J., KOH, K. S. & SONG, W. C. 2017. Anatomy of the lateral femoral cutaneous nerve relevant to clinical findings in meralgia paresthetica. *Muscle & nerve,* 55**,** 646-650.

MALATRAY, M., AL QAHTANI, T., MONNEUSE, O., PIBAROT, V. & WEGRZYN, J. 2018. Bone and parietal anterior iliac crest reconstruction for trans-iliac hernia after tricortical graft harvesting: An original technique. *Orthopaedics & Traumatology: Surgery & Research,* 104**,** 1069-1072.

MASSEY, E. 1980. Meralgia paresthetica secondary to trauma of bone graft. *The Journal of trauma,* 20**,** 342-343.

MURATA, Y., TAKAHASHI, K., YAMAGATA, M., SHIMADA, Y. & MORIYA, H. 2000. The anatomy of the lateral femoral cutaneous nerve, with special reference to the harvesting of iliac bone graft. *JBJS,* 82**,** 746.

NERSESJAN, M., HÄGI-PEDERSEN, D., ANDERSEN, J., MATHIESEN, O., DAHL, J., BROENG, L. & THYBO, K. 2018. Sensory distribution of the lateral femoral cutaneous nerve block–a randomised, blinded trial. *Acta Anaesthesiologica Scandinavica,* 62**,** 863-873.

NIELSEN, T. D., MORIGGL, B., BARCKMAN, J., KØLSEN-PETERSEN, J. A., SØBALLE, K., BØRGLUM, J. & BENDTSEN, T. F. 2018. The lateral femoral

cutaneous nerve: description of the sensory Territory and a novel ultrasound-guided nerve block technique. *Regional Anesthesia & Pain Medicine,* 43**,** 357-366.

OZAKI, Y., HOMMA, Y., BABA, T., SANO, K., DESROCHES, A. & KANEKO, K. 2017. Spontaneous healing of lateral femoral cutaneous nerve injury and improved quality of life after total hip arthroplasty via a direct anterior approach: Survey at average 12.8 and 26.2 months of follow-up. *Journal of Orthopaedic Surgery,* 25**,** 2309499016684750.

ÖZÇAKAR, L., KARA, M., CHANG, K.-V., ÇARL, A. B., AKKAYA, N., TOK, F., CHEN, W.-S., WANG, T.-G., TEKIN, L. & ULASL, A. M. 2015. Nineteen reasons why physiatrists should do musculoskeletal ultrasound: EURO-MUSCULUS/USPRM recommendations. *American journal of physical medicine & rehabilitation,* 94**,** e45-e49.

PAUL, S., NUNES, S. E. V. & BRONKHORST, M. W. 2015. Anatomical variations of the lateral femoral cutaneous nerve and iatrogenic injury after autologous bone grafting from the iliac crest. *Journal of orthopaedic trauma,* 29**,** 549-553.

REINPOLD, W., SCHROEDER, A., SCHROEDER, M., BERGER, C., ROHR, M. & WEHRENBERG, U. 2015. Retroperitoneal anatomy of the iliohypogastric, ilioinguinal, genitofemoral, and lateral femoral cutaneous nerve: consequences for prevention and treatment of chronic inguinodynia. *Hernia,* 19**,** 539-548.

RUDIN, D., MANESTAR, M., ULLRICH, O., ERHARDT, J. & GROB, K. 2016. The anatomical course of the lateral femoral cutaneous nerve with special attention to the anterior approach to the hip joint. *JBJS,* 98**,** 561-567.

SHANNON, J., LANG, S., YIP, R. & GERARD, M. 1994. Lateral femoral cutaneous nerve block revisited. A nerve stimulator technique. *Regional anesthesia,* 20**,** 100-104.

SHEHA, E. D., MEREDITH, D. S., SHIFFLETT, G. D., BJERKE, B. T., IYER, S., SHUE, J., NGUYEN, J. & HUANG, R. C. 2018. Post-operative pain following posterior iliac crest bone graft harvesting in spine surgery: a prospective, randomized trial. *The Spine Journal,* 18**,** 986-992.

SHIN, S. R. & TORNETTA III, P. 2016. Donor site morbidity after anterior iliac bone graft harvesting. *Journal of orthopaedic trauma,* 30**,** 340-343.

SUDA, A. J., SCHAMBERGER, C. T. & VIERGUTZ, T. 2019. Donor site complications following anterior iliac crest bone graft for treatment of distal radius fractures. *Archives of orthopaedic and trauma surgery,* 139**,** 423-428.

THYBO, K., MATHIESEN, O., DAHL, J., SCHMIDT, H. & HÄGI-PEDERSEN, D. 2016. Lateral femoral cutaneous nerve block after total hip arthroplasty: a randomised trial. *Acta Anaesthesiologica Scandinavica,* 60**,** 1297-1305.

TOMASZEWSKI, K., POPIELUSZKO, P., HENRY, B., ROY, J., SANNA, B., KIJEK, M. & WALOCHA, J. 2016. The surgical anatomy of the lateral femoral cutaneous nerve in the inguinal region: a meta-analysis. *Hernia,* 20**,** 649-657.

ÜZEL, M., AKKIN, S. M., TANYELI, E. & KOEBKE, J. 2011. Relationships of the lateral femoral cutaneous nerve to bony landmarks. *Clinical Orthopaedics and Related Research®,* 469**,** 2605-2611.

VANDEBROEK, A., VERTOMMEN, M., HUYGHE, M. & VAN HOUWE, P. 2014. Ultrasound guided femoral nerve block and lateral femoral cutaneous nerve block for post-operative pain control after primary hip arthroplasty: a retrospective study. *Acta Anæsthesiologica Belgica,* 65**,** 39-44.

Chapter 6 – Obturator nerve (ON)

6.1. Introduction and problem statement

The ON is a motor and sensory nerve that innervates the medial compartment of the thigh, the knee and hip. It is one the terminal branches of the lumbar plexus and has a unique course as it is the only branch that runs medial to the psoas major muscle.

Damage to the ON may present with motor and/or sensory fallouts such as paraesthesia or loss of sensation to the medial third of the thigh and weakness of the adductor muscles, which may lead to atrophy of the medial compartment. (Ghaemmaghami et al., 2009; Bachar Avnieli et al., 2018; Kanezaki et al., 2018; Osório et al., 2018). The ON and its branches are most frequently injured by the trocars used in transobturator tape (TOT) and tension-free vaginal tape-obturator (TVT-O) procedures for the treatment of urinary incontinence in males and females, respectively. The nerves are injured as the trocars are passed through the obturator foramen in order to secure them, in close proximity to the pathway of the ON in the pelvis and its branches as it exits in the medial thigh (Aydogmus et al., 2014; Kuponiyi et al., 2014; Sanderson and Ghomi, 2015; Tshabalala et al., 2016). Clinicians must understand the detailed anatomy of the ON throughout its course in order to do proper pre-operative planning of their procedures and to be able to adapt to variable anatomy observed peri-operatively.

6.2. Literature review

6.2.1. Obturator nerve (ON)

The ON arises from the ventral rami of the L2, L3 and L4 spinal nerves. The ON is the only nerve of the lumbar plexus to emerge from the medial border of the psoas major muscle. It then descends towards the pelvis, running on the pelvic brim and then entering the lesser pelvis at the level of the sacroiliac joint. The nerve passes through the obturator foramen and the obturator canal, to then enter the medial compartment of the thigh. After entering the obturator canal, the nerve terminates into its anterior and posterior branches to give motor supply to the medial compartment of the thigh. The anterior division of the ON innervates the adductor longus, adductor brevis and gracilis muscles, whereby the posterior division innervates the obturator externus and adductor magnus muscles. The anterior and posterior divisions are separated by the obturator externus muscle as the ON courses into the medial compartment of the

thigh. The anterior division of the ON gives additional sensory innervation to the skin over the medial thigh, up to the level of the knee (Anagnostopoulou et al., 2009; Anloague and Huijbregts, 2009; Nielsen et al., 2017; Yoshida et al., 2017).
Some studies have reported variations in the terminal motor branches of the ON, with the anterior division innervating the pectineus muscle and the posterior division giving additional supply to the adductor brevis muscle, together with the anterior division (Anagnostopoulou et al., 2009; Vandana et al., 2011).

6.2.2. Obturator nerve block

The ON block is a procedure performed to provide analgesia and anaesthesia during hip and knee surgery. The procedure is commonly used in conjunction with ultrasound imaging in order to identify the ON and its branches in the medial compartment of the thigh. To begin the procedure, the patient is placed in a lithotomy position with the hip abducted and laterally rotated. The probe is placed distal to the inguinal crease on the medial side; this allows the operator to visualize the fascial planes between the pectineus-, adductor longus- and adductor brevis muscles. Once the ON is observed within the fascial planes between the muscles, the needle is inserted and advanced towards the nerve until it is in a safe proximity to the ON and/or its branches. The anaesthetic solution is then injected (Runge et al., 2016; Nielsen et al., 2017; Yoshida et al., 2017).

6.2.3. Transobturator procedures

Stress urinary incontinence (SUI) is a common condition where there is involuntary leakage of urine after coughing, sneezing, exertion or laughing, any activity which increases the intra-abdominal pressure (Ross et al., 2016; Kurkijärvi et al., 2016; Capobianco et al., 2018). Menopause, obesity and pregnancy are amongst the reported bases of pelvic floor weakness that causes SUI in females (Jahromi et al., 2015; Jung et al., 2016; de Mattos Lourenco et al., 2018). In males, SUI has been commonly observed after surgical procedures involving the prostate (Friedl et al., 2017; Angulo et al., 2017; Angulo et al., 2018; Sacco et al., 2018). To treat the condition, a mesh is placed against the urethra using needles that are passed through the obturator foramen bilaterally (Bozkurt et al., 2015; Huri et al., 2015; Friedl et al., 2017).

Female patients are placed in the lithotomy position. A vertical incision of 20mm is made 10mm inferior to the urethral meatus. All soft tissue and fascia on either side of the urethra is dissected out laterally towards the ishiopubic ramus until the urethra has been clearly identified (Dmochowski et al., 2012; Huri et al., 2015; Barbier et al., 2018). For the outside-in technique, a 10mm vertical incision is made in the upper medial thigh, distal to the origin of the adductor longus muscle at the body of the pubis. The needle is then introduced through the incision and advanced into the medial compartment of the thigh through the obturator foramen into the perineum, ensuring that the trajectory of the needle is as medial as possible. A finger is inserted through the vaginal incision and is pushed laterally in order to palpate the ischiopubic ramus and guide the needle tip (ElSheemy et al., 2015; Huri et al., 2015; Barbier et al., 2018).

With the inside-out technique, a vertical 20mm incision inferior to the urethra is made and dissection of the tissue and fascia is done. Instead of passing the needle through the thigh, the needle is introduced through the vaginal incision. The needle is advanced as close to the ischiopubic ramus as possible before it is allowed to pierce the obturator internus muscle and the obturator membrane; this allows the needle to be passed through the obturator foramen into the thigh. The tip of the needle is pushed until it pierces the skin of the medial compartment of the thigh to exit (Huri et al., 2015; ElSheemy et al., 2015).

The procedure for males is similar to the techniques used in females, where the patient is first placed in the lithotomy position. An approximately 50mm midsaggital incision is made from the inferior surface of the scrotum to near the perineal body. All tissue and fascia is dissected away in order to expose the bulbospongiosus muscle at the bulb of the penis. This dissection is extended laterally until the ishiocavernosus muscles are exposed bilaterally along the ischiopubic rami. The procedures for the introduction of the needle and the trajectory thereof in the inside-out and outside-in techniques are as described earlier in the female procedure. The difference only exists where the needle will be introduced in relation to the bulbospongiosus- and ischiocavernosus muscles in males, as opposed to introducing the needle in relation to the urethra in females (Sacco et al., 2018; Hoda et al., 2012; Seweryn et al., 2012)

6.3. Aim

The aim of this study was to accurately describe the course of the ON in the abdomen, pelvis and the thigh and its location within the obturator foramen for correlation with current procedural guidelines for the performance of the ON block and transobturator procedures.

6.4. Research objectives

1. Describe the spinal nerve rami that contribute to the formation of the ON, as well as the course of the nerve throughout the abdomen, pelvis and thigh.
2. Observe the branching pattern of the ON as it enters the thigh.
3. Determine the location of the ON within the obturator foramen by measuring the distance from the nerve to the most superior-, inferior- and medial points of the foramen.
4. Use the results of this study to correlate with current guidelines for the performance of ON blocks and transobturator procedures for the treatment of urinary incontinence.

6.5. Materials and methods

6.5.1. Root values of the ON and its bifurcation pattern at the obturator foramen

Bilateral dissections were performed on 105 formalin-fixed cadavers (102 left and 103 right; 91 females and 114 males; 70 ± 15 years). In order to expose the rami contributing to the ON, the dissection was carried out as detailed in the lumbar plexus chapter. Once the roots were exposed, the rami contributing to the ON were separated from those of the femoral nerve (FN) using blunt dissection. Thereafter, the rami were traced back to the intervertebral foramina from which they exited (Figure 21).

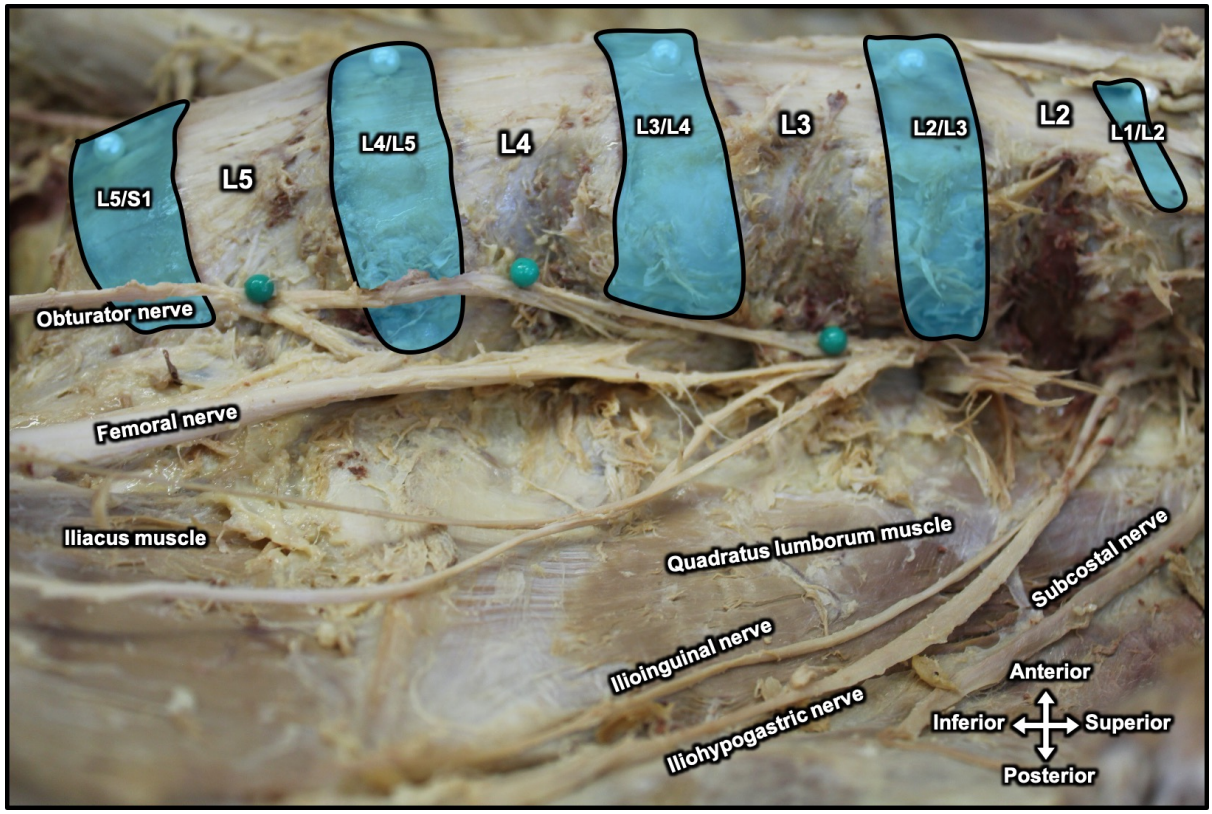

Figure 21: Lateral view of the posterior abdominal wall indicating roots of the ON on the left side.

After the ON was observed paravertebrally, it was followed over the posterior abdominal wall and as it descended into the pelvis before passing through the obturator foramen. At this point, the location where the ON bifurcated into its terminal branches was observed. The bifurcation was regarded as intrapelvic if it occurred before it entered the obturator canal, while the bifurcation was considered within the obturator canal if it occurred between the obturator membrane and the obturator externus muscle. The last category was extrapelvic, where the ON bifurcated after exiting the obturator externus muscles, within the thigh.

6.5.2. Location of the ON within the obturator foramen

To determine the location of the ON within the obturator foramen, the distances from the most superior-, inferior- and medial points of the obturator foramen to the ON were measured. The distances were determined using a mechanical dial sliding calliper (accuracy = 0.01mm) by placing the calliper against the bone and measuring to the closest border of the ON in a straight line (Figure 22).

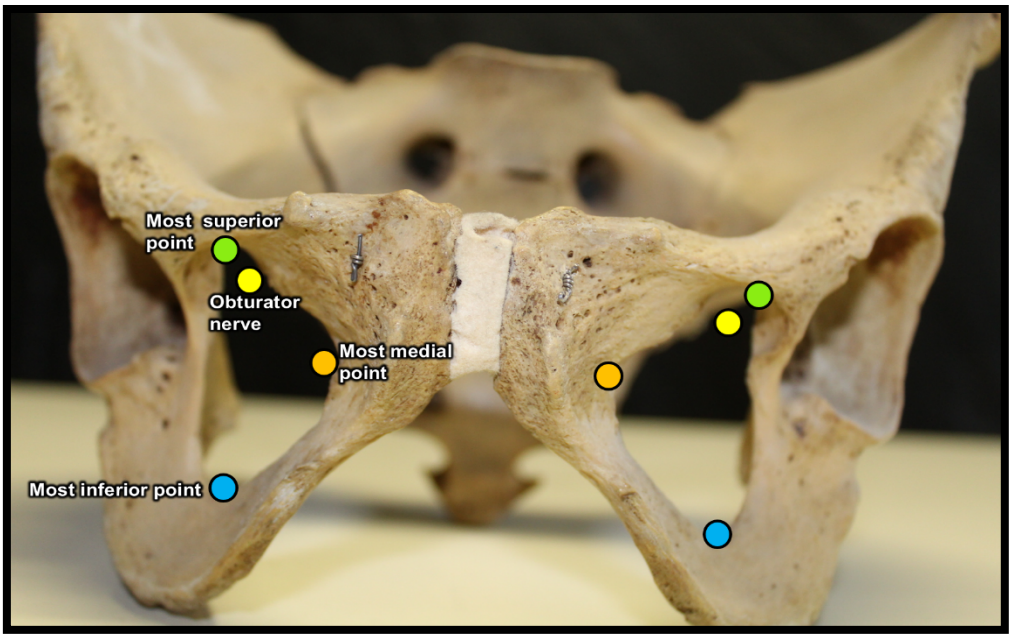

Figure 22: Anterior view of a bony pelvis representing the most superior, -medial and –inferior points of the obturator foramen that are used to locate the ON within the foramen.

6.5.3. Clinical applications

An extensive literature study was conducted using PubMed, Science Direct, Ovid and Google Scholar journal databases, as well as current anatomy-, surgical- and anaesthetic textbooks/guidelines as resources.

6.5.4. Statistical analysis

Statistical testing was performed using IBM® SPSS® Statistics version 25. Chi-squared tests for the influence of sex, sides, age, height, weight and BMI on the root values contributing to the formation of the ON and its bifurcation pattern at the obturator foramen, were performed. A p-value larger than 0.05 would indicate no statistically significant difference for these factors.

In order to determine the distribution of the data, a Shapiro-Wilk test was done on the measurements for the location of the ON in the obturator foramen. Where the data was observed to be normally distributed, a paired t-test was performed to determine whether there is a difference in the results between the left and right sides. A p-value exceeding 0.05 would indicate that there is no statistically significant difference between the data of the left and right sides. To test for the influence of sex on the

location of the ON in obturator foramen, a Chi-square test was performed, where $p > 0.05$ indicates no statistically significant difference. To determine the role that age, height, weight and BMI play in the results, a Pearson's correlation test was performed against each factor on the left and right sides.

6.6. Results

6.6.1. Root values of the ON and its bifurcation at the obturator foramen

The ON on the left side (n = 105) in females (n = 46; 43.81%) was observed originating from L2-L4 in 36 cases (34.29%), L2-3 in 1 case (0.95%) and L3-4 in 9 cases (8.57%). In males (n = 59; 56.19%), L2-L4 origin was observed in 48 cases (45.71%), L2-L3 origin in 4 cases (3.81%) and L3-L4 in 7 cases (6.67%) (Figure 23). On the right side (n = 105) of the female sample (n = 46; 43.81%) the origin of ON was from L2-L4 in 31 cases (29.52%), from L2-L3 in 3 cases (2.86%) and from L3-L4 in 12 cases (11.43%). In males (n = 59; 56.19%), the ON was observed originating from L2-L4 in 50 cases (47.62%), L2-3 in 2 cases (1.90%) and from L3-L4 in 7 cases (6.67%) (Figure 24).

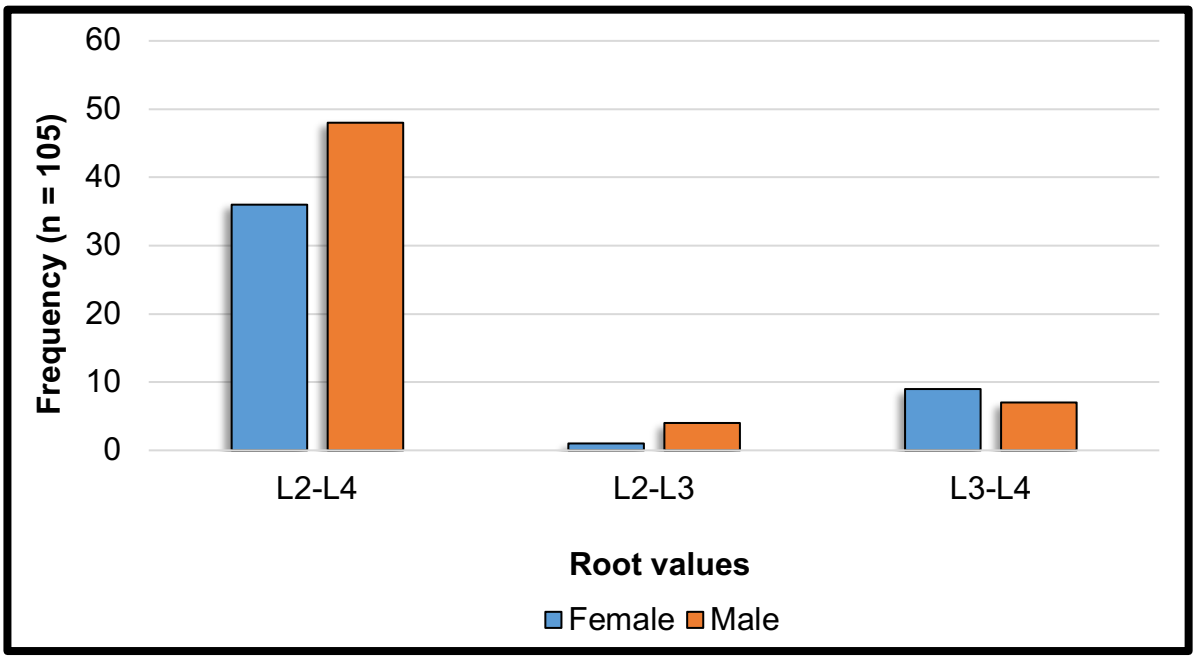

Figure 23: Bar graph indicating the frequency of the nerve root contributions to the formation of the ON on the left side for both males and females.

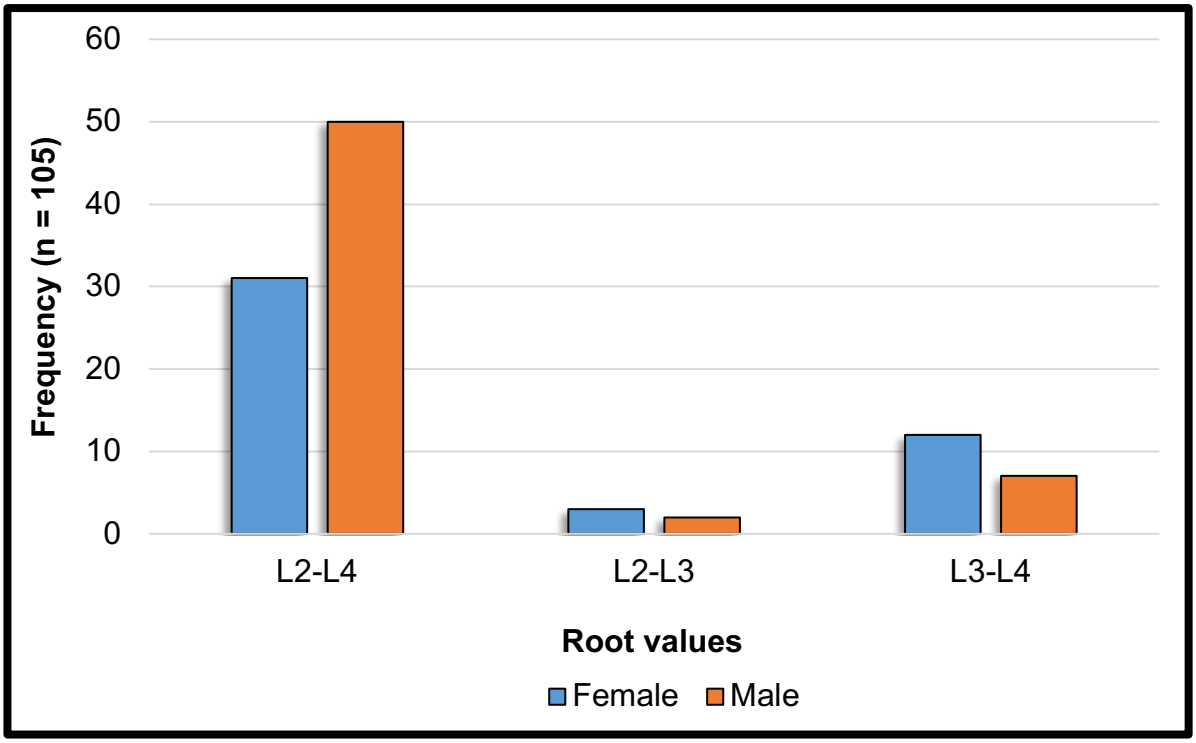

Figure 24: Bar graph showing the frequency of different nerves root contribution to the formation on the ON on the right side for both males and females.

To determine whether sex had an influence on the results of each side, Chi-squared tests were performed using cross-tabulations. The tests resulted in p-values of 0.34 for the left side and 0.11 for the right side, indicating that sex had no statistically significant influence on the contribution of the nerve roots. This allowed the male and females samples to be combined for each side.

On the left side (n = 105), the ON predominantly originated from L2-L4 in 84 cases (80.95%), L2-L3 in 5 cases (4.76%) and 16 cases (15.24%) of origin from L3-L4. On the right side (n = 105), there were 81 observed cases (77.14%) of L2-L4 origin, 5 cases (4.76%) of L2-L3 origin and 19 cases (18.10%) of L3-L4 origin (Figure 25).

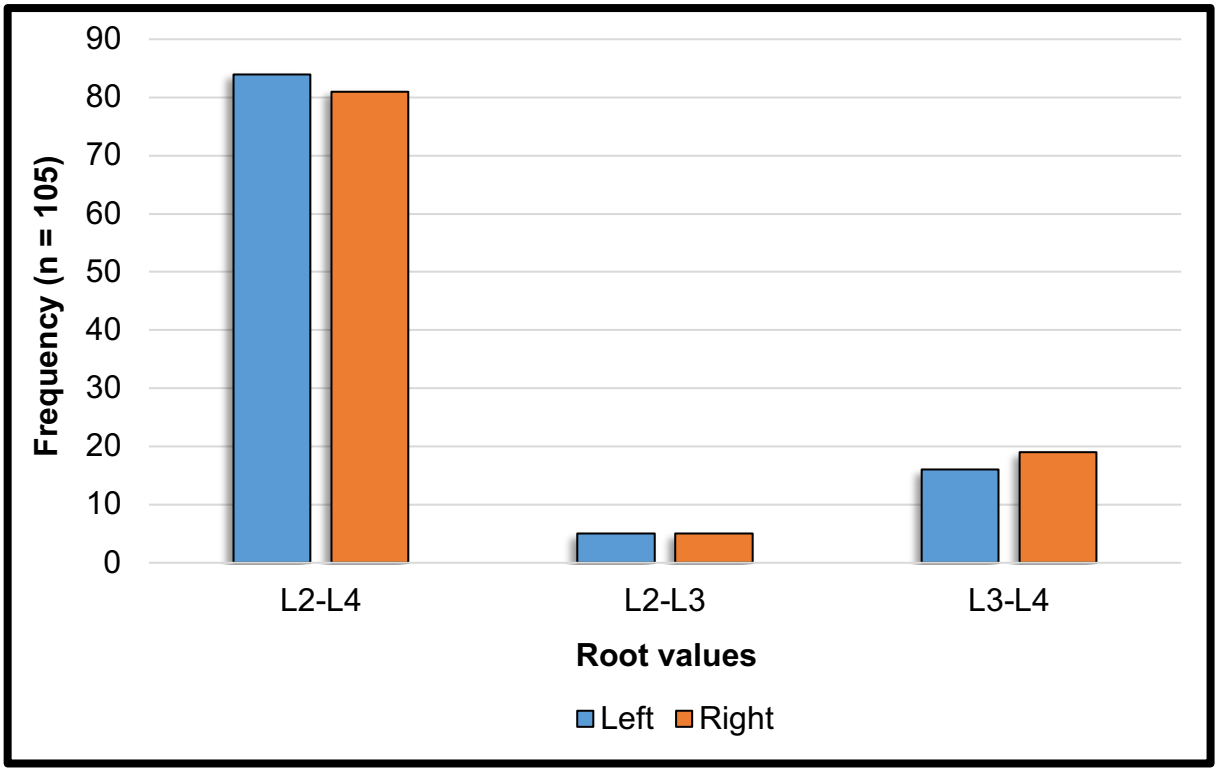

Figure 25: Graphic representation comparing the frequency of nerve root contributions to the formation of the ON on the left- and right sides.

A Chi-squared test was performed to determine the influence of sides on the results indicated no statistically significant influence of sides on the root value contributions ($p = 0.86$). The sample was pooled into an overall size of 210 sides. In the pooled sample, the ON originated from L2-L4 was observed in 165 cases (78.57%), from L2-L3 in 10 cases (4.76%) and from L3-L4 in 35 cases (16.67%) (Figure 26)

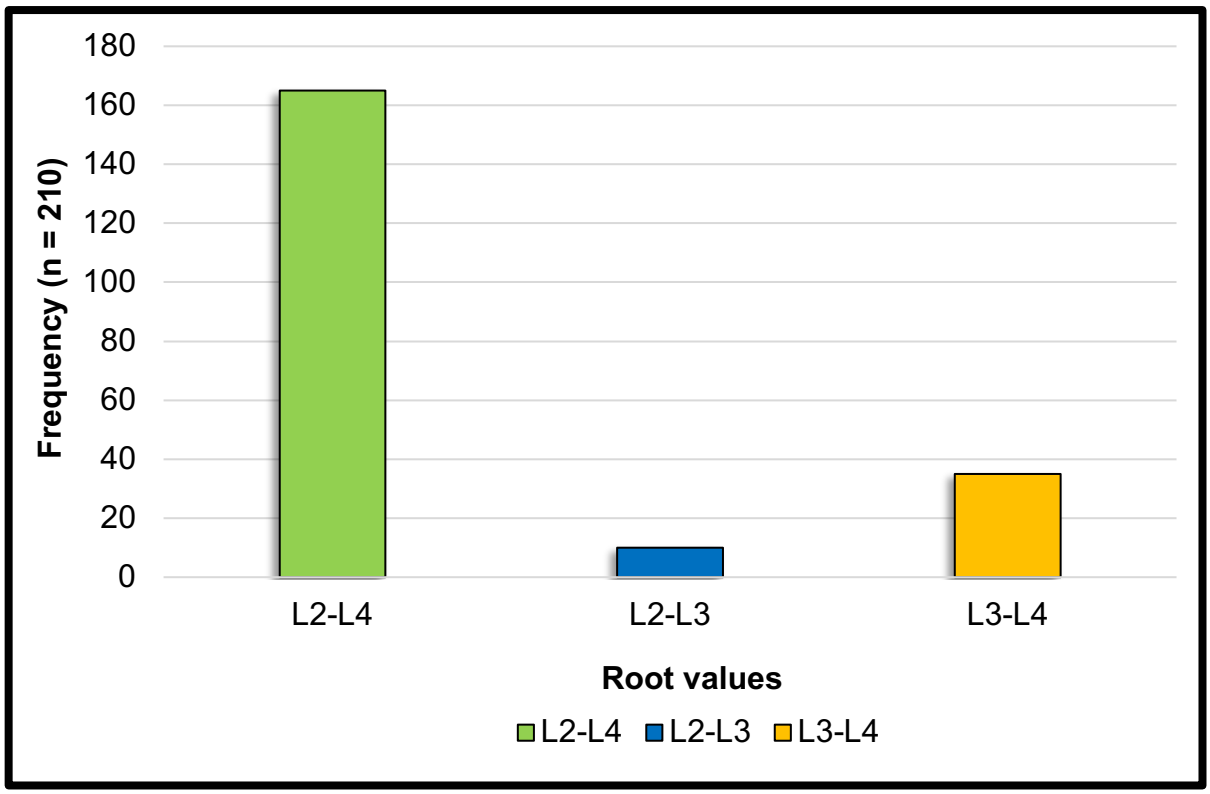

Figure 26: Graphic representation comparing the frequency of nerve root contributions to the origin of the ON.

After the ON had formed, it descended medial to the psoas major muscle into the pelvis to where it ran against the lateral pelvic wall to enter the obturator foramen. At the obturator foramen, the ON was observed as it bifurcated into its terminal branches. The bifurcation of the ON on the left side (n = 105) was observed intrapelvically in 2 cases (1.90%), within the obturator canal in 100 cases (95.24%) and extrapelvically in 3 cases (2.86%). On the right side (n = 100), the bifurcation occurred intrapelvically in 5 cases (5%), within the obturator canal in 93 cases (93%) and extrapelvically in 2 cases (2%). A Chi-square test indicated no statistically significant influence of sides, sex, height, weight and BMI on the bifurcation pattern of the ON ($p > 0.05$) (Table 11).

Table 11: A representation of the p-values obtained from Chi-square tests done to test the influence of sex, side, age, height, weight and BMI on the location of bifurcation of the ON at the obturator foramen on the left and right sides

		p-value
Sides		0.12
Sex	Left	0.42
	Right	0.99
Age	Left	0.06
	Right	0.12
Height	Left	0.24
	Right	0.91
Weight	Left	0.06
	Right	0.07
BMI	Left	0.33
	Right	0.31

The yielded results permitted the data to be combined into one sample of 205 sides, where 4 cases (1.95%) were intrapelvic, 193 cases (94.15%) were within the obturator canal and 8 cases (3.90%) were extrapelvic (Figure 27).

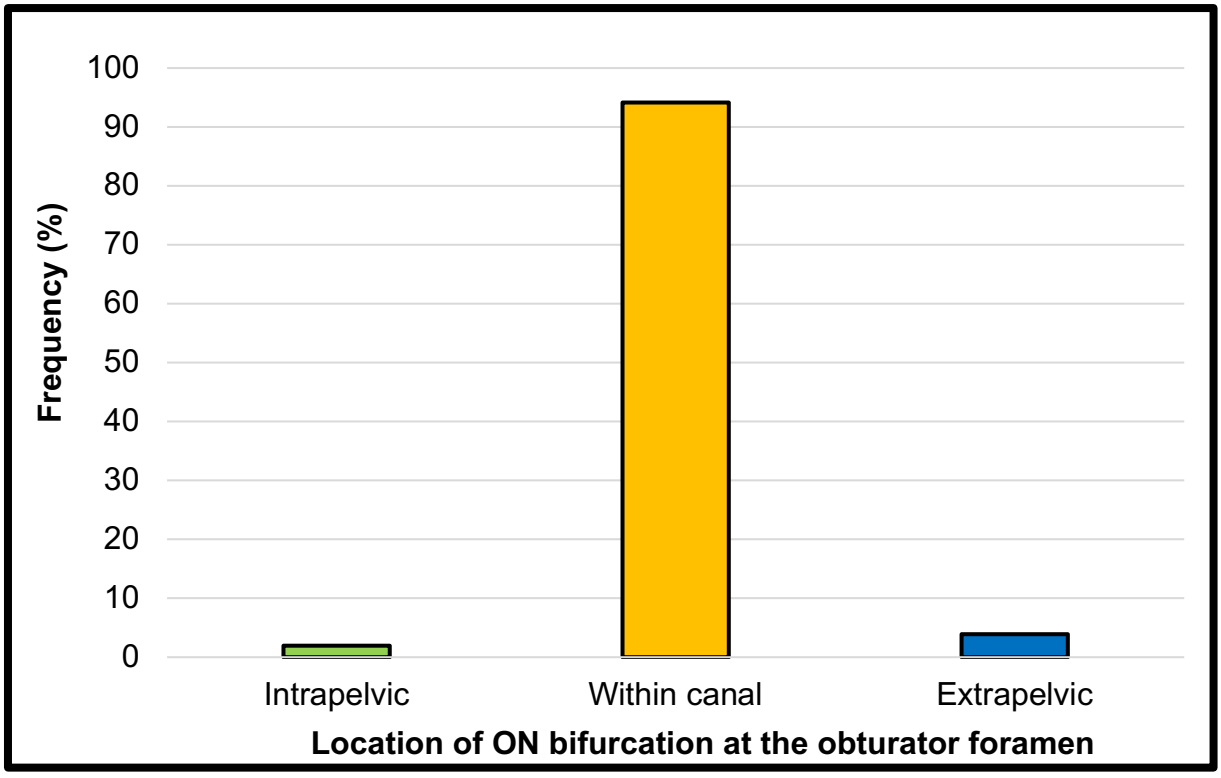

Figure 27: Diagram representing the combined frequency (%) of the bifurcation of the ON at different locations in relation to the obturator foramen.

6.6.2. Location of the ON within the obturator foramen

The measurement from the most superior point of the obturator foramen to the ON was on average 7.0 ± 1.8mm (CI – 6.6, 7.3) on the left side and 7.0 ± 1.7mm (CI – 6.7, 7.4) on the right side. The average distance from the most medial point of the obturator foramen to the ON on the left side was 30.6 ± 3.8mm (CI – 29.9, 31.4) and 30.9 ± 3.6mm (CI – 30.1, 31.6) on the right side. The measurement from the most inferior point of the obturator foramen to the ON resulted in an average distance of 46.7 ± 3.9mm (CI – 45.9, 47.4) on the left side and 47.3 ± 4.5mm (CI – 46.4, 48.2) on the right side. The location of the ON in the obturator foramen was determined by firstly performing a Shapiro-Wilk test to determine whether the data of each side is normally distributed or not. For the measurements on the left and right sides, the data was observed to be normally distributed, with all the data resulting in a p-value above 0.05 (Table 12).

Table 12: The p-values of a Shapiro-Wilk tests performed on measurements from bony landmarks of the obturator foramen to the ON for the left and right sides

		p-value
Most superior point of the obturator foramen to ON	Left	0.09
	Right	0.16
Most medial point of the obturator foramen to ON	Left	0.66
	Right	0.29
Most inferior point of the obturator foramen to ON	Left	0.98
	Right	0.13

A Chi-squared test was performed to determine whether sex had an influence on the position of the ON. The tests resulted in p-values above 0.05 for all measurements, suggesting no statistically significant influence of sex on the location of the ON (Table 13).

Table 13: The p-values of Chi-squared tests to determine whether sex had a statistically significant influence on measurements from bony landmarks to the ON on the left and right sides

		p-value
Most superior point of the obturator foramen to ON	Left	0.51
	Right	0.57
Most medial point of the obturator foramen to ON	Left	0.43
	Right	0.42
Most inferior point of the obturator foramen to ON	Left	0.40
	Right	0.40

To determine whether there was a difference between left- and right sides, a paired t-test was performed. A p-value of 0.38 was obtained for the measurement from the most superior point to the ON, 0.77 from the most medial point and 0.06 from the most inferior point of the obturator foramen. The p-values indicated no statistically significant difference between the sides, which allowed the data of the two sides to be combined into one sample. The average distance from the most superior point of the obturator

foramen to the ON was 6.8 ± 1.8mm (CI – 6.8, 7.2), 30.7 ± 3.7mm (CI – 30.2, 31.3) from the most medial point to the ON and 47.0 ± 4.2mm (CI – 46.4, 47.5) from the most inferior point to the ON.

A Pearson's correlation test for the overall results indicated a weak correlation between age, height, weight and BMI and the measurements from the most medial superior-, most medial- and most inferior points of the obturator foramen to the ON (Table 14).

Table 14: Pearson's correlation test results for the measurements from the three landmarks of the obturator foramen to the ON against age, height, weight and BMI

	Age		**Height**		**Weight**		**BMI**	
	r	**p**	**r**	**p**	**r**	**p**	**r**	**p**
Most superior	0.06	0.55	0.02	0.81	-0.09	0.21	-0.12	0.22
Most medial	0.09	0.37	0.09	0.19	0.06	0.40	0.08	0.44
Most inferior	-0.12	0.23	0.32	<0.01	0.01	0.94	<0.01	0.98

Inter- and intra-observer reliability test results may be found in Annexure A.

6.6.3. Clinical applications

A study of the literature was conducted to identify relevant clinical and surgical procedures using the following keywords: *obturator nerve anatomy, obturator nerve variation, obturator nerve injury, obturator nerve block, obturator nerve procedures, urinary incontinence treatment, transobturator procedures females, transobturator procedures males.*

6.7. Discussion

6.7.1. Root values of the ON and its bifurcation at the obturator foramen

To understand the variation in the root values of the ON, the roots were traced back to their exit lateral to the intervertebral discs. Variations were observed with regard to the root contribution combinations in the formation of the ON. The ON predominantly originated from the ventral rami of L2-L4 (78.57%), followed by the ventral rami of

L3-L4 (16.67%) while the least frequent origin was from the ventral rami of L2-L3 (4.76%). A study by Anloague and Huijbregts (2009) reported the ON as only originating from the ventral rami of L2-L4 (n = 38). A study by Nontasaen et al. (2016) reported the same result, with all observed ON originating from L2-L4 (n = 131). A study by Arora et al. (2014) observed variable root value contributions of the ON (n = 60). They reported a L2-L4 origin in 33% of cases and an origin from T12-L3 in 2% of cases. The remaining root values were not reported by the authors (Table 15).

Table 15: Comparison of the results found in literature for the root values observed contributing to the formation of the ON

			Prevalence (%)			
	Country	**n**	**L2-L4**	**L2-L3**	**L3-L4**	**T12-L3**
Anloague and Huijbregts (2009)	USA	38	100	0	0	0
Arora et al. (2014)	India	60	33.33	NR*	NR*	1.67
Nontasaen et al. (2016)	Thailand	131	100	0	0	0
Current study (2019)	South Africa	205	78.57	4.76	16.67	0

NR* = Not reported

After its formation, the ON was observed as it descended medial to the psoas major muscle and was the only branch of the lumbar plexus to do so. It exited the abdomen to enter the pelvis at the level of the sacroiliac joint and runs against the lateral pelvic wall to enter the obturator canal. At this point, the ON bifurcated into its anterior and posterior terminal branches. In the current study, it was observed to have predominantly bifurcated within the obturator canal (94.15%), followed by extrapelvic bifurcation (3.90%) and the least number of bifurcations intrapelvically (1.95%). In a study by Anagnostopoulou et al. (2009) (n = 168) the bifurcation of the ON was observed as intrapelvic in 39 cases (23.22%), within the obturator canal in 87 cases (51.78%) and extrapelvic in 42 cases (25%). In that study, the bifurcation was described as within the obturator canal if it was observed after the ON entered the canal. Extrapelvic bifurcation was described as the bifurcation of the ON within the medial thigh. In the current study, the obturator externus muscle was used as the border to determine bifurcation within the obturator canal and extrapelvic bifurcation in order to have a consistent landmark for the observations at the obturator foramen.

6.7.2. Location of the ON within the obturator foramen

To give an accurate description of the ON within the obturator foramen, three bony landmarks of the foramen were used: the most superior point of the foramen, the most medial point of the foramen and the most inferior point of the foramen. The ON was closest to the most superior point of the obturator foramen at a mean distance of 6.8 ± 1.8mm. The distances of the ON from the most medial- and most inferior points were relatively large at 30.7 ± 3.7mm and 47.0 ± 4.2mm, respectively.

The bony landmarks used to locate the ON in the obturator foramen will assist in the performance of procedures in the area of the obturator foramen by giving a safe area for needle insertion, to ensure that the trajectory of the needle is far from the ON and its branches. In that way, placement of needles and other instruments can be planned properly using these landmarks and knowledge of their approximate locations.

6.7.3. Clinical implications

The ON block is an essential procedure for post-operative analgesia after hip- and knee surgery. The current literature guidelines of abducting and laterally rotating the thigh is supported by the current study, as this will expose the muscles in the medial compartment (Yoshida et al., 2017). The advancement of the needle between the obturator externus muscle and the pectineus muscle has been reported to mainly block the anterior branch of the ON, but may also block the posterior branch, should the anaesthetic solution spread deeper into the medial compartment (Nielsen et al., 2017; Taha and Darwich, 2017; Yoshida et al., 2017; Nielsen et al., 2019). The results of the current study support the technique used for the approaches to the ON blocks, where the location of the nerves were identified within the planes at which the blocks are performed.

The placement of the needle insertion site on the lateral side of the medial compartment of the thigh, distal to the inguinal ligament, as recommended in the guidelines, correlates with the results of the current study which located the ON near the most superior point of the obturator foramen. This point is found superolaterally within the obturator foramen. Therefore, the needle insertion site will likely in line with the ON, making it easier to advance the needle close to the ON, especially during a blind block. The advancement of the needle deep to the pectineus muscle and

superficial to the obturator externus and adductor longus muscle for blocking the ON, as described in the literature, correlates with the observations in this study, where the ON was observed as it bifurcated in relation to the obturator externus muscle. In this plane is where the anaesthetic solution is described to being administered (Runge et al., 2016; Nielsen et al., 2017; Yoshida et al., 2017). The bifurcation patterns observed in the current study, where the ON predominantly bifurcated within the obturator canal, correlates with reported results where the anterior branch was most likely to be blocked in the procedure (Yoshida et al., 2017). Although the ON block is performed with the assistance of ultrasound scans, it is important for the operator to know the anatomy and variability of the ON in the obturator foramen. Correct visualization of the nerves in relation to the muscles is important for the correct insertion of the needle and advancement towards the ON for a safe and complete block of the ON. Although the ON block is described as a single injection block, it may be necessary to advance the needle deep to the level of the anterior branch of the ON in order to reach the posterior branch (Lin et al., 2015; Yoshida et al., 2017; Han et al., 2019). This additional injection will then be directed solely at the posterior branch of the ON. The injection of the anaesthetic solution through two injections should however be performed with caution to prevent damaging the anterior branch of the ON by piercing it.

In procedures for the treatment of urinary incontinence, trocars are passed through the obturator foramen in order to secure a mesh, thereby placing the ON and its branches in danger (Favors et al., 2016; Cooke et al., 2019; Duckett et al., 2019). The approach of insertion of the mesh may differ, but the common path of the needle is through the obturator foramen and is, therefore, in relation to the ON and its branches (Huri et al., 2015). The mesh that is placed to support the urethra may also impinge the ON within the obturator foramen if improperly placed (Van Ba et al., 2014; Boț et al., 2017; Barisiene et al., 2018; Kaufman et al., 2019). This complication may be as a result of the needle being advanced too far superiorly towards the superior pubic ramus.

Accurate and safe passing of the needle through the obturator foramen will prevent the impingement of the ON by the mesh. A safe trajectory that is suggested by the current study is as outlined in the guidelines for the inside-out transobturator- and

tension-free vaginal tape-obturator approaches. The insertion of the needle from the region of the urethra will allow the clinician to palpate and visualize the ischiopubic ramus before inserting the needle. The results of the current study suggest that the most medial point of the obturator foramen be used as a landmark for needle insertion, as this landmark is relatively far removed from the ON at an average distance of 30.74 ± 3.69mm. Placing the needle in relation to the most medial point of the obturator foramen will allow the needle to run towards the medial thigh instead, while ensuring that mesh is placed at a safe distance from the ON, its branches and its accompanying vessels. A study by Bozkurt et al. (2015) suggests the same pathway of the needle through the obturator foramen. In this regard, the number of complications during procedures for mesh placement through the obturator foramen will diminish.

6.8. Conclusion

There was some variation in the root value origins of the ON, as expected. However, it predominantly received contributions from the ventral rami of the L2-L4 spinal nerve roots. After its formation, the ON exits the psoas major muscle from its medial border as it enters the true pelvis at the sacroiliac joint, where it courses on the lateral pelvic wall. It exits the pelvis by entering the obturator canal of the obturator foramen.

The ON bifurcates predominantly within the obturator canal, where it is described in the current study to enter the thigh after crossing the obturator externus muscle. In the obturator foramen, the ON is closest to the most superior point of the obturator foramen. This places the ON in close proximity to the superolateral end of the obturator foramen and a safe distance from the most medial- and most inferior points of the foramen. In this sample, the distance of the ON from the most inferior point of the obturator foramen showed a positive correlation with the height of the cadavers ($r = 0.32$). This should be considered when placing sharp instruments in the area of individuals with a shorter stature, as the ON will be near the bony landmark.

The results of this study support the current guidelines for the performance of the ON block. Inserting the needle on the lateral side of the medial compartment of the thigh, distal to the inguinal ligament, will place the needle in close proximity to the ON as it exits the obturator canal. It is important for clinicians to bear in mind that the bifurcation of the ON within the obturator canal means that the anterior branch is most likely to be

blocked in the procedure and a further effort must be made to ensure that the posterior branch is blocked as well, to avoid muscle spasms during procedures in the medial thigh.

For the transobturator procedures, in both males and females, the inside-out technique is suggested as a safer option for needle insertion. The most medial point of the obturator foramen is suggested as the bony landmark to be used during the procedure as it is easily palpable and is a safe distance from the ON. Aiming for the needle to pass through the obturator foramen closer to its most medial point will prevent damage to the ON and entrapment of the nerve by the mesh attached to the needle.

Having an accurate and current understanding of the anatomy and variability of the ON and its branches is important, even with the availability of ultrasound machines, as it will assist clinicians in pre-operative planning. This will decrease complication rates and ensure successful performance of all procedures performed near, and on the ON and its branches. Preventing damage to the nerves during the procedures will decrease the possibility of post-operative complications in patients and will improve their quality of life.

It is suggested that further studies be conducted in a clinical setting and on fresh cadavers, so to correlate the results with those of the current study. Further, it is suggested that additional studies be conducted on the depth of the ON within muscle planes and from the skin using ultrasound- and CT scans. Furthermore, a study using bony landmarks to determine the exact needle insertion site for the ON block should also be conducted. This could assist clinicians operating in countries where ultrasound technology is not readily available. This study will contribute to further studies on the safe and successful performance of procedures in the region of the ON, specifically.

6.9. References

ANAGNOSTOPOULOU, S., KOSTOPANAGIOTOU, G., PARASKEUOPOULOS, T., CHANTZI, C., LOLIS, E. & SARANTEAS, T. 2009. Anatomic variations of the obturator nerve in the inguinal region: implications in conventional and ultrasound regional anesthesia techniques. *Regional anesthesia and pain medicine,* 34**,** 33-39.

ANGULO, J. C., ARANCE, I., ESQUINAS, C., DORADO, J. F., MARCELINO, J. P. & MARTINS, F. E. 2017. Outcome measures of adjustable transobturator male system with pre-attached scrotal port for male stress urinary incontinence after radical prostatectomy: a prospective study. *Advances in therapy,* 34**,** 1173-1183.

ANGULO, J. C., CRUZ, F., ESQUINAS, C., ARANCE, I., MANSO, M., RODRÍGUEZ, A., PEREIRA, J., OJEA, A., CARBALLO, M. & RABASSA, M. 2018. Treatment of male stress urinary incontinence with the adjustable transobturator male system: Outcomes of a multi-center Iberian study. *Neurourology and urodynamics,* 37**,** 1458-1466.

ANLOAGUE, P. A. & HUIJBREGTS, P. 2009. Anatomical variations of the lumbar plexus: a descriptive anatomy study with proposed clinical implications. *Journal of Manual & Manipulative Therapy,* 17**,** 107E-114E.

ARORA, D., KAUSHAL, S. & SINGH, G. 2014. VARIATIONS OF LUMBAR PLEXUS IN 30 ADULT HUMAN CADAVERS-A UNILATERAL PREFIXED PLEXUS. *IJPAES,* 4**,** 225-8.

AYDOGMUS, S., KELEKCI, S., AYDOGMUS, H., EKMEKCI, E., SECIL, Y. & TURE, S. 2014. Obturator nerve injury: an infrequent complication of TOT procedure. *Case reports in obstetrics and gynecology,* 2014.

BACHAR AVNIELI, I., AMAR, E., EFRIMA, B., KOLLANDER, Y., RATH, E. & VOLASKI, H. 2018. Hip arthroscopy as a treatment for obturator neuropathy secondary to intra-pelvic ganglion: a case report. *Journal of hip preservation surgery,* 5**,** 319-322.

BARBIER, V., DUPPERON, C. & DELORME, E. 2018. Evolution of the TOT OUT/IN technique: retropubic TOT. Morbidity and 5-year functional outcomes. *PELVIPERINEOLOGY***,** 74.

BARISIENE, M., CERNIAUSKIENE, A. & MATULEVICIUS, A. 2018. Complications and their treatment after midurethral tape implantation using retropubic and

transobturator approaches for treatment of female stress urinary incontinence. *Videosurgery and Other Miniinvasive Techniques,* 13**,** 501.

BOȚ, M., VLĂDĂREANU, S., VLĂDĂREANU, R., PETCA, R., ZVÂNCĂ, M., RADU, D. C. & PETCA, A. Painful Complications after Pelvic Floor Reconstructive Surgery in Transobturator Suburethral Vaginal Slings. Key Engineering Materials, 2017. Trans Tech Publ, 49-53.

BOZKURT, M., YUMRU, A. & SALMAN, S. 2015. Assessment of peri-operative, early, and late post-operative complications of the inside-out transobturator tape procedure in the treatment of stress urinary incontinence. *Clin Exp Obstet Gynecol,* 42**,** 82-9.

CAPOBIANCO, G., MADONIA, M., MORELLI, S., DESSOLE, F., DE VITA, D., CHERCHI, P. L. & DESSOLE, S. 2018. Management of female stress urinary incontinence: a care pathway and update. *Maturitas,* 109**,** 32-38.

COOKE, W. R., CARTWRIGHT, R., FRIES, C. A. & PRICE, N. 2019. Complete laparoscopic removal of retropubic midurethral tape (tension-free vaginal tape) from the obturator nerve: a multidisciplinary approach. *International urogynecology journal***,** 1-2.

DE MATTOS LOURENCO, T. R., MATSUOKA, P. K., BARACAT, E. C. & HADDAD, J. M. 2018. Urinary incontinence in female athletes: a systematic review. *International urogynecology journal,* 29**,** 1757-1763.

DMOCHOWSKI, R., PADMANABHAN, P. & SCARPERO, H. 2012. Slings: autologous, biologic, synthetic, and midurethral. *Campbell-Walsh Urology,* 3**,** 2115-2167.

DUCKETT, J., BODNER-ADLER, B., RACHANENI, S. & LATTHE, P. 2019. Management of complications arising from the use of mesh for stress urinary incontinence—International Urogynecology Association Research and Development Committee opinion. *International urogynecology journal***,** 1-5.

ELSHEEMY, M. S., ELSERGANY, R. & ELSHENOUFY, A. 2015. Low-cost transobturator vaginal tape inside-out procedure for the treatment of female stress urinary incontinence using ordinary polypropylene mesh. *International urogynecology journal,* 26**,** 577-584.

FAVORS, S., CHINTHAKANAN, O., MIKLOS, J. & MOORE, R. 2016. Obturator Neuralgia: Complete Resolution after Laparoscopic Retropubic Sling Removal: A Report of 2 Cases. J Genit Syst Disor 5: 4. *of,* 4**,** 2.

FRIEDL, A., MÜHLSTÄDT, S., ZACHOVAL, R., GIAMMÒ, A., KIVARANOVIC, D., ROM, M., FORNARA, P. & BRÖSSNER, C. 2017. Long-term outcome of the adjustable transobturator male system (ATOMS): results of a European multicentre study. *BJU international,* 119**,** 785-792.

GHAEMMAGHAMI, F., BEHNAMFAR, F. & SABERI, H. 2009. Immediate grafting of transected obturator nerve during radical hysterectomy. *International Journal of Surgery,* 7**,** 168-169.

HAN, C., MA, T., LEI, D., XIE, S. & GE, Z. 2019. Effect of ultrasound-guided proximal and distal approach for obturator nerve block in transurethral resection of bladder cancer under spinal anesthesia. *Cancer management and research,* 11**,** 2499.

HODA, M., PRIMUS, G., SCHUMANN, A., FISCHEREDER, K., SCHMID, N., MOLL, V., HAMZA, A., KARSCH, J., STEINBACH, F. & BRÖSSNER, C. 2012. Treatment of stress urinary incontinence after radical prostatectomy: adjustable transobturator male system-results of a multicenter prospective observational study. *Der Urologe. Ausg. A,* 51**,** 1576-1583.

HURI, E., EZER, M., AYDOĞAN, B., TATAR, İ. & SARGON, M. F. 2015. Anatomic transobturator tape (TOT) technique: clinical anatomic landmarks of obturator foramen on female cadavers. *Anatomy,* 9.

JAHROMI, M. K., TALEBIZADEH, M. & MIRZAEI, M. 2015. The effect of pelvic muscle exercises on urinary incontinency and self-esteem of elderly females with stress urinary incontinency, 2013. *Global journal of health science,* 7**,** 71.

JUNG, B. C., TRAN, N.-A., VERMA, S., DUTTA, R., TUNG, P., MOUSA, M., HERNANDEZ-RANGEL, E., NAYYAR, M. & LALL, C. 2016. Cross-sectional imaging following surgical interventions for stress urinary incontinence in females. *Abdominal Radiology,* 41**,** 1178-1186.

KANEZAKI, S., SAKAI, A., NAKAMURA, E. & UCHIDA, S. 2018. Surgical management of obturator neuropathy with a concomitant acetabular labral tear—a case report. *Acta orthopaedica,* 89**,** 591-593.

KAUFMAN, M. R., CHANG-KIT, L., BROWN, E. T. & DMOCHOWSKI, R. R. 2019. Complications of Transobturator Synthetic Slings. *The Innovation and Evolution of Medical Devices.* Springer.

KUPONIYI, O., ALLEEMUDDER, D. I., LATUNDE-DADA, A. & EEDARAPALLI, P. 2014. Nerve injuries associated with gynaecological surgery. *The Obstetrician & Gynaecologist,* 16**,** 29-36.

KURKIJÄRVI, K., AALTONEN, R., GISSLER, M. & MÄKINEN, J. 2016. Surgery for stress urinary incontinence in Finland 1987–2009. *International urogynecology journal,* 27**,** 1021-1027.

LIN, J., NAKAMOTO, T. & YEH, S. 2015. Ultrasound standard for obturator nerve block: the modified Taha's approach. *British Journal of Anaesthesia,* 114**,** 337-339.

NIELSEN, N. D., RUNGE, C., CLEMMESEN, L., BØRGLUM, J., MIKKELSEN, L. R., LARSEN, J. R., NIELSEN, T. D., SØBALLE, K. & BENDTSEN, T. F. 2019. An Obturator Nerve Block does not Alleviate Post-operative Pain after Total Hip Arthroplasty: a Randomized Clinical Trial.

NIELSEN, T. D., MORIGGL, B., SØBALLE, K., KOLSEN-PETERSEN, J. A., BØRGLUM, J. & BENDTSEN, T. F. 2017. A cadaveric study of ultrasound-guided subpectineal injectate spread around the obturator nerve and its hip articular branches. *Reg Anesth Pain Med,* 42**,** 357-361.

NONTASAEN, P., DAS, S., NISUNG, C., SINTHUBUA, A. & MAHAKKANUKRAUH, P. 2016. A cadaveric study of the anatomical variations of the lumbar plexus with clinical implications. *Journal of the Anatomical Society of India,* 65**,** 24-28.

OSÓRIO, F., ALVES, J., PEREIRA, J., MAGRO, M., BARATA, S., GUERRA, A. & SETÚBAL, A. 2018. Obturator internus muscle endometriosis with nerve involvement: a rare clinical presentation. *Journal of minimally invasive gynecology,* 25**,** 330-333.

ROSS, S., TANG, S., ELIASZIW, M., LIER, D., GIRARD, I., BRENNAND, E., DEDERER, L., JACOBS, P. & ROBERT, M. 2016. Transobturator tape versus retropubic tension-free vaginal tape for stress urinary incontinence: 5-year safety and effectiveness outcomes following a randomised trial. *International urogynecology journal,* 27**,** 879-886.

RUNGE, C., BØRGLUM, J., JENSEN, J. M., KOBBORG, T., PEDERSEN, A., SANDBERG, J., MIKKELSEN, L. R., VASE, M. & BENDTSEN, T. F. 2016. The analgesic effect of obturator nerve block added to a femoral triangle block after total knee arthroplasty: a randomized controlled trial.

SACCO, E., GANDI, C., VACCARELLA, L., RECUPERO, S., RACIOPPI, M., PINTO, F., TOTARO, A., FOSCHI, N., PALERMO, G. & PIERCONTI, F. 2018. Titanized transobturator sling placement for male stress urinary incontinence using an inside-out single-incision technique: minimum 12-months follow-up study. *Urology,* 115**,** 144-150.

SANDERSON, D. J. & GHOMI, A. 2015. Bilateral obturator neuropathy after transobturator vaginal sling: a case report. *Female pelvic medicine & reconstructive surgery,* 21**,** e21-e22.

SEWERYN, J., BAUER, W., PONHOLZER, A. & SCHRAMEK, P. 2012. Initial experience and results with a new adjustable transobturator male system for the treatment of stress urinary incontinence. *The Journal of urology,* 187**,** 956-961.

TAHA, A. M. & DARWICH, N. 2017. SOFT block (Sciatic, Obturator and Femoral nerve block Technique): a single-puncture, sole anesthetic for knee surgery. *Canadian Journal of Anesthesia/Journal canadien d'anesthésie,* 64**,** 1279-1281.

TSHABALALA, Z. N., VAN SCHOOR, A., HUMAN-BARON, R. & VAN DER WALT, S. 2016. *The anatomy and clinical implications of the obturator nerve and its branches (Unpublished thesis).* MSc Anatomy, University of Pretoria.

VAN BA, O. L., WAGNER, L. & DE TAYRAC, R. 2014. Obturator neuropathy: an adverse outcome of a trans-obturator vaginal mesh to repair pelvic organ prolapse. *International Urogynecology Journal,* 25**,** 145-146.

VANDANA, M., SURI, R., RAVI, S., VANDANA, D. & GAYATRI, R. 2011. Clinical submission of supernumerary head of adducter brevis muscle. *Journal of Surgical Academia,* 1**,** 78-81.

YOSHIDA, T., NAKAMOTO, T. & KAMIBAYASHI, T. 2017. Ultrasound-guided obturator nerve block: a focused review on anatomy and updated techniques. *BioMed research international,* 2017.

Chapter 7 – Femoral nerve (FN)

7.1. Introduction and problem statement

More than 1 million total hip replacement surgeries are performed in the United States of America alone, annually (Shan et al., 2014). In Australia, it has been reported that approximately 19000 patients are admitted to hospital with a fracture to the femur (Cooper et al., 2019). Globally, hip fractures and the repair thereof are on the rise, especially in the elderly (Kates, 2016; McFarlane et al., 2017) and the incidence is projected to increase annually (Wennberg et al., 2019). One of the indications of the femoral nerve block and the fascia iliaca compartment block performed in the inguinal region, is to give post-operative pain relief to patients (McGraw-Tatum et al., 2017; Wennberg et al., 2019). In addition to giving analgesia for hip surgery, the femoral nerve block can also provide analgesia after knee surgery (Dong et al., 2016; Grape et al., 2016; Light et al., 2019). This indicates the multi-purpose ability of these nerve blocks in ensuring that patients are relatively comfortable after major surgery by reducing the severe pain experienced post-operatively.

The femoral nerve block and fascia iliaca compartment block differ in their guidelines as a result of their proximity to the FN, with the needle in the femoral nerve block being inserted closer to the FN, as opposed to the fascia iliaca compartment block (McGraw-Tatum et al., 2017; Cooper et al., 2019; Wennberg et al., 2019). For both procedures, the most reported complication was failure of the nerve blocks, with low incidence of neurovascular injury (Yu et al., 2016; Cooper et al., 2019). Familiarity with the neurovascular anatomy of the femoral neurovascular bundle will assist with identification and approximation of the location of the FN during needle insertion, thereby decreasing the rate of peri-operative complications. The study of the course of the FN and its location in the inguinal region, together with the femoral artery (FA) and femoral vein (FV), will reaffirm the current knowledge of the FN for the blockade of the nerve.

7.2. Literature review

7.2.1. Femoral nerve (FN)

The FN arises from the posterior divisions of the ventral rami of the L2, L3 and L4 spinal nerves. As it emerges from the lateral border of the psoas major muscle, it descends anterior to the iliacus muscle towards the inguinal ligament. As it reaches

the inguinal ligament, it passes posterior to it before entering the anterior compartment of the thigh, lateral to femoral sheath, within which the femoral artery and vein are found. Upon entering the thigh, it divides into various motor and sensory branches. The sensory branches innervate the skin over the anterior surface of the thigh and the medial surface of the knee joint and the leg. The motor branches innervate the iliacus, rectus femoris, sartorius, pectineus and the vastus medialis, -intermedius and -lateralis muscles (Anloague and Huijbregts, 2009; Moore and Stringer, 2011).

Anloague and Huijbregts (2009) reported a variation in the bifurcation of the FN in relation to the psoas major muscle. The authors reported that the FN bifurcated into what they describe as slips, within the substance of the muscle, instead of exiting the muscle as a complete nerve. The slips would then join as they approached the pelvic cavity.

For total hip arthroplasty, FN blocks are performed for anaesthesia and post-operative analgesia along the fascial plane of the fascia iliaca (Nielsen et al., 2003; Gray et al., 2004). Lack of knowledge of the anatomy of the nerve and its relations may lead to incomplete anaesthesia of the FN and damage to vascular structures (Cuvillon et al., 2001; Nielsen et al., 2003; Salinas et al., 2006; Sharma et al., 2010). It is important to understand the anatomical basis of the femoral nerve block and fascia iliaca compartment block to allow for safe performance of these procedures.

7.2.2. Femoral nerve block

Total hip and knee arthroplasty can leave patients with severe pain post-operatively. To provide relief for these patients, the femoral nerve block is performed in the inguinal region. Although it can be performed either blind, or using a nerve stimulator, most femoral nerve blocks are performed with the assistance of an ultrasound machine. A linear ultrasound probe is placed horizontally over the femoral triangle, distal to the inguinal crease, in order to locate the FA and FV. Once their location has been confirmed, the FN is identified lateral to the FA. Thereafter, the needle is inserted and advanced in-line with the FN until it rests adjacent and lateral to the nerve, where the anaesthetic solution is injected (Cooper et al., 2019).

7.2.3. Fascia iliaca compartment block

The fascia iliaca compartment block has been reported to be successful in pain relief after hip and knee surgery and was first described by Dalens et al. (1989). In order to determine the needle insertion site, a line is drawn between the ASIS and the pubic tubercle and then divided into thirds. The needle is inserted along a vertical line approximately 10mm inferior to the junction between the medial two-thirds and the lateral one-third of the line between the ASIS and pubic tubercle. The needle is then advanced until resistance against movement can be felt. At this point, the needle has reached the fascia lata, the first indication of the level at which the needle is. More force is applied to the needle until it pierces the fascia lata and reaches another point of resistance, the last indication of needle depth, which is the fascia iliaca. The needle is carefully advanced until no further resistance to movement can be felt. Thereafter, the anaesthetic solution is administered (Pinson, 2015; KumAr et al., 2016; Cooper et al., 2019).

The complication rate of fascia iliaca compartment block has been reported to be three in 10 000 patients (Sharma et al., 2010). Although this may not seem significant, the vast area of innervation of the femoral nerve will have adverse effects on patients, as it gives motor and sensory innervation to the thigh, hip and knee. Damage to the nerve may then result in loss of function of the quadriceps femoris muscle group and pain in the hip and knee joints. Awareness of the anatomy of the FN and its relation to vascular and bony structures will assist in the prevention of these complications.

7.3. Aim

The aim of this study was to accurately describe the course of the FN from its origin to where it enters the anterior compartment of the thigh, the knowledge which will assist in femoral nerve block and fascia iliaca compartment block.

7.4. Research objectives

1. Describe the anatomy and course of the FN from its paravertebral spinal nerve root origins to where it enters the thigh.
2. Describe the location of the FN in relation to the ASIS as it enters the thigh deep to the inguinal ligament.

3. Compare the results of the current study to currently followed surgical and clinical guidelines for the performance of femoral nerve block and fascia iliaca compartment block.

7.5. Materials and methods

7.5.1. Root values of the FN

Dissection was performed on 205 sides (102 left and 103 right; 91 females and 114 males; 70 ± 15 years) to expose the roots that contribute to the formation of the FN, as highlighted in the materials and methods section in the chapter two on the lumbar plexus. Furthermore, the root values were only investigated after the roots of the ON had been isolated and identified. Once this was done, the roots contributing to the FN were followed superomedially towards the intervertebral foramen from which they came.

7.5.2. Location of the FN, femoral artery and femoral vein in relation to the ASIS

To determine the location of the FN, measurements were taken from the ASIS to the FN as it entered the anterior thigh deep to the inguinal ligament. The measurement was taken in a straight line from the most anterior point of the ASIS to the most anterior point of the FN, inferior to the inguinal ligament and before the nerve terminated into its branches. The FN lies in close proximity to the femoral artery (FA) and femoral vein (FV). To further give clinical relevance for use of the results, similar measurements were also taken from the ASIS to the lateral border of the FA and FV, just inferior to the inguinal ligament (Figure 28). Further locating the FA and FV will give clinicians and surgeons an awareness of structures that may be in danger when performing procedures in the vicinity. All measurements were taken using a mechanical dial sliding calliper (accuracy = 0.01mm) and were captured in a Microsoft Excel (2013) spreadsheet.

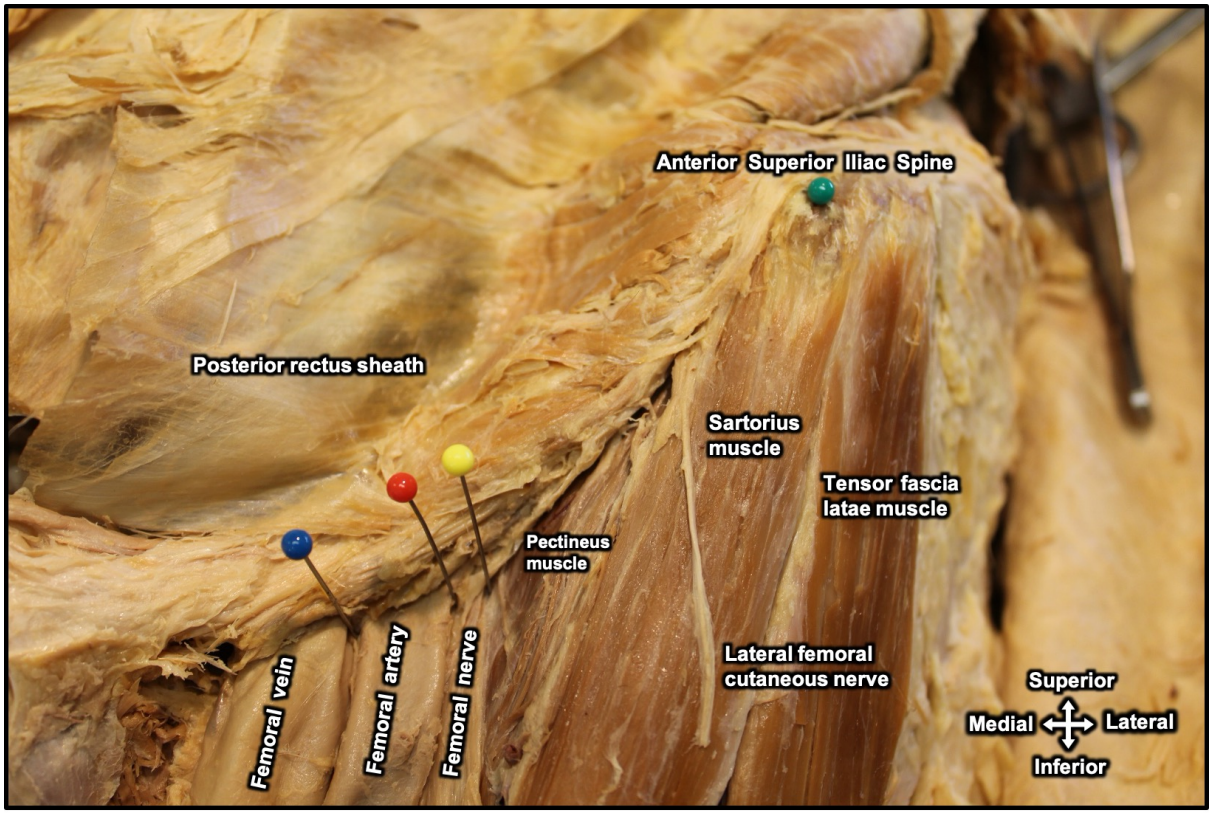

Figure 28: Anterior view of the anterior thigh indicating the measurements from the ASIS to the FN (Yellow), FA (Red) and FV (Blue) using pins.

7.5.3. Clinical applications

Clinically relevant procedures were studied by using literature obtained using PubMed, Science Direct, Ovid and Google Scholar journal databases. In addition to these electronic resources, currently utilised anatomy, surgical and anaesthetic textbooks/guidelines were consulted.

7.5.4. Statistical analysis

Statistical testing was performed using IBM® SPSS® Statistics version 25. Chi-squared tests to determine the influence of sex and sides on the root values contributing to the formation of the FN were conducted. A p-value greater than 0.05 would indicate no statistically significant influence for these factors.

To analyse the measurements taken from the ASIS to the FN, FA and FV, a Shapiro-Wilk test was performed to test whether the data is normally distributed. Where the data was normally distributed, a paired t-test was performed to test whether there was a statistically significant difference between the sides, which would be

determined by a p-value of smaller than 0.05. To determine whether sex had an influence on the measurements, a contingency table was drawn up. Thereafter, descriptive statistics such as the mean, standard deviation and 95% confidence interval were obtained. A Pearson's correlation test was performed to determine whether age, height, weight and BMI of the individuals had an influence on the results on the left and right sides.

7.6. Results

7.6.1. Root values of the FN

The investigation revealed that the root contributions to the FN were all (n = 205) from the posterior divisions of the ventral rami of the L2-L4 spinal nerves (Figure 29). The influence of sex and sides could not be tested as the results were constant across all samples. The FN appeared lateral to the psoas major muscle and descended into the false pelvis, towards the inguinal ligament, where it crossed deep to it before entering the thigh.

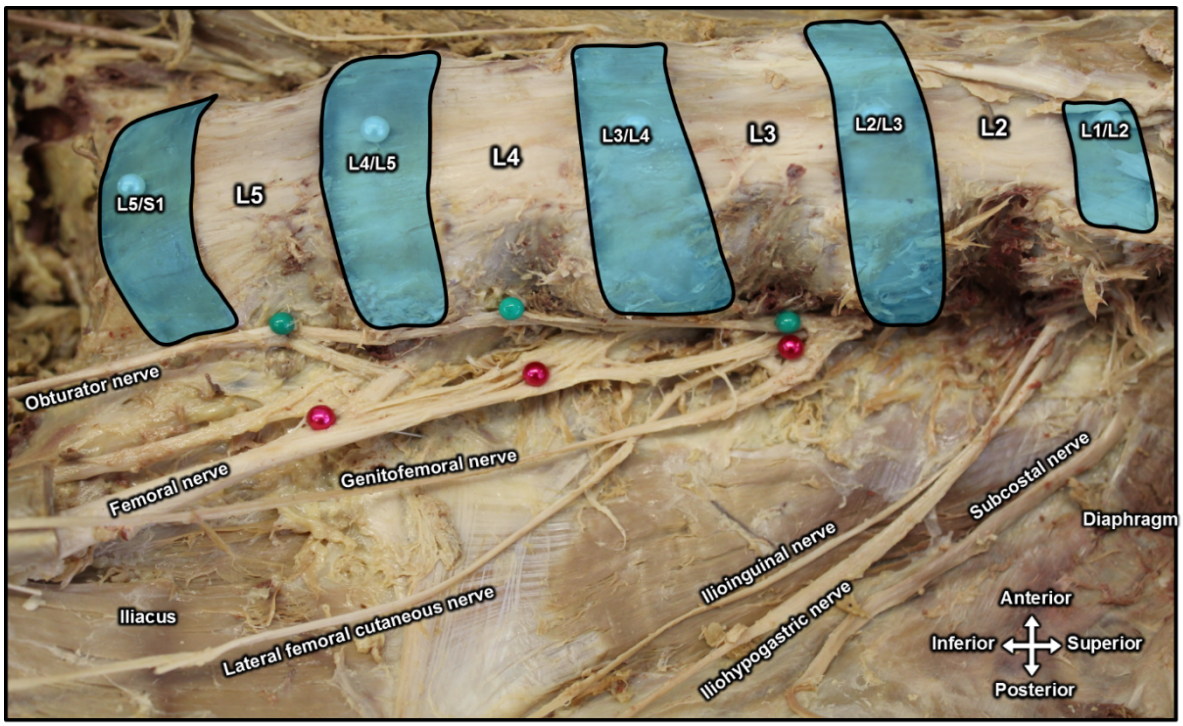

Figure 29: Anterolateral view of the posterior abdominal wall exposing roots of the FN and other nerves of the lumbar plexus, after removal of the fibres of the psoas major muscle.

7.6.2. Location of the FN, femoral artery and femoral vein in relation to the ASIS

A Shapiro-Wilk test revealed that all the data of the measurements taken from the ASIS to the FN, FA and FV were normally distributed, where the p-values obtained were larger than 0.05 (Table 16).

Table 16: A representation of the p-values obtained after a Shapiro-Wilk test for measurements from the ASIS to the FN, FA and FV on the left and right sides

		p-value
ASIS to FN	Left	0.07
	Right	0.65
ASIS to FA	Left	0.73
	Right	0.65
ASIS to FV	Left	0.66
	Right	0.11

A Chi-squared test was performed to determine whether sex had a significant influence on the measurements obtained. No statistically significant influence of sex was revealed, where all the p-values were above 0.05 on both the left and the right sides (Table 17).

Table 17: Results of a Chi-squared test to determine the influence of sex on the data on the left and right sides

		p-value
ASIS to FN	Left	0.51
	Right	0.40
ASIS to FA	Left	0.45
	Right	0.40
ASIS to FV	Left	0.43
	Right	0.45

A paired t-test was performed and revealed no statistically significant difference between the data on the left and right sides for the measurements from the ASIS to

the FN ($p = 0.06$), FA ($p = 0.051$) and FV ($p = 0.22$). This allowed for the data of the left and right sides for all measurements to be combined into one sample. The mean distances of the combined sample is represented in Table 18.

Table 18: Representation of the mean distances from the ASIS to the FN, the FA and the FV of the pooled sample

	Mean distance ± SD	**95% Confidence interval**
ASIS to FN	54.99 ± 8.13mm	53.85; 56.12
ASIS to FA	67.40 ± 8.89mm	66.16; 68.64
ASIS to FV	80.51 ± 9.28mm	79.22; 81.81

Pearson's correlation tests between age and the distances from the ASIS to the FN and the FV revealed weak correlations. The measurement from the ASIS to the FV had borderline weak to moderate correlation on both the left and right sides, where the r-values where slightly over the 0.30 threshold between weak and moderate correlations. These r-values also appeared to have a statistically significant difference. The correlation test of height, weight and BMI to the measurements revealed weak correlations ($r < 0.3$) (Table 19). All the measurements had positive weak correlations except for the test of the left ASIS to FN and BMI which had a negative weak correlation. Except for the right ASIS to FV, the measurements had a statistically significant positive weak correlation with height ($p < 0.05$). Similarly, the right ASIS to FN-, FA- and FV measurements and weight had statistically significant positive weak correlations ($p < 0.05$).

Table 19: Pearson's correlation test between distances from the ASIS to the FN, FA and FV and age, height, weight and BMI on the left and right sides

		Age		Height		Weight		BMI	
		r	**p**	**r**	**p**	**r**	**p**	**r**	**p**
ASIS to FN	Left	0.26	0.10	0.24	0.02	0.04	0.69	-0.07	0.53
	Right	0.12	0.25	0.23	0.02	0.27	<0.01	0.16	0.12
ASIS to FA	Left	0.27	0.01	0.25	0.01	0.13	0.19	0.02	0.87
	Right	0.19	0.06	0.30	<0.01	0.24	0.02	0.10	0.34
ASIS to FV	Left	0.31	<0.01	0.22	0.03	0.15	0.14	0.04	0.67
	Right	0.32	<0.01	0.17	0.09	0.23	0.02	0.13	0.21

Inter- and intra-observer reliability test results may be found in Annexure A.

7.6.3. Clinical applications

The fascia iliaca compartment block was identified as the most relevant procedure to correlate with the results of the current study. The keywords entered into the databases were *anterior total hip arthroplasty, anterior total hip arthroplasty complication, femoral nerve procedures, fascia iliaca compartment block.*

7.7. Discussion

7.7.1. Root values of the FN

The aim of this study was to investigate the posterior divisions of the ventral rami which contributed to the formation of the FN. The FN consistently received contributions from the posterior divisions of the ventral rami of the spinal nerves L2-L4 for the entire sample. This was also true for its exit lateral to the psoas major muscle and its descending into the false pelvis towards the inguinal ligament, where it entered the thigh deep to it. There was no observed statistically significant influence of the demographics of the sample on the root values of the FN. According to our knowledge, there is no recent literature that investigated the root values of the FN paravertebrally. Current anatomical textbooks and literature consistently describe the root values of the FN as L2-L4 (Moore et al., 2013; Drake et al., 2014; Mirjalili, 2015; Radić et al., 2018; Sripriya and Sivashanmugam, 2018).

7.7.2. Location of the FN, femoral artery and femoral vein in relation to the ASIS

The FN, FA and FV lie in very close proximity to one another in the femoral triangle, with the FA and FV lying within the femoral sheath and the FN lying lateral to the sheath (Moore et al., 2013; Drake et al., 2014). As a result, procedures performed on any of these structures poses a threat to the surrounding structures. In the current study, the locations of the FN, FA and FV were investigated in relation to the ASIS. The closest to the ASIS was the FN (54.99 ± 8.13mm), followed by the FA at 67.40 ± 8.89mm, with the FV being the most medial at a distance of 80.51 ± 9.28mm. In a study by Botham et al. (2019), the authors reported the FA at a mean distance range between 50 ± 1mm and 58 ± 3mm in 103 live patients (0 – 19 years, respectively) using CT scans. In the same study, the researchers observed the FV at a mean distance range between 61 ± 3mm in 0 year olds and 65 ± 3mm in 19 year olds. Concluding that the FA and FV move in position as one ages. The common procedure for the nerve block is to use the junction between the medial two-thirds- and the lateral one-third of a line drawn between the ASIS and the pubic tubercle as a landmark for needle insertion (Dolan et al., 2008; Pinson, 2015; Cooper et al., 2019)

7.7.3. Clinical implications

The fascia Iliaca compartment block and femoral nerve block are essential in achieving anaesthesia and analgesia to the FN during and after hip surgery (McGraw-Tatum et al., 2017; Wennberg et al., 2019). It is essential that the needle be inserted correctly to avoid vascular damage and intravascular injection of the anaesthetic solution into the FA and FV, which are located in close proximity medial to the FN. In the current study, the difference of the mean distances of the FN and FA from the ASIS places the lateral border of the FN within 12.4mm from the lateral border of the FA. The needle insertion site in the fascia iliaca compartment block is determined by dividing the inguinal ligament into thirds and inserting the needle 10mm distal to the junction of the lateral third and medial two-thirds (McGraw-Tatum et al., 2017; Cooper et al., 2019; Wennberg et al., 2019). In the femoral nerve block, with the assistance of ultrasound, the needle is inserted directly lateral, cranially and adjacent to the FN. (Sharma et al., 2010; Yu et al., 2016; Cooper et al., 2019). The current study suggests that the needle be inserted at a distance more than 12.4mm will be a safe zone to ensure that the FN is not damaged by the needle.

A recent study of 100 patients by Cooper et al. (2019) compared the success of the femoral nerve block (n = 48) and the fascia iliaca compartment block (n = 52) in achieving analgesia in patients with fractures of the neck- or proximal end of the femur. The techniques were compared according to success of the block and incidence of complications. The authors reported no significant difference in the success of the femoral nerve block and fascia iliaca compartment block, with the fascia iliaca compartment block having a higher success rate at 87% as opposed to 81% for the femoral nerve block. A study of 60 patients by Yu et al. (2016) observed similar success rates of the femoral nerve block (n = 30) and fascia iliaca compartment block (n = 30) techniques in providing analgesia to patients and in observed complications. The predominant reported complication experienced by clinicians in these procedures was failure in blocking the FN, even with the assistance of ultrasound technology.

Knowledge of the anatomy of the FN and its relation to the FA and FV will assist in the safe performance of the femoral nerve block and fascia iliaca compartment block. These neurovascular structures have been observed in close proximity to each other in the current study, when looking at their relative distances from the ASIS. This indicates that vascular puncture is a possible complication of the blocks if the proximity is not taken into account during procedures. A literature study yielded no results for studies that investigated the distances from the ASIS to the FN, FA and FV.

A study by Hunt and Harris (1996) investigated the distance from the pubic symphysis to the FA. They reported a mean distance of 79.9 ± 5.1mm from the pubic symphysis. However, the current study does not support the use of the pubic symphysis as a landmark as the fascia iliaca- and femoral nerve blocks are executed closer to the ASIS that the pubic symphysis. Therefore, utilizing the results of the current study will provide clinicians with a map of the location of the FN, FA and FV in the inguinal area when using ultrasound technology. When such technology is not available, palpation of the pulse of the FA to approximate the location of the FN is supported by the results of this study. Identification of the femoral pulse and observing its relation to the junction between the lateral two-thirds and the medial one-third of the line between ASIS and the pubic tubercle will allow the needle to be advanced into the correct plane to block the FN and to avoid piercing the FA and FV.

7.8. Conclusion

The aim of this study was to expand the knowledge of the FN from its paravertebral origin from the spinal roots and its to course to the thigh. The FN was consistent in its origin from the posterior divisions of the ventral rami of the L2-L4 in all the samples. It was also consistent in its descent into the false pelvis as it exited lateral to the psoas major muscle. It was observed that there were, to the knowledge of the authors, no recent studies conducted to investigate the roots of the FN. The study validated the currently taught anatomy of the FN as described in the literature through the extensive observations of the FN throughout its course.

In the inguinal regional, clinicians should constantly be aware of the close relation of the FN to the FA and FV. The FN is the most lateral of the three structures, followed by the FA and the FV, respectively. To avoid vascular damage to the FA and FV, the femoral nerve block and fascia iliaca compartment block should be performed lateral to the FN. This will also increase the probability of the success of the blocks. The results of the current study support the current guidelines for the femoral nerve block and fascia iliaca compartment block, as they underscore the importance of knowing the anatomy of the inguinal region for the successful performance of these procedures.

It is suggested that further research be performed on the FN, FA and FV using ultrasound and/or CT in order to further strengthen the guidelines for the femoral nerve block and fascia iliaca compartment block. Using these modalities, the depth of the FN, FA and FV, together with the fascial planes of the muscles, could be investigated in populations of different ancestries. The results should be correlated with the current practice of using resistance of the fascial layers in needle advancement as an indicator of its location in the thigh. Although no strong correlation was observed for the height and weight of the cadavers for the location of the FN, FA and FV, it is important to note that the resultant r-values were close to a moderate correlation, where they were predominantly larger than 0.2. These should be considered when locating these structures on patients of different height and weight.

Investigating the sex and the side of the body did not result in a statistically significant difference on the measurements. The results support the use of current procedural guidelines on both the left and right sides in males and females. It must be stated that

the visualization of the neurovascular structures is the most important step that should be followed in all procedures in order to decrease the possibility of damaging them.

7.9. References

ANLOAGUE, P. A. & HUIJBREGTS, P. 2009. Anatomical variations of the lumbar plexus: a descriptive anatomy study with proposed clinical implications. *Journal of Manual & Manipulative Therapy,* 17**,** 107E-114E.

COOPER, A. L., NAGREE, Y., GOUDIE, A., WATSON, P. R. & ARENDTS, G. 2019. Ultrasound-guided femoral nerve blocks are not superior to ultrasound-guided fascia iliaca blocks for fractured neck of femur. *Emergency Medicine Australasia,* 31**,** 393-398.

CUVILLON, P., RIPART, J., LALOURCEY, L., VEYRAT, E., L'HERMITE, J., BOISSON, C., THOUABTIA, E. & ELEDJAM, J. J. 2001. The continuous femoral nerve block catheter for post-operative analgesia: bacterial colonization, infectious rate and adverse effects. *Anesthesia & Analgesia,* 93**,** 1045-1049.

DALENS, B., TANGUY, A. & VANNEUVILLE, G. 1989. Lumbar plexus blocks and lumbar plexus nerve blocks. *Anesthesia & Analgesia,* 69**,** 852-854.

DOLAN, J., WILLIAMS, A., MURNEY, E., SMITH, M. & KENNY, G. N. 2008. Ultrasound guided fascia iliaca block: a comparison with the loss of resistance technique.

DONG, C.-C., DONG, S.-L. & HE, F.-C. 2016. Comparison of adductor canal block and femoral nerve block for post-operative pain in total knee arthroplasty: a systematic review and meta-analysis. *Medicine,* 95.

DRAKE, R., VOGL, A. W. & MITCHELL, A. W. 2014. *Gray's anatomy for students*, Elsevier Health Sciences.

GRAPE, S., KIRKHAM, K., BAERISWYL, M. & ALBRECHT, E. 2016. The analgesic efficacy of sciatic nerve block in addition to femoral nerve block in patients undergoing total knee arthroplasty: a systematic review and meta-analysis. *Anaesthesia,* 71**,** 1198-1209.

GRAY, A. T., COLLINS, A. B. & SCHAFHALTER-ZOPPOTH, I. 2004. An introduction to femoral nerve and associated lumbar plexus nerve blocks under ultrasonic guidance. *Techniques in Regional Anesthesia and Pain Management,* 8**,** 155-163.

HUNT, J. A. & HARRIS, J. P. 1996. Is the mid-inguinal point an accurate landmark for the common femoral artery in vascular patients? *Australian and New Zealand journal of surgery,* 66**,** 43-45.

KATES, S. L. 2016. Hip fracture programs: are they effective? *Injury,* 47**,** S25-S27.

KUMAR, D., HOODA, S., KIRAN, S. & DEVI, J. 2016. Analgesic efficacy of ultrasound guided FICB in patients with hip fracture. *Journal of clinical and diagnostic research: JCDR,* 10**,** UC13.

LIGHT, J., TREHAN, G. & MCCAUGHAN, S. 2019. Femoral Nerve. *Pain.* Springer.

MCFARLANE, R. A., ISBEL, S. T. & JAMIESON, M. I. 2017. Factors determining eligibility and access to subacute rehabilitation for elderly people with dementia and hip fracture. *Dementia,* 16**,** 413-423.

MCGRAW-TATUM, M. A., GROOVER, M. T., GEORGE, N. E., URSE, J. S. & HEH, V. 2017. A prospective, randomized trial comparing liposomal bupivacaine vs fascia iliaca compartment block for post-operative pain control in total hip arthroplasty. *The Journal of arthroplasty,* 32**,** 2181-2185.

MIRJALILI, S. A. 2015. Anatomy of the lumbar plexus. *Nerves and Nerve Injuries.* Elsevier.

MOORE, A. E. & STRINGER, M. D. 2011. Iatrogenic femoral nerve injury: a systematic review. *Surgical and radiologic anatomy,* 33**,** 649-658.

MOORE, K. L., DALLEY, A. F. & AGUR, A. M. 2013. *Clinically oriented anatomy*, Lippincott Williams & Wilkins.

NIELSEN, K. C., KLEIN, S. M. & STEELE, S. M. 2003. Femoral nerve blocks. *Techniques in Regional Anesthesia and Pain Management,* 7**,** 8-17.

PINSON, S. 2015. Fascia Iliaca (FICB) block in the emergency department for adults with neck of femur fractures: A review of the literature. *International emergency nursing,* 23**,** 323-328.

RADIĆ, B., RADIĆ, P. & DURAKOVIĆ, D. 2018. Peripheral Nerve Injury in Sports. *Acta clinica Croatica,* 57**,** 561-569.

SALINAS, F. V., LIU, S. S. & MULROY, M. F. 2006. The effect of single-injection femoral nerve block versus continuous femoral nerve block after total knee arthroplasty on hospital length of stay and long-term functional recovery within an established clinical pathway. *Anesthesia & Analgesia,* 102**,** 1234-1239.

SHAN, L., SHAN, B., GRAHAM, D. & SAXENA, A. 2014. Total hip replacement: a systematic review and meta-analysis on mid-term quality of life. *Osteoarthritis and cartilage,* 22**,** 389-406.

SHARMA, S., IORIO, R., SPECHT, L. M., DAVIES-LEPIE, S. & HEALY, W. L. 2010. Complications of femoral nerve block for total knee arthroplasty. *Clinical Orthopaedics and Related Research®,* 468**,** 135-140.

SRIPRIYA, R. & SIVASHANMUGAM, T. 2018. Aberrant femoral nerve anatomy: No longer a cause of block failure when using ultrasound guidance. *Indian journal of anaesthesia,* 62**,** 997.

WENNBERG, P., MÖLLER, M., HERLITZ, J. & SARENMALM, E. K. 2019. Fascia iliaca compartment block as a preoperative analgesic in elderly patients with hip fractures–effects on cognition. *BMC geriatrics,* 19**,** 252.

YU, B., HE, M., CAI, G.-Y., ZOU, T.-X. & ZHANG, N. 2016. Ultrasound-guided continuous femoral nerve block vs continuous fascia iliaca compartment block for hip replacement in the elderly: a randomized controlled clinical trial (CONSORT). *Medicine,* 95.

Chapter 8 - General conclusion

The aim of this study was correlate the results that were obtained to currently prescribed in clinical and surgical procedural guidelines in order to validate and suggest improvements for the safe and successful execution of these procedures. This was achieved through extensive and careful dissection of the lumbar plexus and its branches from their origin in the abdomen until their termination in the lower limb. It is essential that the described anatomy and variations of these nerves be considered during all pre-operative planning.

The lumbar plexus was investigated from where the rami exited entered the abdominal cavity until where they enter the lower limbs. The root values of the plexus were consistent in all cases. The lumbar plexus was observed predominantly in the substance of the psoas major muscle. This observation was also revealed in the study using CT scans. This result may be used in the planning of psoas compartment blocks, using that the needle is advanced with the substance of the psoas major muscle in order for the anaesthetic solution to reach the rami of the lumbar plexus effectively, for successful analgesia and paraesthesia.

The IHN and IIN received contribution from the L1 spinal nerve only in all cases. Although there are studies that report contribution from the T12 spinal nerve, this was not found in the current study. Along its course, the L1 spinal nerve predominantly bifurcated into the IHN and IIN within the transversus abdominis muscle. At the pelvis, the IHN was further posterior from the ASIS than the IIN, this reveals that the IIN is more danger than the IHN during procedures performed in the vicinity and on the ASIS and the iliac crest.

The GFN had variations of the spinal nerves that contribute to its formation. It predominantly received contribution from the rami of the L1-L2 spinal nerves, followed by the L2 spinal nerve only and received the least contribution from the L1 spinal nerve only. There were no contributions from the T12 and L3 spinal nerves found in this study, as reported by other studies. In the inguinal region, the GFN lies within the limits of the incisions made for the treatment of inguinal hernias. With this, it is recommended that the GFN be visualised using blunt dissection before repairs can be done in the groin area, so to ensure not to damage the nerve.

The LFCN predominantly received from the L2-L3 spinal nerves, followed by the L2 only and received the least contribution from the L3 only. Although L1-L2 contribution and branching of the LFCN from the femoral nerve were reported in the literature, it was not observed in the current study. As the LFCN entered the thigh, it was found in close proximity to the ASIS and caution should be taken when performing iliac crest bone harvesting, as it performed close to the ASIS. The area should be explored and the LFCN identified before bone is excised, so not to damage the nerve.

The ON received contribution from the L2-L4 spinal nerves predominantly. Thereafter, it received contribution from L3-L4 spinal nerves only and the least contribution from the L2-L3 spinal nerves only. These observations were similar to those reported in the literature. Within the obturator canal, the ON was in closest proximity to the most superior point of the obturator foramen. It was furthest from the most inferior point of the obturator foramen and was at an intermediate distance from the most medial point of the obturator foramen. In the obturator canal, it also bifurcated with in the canal, followed by its extrapelvic bifurcation and was least observed bifurcating intrapelvically. These results should be used in planning of procedures done in the vicinity of the ON, its branch and through the obturator foramen, so not to damage them with the instruments used for the procedures.

The FN received contribution from the rami of the L2-L4 spinal nerves in all the cases, this is consistent with the literature. As the FN enters the anterior thigh, deep to the inguinal ligament, it lies in relation to the FA and the FV. The FN is at the closest proximity to the ASIS, followed by the FA and then the FV. Femoral nerve blocks are suggested to be performed lateral to the FN, so to avoid piercing the FA and FV with the advancement of the needle closer to the proximity of the FN. Similarly, ensuring that the needle is a significant distance from the FN will ensure that it is not damage by the needle.

Ensuring that there is a low incidence rate of nerve injury and nerve entrapment as a result of clinical instruments and installed devices is imperative in giving patients a better post-operative quality of life. This goes hand-in-hand with ensuring that clinicians regularly consult the literature to determine the safest and most efficient ways to successful complete procedures. This study will assist clinicians in the pursuit

of knowledge of the anatomy of the lumbar plexus and its branches throughout their course. It is suggested that further studies be conducted in clinical settings using the results of this study, in order to further expand the knowledge base on the lumbar plexus and its branches. Cadaver dissections are an important resource to be used together with clinical practice for the advancement of patient care.

Chapter 1 References

ARMAGHANI, S. J., EVEN, J. L., ZERN, E. K., BRALY, B. A., KANG, J. D. & DEVIN, C. J. 2016. The evaluation of donor site pain after harvest of tricortical anterior iliac crest bone graft for spinal surgery: a prospective study. *Spine,* 41**,** E191-E196.

AYDOGMUS, S., KELEKCI, S., AYDOGMUS, H., EKMEKCI, E., SECIL, Y. & TURE, S. 2014. Obturator nerve injury: an infrequent complication of TOT procedure. *Case reports in obstetrics and gynecology,* 2014.

BOMBERG, H., WETJEN, L., WAGENPFEIL, S., SCHÖPE, J., KESSLER, P., WULF, H., WIESMANN, T., STANDL, T., GOTTSCHALK, A. & DÖFFERT, J. 2018. Risks and benefits of ultrasound, nerve stimulation, and their combination for guiding peripheral nerve blocks: a retrospective registry analysis. *Anesthesia & Analgesia,* 127**,** 1035-1043.

BOZKURT, M., YUMRU, A. & SALMAN, S. 2015. Assessment of perioperative, early, and late postoperative complications of the inside-out transobturator tape procedure in the treatment of stress urinary incontinence. *Clin Exp Obstet Gynecol,* 42**,** 82-9.

DUCKETT, J., BODNER-ADLER, B., RACHANENI, S. & LATTHE, P. 2019. Management of complications arising from the use of mesh for stress urinary incontinence—International Urogynecology Association Research and Development Committee opinion. *International urogynecology journal***,** 1-5.

GUAY, J., PARKER, M. J., GRIFFITHS, R. & KOPP, S. 2017. Peripheral nerve blocks for hip fractures. *Cochrane Database of Systematic Reviews*.

HORLOCKER, T. T., KOPP, S. L. & WEDEL, D. J. 2015. Peripheral nerve blocks. *Miller's Anesthesia. 8th ed. Philadelphia: Elsevier Saunders***,** 1730-740.

HURI, E., EZER, M., AYDOĞAN, B., TATAR, İ. & SARGON, M. F. 2015. Anatomic transobturator tape (TOT) technique: clinical anatomic landmarks of obturator foramen on female cadavers. *Anatomy,* 9.

KATZEN, B. T. 2019. Clinical diagnosis and prognosis of acute limb ischemia. *Reviews in cardiovascular medicine,* 3**,** 2-6.

LANGE, J., KAUFMANN, R., WIJSMULLER, A., PIERIE, J., PLOEG, R., CHEN, D. & AMID, P. 2015. An international consensus algorithm for management of chronic postoperative inguinal pain. *Hernia,* 19**,** 33-43.

LEE, R., SIDESO, E., UBEROI, R. & HANDA, A. 2016. Abdominal aortic aneurysm and lumbar plexus palsy. *European heart journal,* 37**,** 977-977.

LEWIS, S. R., PRICE, A., WALKER, K. J., MCGRATTAN, K. & SMITH, A. F. 2015. Ultrasound guidance for upper and lower limb blocks. *Cochrane Database of Systematic Reviews*.

PARK, A. G., SHAFI, K., FRIED, T. & VACCARO, A. R. 2016. Leg Pain/Weakness/Numbness. *Differential Diagnosis in Spine Surgery***,** 80.

SUDA, A. J., SCHAMBERGER, C. T. & VIERGUTZ, T. 2019. Donor site complications following anterior iliac crest bone graft for treatment of distal radius fractures. *Archives of orthopaedic and trauma surgery,* 139**,** 423-428.

SUGIMOTO, Y., ITO, Y., TOMIOKA, M., TANAKA, M., HASEGAWA, Y., NAKAGO, K. & YAGATA, Y. 2010. Risk factors for lumbosacral plexus palsy related to pelvic fracture. *Spine,* 35**,** 963-966.

THOMAS, A. C., WOJTYS, E. M., BRANDON, C. & PALMIERI-SMITH, R. M. 2016. Muscle atrophy contributes to quadriceps weakness after anterior cruciate ligament reconstruction. *Journal of science and medicine in sport,* 19**,** 7-11.

VASU, S. & SAGAR, K. 2018. A clinical study of post operative complications of Lichtenstein's hernioplasty for inguinal hernia. *International Surgery Journal,* 6**,** 13-16.
WILLIAMS, B. A., IBINSON, J. W., GOULD, A. J. & MANGIONE, M. P. 2017. The incidence of peripheral nerve injury after multimodal perineural anesthesia/analgesia does not appear to differ from that following single-drug nerve blocks (2011–2014). *Pain Medicine,* 18**,** 628-636.
XU, D. & HADZIC, A. 2015. Complications of Peripheral Nerve Blocks. *Regional Nerve Blocks in Anesthesia and Pain Therapy.* Springer.
YANG, L., LI, M., CHEN, C., SHEN, J. & BU, X. 2017. Fascia iliaca compartment block versus no block for pain control after lower limb surgery: a meta-analysis. *Journal of pain research,* 10**,** 2833.

ANNEXURE A

Inter and intra-observer error

Bland-Altman plots were performed on 10% of the sample size for each measurement to determine inter and intra-observer reliability. Thereafter, linear regression was performed on the inter- and intra-observer means, to determine whether there was any directional biase in the measurements. A linear regression test result t-value close to 0 indicates strong agreement between the measurements. A p-value larger than 0.05 indicates that there is no statistically significant difference in the measurement and strengthens the result of the t-value. In a case where the t-value is large, therefore indicating that there is moderate to low agreement, the p-value will determine whether the weakness is statistically significant ($p>0.05$). The results of the Bland-Altman plots and linear regression tests for each of the nerves, both on the left and the right sides may be found in the subsequent pages.

1. ILIOHYPOGASTRIC AND ILIOINGUINAL NERVES

Inter-observer tests for the measurements from the ASIS to the IHN

Left side

Table 1: The mean, standard deviation (SD), standard error (SE) and the upper and the upper and lower limits of the 95% confidence interval of the inter-observer measurements

	N	Mean	SD	SE	Upper	Lower
ASIS to IHN (Inter-observer)	10	-1,99	8,66	2,74	14,99	-18,97

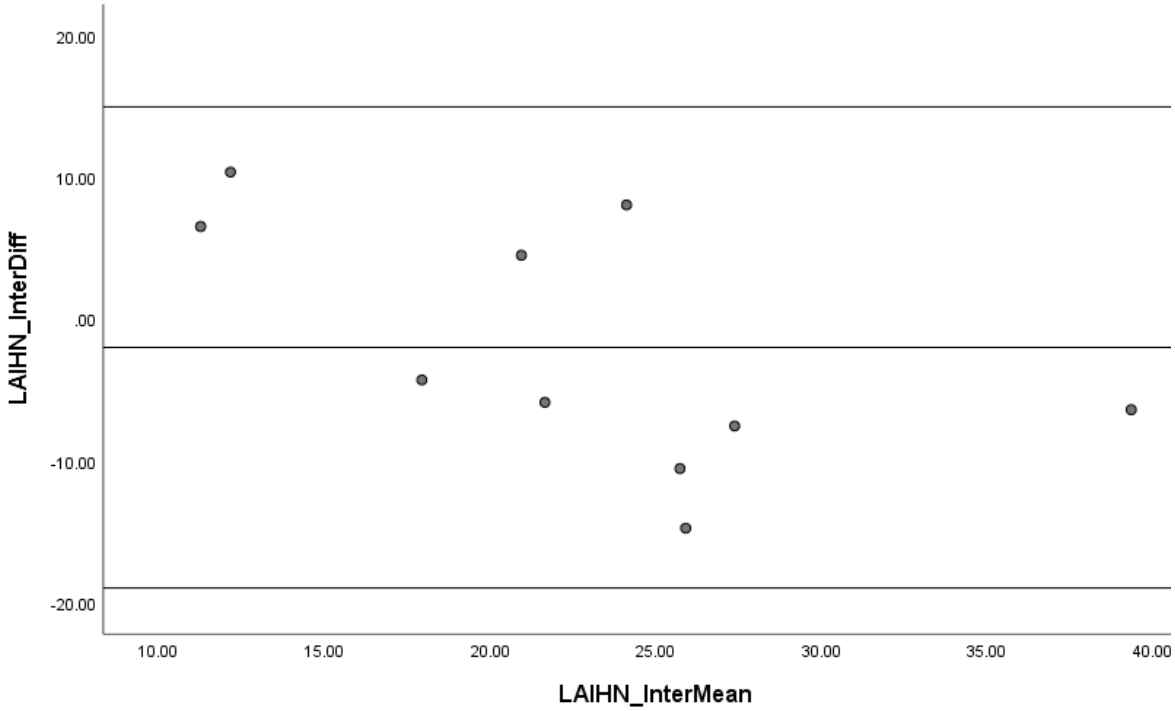

Figure 1: Bland-Altman plot for the left inter-observer (Inter) measurements from the ASIS to the IHN (LAIHN)

Table 2: Results of a linear regression test to determine the presence of directional bias of measurements

	Unstandardized Coefficients		Standardized Coefficients	t	p
	B	SE	Beta		
ASIS to IHN (Inter-observer)	-0,64	0,30	-0,60	-2,10	0,07

Right side

Table 3: The mean, standard deviation (SD), standard error (SE) and the upper and the upper and lower limits of the 95% confidence interval of the inter-observer measurements

	N	Mean	SD	SE	Upper	Lower
ASIS to IHN (Inter-observer)	10	-4,05	9,25	2,92	14,07	-22,18

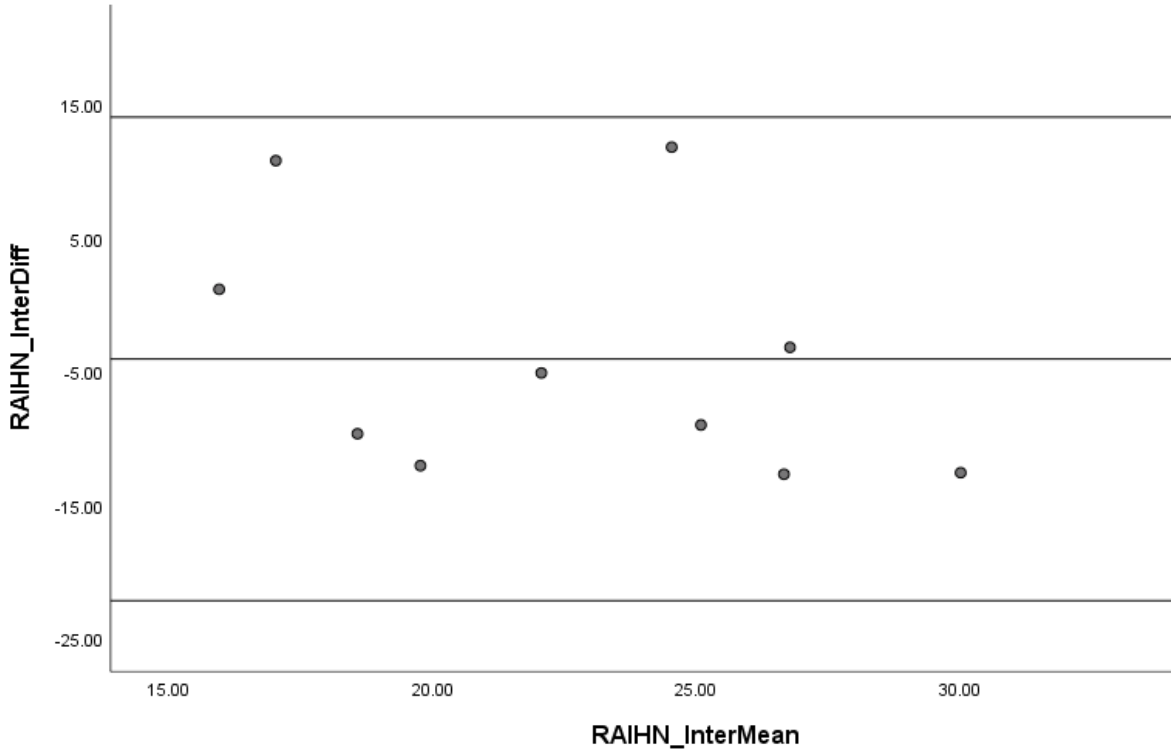

Figure 2: Bland-Altman plot for the right inter-observer (Inter) measurements from the ASIS to the IHN (LAIHN)

Table 4: Results of a linear regression test to determine the presence of directional bias of measurements

	Unstandardized Coefficients		Standardized Coefficients	t	p
	B	SE	Beta		
ASIS to IHN (Inter-observer)	-0,75	0,64	-0,38	-1,16	0,28

Inter-observer tests for the measurements from the ASIS to the IIN

Left side

Table 5: The mean, standard deviation (SD), standard error (SE) and the upper and the upper and lower limits of the 95% confidence interval of the inter-observer measurements

	N	Mean	SD	SE	Upper	Lower
ASIS to IIN (Inter-observer)	10	-1,40	20,35	6,43	38,48	-41,28

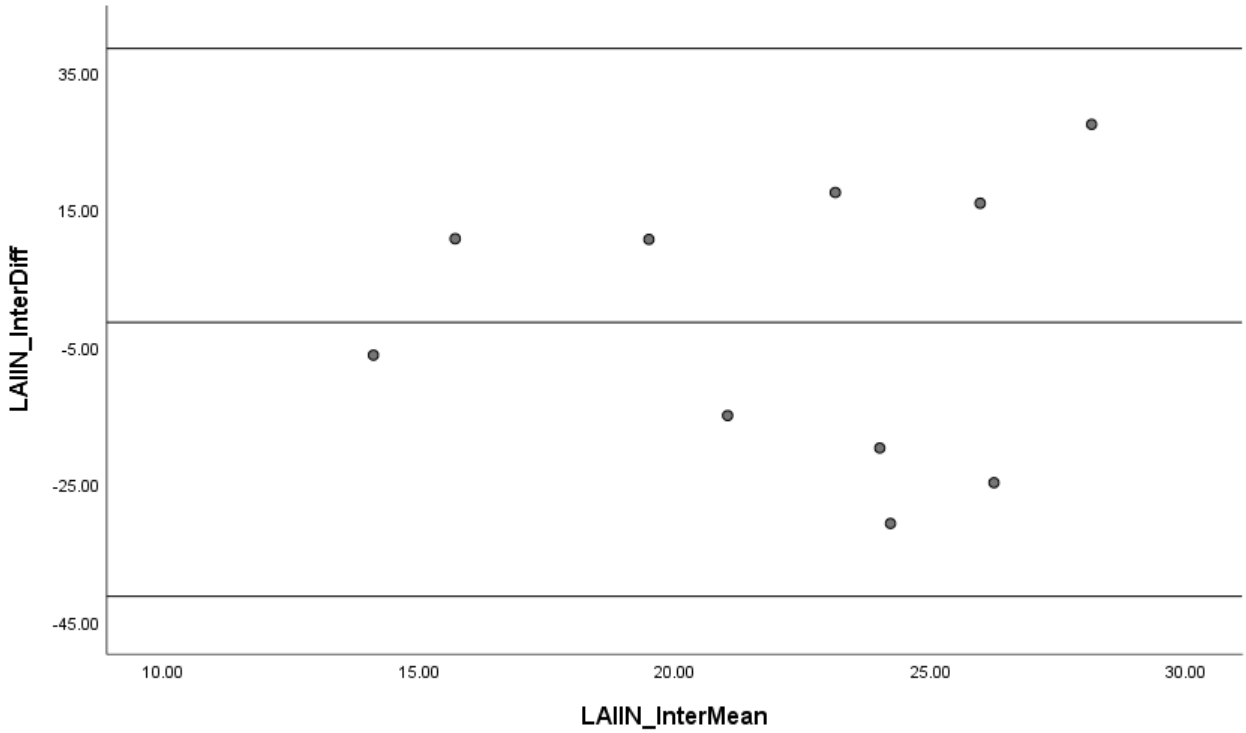

Figure 3: Bland-Altman plot for the left inter-observer (Inter) measurements from the ASIS to the IIN (LAIIN)

Table 6: Results of a linear regression test to determine the presence of directional bias of measurements

	Unstandardized Coefficients		Standardized Coefficients	t	p
	B	SE	Beta		
ASIS to IIN (Inter-observer)	0,06	1,56	0,01	0,04	0,97

Right side

Table 7: The mean, standard deviation (SD), standard error (SE) and the upper and the upper and lower limits of the 95% confidence interval of the inter-observer measurements

	N	Mean	SD	SE	Upper	Lower
ASIS to IIN (Inter-observer)	10	3,29	20,27	6,41	43,01	-36,44

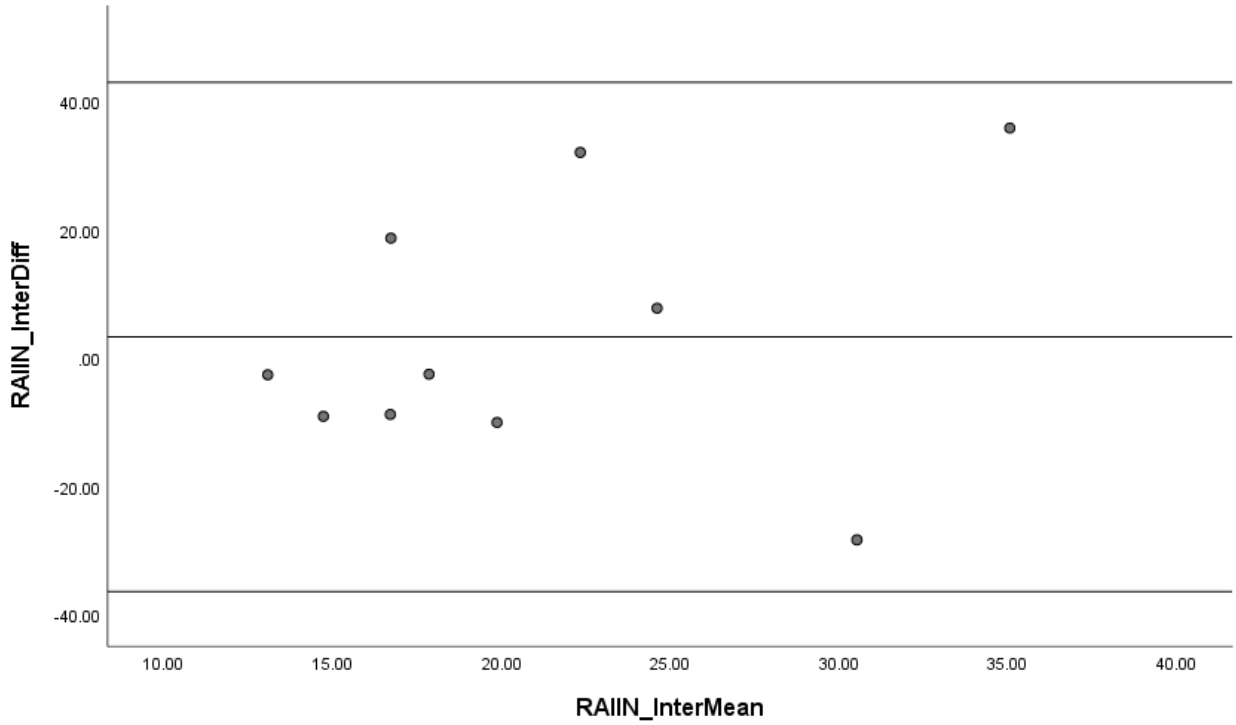

Figure 4: Bland-Altman plot for the right inter-observer (Inter) measurements from the ASIS to the IIN (RAIIN)

Table 8: Results of a linear regression test to determine the presence of directional bias of measurements

	Unstandardized Coefficients		Standardized Coefficients	t	p
	B	SE	Beta		
ASIS to IIN (Inter-observer)	0,78	0,97	0,27	0,81	0,44

Intra-observer tests for the measurements from the ASIS to the IHN

Left side

Table 9: The mean, standard deviation (SD), standard error (SE) and the upper and the upper and lower limits of the 95% confidence interval of the intra-observer measurements

	N	Mean	SD	SE	Upper	Lower
ASIS to IHN (Intra-observer)	10	-5,45	9,04	2,86	12,26	-23,16

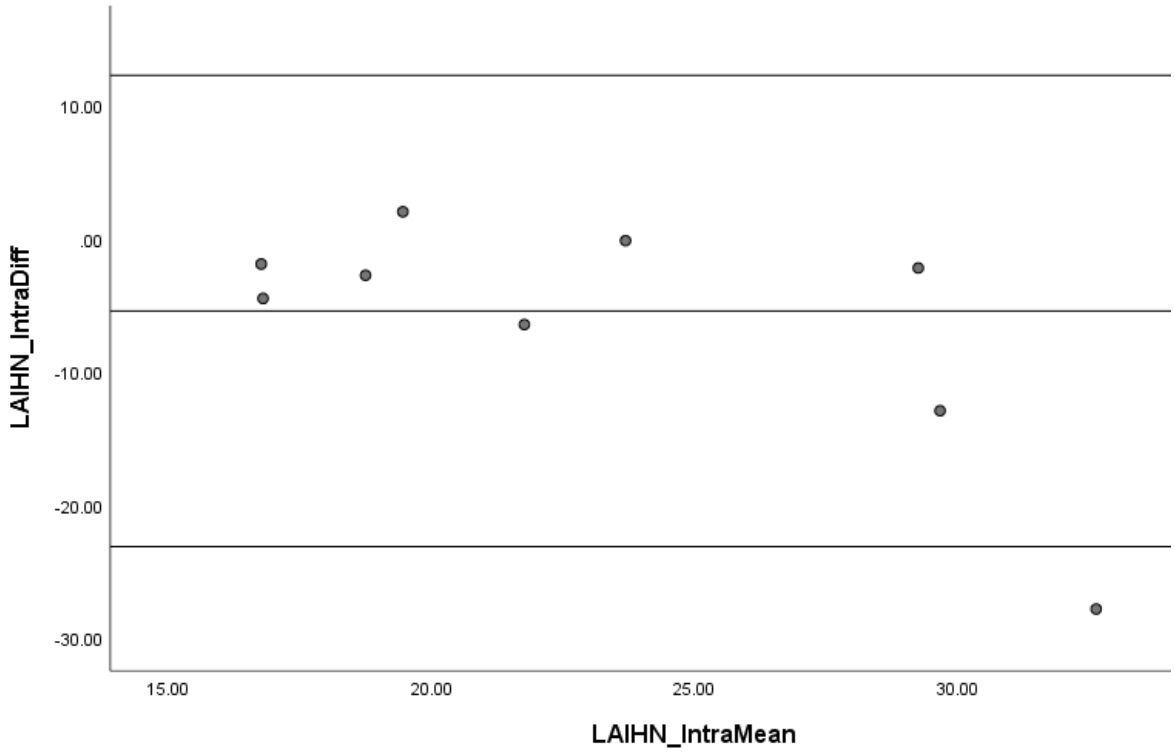

Figure 5: Bland-Altman plot for the left intra-observer (Intra) measurements from the ASIS to the IHN (LAIHN)

Table 10: Results of a linear regression test to determine the presence of directional bias of measurements

	Unstandardized Coefficients		Standardized Coefficients	t	p
	B	SE	Beta		
ASIS to IHN (Intra-observer)	-0,52	0,44	-0,39	-1,19	0,27

Right side

Table 11: The mean, standard deviation (SD), standard error (SE) and the upper and the upper and lower limits of the 95% confidence interval of the intra-observer measurements

	N	Mean	SD	SE	Upper	Lower
ASIS to IHN (Intra-observer)	10	-1,58	4,93	1,56	8,07	-11,24

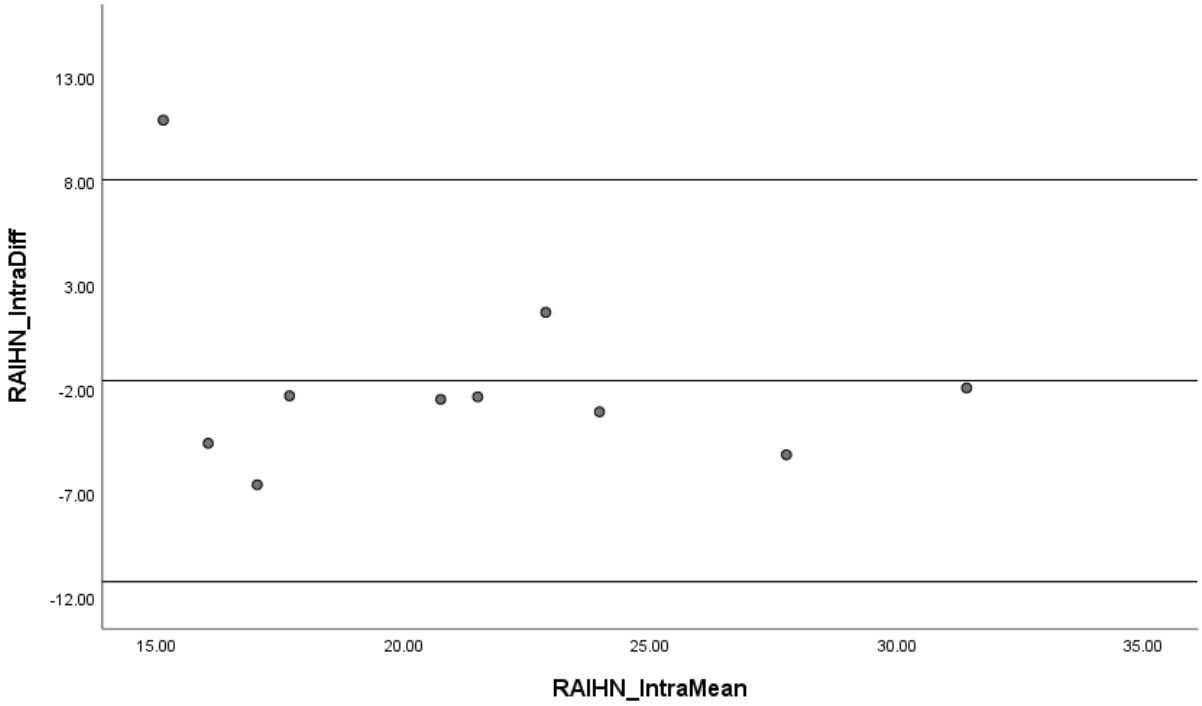

Figure 6: Bland-Altman plot for the right intra-observer (Intra) measurements from the ASIS to the IHN (RAIHN)

Table 12: Results of a linear regression test to determine the presence of directional bias of measurements

	Unstandardized Coefficients		Standardized Coefficients	t	p
	B	SE	Beta		
ASIS to IHN (Intra-observer)	-0,25	0,32	-0,27	-0,78	0,46

Intra-observer tests for the measurements from the ASIS to the IIN

Left side

Table 13: The mean, standard deviation (SD), standard error (SE) and the upper and the upper and lower limits of the 95% confidence interval of the intra-observer measurements

	N	Mean	SD	SE	Upper	Lower
ASIS to IIN (Intra-observer)	10	0,36	7,16	2,26	14,40	-13,68

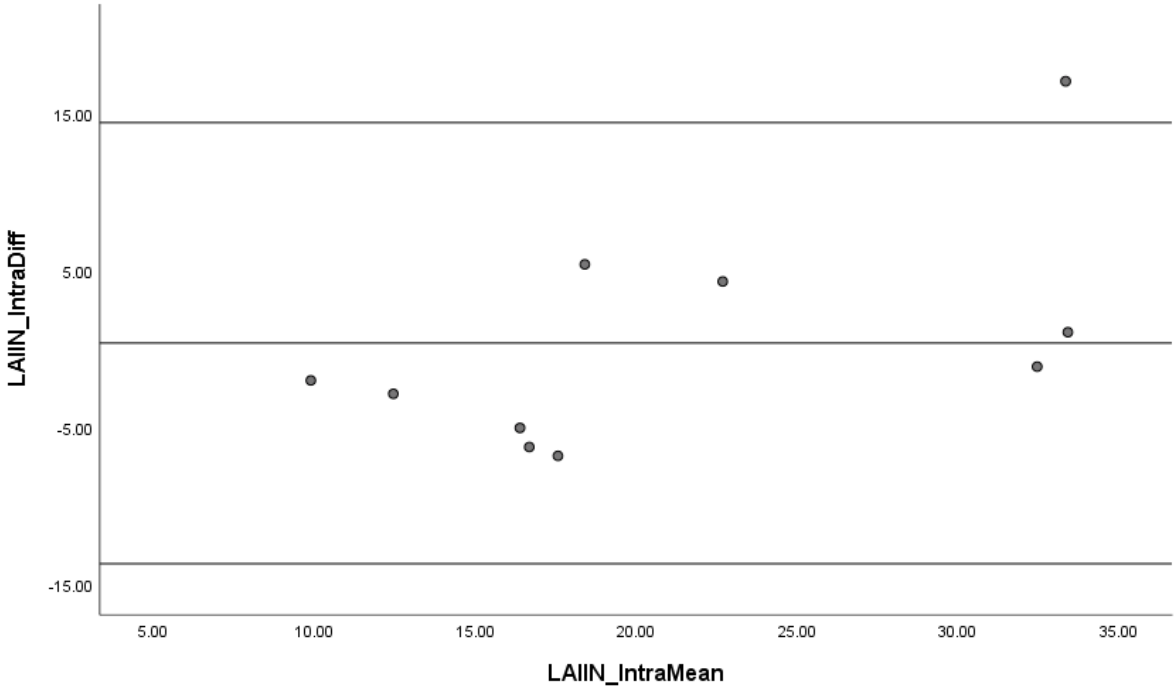

Figure 7: Bland-Altman plot for the left intra-observer (Intra) measurements from the ASIS to the IIN (LAIIN)

Table 14: Results of a linear regression test to determine the presence of directional bias of measurements

	Unstandardized Coefficients		Standardized Coefficients	t	p
	B	SE	Beta		
ASIS to IIN (Intra-observer)	0,47	0,24	0,57	1,96	0,09

Right side

Table 15: The mean, standard deviation (SD), standard error (SE) and the upper and the upper and lower limits of the 95% confidence interval of the intra-observer measurements

	N	Mean	SD	SE	Upper	Lower
ASIS to IIN (Intra-observer)	10	1,41	14,14	4,47	29,12	-26,30

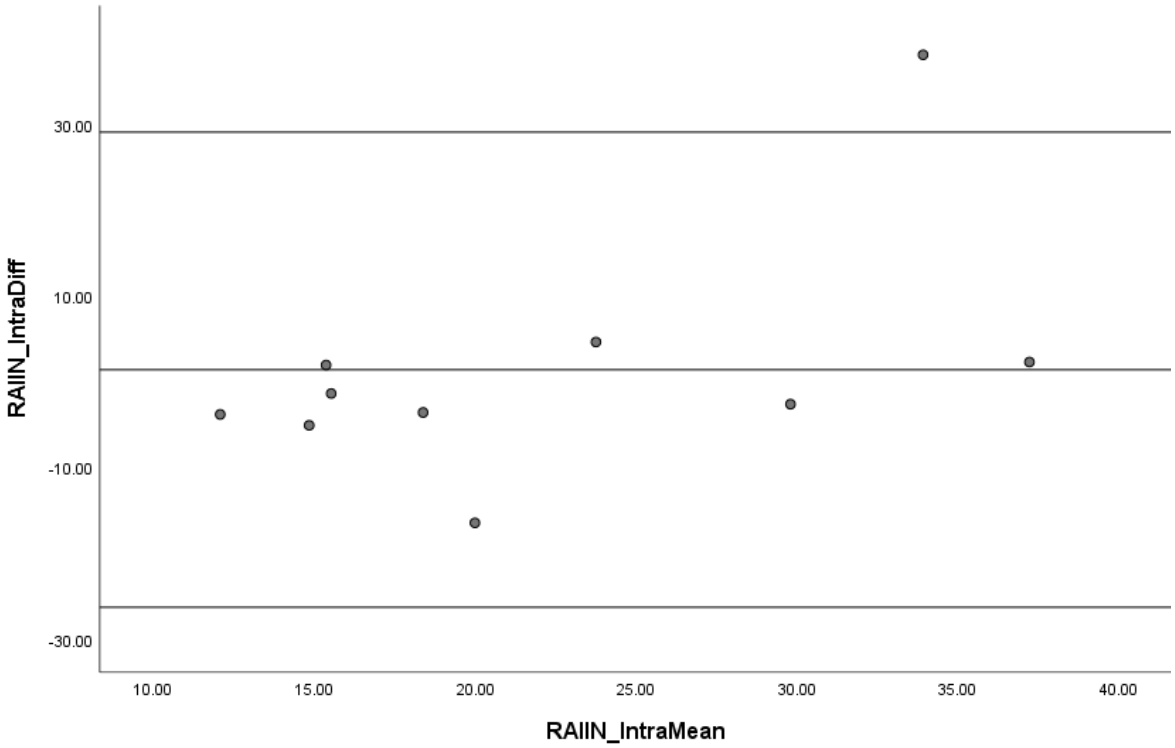

Figure 8: Bland-Altman plot for the right intra-observer (Intra) measurements from the ASIS to the IIN (RAIIN)

Table 16: Results of a linear regression test to determine the presence of directional bias of measurements

	Unstandardized Coefficients		Standardized Coefficients	t	p
	B	SE	Beta		
ASIS to IIN (Intra-observer)	0,86	0,48	0,53	1,78	0,11

2. GENITOFEMORAL NERVE

Inter-observer tests for the measurements from the midline of the body to the exit of the GFN

Left side

Table 17: The mean, standard deviation (SD), standard error (SE) and the upper and the upper and lower limits of the 95% confidence interval of the inter-observer measurements

	N	Mean	SD	SE	Upper	Lower
Midline to GFN exit (Inter-observer)	7	-5,09	7,74	2,93	10,08	-20,26

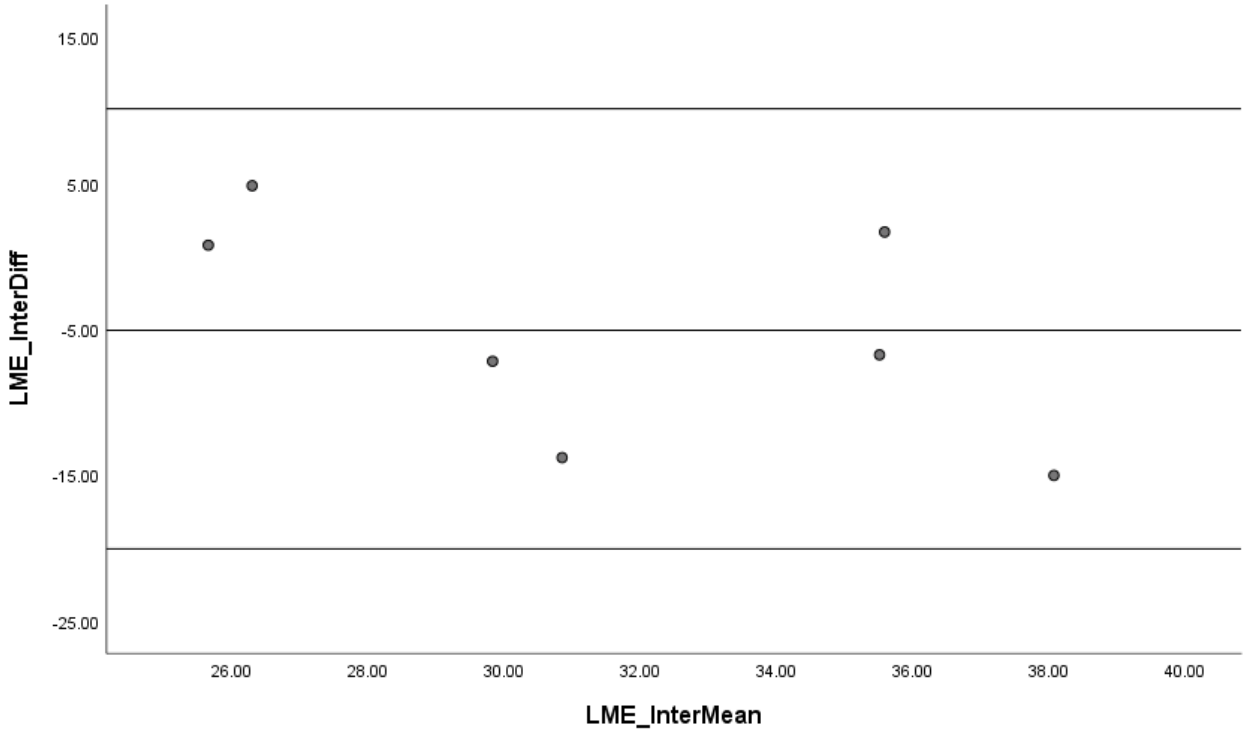

Figure 9: Bland-Altman plot for the left inter-observer (Inter) measurements from the from the midline of the body to the exit of the GFN (LME)

Table 18: Results of a linear regression test to determine the presence of directional bias of measurements

	Unstandardized Coefficients		Standardized Coefficients	t	p
	B	SE	Beta		
Midline to GFN exit (Inter-observer)	-0,86	0,60	-0,54	-1,43	0,21

Right side

Table 19: The mean, standard deviation (SD), standard error (SE) and the upper and the upper and lower limits of the 95% confidence interval of the inter-observer measurements

	N	Mean	SD	SE	Upper	Lower
Midline to GFN exit (Inter-observer)	7	-5,72	7,69	2,91	9,35	-20,80

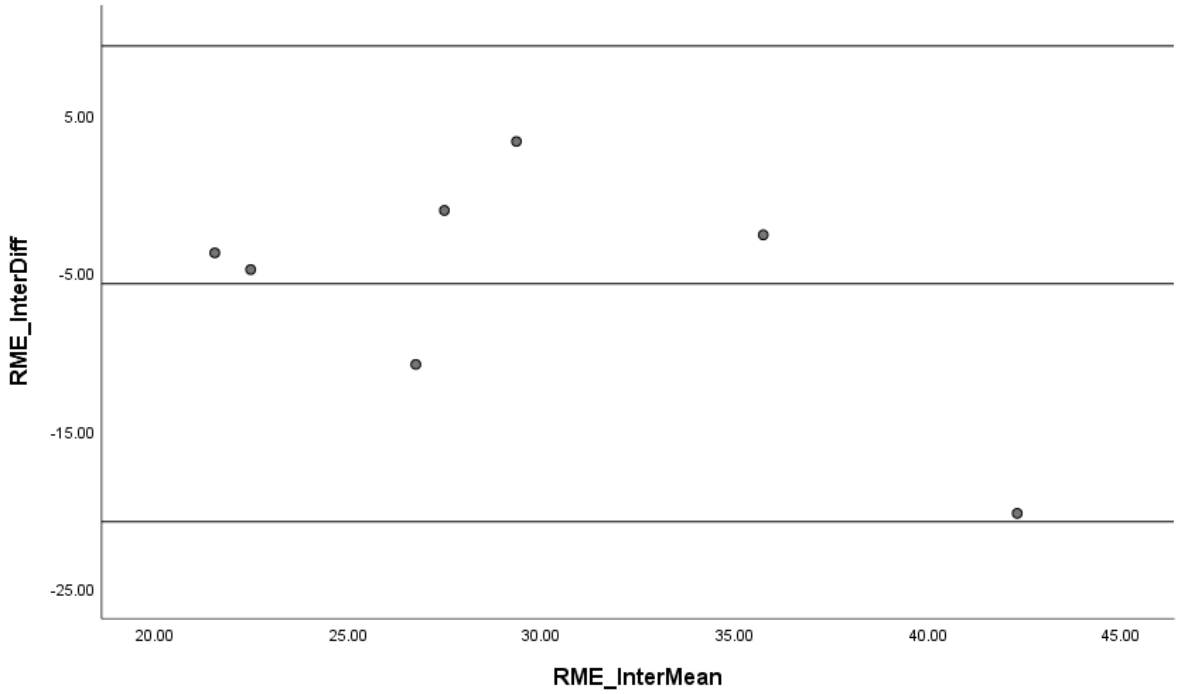

Figure 10: Bland-Altman plot for the right inter-observer (Inter) measurements from the from the midline of the body to the exit of the GFN (LME)

Table 20: Results of a linear regression test to determine the presence of directional bias of measurements

	Unstandardized Coefficients		Standardized Coefficients	t	p
	B	SE	Beta		
Midline to GFN exit (Inter-observer)	-0,57	0,39	-0,55	-1,45	0,21

Inter-observer tests for the measurements from the pubic tubercle (PT) to femoral branch of the GFN (FB-GFN)

Left side

Table 21: The mean, standard deviation (SD), standard error (SE) and the upper and the upper and lower limits of the 95% confidence interval of the inter-observer measurements

	N	Mean	SD	SE	Upper	Lower
PT to FB-GFN (Inter-observer)	7	-2,54	8,15	3,08	13,43	-18,51

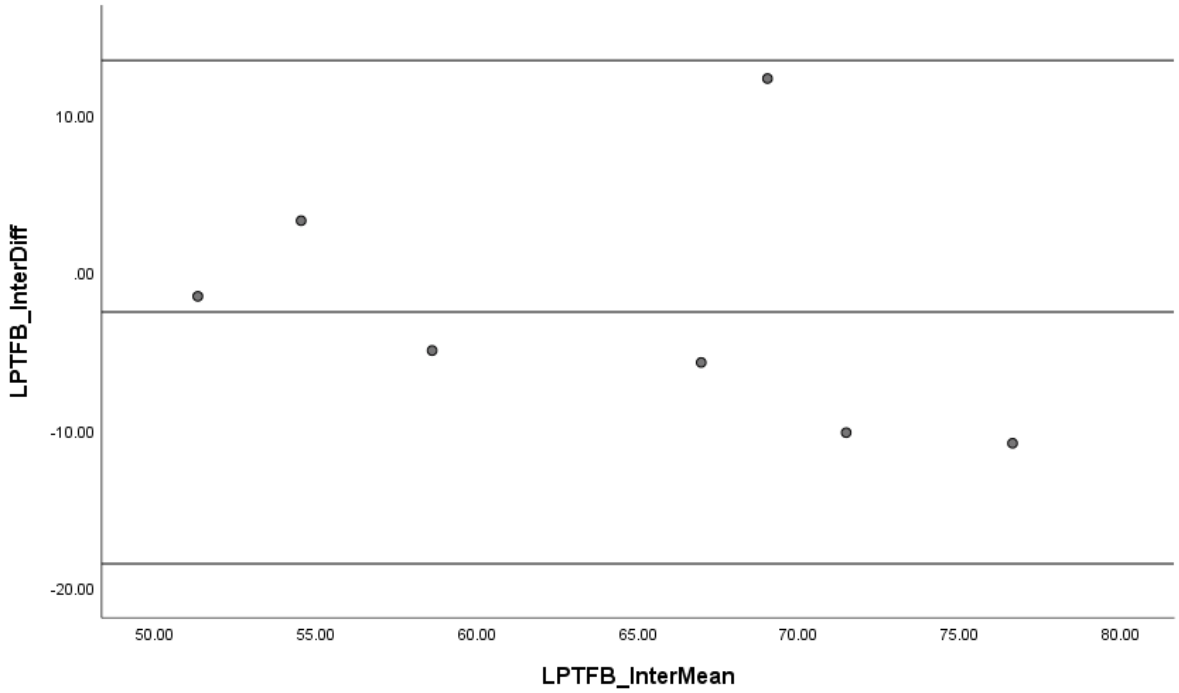

Figure 11: Bland-Altman plot for the left inter-observer (Inter) measurements from the from the pubic tubercle to the femoral branch of the GFN (PTFB)

Table 22: Results of a linear regression test to determine the presence of directional bias of measurements

	Unstandardized Coefficients		Standardized Coefficients	t	p
	B	SE	Beta		
PT to FB-GFN (Inter-observer)	-0,29	0,37	-0,33	-0,78	0,47

Right side

Table 23: The mean, standard deviation (SD), standard error (SE) and the upper and the upper and lower limits of the 95% confidence interval of the inter-observer measurements

	N	Mean	SD	SE	Upper	Lower
PT to FB-GFN (Inter-observer)	7	-0,94	8,67	3,28	16,06	-17,94

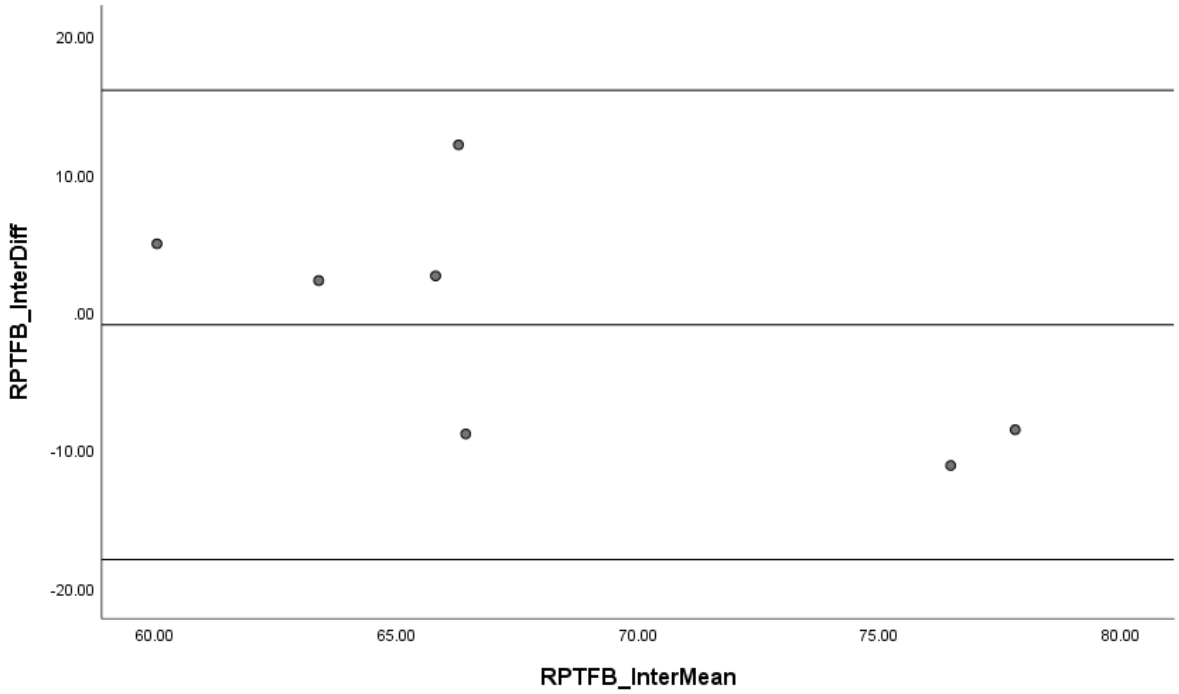

Figure 12: Bland-Altman plot for the right inter-observer (Inter) measurements from the from the pubic tubercle to the femoral branch of the GFN (PTFB)

Table 24: Results of a linear regression test to determine the presence of directional bias of measurements

	Unstandardized Coefficients		Standardized Coefficients	t	p
	B	SE	Beta		
PT to FB-GFN (Inter-observer)	-0,91	0,42	-0,70	-2,18	0,08

Inter-observer tests for the measurements from the pubic tubercle (PT) to genital branch of the GFN (GB-GFN)

Left side

Table 25: The mean, standard deviation (SD), standard error (SE) and the upper and the upper and lower limits of the 95% confidence interval of the inter-observer measurements

	N	Mean	SD	SE	Upper	Lower
PT to GB-GFN (Inter-observer)	7	0,76	7,04	2,66	14,55	-13,04

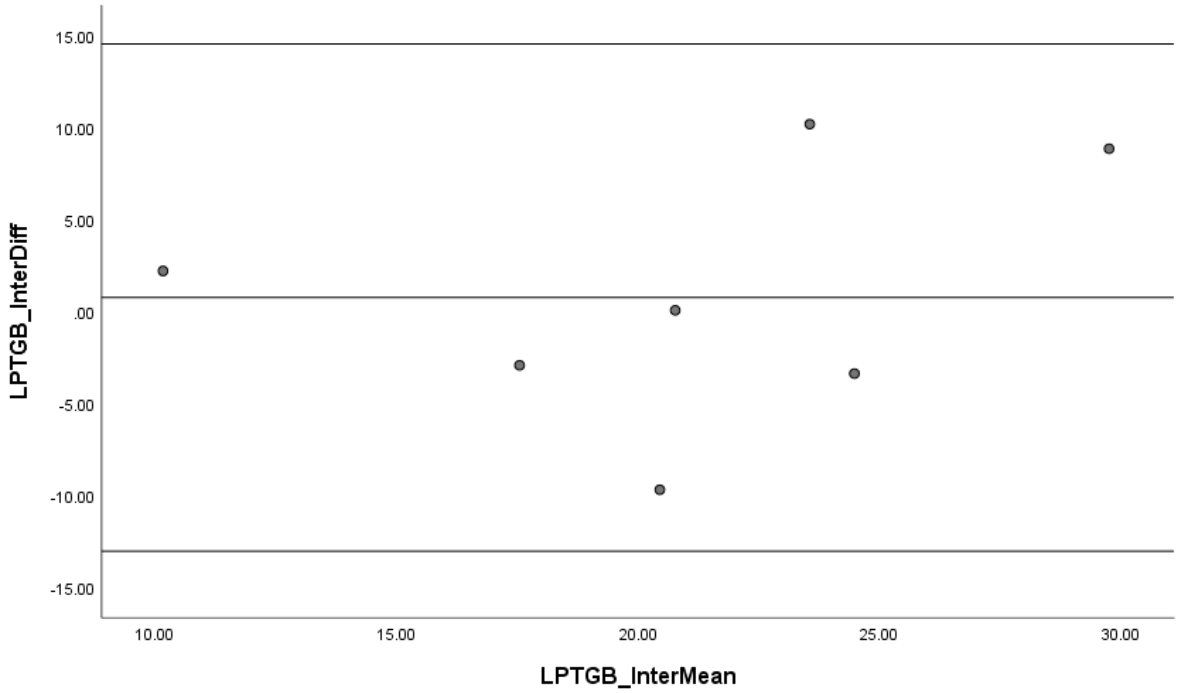

Figure 13: Bland-Altman plot for the left inter-observer (Inter) measurements from the from the pubic tubercle to the genital branch of the GFN (GTFB)

Table 26: Results of a linear regression test to determine the presence of directional bias of measurements

	Unstandardized Coefficients		Standardized Coefficients	t	p
	B	SE	Beta		
PT to GB-GFN (Inter-observer)	0,37	0,49	0,32	0,76	0,48

Right side

Table 27: The mean, standard deviation (SD), standard error (SE) and the upper and the upper and lower limits of the 95% confidence interval of the inter-observer measurements

	N	Mean	SD	SE	Upper	Lower
PT to GB-GFN (Inter-observer)	6	2,58	9,58	3,91	21,36	-16,20

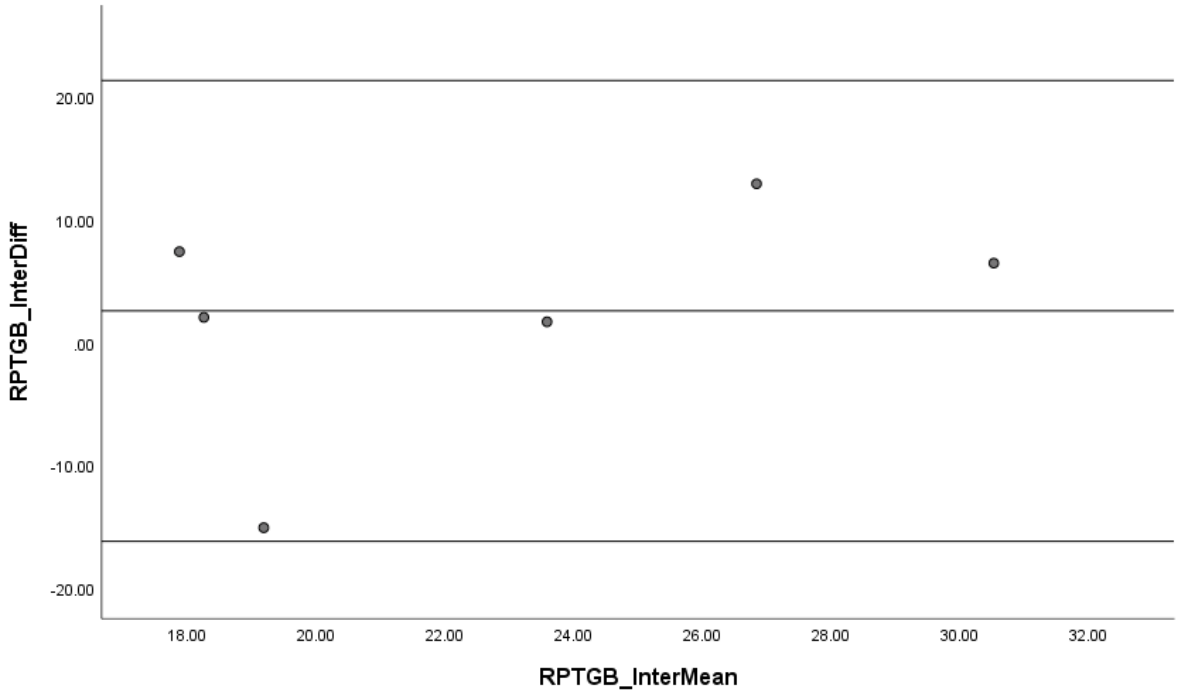

Figure 14: Bland-Altman plot for the right inter-observer (Inter) measurements from the from the pubic tubercle to the genital branch of the GFN (PTFB)

Table 28: Results of a linear regression test to determine the presence of directional bias of measurements

	Unstandardized Coefficients		Standardized Coefficients	t	p
	B	SE	Beta		
PT to GB-GFN (Inter-observer)	0,85	0,82	0,46	1,03	0,36

Intra-observer tests for the measurements from the midline of the body to the exit of the GFN

Left side

Table 29: The mean, standard deviation (SD), standard error (SE) and the upper and the upper and lower limits of the 95% confidence interval of the intra-observer measurements

	N	Mean	SD	SE	Upper	Lower
Midline to GFN exit (Intra-observer)	7	-6,55	7,96	3,01	9,05	-22,16

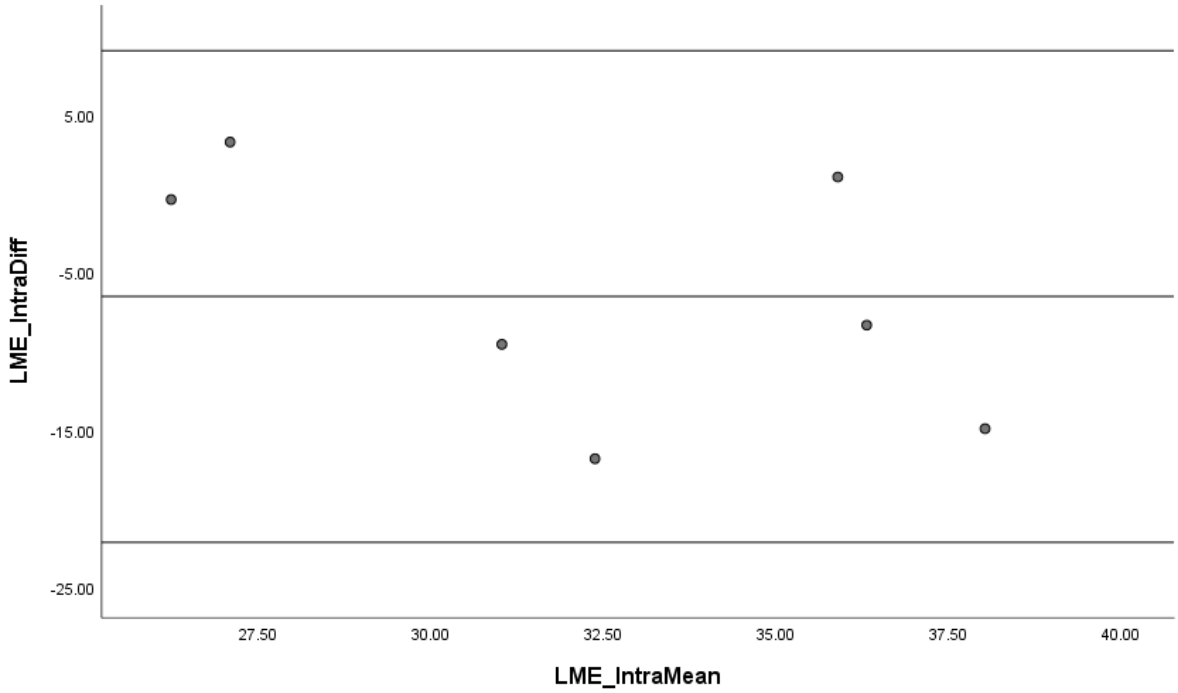

Figure 15: Bland-Altman plot for the left intra-observer (Intra) measurements from the from the midline of the body to the exit of the GFN (LME)

Table 30: Results of a linear regression test to determine the presence of directional bias of measurements

	Unstandardized Coefficients		Standardized Coefficients	t	p
	B	SE	Beta		
Midline to GFN exit (Intra-observer)	-0,89	0,66	-0,52	-1,35	0,24

Right side

Table 31: The mean, standard deviation (SD), standard error (SE) and the upper and the upper and lower limits of the 95% confidence interval of the intra-observer measurements

	N	Mean	SD	SE	Upper	Lower
Midline to GFN exit (Intra-observer)	7	-5,07	7,18	2,72	9,01	-19,15

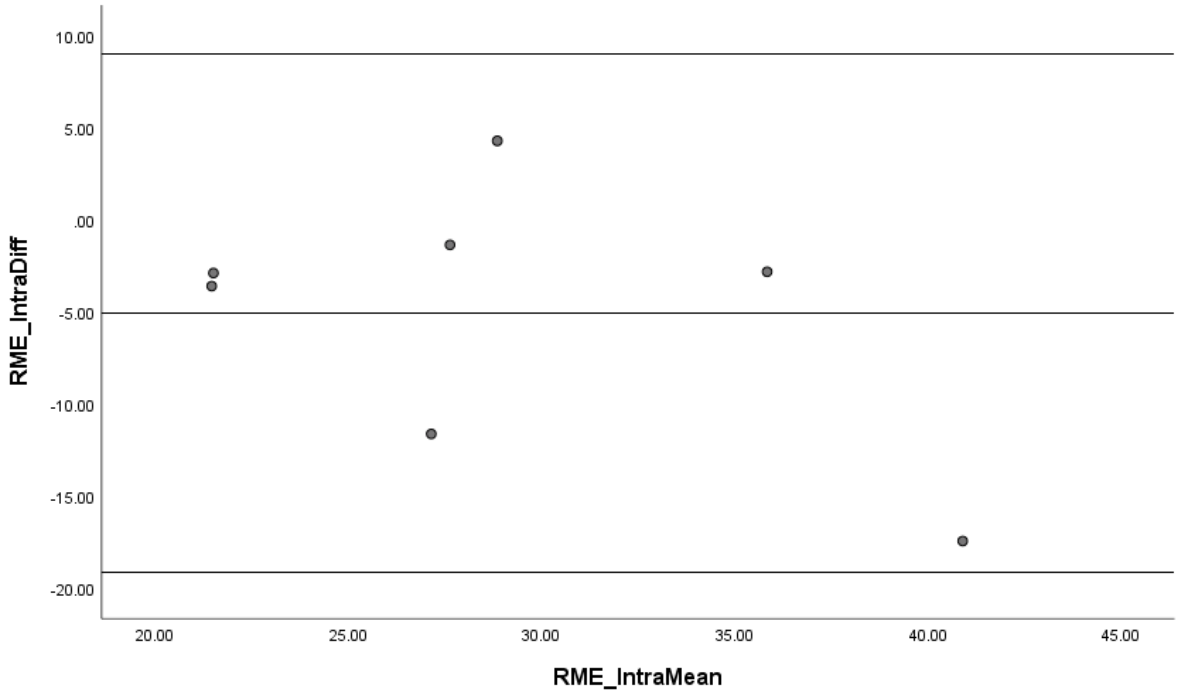

Figure 16: Bland-Altman plot for the right intra-observer (Inter) measurements from the from the midline of the body to the exit of the GFN (LME)

Table 32: Results of a linear regression test to determine the presence of directional bias of measurements

	Unstandardized Coefficients		Standardized Coefficients	t	p
	B	SE	Beta		
Midline to GFN exit (Intra-observer)	-0,50	0,39	-0,50	-1,29	0,26

Intra-observer tests for the measurements from the pubic tubercle (PT) to femoral branch of the GFN (FB-GFN)

Left side

Table 33: The mean, standard deviation (SD), standard error (SE) and the upper and the upper and lower limits of the 95% confidence interval of the intra-observer measurements

	N	Mean	SD	SE	Upper	Lower
PT to FB-GFN (Intra-observer)	7	-3,35	7,45	2,81	11,25	-17,94

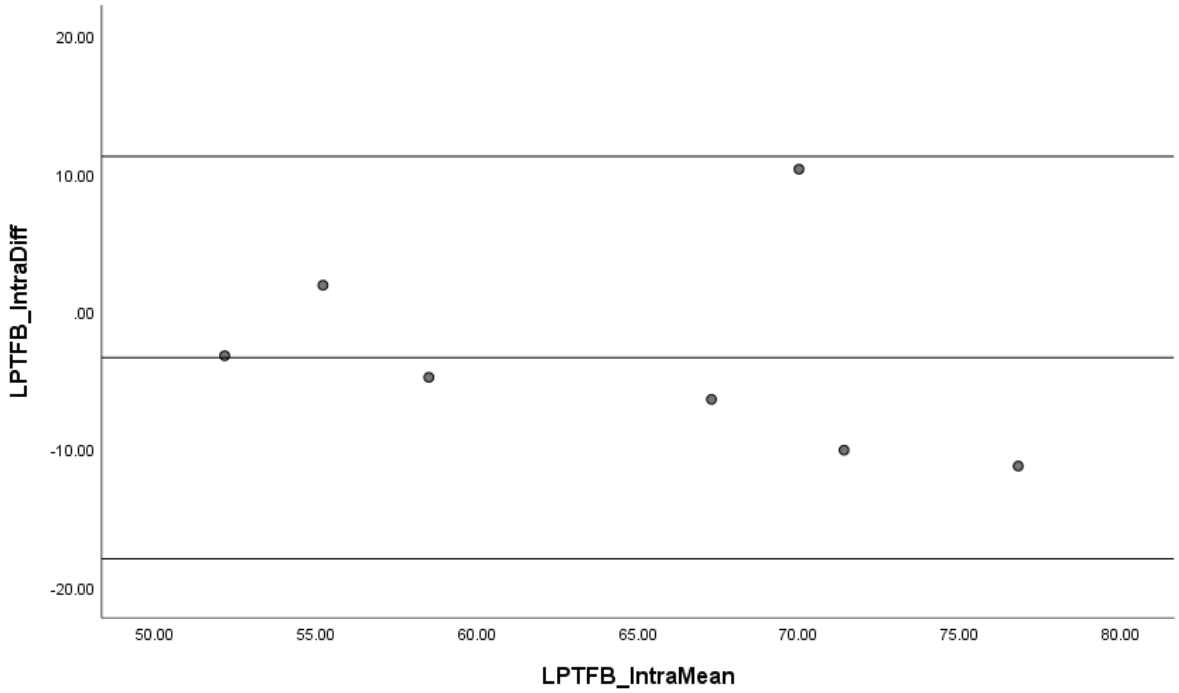

Figure 17: Bland-Altman plot for the left intra-observer (Inter) measurements from the from the pubic tubercle to the femoral branch of the GFN (PTFB)

Table 34: Results of a linear regression test to determine the presence of directional bias of measurements

	Unstandardized Coefficients		Standardized Coefficients	t	p
	B	SE	Beta		
PT to FB-GFN (Intra-observer)	-0,23	0,35	-0,29	-0,67	0,53

Right side

Table 35: The mean, standard deviation (SD), standard error (SE) and the upper and the upper and lower limits of the 95% confidence interval of the intra-observer measurements

	N	Mean	SD	SE	Upper	Lower
PT to FB-GFN (Intra-observer)	7	0,68	6,36	2,40	13,15	-11,79

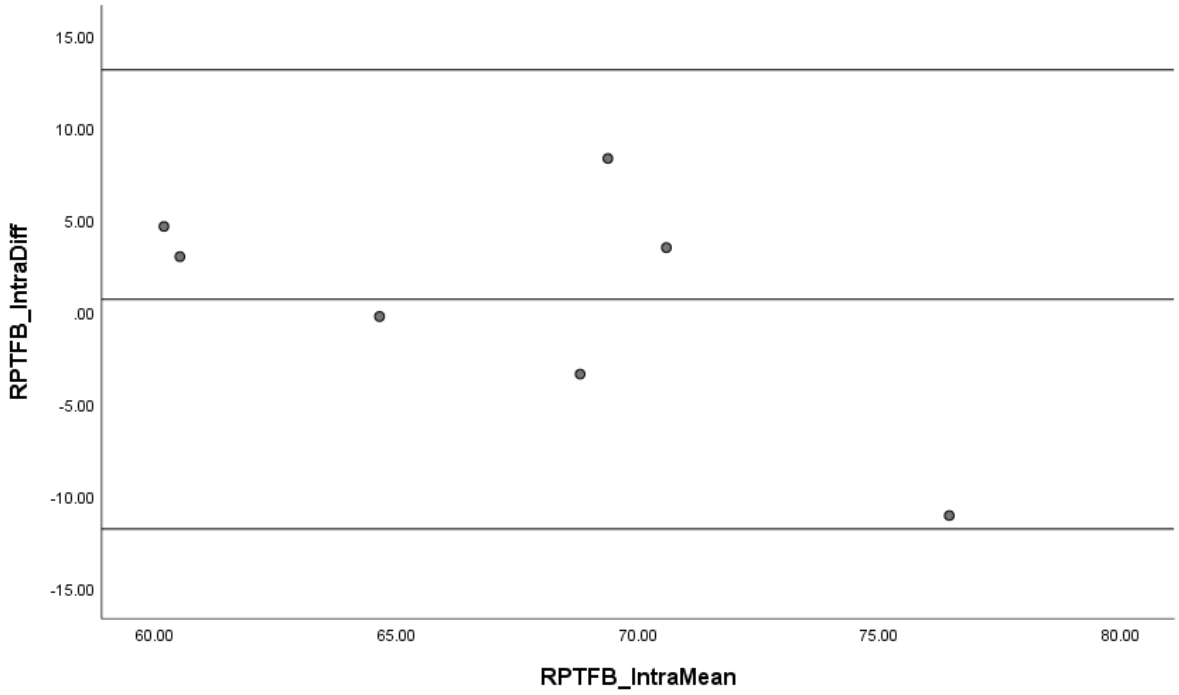

Figure 18: Bland-Altman plot for the right intra-observer (Inter) measurements from the from the pubic tubercle to the femoral branch of the GFN (PTFB)

Table 36: Results of a linear regression test to determine the presence of directional bias of measurements

	Unstandardized Coefficients		Standardized Coefficients	t	p
	B	SE	Beta		
PT to FB-GFN (Intra-observer)	-0,63	0,40	-0,58	-1,60	0,17

Intra-observer tests for the measurements from the pubic tubercle (PT) to genital branch of the GFN (GB-GFN)

Left side

Table 37: The mean, standard deviation (SD), standard error (SE) and the upper and the upper and lower limits of the 95% confidence interval of the intra-observer measurements

	N	Mean	SD	SE	Upper	Lower
PT to GB-GFN (Intra-observer)	7	1,14	7,07	2,67	14,99	-12,71

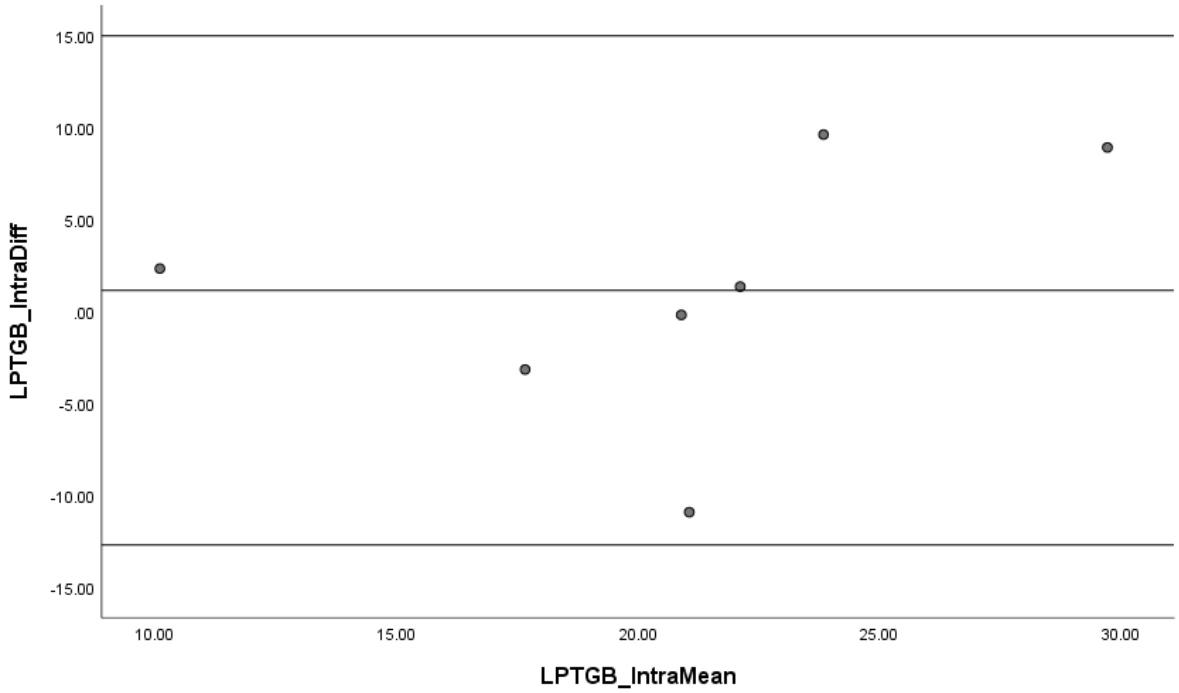

Figure 19: Bland-Altman plot for the left intra-observer (Intra) measurements from the from the pubic tubercle to the genital branch of the GFN (GTFB)

Table 38: Results of a linear regression test to determine the presence of directional bias of measurements

	Unstandardized Coefficients		Standardized Coefficients	t	p
	B	SE	Beta		
PT to GB-GFN (Intra-observer)	0,43	0,49	0,37	0,88	0,42

Right side

Table 39: The mean, standard deviation (SD), standard error (SE) and the upper and the upper and lower limits of the 95% confidence interval of the intra-observer measurements

	N	Mean	SD	SE	Upper	Lower
PT to GB-GFN (Intra-observer)	6	0,35	5,05	2,06	10,25	-9,54

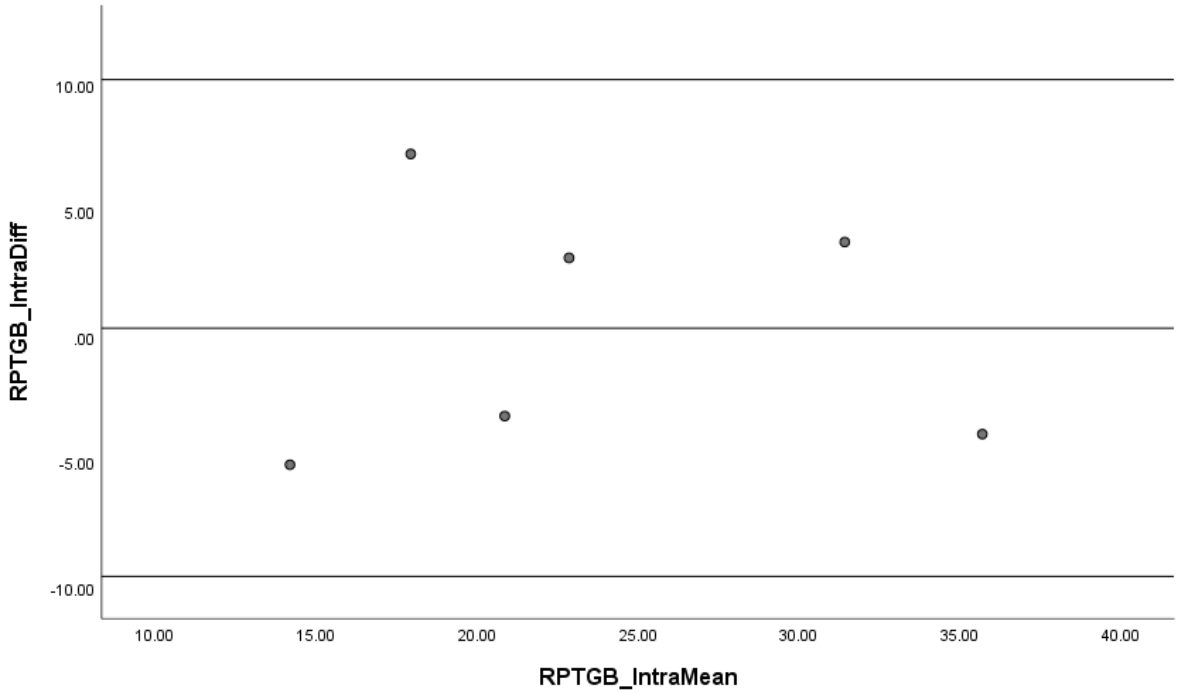

Figure 20: Bland-Altman plot for the right intra-observer (Intra) measurements from the from the pubic tubercle to the genital branch of the GFN (PTFB)

Table 40: Results of a linear regression test to determine the presence of directional bias of measurements

	Unstandardized Coefficients		Standardized Coefficients	t	p
	B	SE	Beta		
PT to GB-GFN (Intra-observer)	-0,01	0,31	-0,02	-0,05	0,97

3. LATERAL FEMORAL CUTANEOUS NERVE (LFCN)
Inter-observer tests for the measurements from the ASIS to the LFCN

Left side

Table 41: The mean, standard deviation (SD), standard error (SE) and the upper and the upper and lower limits of the 95% confidence interval of the inter-observer measurements

	N	Mean	SD	SE	Upper	Lower
ASIS to LFCN (Inter-observer)	10	-1,38	4,22	1,33	6,89	-9,64

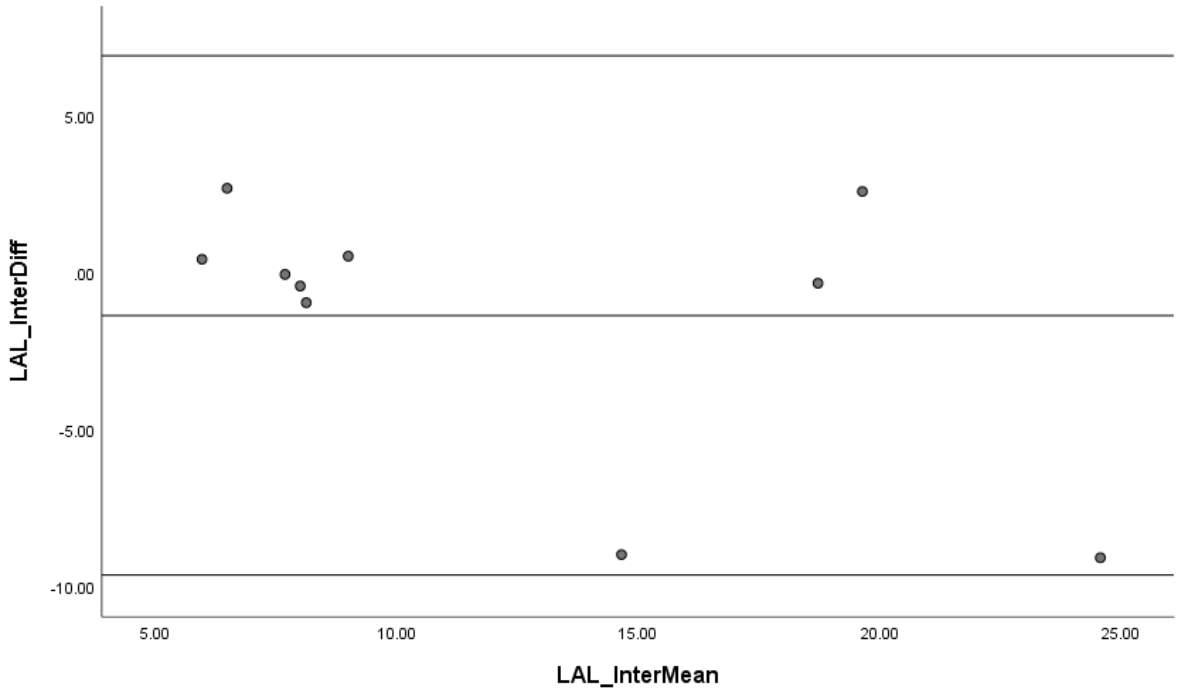

Figure 21: Bland-Altman plot for the left inter-observer (Inter) measurements from the from the ASIS to the LFCN

Table 42: Results of a linear regression test to determine the presence of directional bias of measurements

	Unstandardized Coefficients		Standardized Coefficients	t	p
	B	SE	Beta		
ASIS to LFCN (Inter-observer)	-0,33	0,19	-0,52	-1,71	0,13

Right side

Table 43: The mean, standard deviation (SD), standard error (SE) and the upper and the upper and lower limits of the 95% confidence interval of the inter-observer measurements

	N	Mean	SD	SE	Upper	Lower
ASIS to LFCN (Inter-observer)	10	-0,69	3,13	0,99	5,44	-6,83

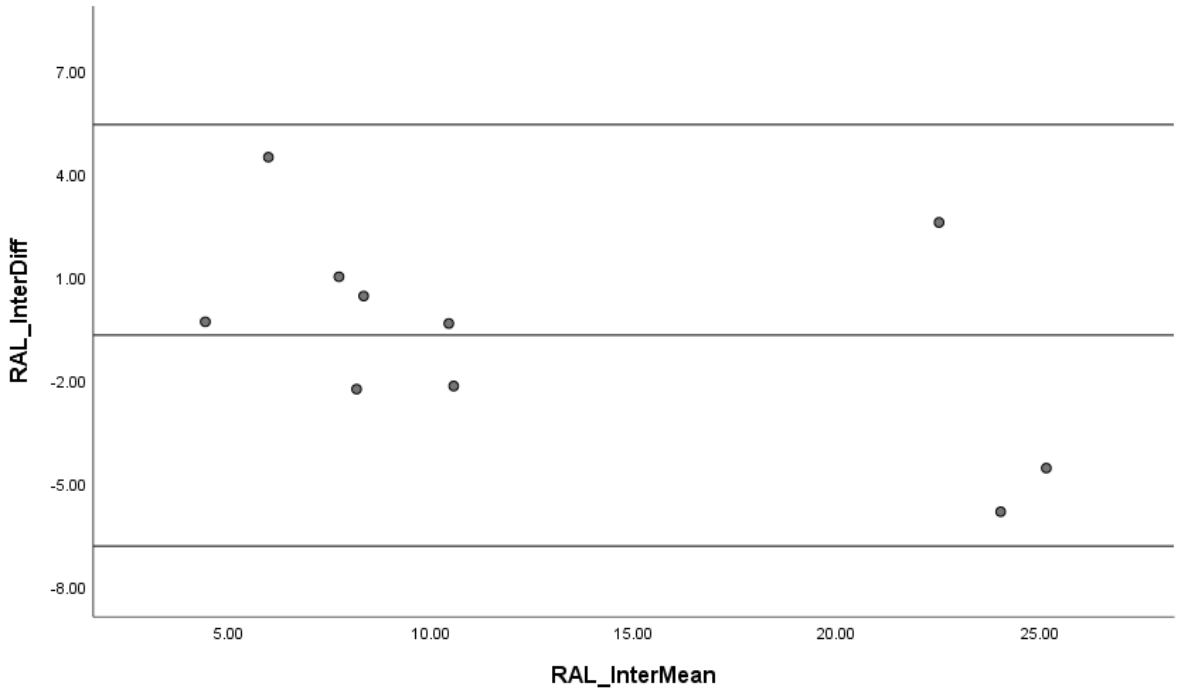

Figure 22: Bland-Altman plot for the right inter-observer (Inter) measurements from the from the ASIS to the LFCN

Table 44: Results of a linear regression test to determine the presence of directional bias of measurements

	Unstandardized Coefficients		Standardized Coefficients	t	p
	B	SE	Beta		
ASIS to LFCN (Inter-observer)	-0,21	0,12	-0,52	-1,72	0,12

Intra-observer tests for the measurements from the ASIS to the LFCN

Left side

Table 45: The mean, standard deviation (SD), standard error (SE) and the upper and the upper and lower limits of the 95% confidence interval of the intra-observer measurements

	N	Mean	SD	SE	Upper	Lower
ASIS to LFCN (Intra-observer)	10	-0,11	1,18	0,37	2,21	-2,42

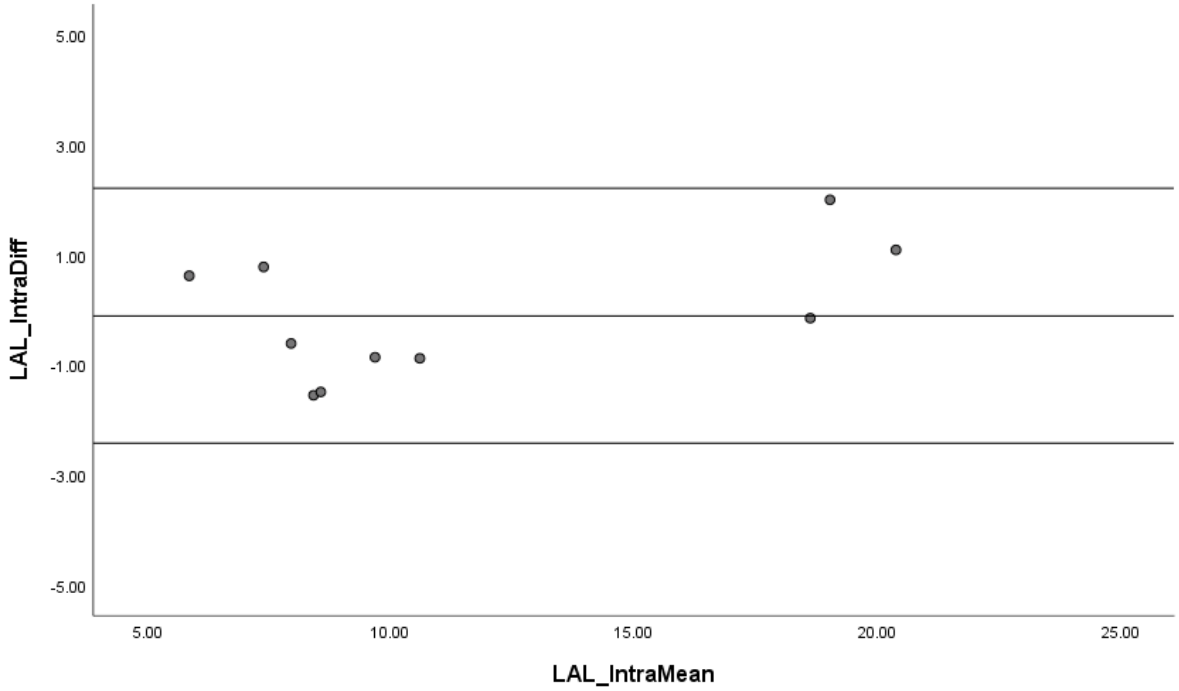

Figure 23: Bland-Altman plot for the left intra-observer (Intra) measurements from the from the ASIS to the LFCN

Table 46: Results of a linear regression test to determine the presence of directional bias of measurements

	Unstandardized Coefficients		Standardized Coefficients	t	p
	B	SE	Beta		
ASIS to LFCN (Intra-observer)	0,11	0,07	0,53	1,76	0,12

Right side

Table 47: The mean, standard deviation (SD), standard error (SE) and the upper and the upper and lower limits of the 95% confidence interval of the intra-observer measurements

	N	Mean	SD	SE	Upper	Lower
ASIS to LFCN (Intra-observer)	10	0,03	1,55	0,49	3,08	-3,01

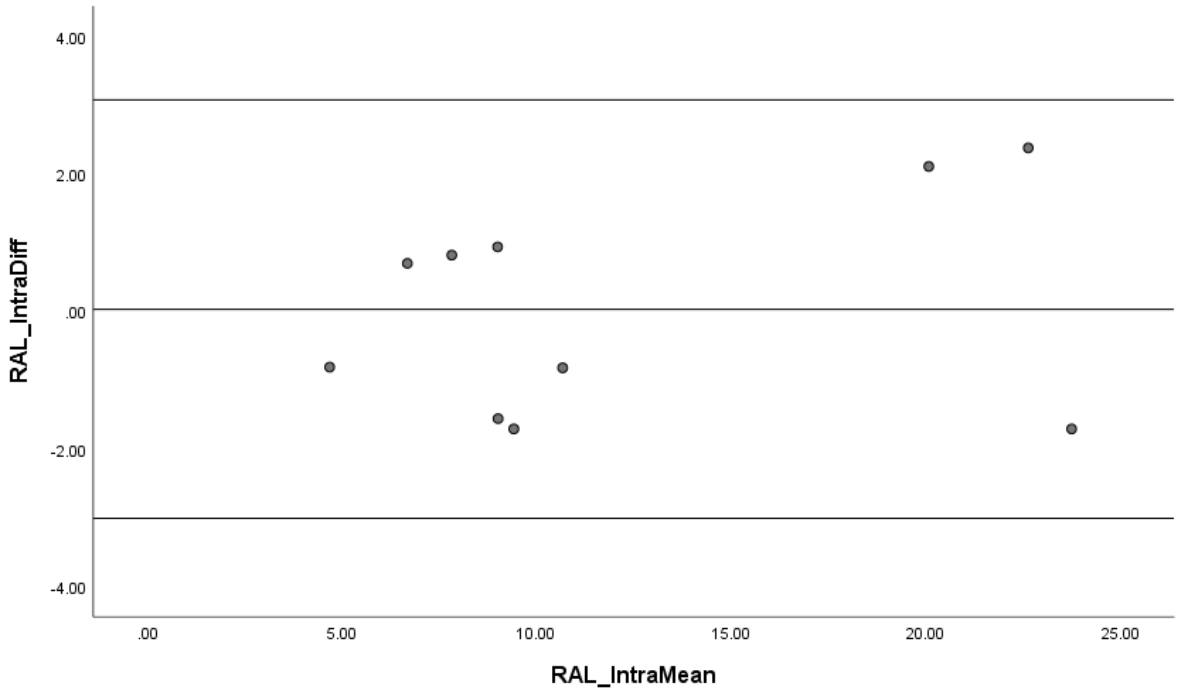

Figure 24: Bland-Altman plot for the right intra-observer (Intra) measurements from the from the ASIS to the LFCN

Table 48: Results of a linear regression test to determine the presence of directional bias of measurements

	Unstandardized Coefficients		Standardized Coefficients	t	p
	B	SE	Beta		
ASIS to LFCN (Intra-observer)	0,06	0,08	0,29	0,85	0,42

4. OBTURATOR NERVE (ON)

Inter-observer tests for the measurements from the most superior point of the obturator foramen (S) to the ON within the obturator foramen (N)

Left side

Table 49: The mean, standard deviation (SD), standard error (SE) and the upper and the upper and lower limits of the 95% confidence interval of the inter-observer measurements

	N	Mean	SD	SE	Upper	Lower
S to N (Inter-observer)	10	-0,17	1,27	0,40	2,33	-2,67

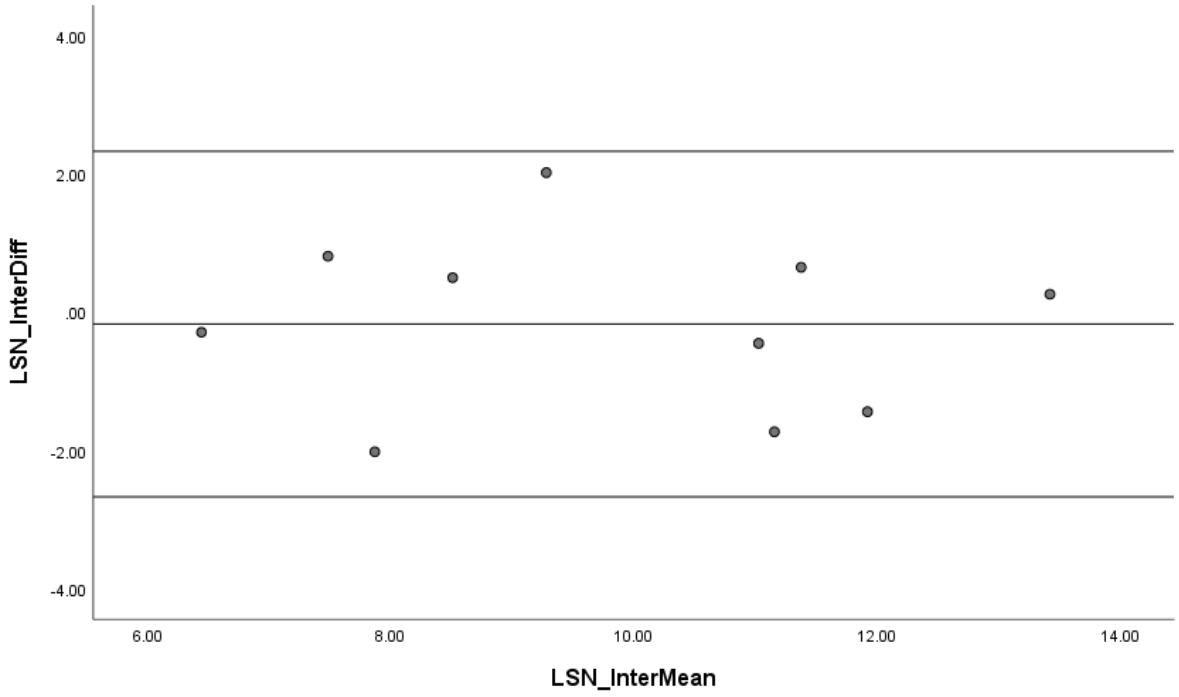

Figure 25: Bland-Altman plot for the left inter-observer (Inter) measurements from the from the S to N

Table 50: Results of a linear regression test to determine the presence of directional bias of measurements

	Unstandardized Coefficients		Standardized Coefficients	t	p
	B	SE	Beta		
S to N (Inter-observer)	-0,06	0,20	-0,10	-0,29	0,78

Right side

Table 51: The mean, standard deviation (SD), standard error (SE) and the upper and the upper and lower limits of the 95% confidence interval of the inter-observer measurements

	N	Mean	SD	SE	Upper	Lower
S to N (Inter-observer)	10	-0,79	3,18	1,00	5,43	-7,02

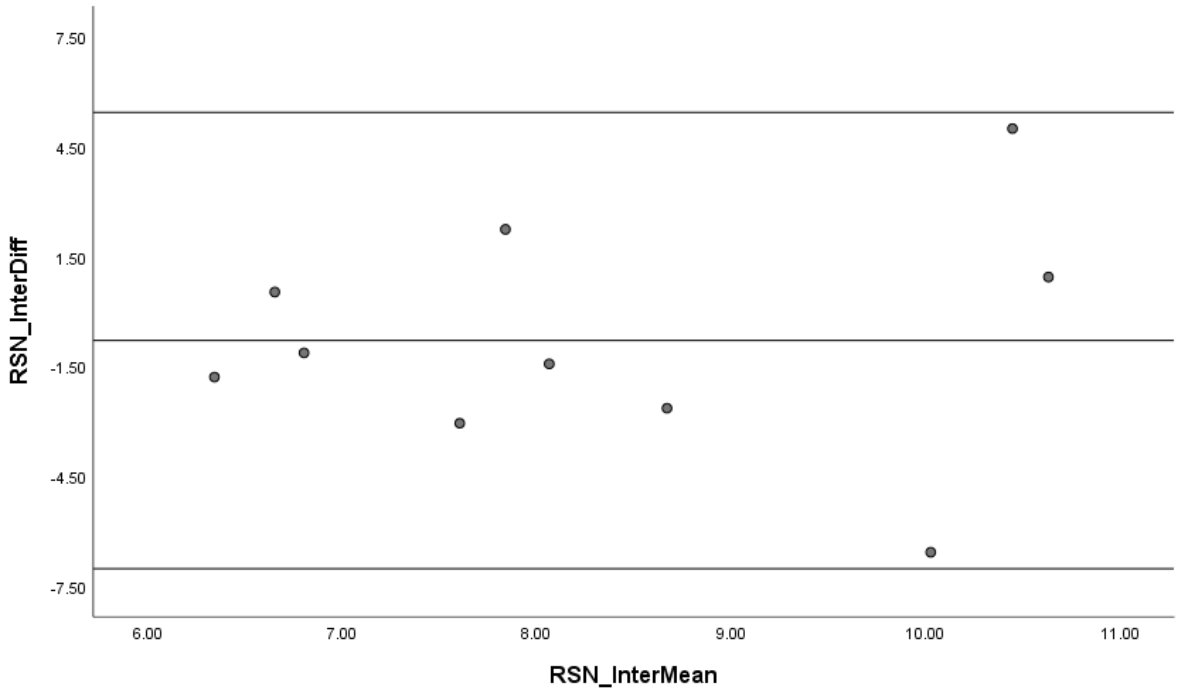

Figure 26: Bland-Altman plot for the right inter-observer (Inter) measurements from the from the S to N

Table 52: Results of a linear regression test to determine the presence of directional bias of measurements

	Unstandardized Coefficients		Standardized Coefficients	t	p
	B	SE	Beta		
S to N (Inter-observer)	0,28	0,70	0,14	0,40	0,70

Inter-observer tests for the measurements from the most medial point of the obturator foramen (M) to the ON within the obturator foramen (N)

Left side

Table 53: The mean, standard deviation (SD), standard error (SE) and the upper and the upper and lower limits of the 95% confidence interval of the inter-observer measurements

	N	Mean	SD	SE	Upper	Lower
M to N (Inter-observer)	10	3,35	5,04	1,59	13,22	-6,53

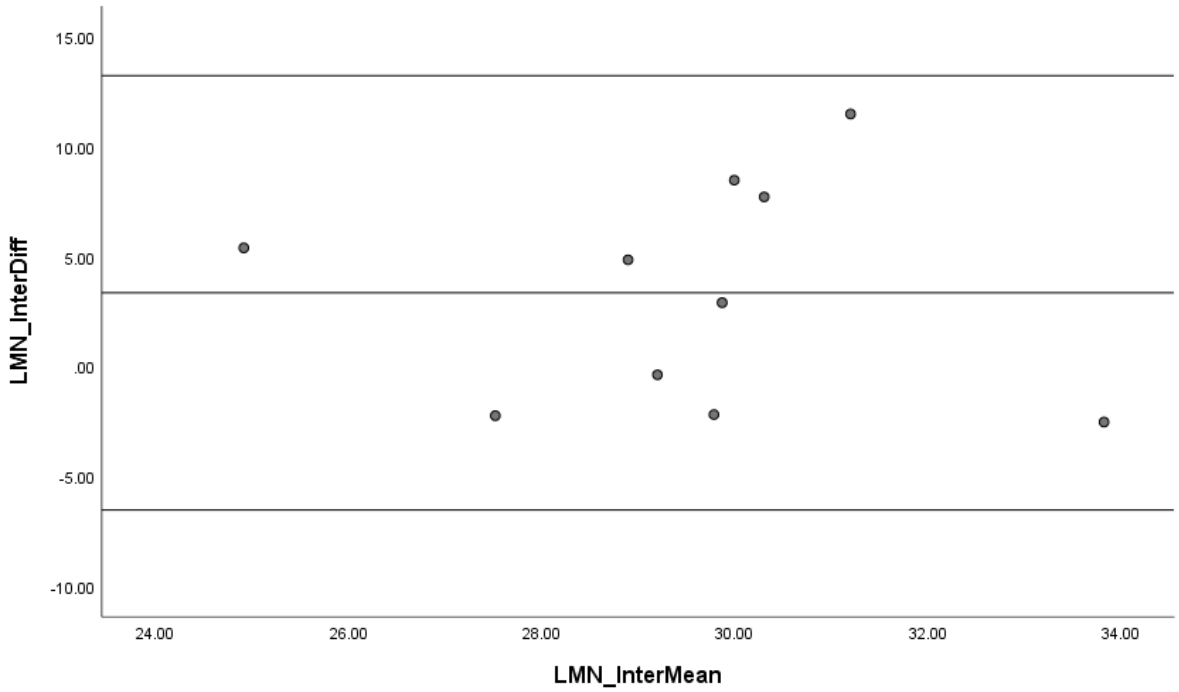

Figure 27: Bland-Altman plot for the left inter-observer (Inter) measurements from the from the M to N

Table 54: Results of a linear regression test to determine the presence of directional bias of measurements

	Unstandardized Coefficients		Standardized Coefficients	t	p
	B	SE	Beta		
M to N (Inter-observer)	-0,11	0,77	-0,05	-0,15	0,89

Right side

Table 55: The mean, standard deviation (SD), standard error (SE) and the upper and the upper and lower limits of the 95% confidence interval of the inter-observer measurements

	N	Mean	SD	SE	Upper	Lower
M to N (Inter-observer)	10	1,79	4,59	1,45	10,78	-7,19

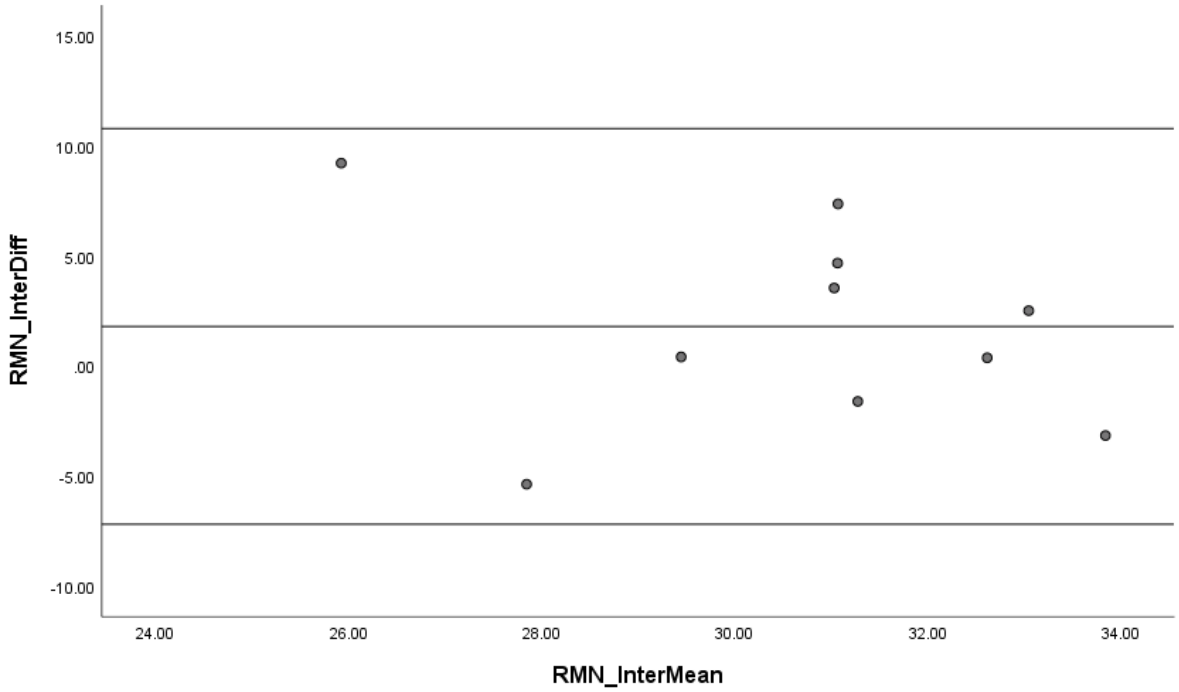

Figure 28: Bland-Altman plot for the right inter-observer (Inter) measurements from the from the M to N

Table 56: Results of a linear regression test to determine the presence of directional bias of measurements

	Unstandardized Coefficients		Standardized Coefficients	t	p
	B	SE	Beta		
M to N (Inter-observer)	-0,54	0,65	-0,28	-0,83	0,43

Inter-observer tests for the measurements from the most inferior point of the obturator foramen (I) to the ON within the obturator foramen (N)

Left side

Table 57: The mean, standard deviation (SD), standard error (SE) and the upper and the upper and lower limits of the 95% confidence interval of the inter-observer measurements

	N	Mean	SD	SE	Upper	Lower
I to N (Inter-observer)	10	0,23	5,93	1,87	11,84	-11,39

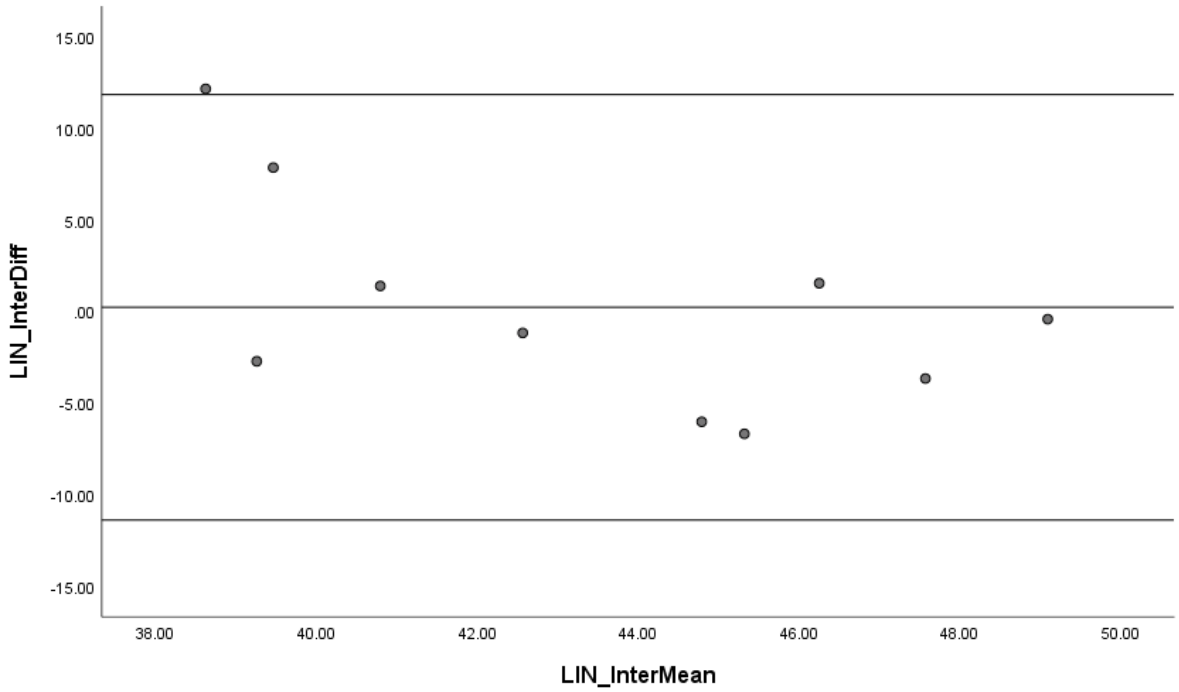

Figure 29: Bland-Altman plot for the left inter-observer (Inter) measurements from the from the I to N

Table 58: Results of a linear regression test to determine the presence of directional bias of measurements

	Unstandardized Coefficients		Standardized Coefficients	t	p
	B	SE	Beta		
I to N (Inter-observer)	-0,91	0,46	-0,57	-1,98	0,08

Right side

Table 59: The mean, standard deviation (SD), standard error (SE) and the upper and the upper and lower limits of the 95% confidence interval of the inter-observer measurements

	N	Mean	SD	SE	Upper	Lower
I to N (Inter-observer)	10	-1,10	7,54	2,38	13,67	-15,87

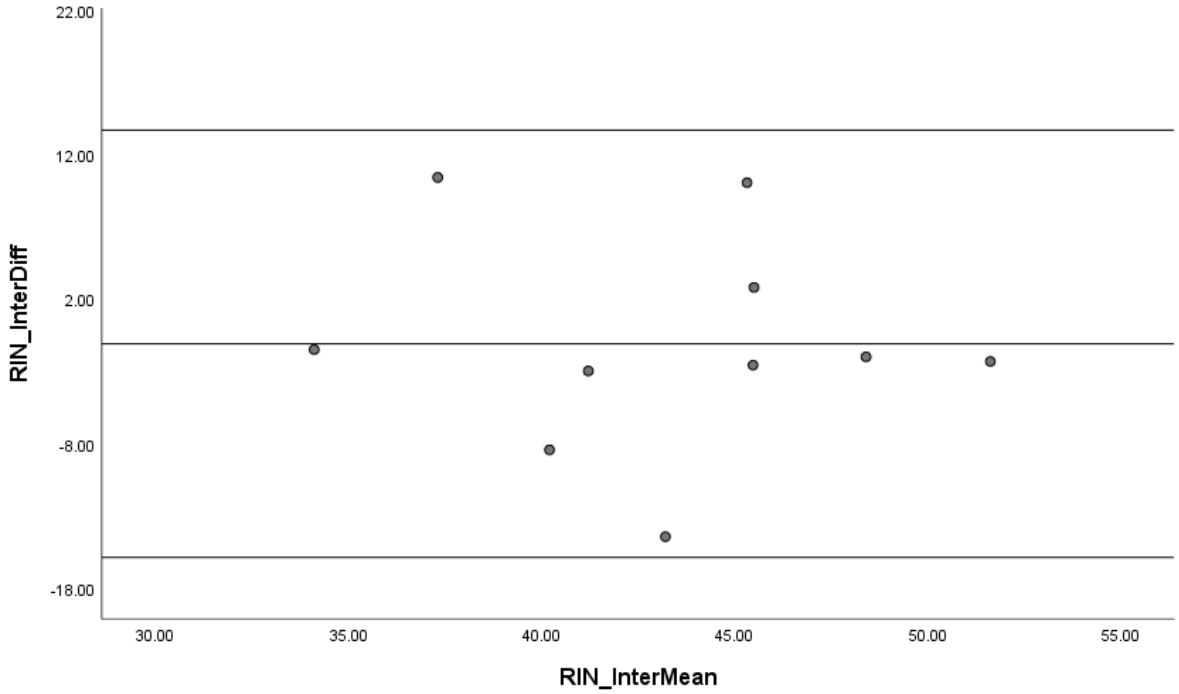

Figure 30: Bland-Altman plot for the right inter-observer (Inter) measurements from the from the I to N

Table 60: Results of a linear regression test to determine the presence of directional bias of measurements

	Unstandardized Coefficients		Standardized Coefficients	t	p
	B	SE	Beta		
I to N (Inter-observer)	-0,10	0,51	-0,07	-0,19	0,85

Intra-observer tests for the measurements from the most superior point of the obturator foramen (S) to the ON within the obturator foramen (N)

Left side

Table 61: The mean, standard deviation (SD), standard error (SE) and the upper and the upper and lower limits of the 95% confidence interval of the intra-observer measurements

	N	Mean	SD	SE	Upper	Lower
S to N (Intra-observer)	10	1,63	2,88	0,91	7,28	-4,02

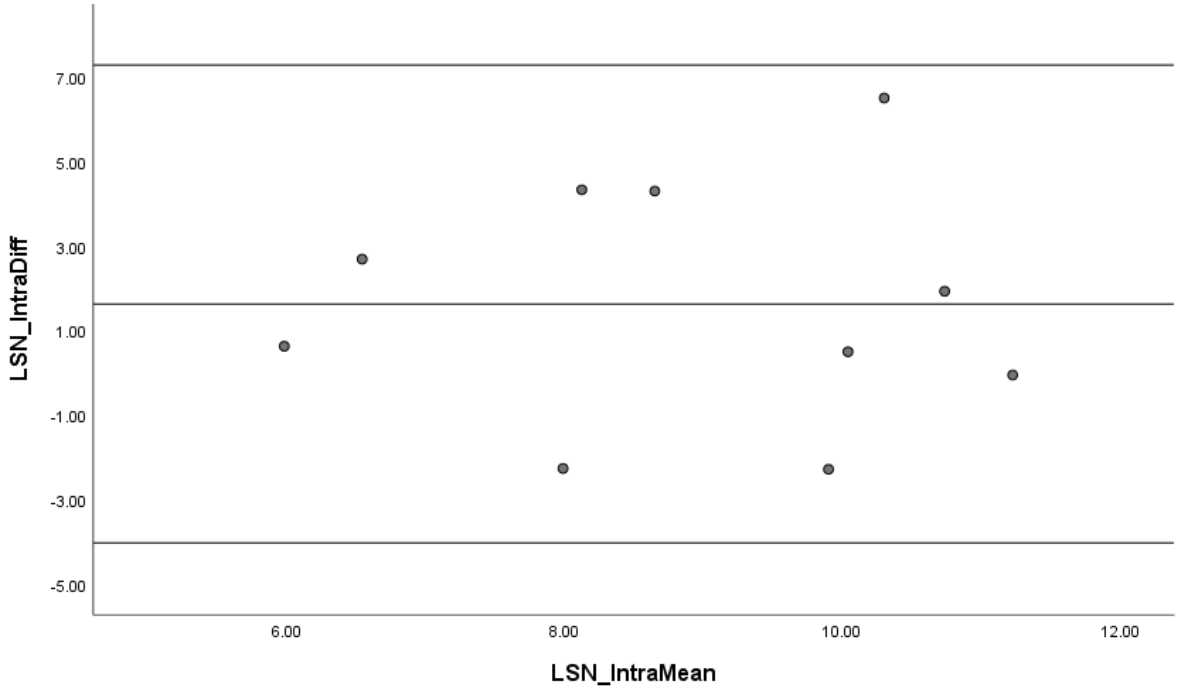

Figure 31: Bland-Altman plot for the left intra-observer (Intra) measurements from the from the S to N (SN)

Table 62: Results of a linear regression test to determine the presence of directional bias of measurements

	Unstandardized Coefficients		Standardized Coefficients	t	p
	B	SE	Beta		
S to N (Intra-observer)	-0,02	0,57	-0,01	-0,03	0,98

Right side

Table 63: The mean, standard deviation (SD), standard error (SE) and the upper and the upper and lower limits of the 95% confidence interval of the intra-observer measurements

	N	Mean	SD	SE	Upper	Lower
S to N (Intra-observer)	10	1,08	1,94	0,61	4,88	-2,72

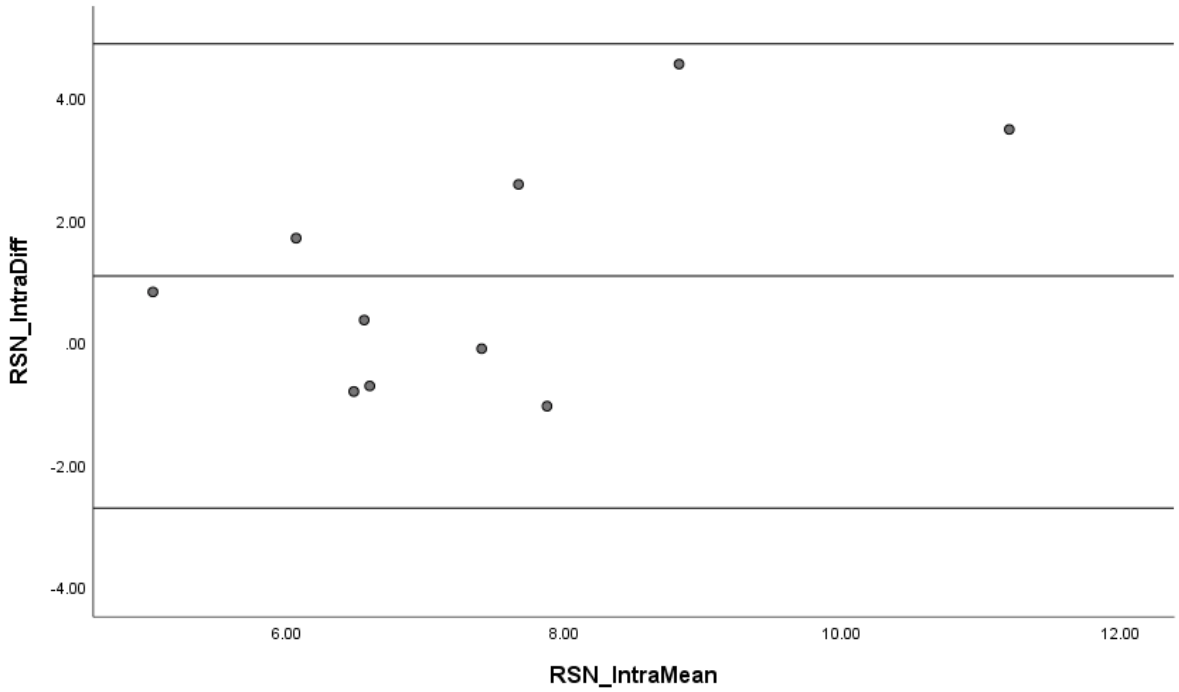

Figure 32: Bland-Altman plot for the right intra-observer (Intra) measurements from the from the S to N (SN)

Table 64: Results of a linear regression test to determine the presence of directional bias of measurements

	Unstandardized Coefficients		Standardized Coefficients	t	p
	B	SE	Beta		
S to N (Intra-observer)	0,65	0,33	0,57	1,97	0,09

Intra-observer tests for the measurements from the most medial point of the obturator foramen (M) to the ON within the obturator foramen (N)

Left side

Table 65: The mean, standard deviation (SD), standard error (SE) and the upper and the upper and lower limits of the 95% confidence interval of the intra-observer measurements

	N	Mean	SD	SE	Upper	Lower
M to N (Intra-observer)	10	4,16	6,31	2,00	16,53	-8,21

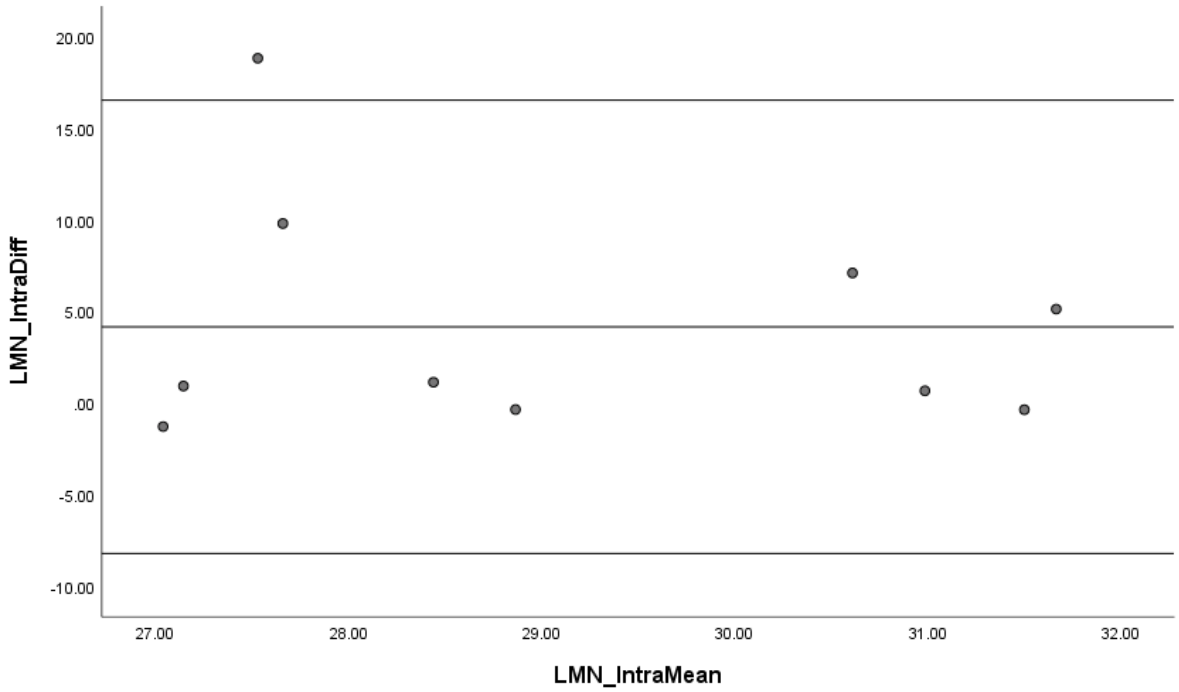

Figure 33: Bland-Altman plot for the left intra-observer (Intra) measurements from the from the M to N (MN)

Table 66: Results of a linear regression test to determine the presence of directional bias of measurements

	Unstandardized Coefficients		Standardized Coefficients	t	p
	B	SE	Beta		
M to N (Intra-observer)	-0,67	1,17	-0,20	-0,57	0,58

Right side

Table 67: The mean, standard deviation (SD), standard error (SE) and the upper and the upper and lower limits of the 95% confidence interval of the intra-observer measurements

	N	Mean	SD	SE	Upper	Lower
M to N (Intra-observer)	10	-0,75	2,75	0,87	4,64	-6,13

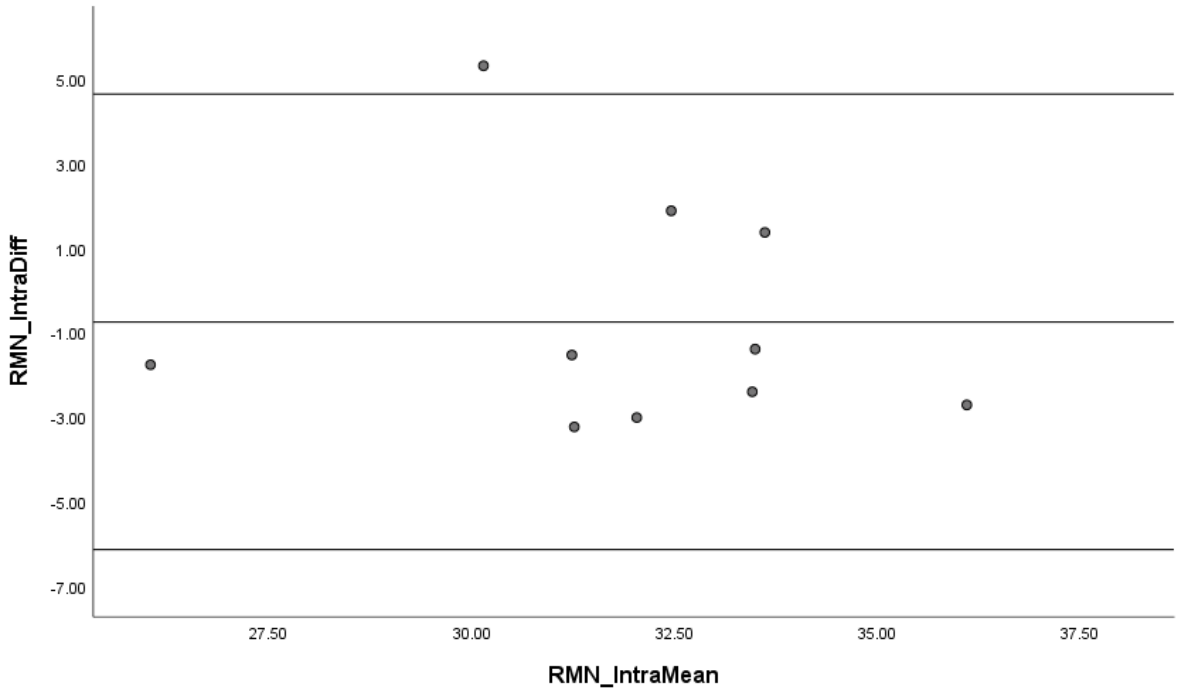

Figure 34: Bland-Altman plot for the right intra-observer (Intra) measurements from the from the M to N (MN)

Table 68: Results of a linear regression test to determine the presence of directional bias of measurements

	Unstandardized Coefficients		Standardized Coefficients	t	p
	B	SE	Beta		
M to N (Intra-observer)	-0,15	0,36	-0,15	-0,42	0,69

Intra-observer tests for the measurements from the most inferior point of the obturator foramen (I) to the ON within the obturator foramen (N)

Left side

Table 69: The mean, standard deviation (SD), standard error (SE) and the upper and the upper and lower limits of the 95% confidence interval of the intra-observer measurements

	N	Mean	SD	SE	Upper	Lower
I to N (Intra-observer)	10	0,64	3,42	1,08	7,34	-6,07

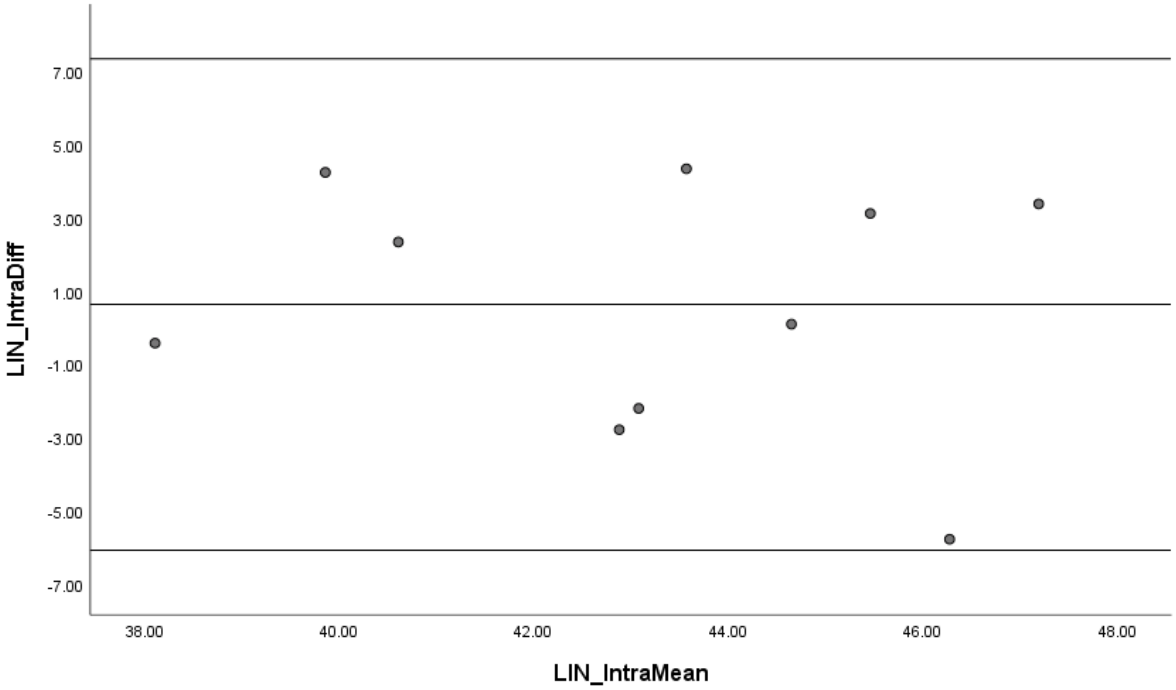

Figure 35: Bland-Altman plot for the left intra-observer (Intra) measurements from the from the I to N (IN)

Table 70: Results of a linear regression test to determine the presence of directional bias of measurements

	Unstandardized Coefficients		Standardized Coefficients	t	p
	B	SE	Beta		
I to N (Intra-observer)	-0,16	0,41	-0,14	-0,39	0,71

Right side

Table 71: The mean, standard deviation (SD), standard error (SE) and the upper and the upper and lower limits of the 95% confidence interval of the intra-observer measurements

	N	Mean	SD	SE	Upper	Lower
I to N (Intra-observer)	10	-1,33	6,86	2,17	12,12	-14,78

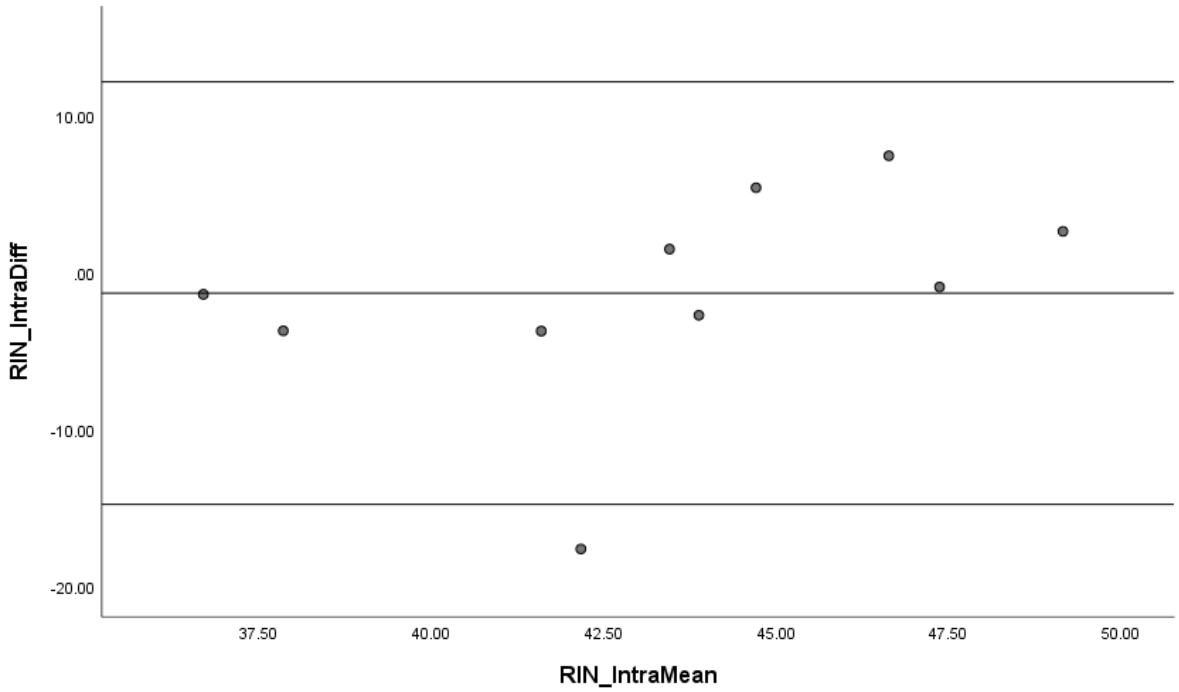

Figure 36: Bland-Altman plot for the right intra-observer (Intra) measurements from the from the I to N (IN)

Table 72: Results of a linear regression test to determine the presence of directional bias of measurements

	Unstandardized Coefficients		Standardized Coefficients	t	p
	B	SE	Beta		
I to N (Intra-observer)	0,70	0,56	0,40	1,25	0,25

5. FEMORAL NERVE (FN)

Inter-observer tests for the measurements from the ASIS to the FN

Left side

Table 69: The mean, standard deviation (SD), standard error (SE) and the upper and the upper and lower limits of the 95% confidence interval of the inter-observer measurements

	N	Mean	SD	SE	Upper	Lower
ASIS to FN (Inter-observer)	10	3,68	9,07	2,87	21,45	-14,10

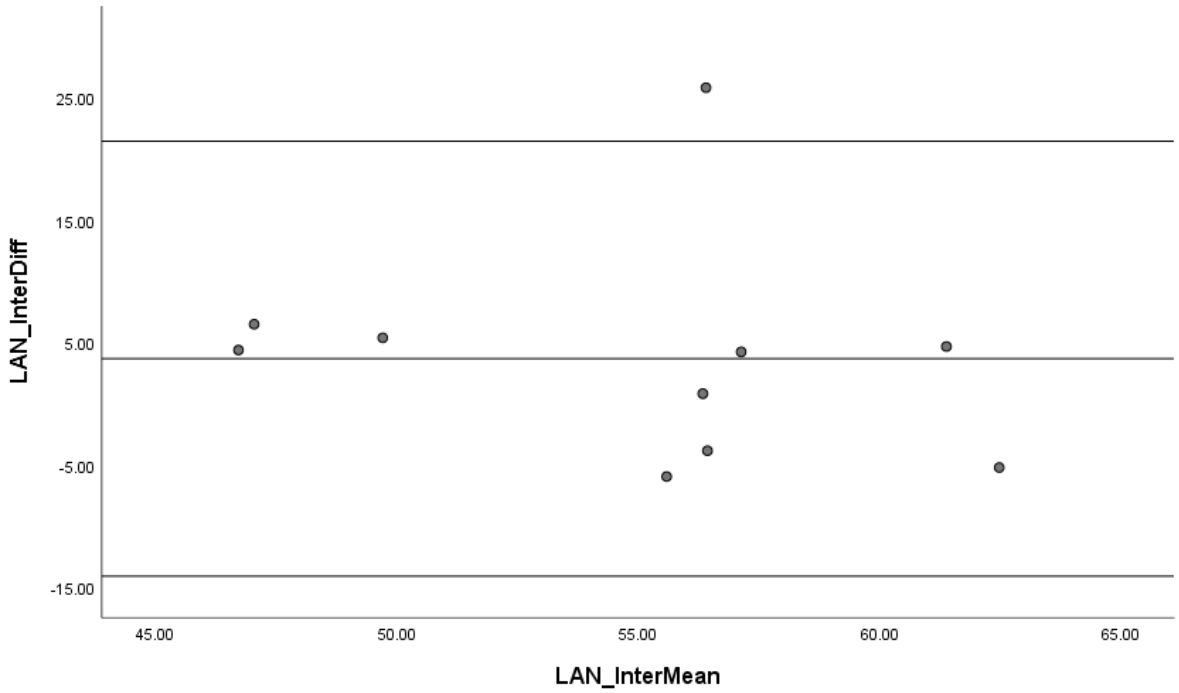

Figure 35: Bland-Altman plot for the left inter-observer (Inter) measurements from the from the ASIS to the FN (AN)

Table 70: Results of a linear regression test to determine the presence of directional bias of measurements

	Unstandardized Coefficients		Standardized Coefficients	t	p
	B	SE	Beta		
ASIS to FN (Inter-observer)	-0,32	0,58	-0,19	-0,55	0,60

Right side

Table 71: The mean, standard deviation (SD), standard error (SE) and the upper and the upper and lower limits of the 95% confidence interval of the inter-observer measurements

	N	Mean	SD	SE	Upper	Lower
ASIS to FN (Inter-observer)	10	0,26	9,95	3,15	19,76	-19,24

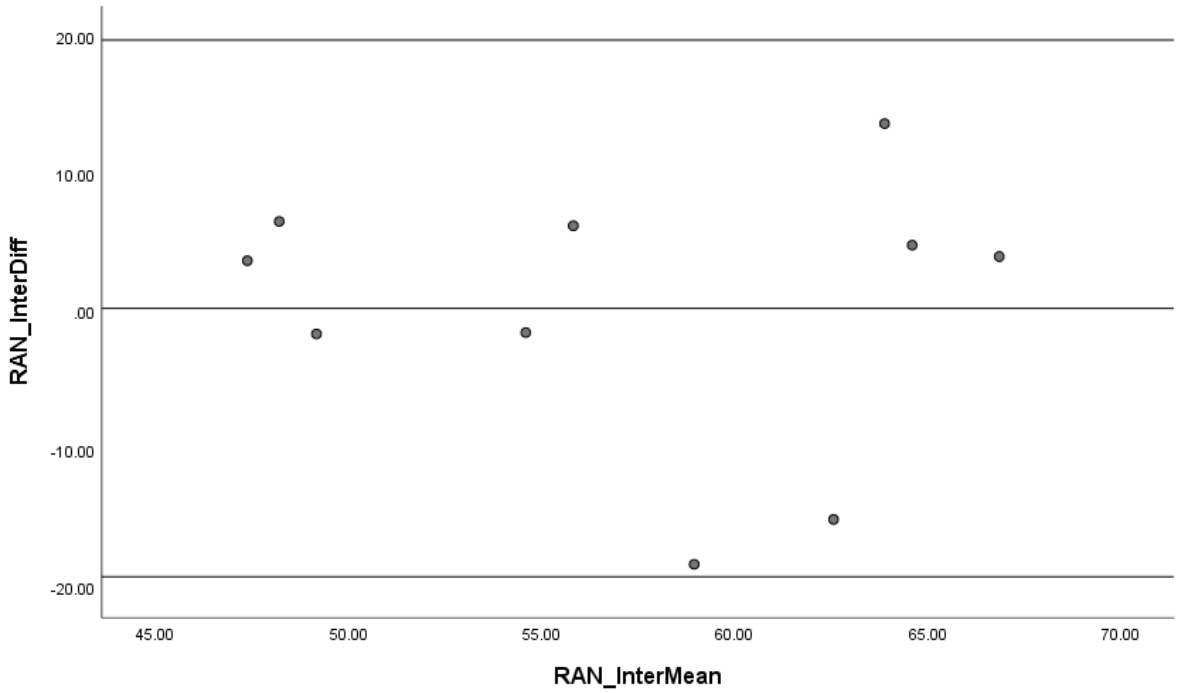

Figure 36: Bland-Altman plot for the right inter-observer (Inter) measurements from the from the ASIS to the FN (AN)

Table 72: Results of a linear regression test to determine the presence of directional bias of measurements

	Unstandardized Coefficients		Standardized Coefficients	t	p
	B	SE	Beta		
ASIS to FN (Inter-observer)	-0,07	0,48	-0,05	-0,15	0,89

Inter-observer tests for the measurements from the ASIS to the femoral artery (FA)

Left side

Table 69: The mean, standard deviation (SD), standard error (SE) and the upper and the upper and lower limits of the 95% confidence interval of the inter-observer measurements

	N	Mean	SD	SE	Upper	Lower
ASIS to FA (Inter-observer)	10	4,10	11,95	3,78	27,52	-19,32

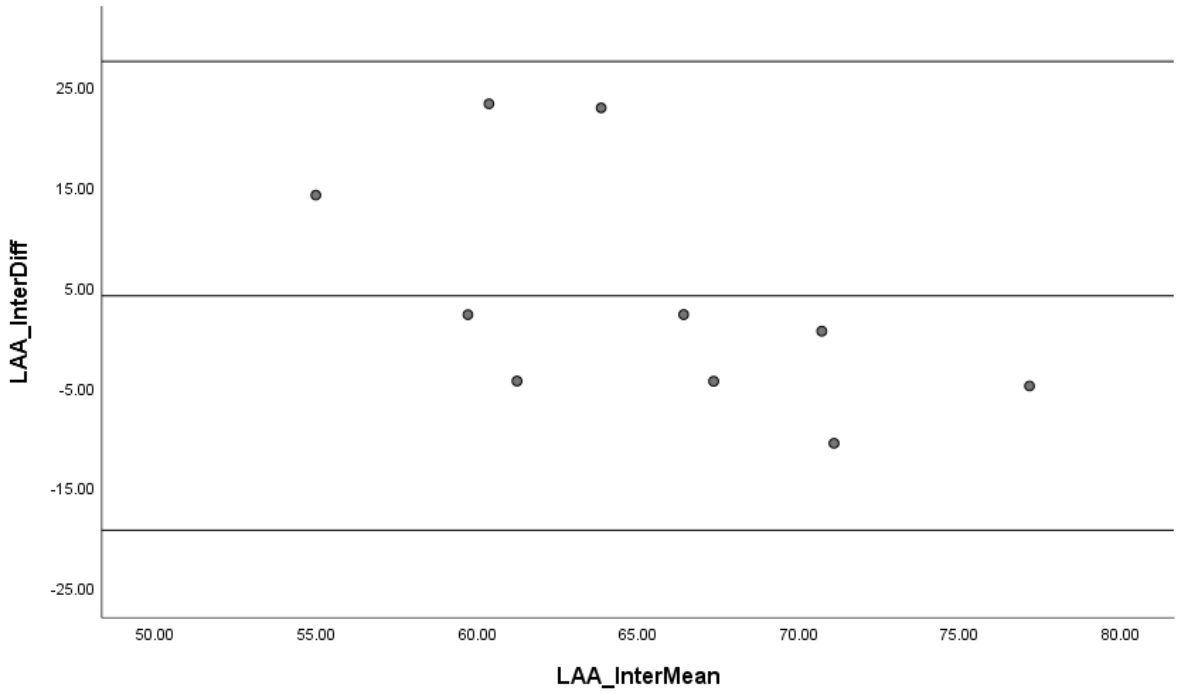

Figure 35: Bland-Altman plot for the left inter-observer (Inter) measurements from the from the ASIS to the FA (AA)

Table 70: Results of a linear regression test to determine the presence of directional bias of measurements

	Unstandardized Coefficients		Standardized Coefficients	t	p
	B	SE	Beta		
ASIS to FA (Inter-observer)	-1,06	0,52	-0,58	-2,02	0,08

Right side

Table 71: The mean, standard deviation (SD), standard error (SE) and the upper and the upper and lower limits of the 95% confidence interval of the inter-observer measurements

	N	Mean	SD	SE	Upper	Lower
ASIS to FA (Inter-observer)	10	5,84	11,82	3,74	29,02	-17,33

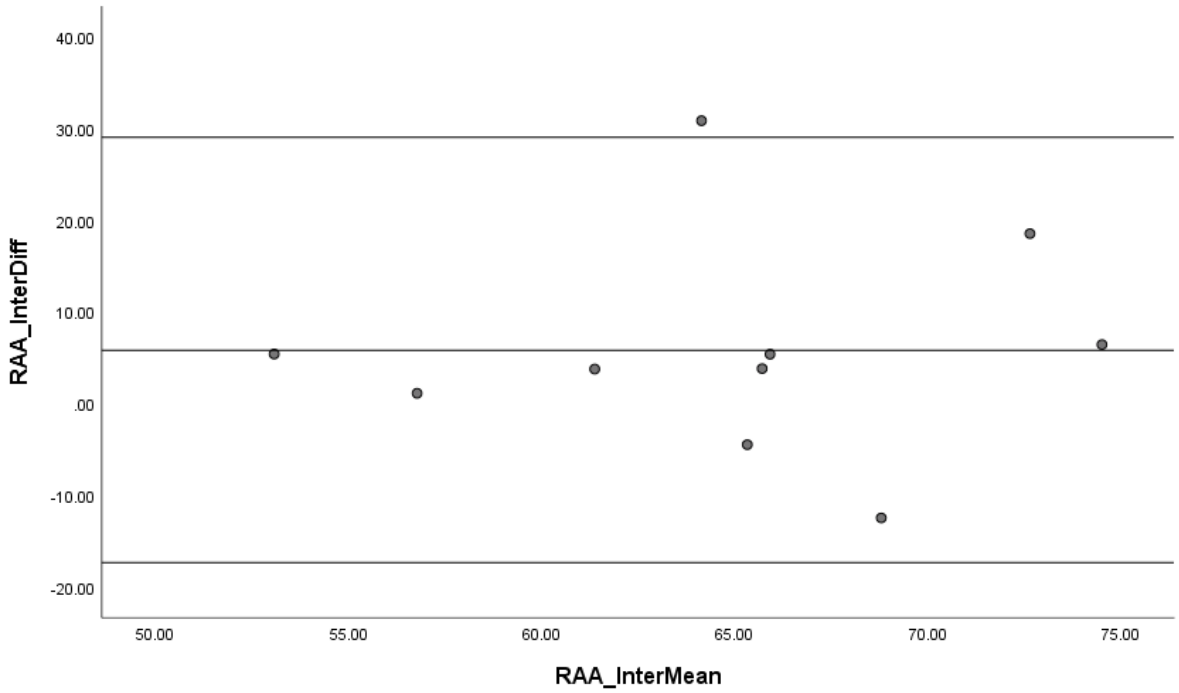

Figure 36: Bland-Altman plot for the right inter-observer (Inter) measurements from the from the ASIS to the FA (AA)

Table 72: Results of a linear regression test to determine the presence of directional bias of measurements

	Unstandardized Coefficients		Standardized Coefficients	t	p
	B	SE	Beta		
ASIS to FA (Inter-observer)	0,15	0,63	0,08	0,24	0,82

Inter-observer tests for the measurements from the ASIS to the femoral vein (FV)

Left side

Table 69: The mean, standard deviation (SD), standard error (SE) and the upper and the upper and lower limits of the 95% confidence interval of the inter-observer measurements

	N	Mean	SD	SE	Upper	Lower
ASIS to FV (Inter-observer)	10	6,61	13,72	4,34	33,49	-20,28

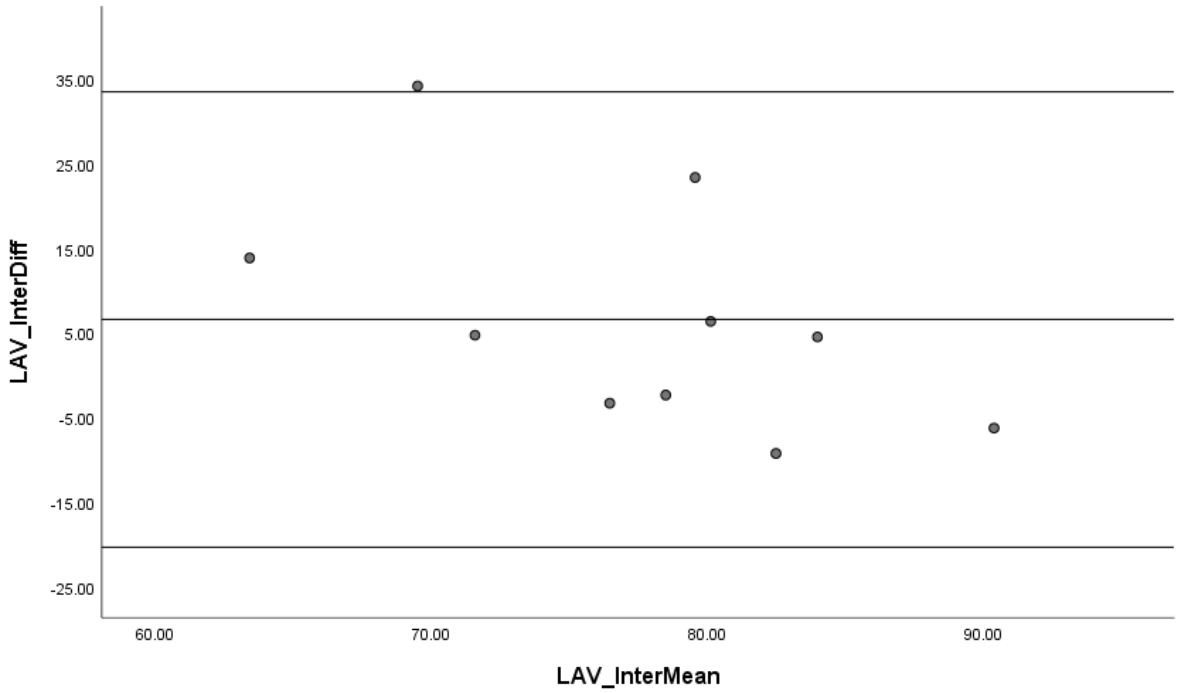

Figure 35: Bland-Altman plot for the left inter-observer (Inter) measurements from the from the ASIS to the FV (AV)

Table 70: Results of a linear regression test to determine the presence of directional bias of measurements

	Unstandardized Coefficients		Standardized Coefficients	t	p
	B	SE	Beta		
ASIS to FV (Inter-observer)	-0,98	0,52	-0,56	-1,90	0,10

Right side

Table 71: The mean, standard deviation (SD), standard error (SE) and the upper and the upper and lower limits of the 95% confidence interval of the inter-observer measurements

	N	Mean	SD	SE	Upper	Lower
ASIS to FV (Inter-observer)	10	5,31	10,63	3,36	26,15	-15,52

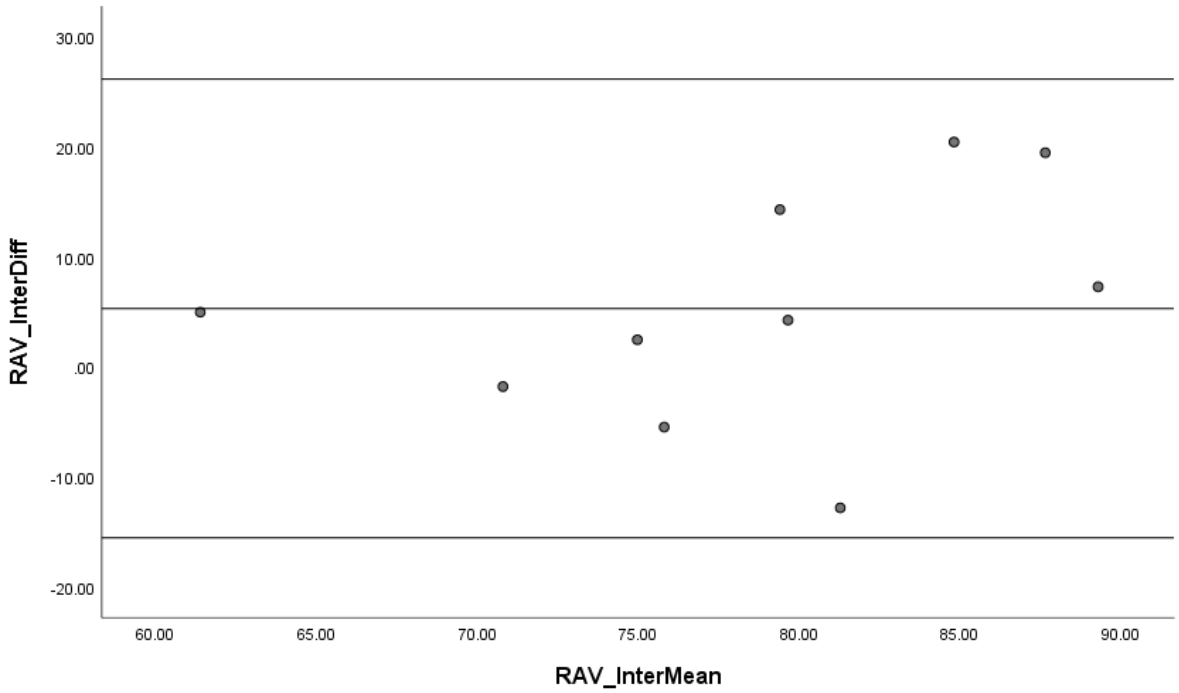

Figure 36: Bland-Altman plot for the right inter-observer (Inter) measurements from the from the ASIS to the FV (AV)

Table 72: Results of a linear regression test to determine the presence of directional bias of measurements

	Unstandardized Coefficients		Standardized Coefficients	t	p
	B	SE	Beta		
ASIS to FV (Inter-observer)	0,49	0,42	0,38	1,16	0,28

Intra-observer tests for the measurements from the ASIS to the FN

Left side

Table 69: The mean, standard deviation (SD), standard error (SE) and the upper and the upper and lower limits of the 95% confidence interval of the intra-observer measurements

	N	Mean	SD	SE	Upper	Lower
ASIS to FN (Intra-observer)	10	3,70	9,15	2,89	21,64	-14,23

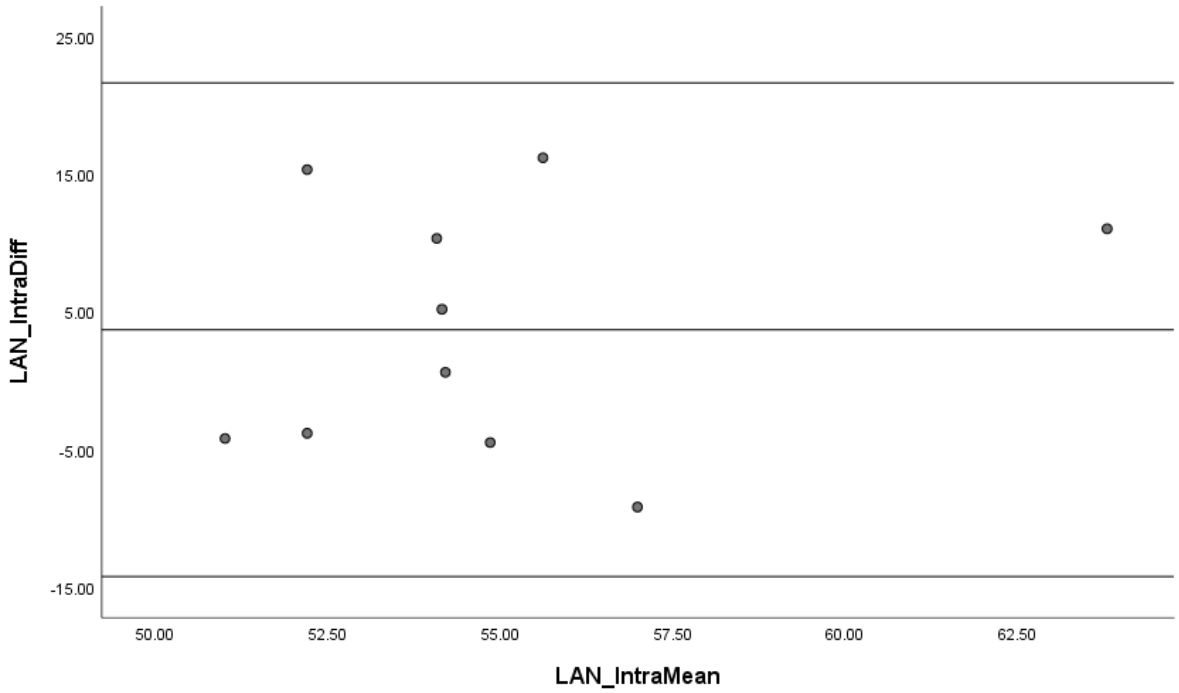

Figure 35: Bland-Altman plot for the left intra-observer (Intra) measurements from the from the ASIS to the FN (AN)

Table 70: Results of a linear regression test to determine the presence of directional bias of measurements

	Unstandardized Coefficients		Standardized Coefficients	t	p
	B	SE	Beta		
ASIS to FN (Intra-observer)	0,55	0,88	0,21	0,62	0,55

Right side

Table 71: The mean, standard deviation (SD), standard error (SE) and the upper and the upper and lower limits of the 95% confidence interval of the intra-observer measurements

	N	Mean	SD	SE	Upper	Lower
ASIS to FN (Intra-observer)	10	-0,22	13,25	4,19	25,74	-26,18

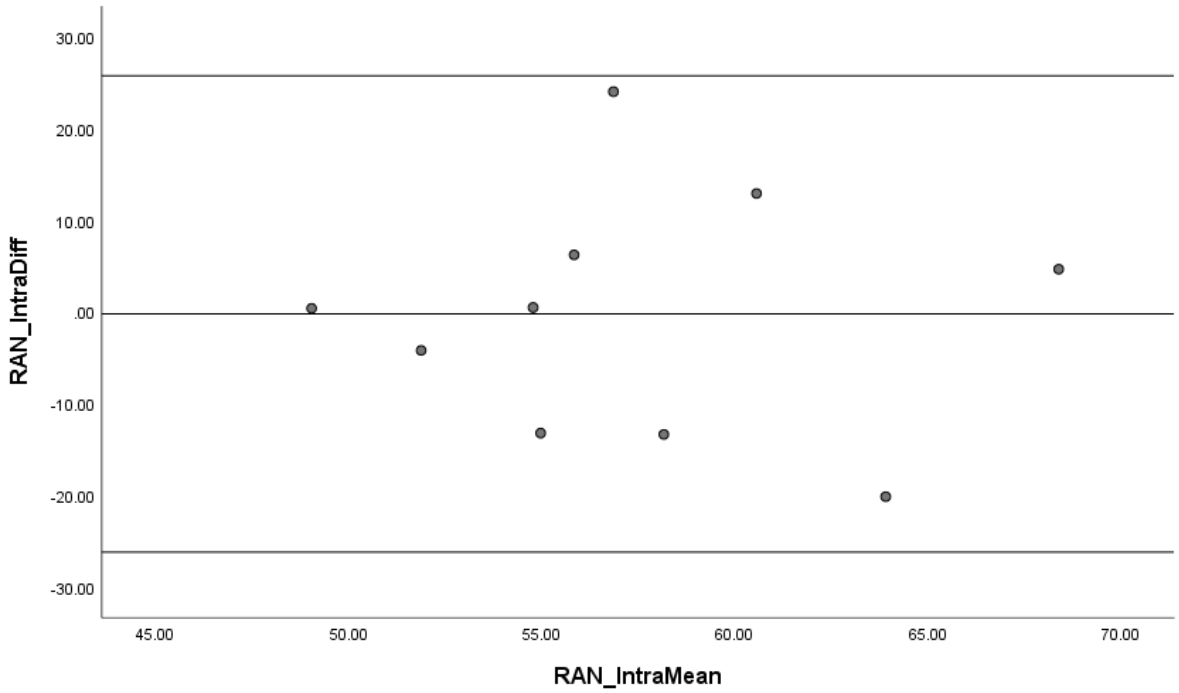

Figure 36: Bland-Altman plot for the right intra-observer (Intra) measurements from the from the ASIS to the FN (AN)

Table 72: Results of a linear regression test to determine the presence of directional bias of measurements

	Unstandardized Coefficients		Standardized Coefficients	t	p
	B	SE	Beta		
ASIS to FN (Intra-observer)	-0,07	0,83	-0,03	-0,09	0,93

Intra-observer tests for the measurements from the ASIS to the femoral artery (FA)

Left side

Table 69: The mean, standard deviation (SD), standard error (SE) and the upper and the upper and lower limits of the 95% confidence interval of the intra-observer measurements

	N	Mean	SD	SE	Upper	Lower
ASIS to FA (Intra-observer)	10	5,17	8,43	2,67	21,70	-11,36

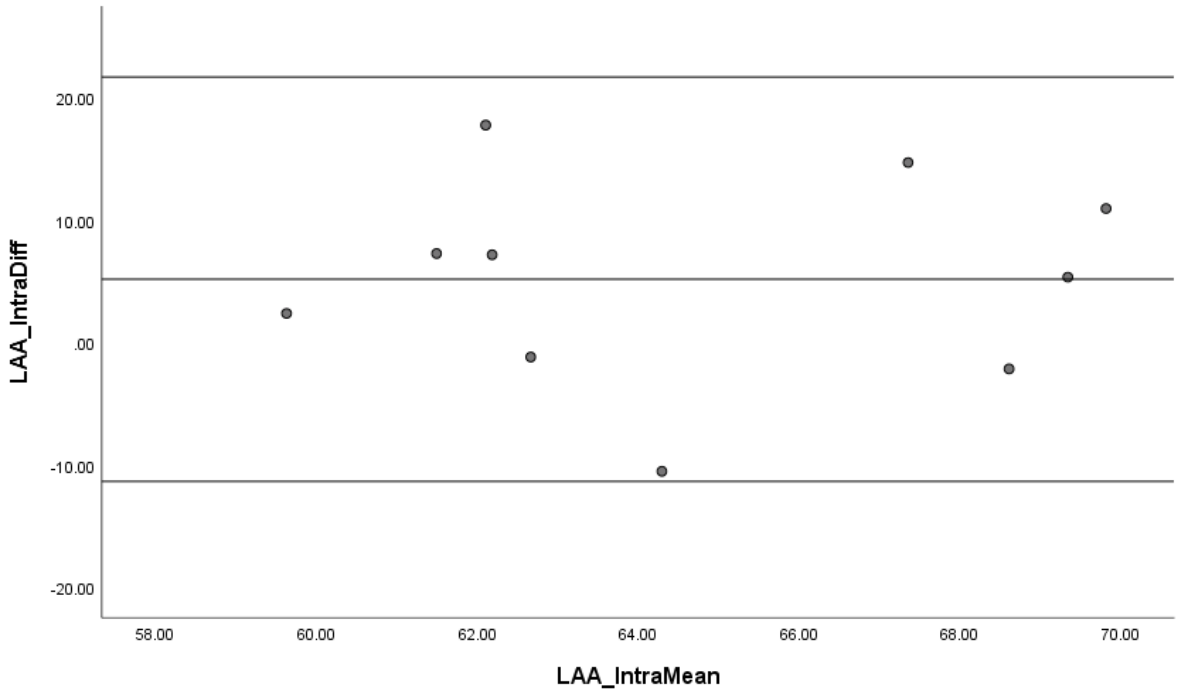

Figure 35: Bland-Altman plot for the left intra-observer (Intra) measurements from the from the ASIS to the FA (AA)

Table 70: Results of a linear regression test to determine the presence of directional bias of measurements

	Unstandardized Coefficients		Standardized Coefficients	t	p
	B	SE	Beta		
ASIS to FA (Intra-observer)	0,13	0,80	0,06	0,16	0,88

Right side

Table 71: The mean, standard deviation (SD), standard error (SE) and the upper and the upper and lower limits of the 95% confidence interval of the intra-observer measurements

	N	Mean	SD	SE	Upper	Lower
ASIS to FA (Intra-observer)	10	3,15	13,27	4,20	29,16	-22,86

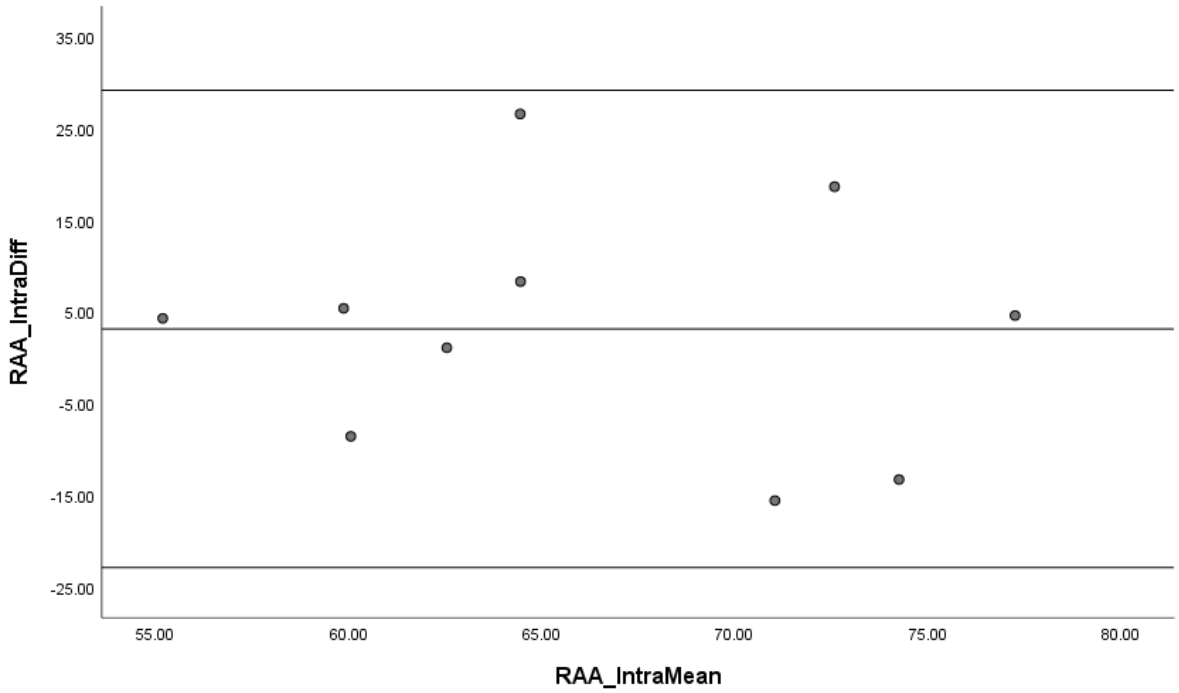

Figure 36: Bland-Altman plot for the right intra-observer (Intra) measurements from the from the ASIS to the FA (AA)

Table 72: Results of a linear regression test to determine the presence of directional bias of measurements

	Unstandardized Coefficients		Standardized Coefficients	t	p
	B	SE	Beta		
ASIS to FA (Intra-observer)	-0,22	0,65	-0,12	-0,35	0,74

Intra-observer tests for the measurements from the ASIS to the femoral vein (FV)

Left side

Table 69: The mean, standard deviation (SD), standard error (SE) and the upper and the upper and lower limits of the 95% confidence interval of the intra-observer measurements

	N	Mean	SD	SE	Upper	Lower
ASIS to FV (Intra-observer)	10	5,85	10,26	3,25	25,96	-14,27

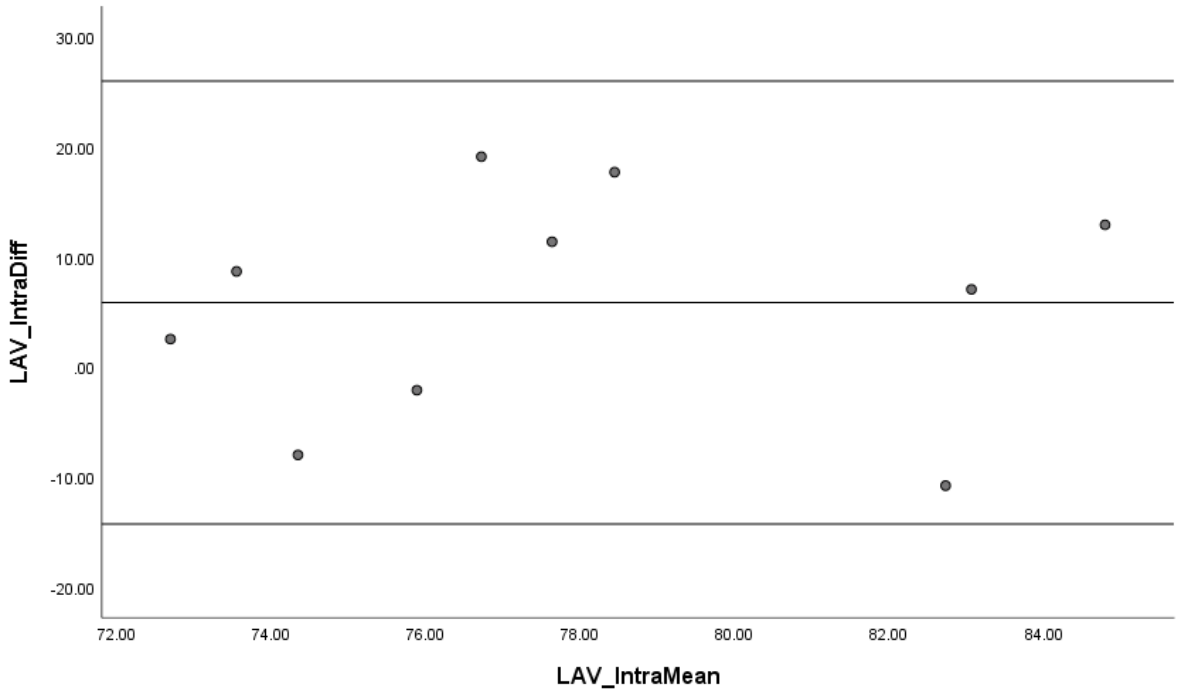

Figure 35: Bland-Altman plot for the left intra-observer (Intra) measurements from the from the ASIS to the FV (AV)

Table 70: Results of a linear regression test to determine the presence of directional bias of measurements

	Unstandardized Coefficients		Standardized Coefficients	t	p
	B	SE	Beta		
ASIS to FV (Intra-observer)	0,21	0,85	0,09	0,25	0,81

Right side

Table 71: The mean, standard deviation (SD), standard error (SE) and the upper and the upper and lower limits of the 95% confidence interval of the intra-observer measurements

	N	Mean	SD	SE	Upper	Lower
ASIS to FV (Intra-observer)	10	6,22	15,67	4,96	36,93	-24,50

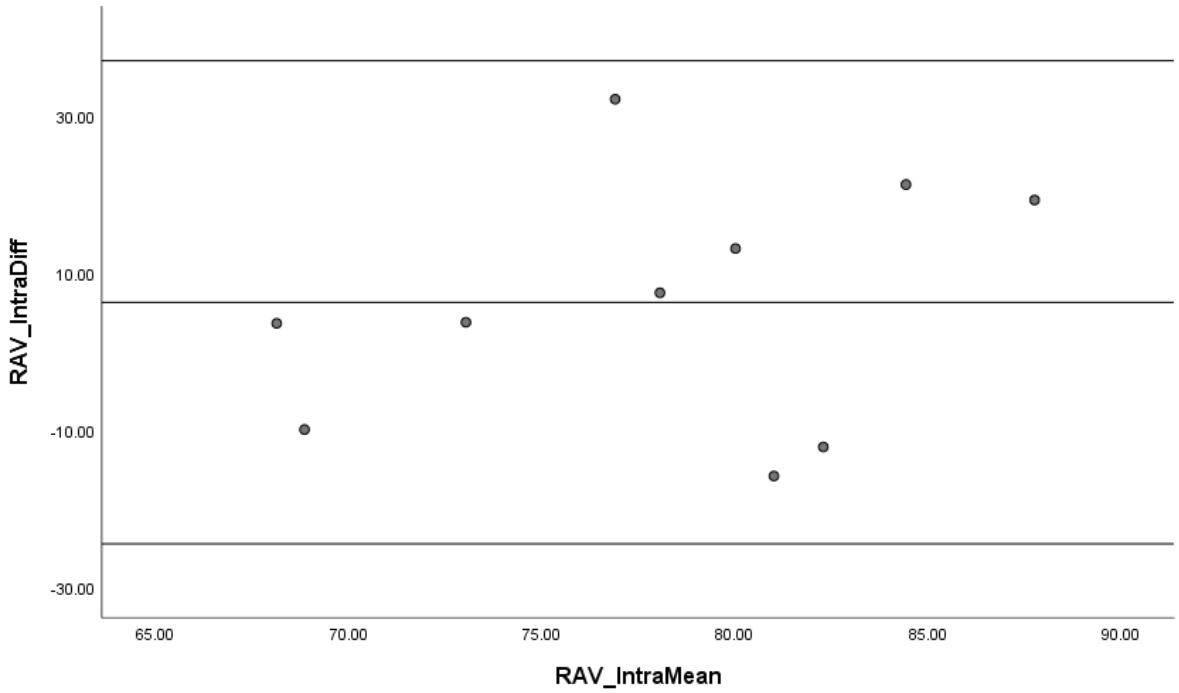

Figure 36: Bland-Altman plot for the right intra-observer (Intra) measurements from the from the ASIS to the FV (AV)

Table 72: Results of a linear regression test to determine the presence of directional bias of measurements

	Unstandardized Coefficients		Standardized Coefficients	t	p
	B	SE	Beta		
ASIS to FV (Intra-observer)	0,67	0,83	0,28	0,81	0,44